

Massless-Massive Amplitude Correspondence II: Constructive Massive Amplitudes in Standard Model

Yu-Han Ni, ^{a,b,e} Chao Wu, ^a Jiang-Hao Yu, ^{a,b,c,d}

^a*Institute of Theoretical Physics, Chinese Academy of Sciences, Beijing 100190, China*

^b*School of Physical Sciences, University of Chinese Academy of Sciences, Beijing 100049, China*

^c*School of Fundamental Physics and Mathematical Sciences, Hangzhou Institute for Advanced Study, UCAS, Hangzhou 310024, China*

^d*International Center for Theoretical Physics Asia-Pacific, Beijing/Hangzhou, China*

^e*School of Science and Engineering, Chinese University of Hong Kong, Shenzhen, Shenzhen 518172, China*

E-mail: niyuhan@cuhk.edu.cn, wuch7@itp.ac.cn, jhyu@itp.ac.cn

ABSTRACT:

In the minimal helicity-chirality formalism, we systematically construct higher-point massive amplitudes from the fundamental building blocks: the contact three-point and four-point massive amplitudes. The inclusion of four-point contact amplitudes is essential to maintain gauge invariance in the spontaneously broken Standard Model. We construct all the standard model massive contact amplitudes and identify the physical light-cone gauge nature of massive amplitudes. Then only using the contact minimal helicity-chirality amplitudes *at the leading order*, we show both bootstrap techniques and on-shell recursion relations can be utilized to compute higher-point massive amplitudes. This provides a systematic framework for constructing various higher-point electroweak amplitudes, analogous to established on-shell methods for massless theories. Finally by deforming the gauge-invariant n -point amplitudes, we extend the massless-massive correspondence from three-and-four point contact amplitudes to general n -point factorized amplitudes.

Contents

1	Introduction	1
2	Minimal Helicity-Chirality Formalism	4
2.1	Spinor-helicity and spin-transversality	4
2.2	Minimal Helicity-Chirality one-particle states	10
2.3	MHC 2-point currents	16
2.4	MHC 3-point amplitudes	21
3	The 3-point Amplitude Matching For SM Amplitudes	35
3.1	Massless and massive 3-point SM amplitudes	35
3.2	3-point matching from MHC amplitude deformation	40
3.3	Matching results for SM amplitudes	48
4	MHC Amplitude Bootstrapping and 4-point Contact MHC amplitudes	53
4.1	Gluing 3-point MHC amplitudes: $u\bar{d} \rightarrow W h$ as example	54
4.2	Massless and MHC amplitudes in light-cone gauge	60
4.3	Contact 4-point MHC amplitudes	63
5	Constructive Amplitudes in 3 Ways: $WW \rightarrow hh$ as Example	75
5.1	Bootstrapping MHC amplitudes	75
5.2	Bootstrapping AHH amplitudes	77
5.3	MHC recursive construction	79
6	Massless-Massive Matching at Leading and Sub-leading Orders	83
6.1	Massless 4-point amplitudes: the gauge-invariant way	86
6.2	Scaling structure for MHC amplitudes	90
6.3	Amplitude deformation and pole separation	95
6.4	Sub-leading MHC matching	102
7	Summary and Outlook	108
A	Higgsing Rules for Internal Particles	109
A.1	MHC internal particles	109
A.2	Internal particle Higgsing	110
B	Contact 4-point Amplitudes from Conserved Current	111
B.1	Contact VVSS amplitudes	112
B.2	Contact VVVV amplitudes	115

C	$WW \rightarrow ZZ$ Amplitudes	118
C.1	Bootstrapping MHC amplitudes	118
C.2	Bootstrapping AHH amplitudes	120

1 Introduction

Over recent decades, the on-shell method has become a central and powerful technique in scattering amplitude calculations. It uses the spinor-helicity formalism to represent scattering amplitudes purely in terms of on-shell states, which automatically enforces equations of motion and makes gauge invariance explicit for massless particles [1–8]. This physical transparency stems from a key distinction: while a massless gauge boson possesses only two physical helicity states, its corresponding gauge field in a local Lagrangian carries redundant degrees of freedom. The on-shell method, by construction, avoids these off-shell redundancies. Consequently, in contrast to the traditional Feynman diagrammatic approach built from Lagrangians and off-shell fields, the on-shell methodology offers a more efficient and physically transparent route to computing scattering amplitudes in gauge theories and gravity.

In the real world, scattering processes involve a variety of massive particles, creating a demand for on-shell methods to compute massive amplitudes. Unlike massless particles, which have one or two helicity states, massive spin- s particles possess $(2s + 1)$ physical states. Consequently, for massive particles there is no distinction between on-shell and off-shell degrees of freedom, nor an underlying gauge symmetry to exploit. This would seem to negate the primary advantages of the on-shell approach, potentially rendering it no more efficient than traditional Feynman diagram methods. However, an important exception exists when the massive theory descends from a massless ultraviolet theory via spontaneous symmetry breaking—as in the Standard Model (SM) and its extensions. In these theories, the underlying gauge symmetry, though hidden, provides a powerful organizing principle for simplifying scattering amplitudes.

In the on-shell method, the fundamental three-point massless amplitudes are fully determined by their scaling behavior under little group transformations [9, 10]. Guided by first principles, symmetry, locality, unitarity, and analyticity, tree-level amplitudes can be constructed recursively from these three-point building blocks to arbitrary multiplicity and extended to loop level via generalized unitarity, which builds loop integrands directly from tree-level amplitudes [11–15]. This foundational logic has been successfully extended to massive scattering amplitudes. Arkani-Hamed, Huang, and Huang (AHH) [16] introduced $SU(2)$ little-group covariant states within a spinor-helicity formalism for massive particles, enabling a systematic enumeration of three-point amplitudes through little-group. The AHH formalism has since been applied to a wide range of areas, including electroweak theory [17–24], effective field theories [25–44], and gravitational wave physics [45–50]. Bootstrap techniques, such as gluing these three-point amplitudes, were then employed to construct several four-point massive amplitudes, involving in massless particles in external leg [18, 22, 36]. Subsequent work has

further demonstrated that on-shell recursive relations, most notably the BCFW recursion, can be effectively generalized to compute scattering amplitudes involving both external massless and massive particles [17, 19–21, 24, 26, 51–55].

The on-shell constructive approach encounters significant challenges in processes where all external particles are massive, particularly when at least one particle carries spin of one or higher. In such cases, standard techniques cannot be directly applied and require specific modifications. For instance, within bootstrap methods, high-energy unitarity constraints [22] often necessitate introducing additional four-point contact amplitudes alongside the standard gluing procedure. Similarly, when applying BCFW recursion to amplitudes involving massive gauge bosons, one must carefully select distinct momentum shifts for longitudinal and transverse polarizations, while also imposing Ward identities to remove spurious boundary terms [24, 55]. In previous work, we build the massless-massive correspondence for 3-point amplitude, and would extend this correspondence for general n-point amplitudes, allowing the full suite of techniques developed for massless amplitudes to be applied directly to the calculation of massive amplitudes.

In this work, we employ the Minimal Helicity-Chirality (MHC) formalism [56] to systematically construct higher-point massive amplitudes from their fundamental building blocks, the contact 3-point and 4-point massive amplitudes. The massive AHH amplitude can be decomposed into primary and descendant MHC amplitudes and the leading MHC amplitudes carry all the information of the massive AHH amplitudes. At the same time, the leading MHC amplitudes possess a definite helicity and are equivalent to massless amplitudes in the light-front gauge, thereby inheriting the calculational advantages of the massless theory. In the massless gauge theory, the on-shell calculation in the light-cone gauge needs the contact four-point amplitudes to ensure the gauge invariance. From massless-massive correspondence, the 3-point leading MHC amplitudes in the SM are the on-shell amplitudes within the light-cone gauge, and thus the AHH massive amplitudes in the SM should be viewed as the massive amplitudes in the light-cone gauge. Therefore, the contact 4-point massive amplitudes, should be naturally included in the massive higher-point construction.

Given the fact that both the contact 3-point and 4-point massive amplitudes are in the light-cone gauge, all of them should be treated as the fundamental building blocks for higher point amplitude construction ¹. Once the correct building blocks are identified, both the bootstrap techniques and on-shell recursion relations can be adapted to compute higher-point massive amplitudes, analogous to massless constructive methods. This procedure applies to both the primary MHC amplitudes, and the AHH amplitudes. Compared to the massless construction, there are several differences:

- In the massless construction, the fundamental 3-point amplitudes are gauge invariant, and thus there is no need to introduce 4-point contact massless amplitudes to ensure gauge invariance. This is the advantage of the massless construction. On the other hand, the massless construction usually involves the ϕ^4 interaction in the Higgs sector, which would induce non-vanishing boundary terms in the recursive construction.
- In the massive construction, the 3-point amplitudes are in the light-cone gauge, and thus 4-point

¹No five-point or higher contact massive amplitudes are needed for renormalizable theories like the SM.

contact massive amplitudes are introduced, but no higher contact one is needed for renormalizable SM. At the same time, the massive construction can avoid the ϕ^4 interaction due to the little group covariance. Unlike independent massless helicity amplitudes, a single MHC amplitude implicitly encodes information about all helicity states of the massive particle. Therefore selecting the MHC helicity without the ϕ^4 interaction would avoid such non-vanishing boundary term.

Let us further specify the common feature and differences between the primary MHC amplitudes, and the AHH amplitudes:

- Both the MHC and AHH amplitudes need the 4-point contact amplitudes as building blocks to obtain higher-point amplitudes in the bootstrap method. For the MHC amplitude construction, choosing one helicity to perform bootstrap is enough to determine the whole massive amplitudes. Since the full set of MHC amplitudes can be combined to form a single, little-group covariant massive amplitude, obtaining the leading MHC amplitude in principle determines all others and allows for the recovery of the complete AHH amplitude. So the leading contact 3-and 4-pt MHC amplitudes are enough to serve as the building blocks for constructive SM.
- In the recursive methods for massive amplitudes, distinct momentum shifts are typically required for different vector boson modes. The MHC framework naturally accommodates different shifts for transverse and longitudinal modes. Furthermore, since little-group covariance ensures that calculating the amplitude for one specific MHC polarization is sufficient, the full amplitude can then be reconstructed without the separate shifts for all helicity states.

To demonstrate the advantage of these bootstrap and recursive techniques within the MHC formalism, we apply them to three exemplary massive scattering processes: $ff \rightarrow Wh$, $WW \rightarrow hh$ and $WW \rightarrow ZZ$, and other processes and higher point calculation should follow the same procedure. Specifically, we calculate the $WW \rightarrow hh$ amplitudes in three different ways: the MHC bootstrap, the AHH bootstrap, and recursive relation.

Finally we have built the massless-massive matching for 3-point amplitudes through the MHC amplitude deformation. It should be extended to higher point amplitudes: first construct the n-point massless amplitudes, and then deform to the n-point leading MHC amplitudes via amplitude deformation. At the same time, this matching offers an alternative route for constructing massive amplitudes, but with some differences:

- The building blocks for gluing amplitudes are different. In the massive constructive method, the building blocks are 3-point and 4-point contact massive amplitudes in the light-cone gauge. However, in the massless-massive matching, the building blocks are 3-point contact massless amplitudes, without the gauge dependence.
- In the massive constructive method, there is no further treatments after construction. But in the massless-massive matching, constructing the higher point massless amplitudes is just the starting point, and further amplitude deformation to the MHC amplitudes in the light-cone gauge, with the pole separation, is needed.

Furthermore, the massless-massive matching is for the leading MHC amplitudes. Beyond the leading matching, sub-leading contributions can be incorporated through established Higgsing rules, which extend the on-shell Higgsing method introduced in Ref. [39]. However, this extension requires further refinement: for processes involving internal massive propagators, a new set of internal particle Higgsing rules should be formulated and applied to correctly perform the matching throughout the entire amplitude.

The paper is organized as follows. Section 2 reviews the Minimal Helicity-Chirality (MHC) formalism, introducing MHC one-particle states, two-particle currents, and three-particle amplitudes. This establishes the massless-massive correspondence at the single-particle, two-particle, and three-particle levels. In Section 3, we turn to the SM, summarizing all three-point MHC amplitudes through the identification of conserved currents and the method of amplitude deformation. Section 4 then demonstrates how three-point MHC amplitudes can be "glued" together to construct four-point amplitudes. We further derive the complete set of four-point contact amplitudes in the light-cone gauge. Building on these results, Section 5 illustrates three complementary approaches to obtaining four-point amplitudes, by direct assembly of the basic three-point and contact four-point MHC and AHH amplitudes, and via BCFW recursion. In Section 6, we detail the procedure for obtaining the massless-massive matching through amplitude deformation and pole separation, and extend the matching to sub-leading contributions using Higgsing rules for both external and internal particles. Finally, Section 7 provides a summary and outlook.

2 Minimal Helicity-Chirality Formalism

2.1 Spinor-helicity and spin-transversality

We employ the spinor-helicity formalism to construct scattering amplitudes, utilizing the isomorphism between the Lorentz group $SO(3, 1)$ and $SL(2, \mathbb{C}) \sim SU(2)_l \times SU(2)_r$. The mapping from the fundamental representation of the $SO(3, 1)$, such as the four-momentum p^μ , to the fundamental representation of the $SU(2)_l \times SU(2)_r$ is implemented via the Pauli matrices $\sigma_{\alpha\dot{\alpha}}^\mu$. For a massless particle, the matrix $p_{\alpha\dot{\alpha}}$ is of rank one and can be factorized as the direct product of two Weyl spinors:

$$p_{\alpha\dot{\alpha}} = p_\mu \sigma_{\alpha\dot{\alpha}}^\mu \equiv \lambda_\alpha \tilde{\lambda}_{\dot{\alpha}}, \quad (2.1)$$

where λ_α transforms under $SU(2)_l$, and $\tilde{\lambda}_{\dot{\alpha}}$ under $SU(2)_r$. For a massive particle, the momentum matrix $\mathbf{p}_{\alpha\dot{\alpha}}$ is of rank two. This necessitates introducing an additional $SU(2)$ index $I = 1, 2$ to form a pair of massive spinors:

$$\mathbf{p}_{\alpha\dot{\alpha}} \equiv \lambda_\alpha^I \tilde{\lambda}_{I\dot{\alpha}}, \quad (2.2)$$

where summation over the index I is implied. The index I labels the two spin states of a spin- $\frac{1}{2}$ particle.

A single-particle state is specified by its momentum and spin, forming an induced representation of the Poincaré group. By definition, a little-group transformation leaves the momentum p invariant while rotating the spinors. For a massless particle, the little group is $U(1)$ and acts as a phase rotation:

$$\lambda_\alpha \rightarrow e^{-i\phi} \lambda_\alpha, \quad \tilde{\lambda}_{\dot{\alpha}} \rightarrow e^{i\phi} \tilde{\lambda}_{\dot{\alpha}}, \quad (2.3)$$

where ϕ is the little-group parameter. Consequently, a massless state of helicity h can be represented as:

$$|p, h\rangle = \begin{cases} \lambda_{\alpha_1} \dots \lambda_{\alpha_{2h}}, & h \geq 0, \\ \tilde{\lambda}_{\dot{\alpha}_1} \dots \tilde{\lambda}_{\dot{\alpha}_{(-2h)}}, & h < 0, \end{cases} \quad (2.4)$$

establishing a one-to-one correspondence between the particle state with different helicity, and the spinor with different Lorentz representation.

For a massive particle, the little group is $SU(2)$. Its action on the massive spinors is given by an $SU(2)$ Wigner rotation W :

$$\lambda_\alpha^I \rightarrow (W^{-1})_J^I \lambda_\alpha^J, \quad \tilde{\lambda}_{\dot{\alpha},I} \rightarrow W_I^J \tilde{\lambda}_{\dot{\alpha},J}, \quad (2.5)$$

where λ_α^I and $\tilde{\lambda}_{\dot{\alpha},I}$ belong to the left- and right-handed Lorentz representations, $(\frac{1}{2}, 0)$ and $(0, \frac{1}{2})$, respectively. Analogous to the massless case, the massive spinors can be used to build Poincaré representations for a particle of spin s

$$|\mathbf{p}, s\rangle = \begin{cases} \lambda_{\alpha_1}^{(I_1} \lambda_{\alpha_2}^{I_2} \dots \lambda_{\alpha_{2s}}^{I_{2s})}, \\ \tilde{\lambda}_{\dot{\alpha}_1}^{(I_1} \lambda_{\alpha_2}^{I_2} \dots \lambda_{\alpha_{2s}}^{I_{2s})}, \\ \dots, \\ \tilde{\lambda}_{\dot{\alpha}_1}^{(I_1} \tilde{\lambda}_{\dot{\alpha}_2}^{I_2} \dots \tilde{\lambda}_{\dot{\alpha}_{2s}}^{I_{2s})}, \end{cases} \quad (2.6)$$

where the indices $(I_1 I_2 \dots I_{2s})$ are fully symmetrized. This formulation makes the $SU(2)$ little-group structure manifest, ensuring that the massive state carries the correct $(2s+1)$ spin degrees of freedom. However, in the massive case, the spinors λ^I and $\tilde{\lambda}^I$ are related by the equation of motion $\mathbf{p}_{\alpha\dot{\alpha}} \tilde{\lambda}^{\dot{\alpha}I} = \mathbf{m} \lambda_\alpha^I$. As a result, all representations in the set are equivalent under the little group. This implies that, unlike for massless particles, there is no one-to-one correspondence between a Lorentz representation, labeled by (j_1, j_2) , and a Poincaré representation, labeled by $|\mathbf{p}, s\rangle$. For example, for a massive spin- $\frac{1}{2}$ particle, one Poincaré representation would have two corresponding Lorentz representations

Poincaré: $ \mathbf{p}, s\rangle$	Lorentz: $ j_1, j_2\rangle$	massive spinor	chirality
$ \mathbf{p}, \frac{1}{2}\rangle$	$ \frac{1}{2}, 0\rangle$ $ 0, \frac{1}{2}\rangle$	λ_α^I $\tilde{\lambda}_{\dot{\alpha}}^I$	$c = -\frac{1}{2}$ $c = +\frac{1}{2}$

where $c = \pm \frac{1}{2}$ denotes the left and right chirality, determined by their Lorentz representations. We classify these chirality representations as follows,

$$c \equiv j_2 - j_1 \rightarrow \begin{cases} c < 0: & \text{chiral representation,} \\ c = 0: & \text{symmetric representation,} \\ c > 0: & \text{anti-chiral representation.} \end{cases} \quad (2.8)$$

For spin- $\frac{1}{2}$ particles, both chiral and anti-chiral representations exist.

To establish the massless-massive correspondence, it is crucial to maintain a one-to-one mapping between the Lorentz and Poincaré representations for massive particles. This can be achieved by introducing an additional $U(1)$ transformation [57, 58], and under which the massive spinors transform as

$$\lambda_\alpha^I \rightarrow e^{-\frac{i}{2}\phi} \lambda_\alpha^J, \quad \tilde{\lambda}_{\dot{\alpha}I} \rightarrow e^{\frac{i}{2}\phi} \tilde{\lambda}_{\dot{\alpha}J}. \quad (2.9)$$

Correspondingly the mass parameter would become complex and transform under this additional $U(1)$ symmetry

$$m \equiv \frac{1}{2} \lambda_{\alpha I} \lambda^{\alpha I} \rightarrow e^{-i\phi} m, \quad \tilde{m} \equiv \frac{1}{2} \tilde{\lambda}_{\dot{\alpha} I} \tilde{\lambda}^{\dot{\alpha} I} \rightarrow e^{i\phi} \tilde{m}. \quad (2.10)$$

This $U(1)$ symmetry identify the quantum number *transversality* t . In this case, the Lorentz group extends to $U(1) \times SO(3, 1)$, with the associated representation now characterized by $[t, j_1, j_2]$, where $|t| \leq s$.

Similar to the Lorentz representation, the Poincaré symmetry is also extended. The $U(1)$ generator D_- , together with m and \tilde{m} , composes the Lie algebra of a $ISO(2)$ group:

$$[D_-, m] = -m, \quad [D_-, \tilde{m}] = +\tilde{m}, \quad [m, \tilde{m}] = 0. \quad (2.11)$$

This extends the Poincaré symmetry to be $ISO(3, 1) \times ISO(2)$. Note that the $ISO(2)$ symmetry is restricted due to the on-shell condition $\mathbf{p}^2 = \mathbf{m}^2 = m\tilde{m}$. The massive little group becomes $U(2) = SU(2) \times U(1)$ because \mathbf{p} is also invariant under the $U(1)$. Correspondingly, the particle states become $|\mathbf{p}, s, t\rangle$. When $t = j_2 - j_1$, this establishes a one-to-one correspondence between the extended Poincaré and Lorentz representations $[t, j_1, j_2] \sim |\mathbf{p}, s, t\rangle$ with

Poincaré: $ \mathbf{p}, s, t\rangle$	Lorentz: $[t, j_1, j_2]$	massive spinor	chirality
$ \mathbf{p}, \frac{1}{2}, \frac{1}{2}\rangle$	$[\frac{1}{2}, \frac{1}{2}, 0]$	λ_α^I	$c = -\frac{1}{2}$
$ \mathbf{p}, \frac{1}{2}, -\frac{1}{2}\rangle$	$[-\frac{1}{2}, 0, \frac{1}{2}]$	$\tilde{\lambda}_{\dot{\alpha}}^I$	$c = +\frac{1}{2}$

where the transversality t plays the role of the chirality in the representation of a particle states. A general spin- s particle state $|\mathbf{p}, s, t\rangle$ can be presented by the massive spinors, transforming under the $[t, j_1, j_2]$ irrep of the $SO(3, 1) \times U(1)$

$$|\mathbf{p}, s, t\rangle = \begin{cases} \lambda_{\alpha_1}^{(I_1} \lambda_{\alpha_2}^{I_2} \dots \lambda_{\alpha_{2s}}^{I_{2s})}, & t = -s, \\ \tilde{\lambda}_{\dot{\alpha}_1}^{(I_1} \lambda_{\alpha_2}^{I_2} \dots \lambda_{\alpha_{2s}}^{I_{2s})}, & t = -(s-1), \\ \dots, \\ \tilde{\lambda}_{\dot{\alpha}_1}^{(I_1} \tilde{\lambda}_{\dot{\alpha}_2}^{I_2} \dots \tilde{\lambda}_{\dot{\alpha}_{2s}}^{I_{2s})}, & t = s. \end{cases} \quad (2.13)$$

The $ISO(2)$ symmetry suggests the particle states $|\mathbf{p}, s, t\rangle$ have both the primary and descendant representations. For a spin- $\frac{1}{2}$ particle, the primary representations are the massive spinors λ_α^I and $\tilde{\lambda}_{\dot{\alpha}}^I$, belonging to different chirality. The descendant representations are expressed as

Poincaré: $ \mathbf{p}, s, t\rangle$	Lorentz: $[t, j_1, j_2]$	massive spinor	chirality
$ \mathbf{p}, \frac{1}{2}, -\frac{1}{2}\rangle$	$[-\frac{1}{2}, \frac{1}{2}, 0]$	$\tilde{m} \lambda_\alpha^I$	$c = -\frac{1}{2}$
$ \mathbf{p}, \frac{1}{2}, \frac{1}{2}\rangle$	$[\frac{1}{2}, 0, \frac{1}{2}]$	$m \tilde{\lambda}_{\dot{\alpha}}^I$	$c = +\frac{1}{2}$

where the transversality is flipped but the chirality does not change. Therefore, the particle states contains both the primary and descendant spinors

	$c = -\frac{1}{2}$	$c = +\frac{1}{2}$
primary	$\lambda_{\alpha}^I(t = -\frac{1}{2})$	$\tilde{\lambda}_{\dot{\alpha}}^I(t = \frac{1}{2})$
descendant	$\tilde{m}\lambda_{\alpha}^I(t = +\frac{1}{2})$	$m\tilde{\lambda}_{\dot{\alpha}}^I(t = -\frac{1}{2})$

(2.15)

which belongs to different transversality and chirality. Given $t \leq s$, there is no 2nd descendant representation for the spin-half particle. For spin-one particle, the particle states are

$\Delta \backslash c$	-1	0	1
primary	$\lambda_{\alpha}^{(I}\lambda_{\beta}^{J)}(t = -1)$	$\lambda_{\alpha}^{(I}\tilde{\lambda}_{\beta}^{J)}(t = 0)$	$\tilde{\lambda}_{\dot{\alpha}}^{(I}\tilde{\lambda}_{\dot{\beta}}^{J)}(t = 1)$
1st descendant	$\tilde{m}\lambda_{\alpha}^{(I}\lambda_{\beta}^{J)}(t = 0)$	$m\lambda_{\alpha}^{(I}\tilde{\lambda}_{\beta}^{J)}(-1), \tilde{m}\lambda_{\alpha}^{(I}\tilde{\lambda}_{\beta}^{J)}(+1)$	$m\tilde{\lambda}_{\dot{\alpha}}^{(I}\tilde{\lambda}_{\dot{\beta}}^{J)}(t = 0)$
2nd descendant	$\tilde{m}^2\lambda_{\alpha}^{(I}\lambda_{\beta}^{J)}(t = 1)$	$m^2\lambda_{\alpha}^{(I}\tilde{\lambda}_{\beta}^{J)}$	$m^2\tilde{\lambda}_{\dot{\alpha}}^{(I}\tilde{\lambda}_{\dot{\beta}}^{J)}(t = -1)$

(2.16)

The one colored in gray, $m^2\lambda_{\alpha}^{(I}\tilde{\lambda}_{\beta}^{J)}$, is considered equivalent to $\lambda_{\alpha}^{(I}\tilde{\lambda}_{\beta}^{J)}$, because we mode out the mass shell m^2 for massive representations. For spin-one particle, since $t \leq s$, there is no 3rd descendant representation.

For the primary representations in a particle states, they can be related by introducing new generators $T_{\alpha\dot{\alpha}}^+ \equiv \tilde{\lambda}_{\dot{\alpha}}^I \frac{\partial}{\partial \lambda^{\alpha I}}$ and $T_{\alpha\dot{\alpha}}^- \equiv \lambda_{\alpha}^I \frac{\partial}{\partial \tilde{\lambda}_{\dot{\alpha}}^I}$:

$$T^+ \circ [t, j_1, j_2] = [t + 1, j_1, j_2], \quad T^- \circ [t, j_1, j_2] = [t - 1, j_1, j_2].$$

Similarly for each descendant representation. Note that these generators play different roles than the equation of motion (EOM), in which the transversality remains unchanged but the chirality is flipped

$$\begin{aligned} t = +\frac{1}{2} : \quad & \mathbf{p}_{\alpha\dot{\alpha}} \tilde{\lambda}^{\dot{\alpha}I} = \tilde{m}\lambda_{\alpha}^I, \quad [\frac{1}{2}, 0, \frac{1}{2}] \rightarrow [\frac{1}{2}, \frac{1}{2}, 0], \\ t = -\frac{1}{2} : \quad & \mathbf{p}_{\alpha\dot{\alpha}} \lambda^{\alpha I} = -m\tilde{\lambda}_{\dot{\alpha}}^I, \quad [-\frac{1}{2}, \frac{1}{2}, 0] \rightarrow [-\frac{1}{2}, 0, \frac{1}{2}]. \end{aligned} \quad (2.17)$$

These EOM would relate different chirality representations in the same t states. Similar to the generators T^\pm , we can treat m and \tilde{m} as new generators, which trivialize the equation of motion.

Consider an n -particle scattering process involving massless particles, with the corresponding amplitude denoted by $\mathcal{A}(1^{h_1}, \dots, n^{h_n})$, where h_i is the helicity of particle i . The amplitude must respect covariance under little-group scaling transformations, which act as

$$\mathcal{A}(1^{h_1}, \dots, n^{h_n}) \longrightarrow e^{2ih_1\phi_1} \dots e^{2ih_n\phi_n} \mathcal{A}(1^{h_1}, \dots, n^{h_n}), \quad (2.18)$$

where ϕ_i is the scaling parameter for particle i . In a general theory, the mass dimension of an amplitude is not fixed by helicity alone, since the number of momentum factors is unconstrained. However, within the renormalizable framework of the Standard Model (SM), amplitudes are required to satisfy the specific dimensional constraint

$$\dim [\mathcal{A}(1, \dots, n)] = 4 - n, \quad (2.19)$$

for both massless and massive cases. If an amplitude is expressed in its simplest kinematic form and still violates Eq. (2.19), it must be excluded on physical grounds: $\dim[\mathcal{A}] < 4 - n$ indicates a non-local interaction, while $\dim[\mathcal{A}] > 4 - n$ signals a violation of unitarity or the presence of higher-dimensional operators beyond the renormalizable SM.

Three-point massless amplitudes are fully constrained by spacetime symmetry, specifically, by their transformation properties under the $U(1)_{\text{LG}}$ little group, along with the requirement of locality. These amplitudes serve as the fundamental building blocks for recursively constructing higher-multiplicity scattering amplitudes. For massless three-particle kinematics, momentum conservation forces the holomorphic spinors to be pairwise proportional, $\lambda_1 \propto \lambda_2 \propto \lambda_3$, or, equivalently, the anti-holomorphic spinors to be pairwise proportional, $\tilde{\lambda}_1 \propto \tilde{\lambda}_2 \propto \tilde{\lambda}_3$. Consequently, a three-point amplitude can depend only on angle brackets $\langle ij \rangle$ or only on square brackets $[ij]$. Combining this observation with little-group covariance and dimensional analysis uniquely determines the functional form of the amplitude, up to an overall coupling constant:

$$\mathcal{A}(1^{h_1}, 2^{h_2}, 3^{h_3}) = \begin{cases} \langle 12 \rangle^{h_1+h_2-h_3} \langle 23 \rangle^{h_2+h_3-h_1} \langle 31 \rangle^{h_3+h_1-h_2}, & h_1 + h_2 + h_3 < 0, \\ [12]^{-h_1-h_2+h_3} [23]^{-h_2-h_3+h_1} [31]^{-h_3-h_1+h_2}, & h_1 + h_2 + h_3 > 0, \end{cases} \quad (2.20)$$

where we employ the standard spinor-helicity notation $|i\rangle_\alpha \equiv \lambda_{i\alpha}$ and $|i]^\alpha \equiv \tilde{\lambda}_i^\alpha$. The case $h_1 + h_2 + h_3 = 0$ corresponds to a constant amplitude, which is admissible only when all three particles are scalars.

Three-point massive amplitudes are similarly constrained by extended Poincaré symmetry [57, 58]. For a given set of spins (s_1, s_2, s_3) , the theory admits a set of amplitudes distinguished by their transversality quantum numbers $[t_1, t_2, t_3]$. The total transversality $t_1 + t_2 + t_3$ acts as a weight under the action of the raising and lowering operators T^\pm . This structure provides a systematic procedure for generating all primary and descendant three-point amplitudes:

- First, determine the highest-weight amplitude, which corresponds to maximal total transversality $t_1 + t_2 + t_3 = s_1 + s_2 + s_3$. This amplitude exhibits simple scaling properties analogous to those of a massless three-point amplitude. Within the SM, its kinematic structure takes the compact form

$$[12]^{s_1+s_2-s_3} [23]^{s_2+s_3-s_1} [31]^{s_3+s_1-s_2}. \quad (2.21)$$

- Next, apply successive lowering operations $T_i^- T_j^-$ (with $i \neq j$) to systematically generate amplitudes with lower total weight. This process is repeated until the lowest-weight representation, with total transversality $t_1 + t_2 + t_3 = -s_1 - s_2 - s_3$, is reached.
- The steps above yield all primary massive amplitudes. To obtain the corresponding descendant amplitudes, one then dresses each primary structure with appropriate powers of the mass spurion, thereby constructing the full tower of descendants up to order $2(s_1 + s_2 + s_3)$.

For the massive FFS amplitude, the highest-weight amplitude is $[12]$, which has total transversality $+1$. Only $T_1^- \cdot T_2^-$ gives a non-vanishing result

$$T_1^- \cdot T_2^- \circ [12] = \langle 12 \rangle, \quad (2.22)$$

producing the lowest-weight amplitude with total transversality -1 . Therefore, the FFS amplitude has two Lorentz structures $[12]$ and $\langle 12 \rangle$, related as

$$[12] \xleftrightarrow{T_1^- \cdot T_2^-} \langle 12 \rangle. \quad (2.23)$$

As a more involved example, consider the FFV amplitude. In the FFV case, the highest-weight amplitude is $[23][31]$. All three products $T_1^- \cdot T_2^-$, $T_2^- \cdot T_3^-$ and $T_3^- \cdot T_1^-$ will generate massive structures with lower weight. Its Lorentz structures are organized as follows,

$$\begin{array}{ccccc} & & [23]\langle 31 \rangle & & \\ & \nearrow T_1^- \cdot T_3^- & & \searrow T_2^- \cdot T_3^- & \\ [23][31] & & & & \langle 23 \rangle\langle 31 \rangle \\ & \searrow T_2^- \cdot T_3^- & & \nearrow T_1^- \cdot T_3^- & \\ & & \langle 23 \rangle[31] & & \end{array} \quad (2.24)$$

Note that the highest-weight amplitude is $[23][31]$ and the lowest-weight amplitude is $\langle 23 \rangle\langle 31 \rangle$. The two intermediate structures, $[23]\langle 31 \rangle$ and $\langle 23 \rangle[31]$, both have total transversality 0.

In the SM, the most complicated amplitude is VVV , whose highest-weight amplitude is $[12][23][31]$. In this case, all three products $T_1^- \cdot T_2^-$, $T_2^- \cdot T_3^-$ and $T_3^- \cdot T_1^-$ will generate massive structures with lower weight:

$$\begin{array}{ccccc} & [12][23]\langle 31 \rangle & & [12]\langle 23 \rangle\langle 31 \rangle & \\ & \nearrow T_2^- \cdot T_3^- & & \nearrow T_1^- \cdot T_2^- & \\ & [12][23][31] & & [12]\langle 23 \rangle[31] & \nearrow T_1^- \cdot T_2^- \\ & \searrow T_1^- \cdot T_3^- & & \searrow T_1^- \cdot T_3^- & \\ & \langle 12 \rangle[23]\langle 31 \rangle & & \langle 12 \rangle[23][31] & \nearrow T_2^- \cdot T_3^- \\ & \nearrow T_2^- \cdot T_3^- & & \nearrow T_1^- \cdot T_2^- & \\ & [12][23][31] & & [12]\langle 23 \rangle[31] & \nearrow T_1^- \cdot T_3^- \\ & \searrow T_1^- \cdot T_2^- & & \searrow T_1^- \cdot T_2^- & \\ & \langle 12 \rangle[23][31] & & \langle 12 \rangle\langle 23 \rangle[31] & \end{array} \quad (2.25)$$

This method allows us to systematically enumerate all independent three-point massive amplitudes for particles of spin 0, $\frac{1}{2}$, and 1:

external particles	SM structures	EFT structures
$(\mathbf{1}^{1/2}, \mathbf{2}^{1/2}, \mathbf{3}^1)$	$\langle 23 \rangle[31], [23]\langle 31 \rangle$	$[23][31], \langle 23 \rangle\langle 31 \rangle$
$(\mathbf{1}^{1/2}, \mathbf{2}^{1/2}, \mathbf{3}^0)$	$[12], \langle 12 \rangle$	
$(\mathbf{1}^1, \mathbf{2}^1, \mathbf{3}^1)$	$[12][23]\langle 31 \rangle, [12]\langle 23 \rangle[31], \langle 12 \rangle[23][31], \langle 12 \rangle[23]\langle 31 \rangle, [12]\langle 23 \rangle\langle 31 \rangle, \langle 12 \rangle\langle 23 \rangle[31]$	$[12][23][31], \langle 12 \rangle\langle 23 \rangle\langle 31 \rangle$
$(\mathbf{1}^1, \mathbf{2}^1, \mathbf{3}^0)$	$\langle 12 \rangle[12]$	$\langle 12 \rangle^2, [12]^2$
$(\mathbf{1}^0, \mathbf{2}^0, \mathbf{3}^0)$	1	

Here, we distinguish between structures that appear in the SM and those that only arise in effective field theory.

After obtaining the primary massive three-point amplitudes, we are ready to obtain the descendant massive amplitudes. We use the massive amplitudes FFV to illustrate the expansion. Take one of the primary amplitudes is $\langle 13 \rangle [32]$, we can obtain its descendant amplitudes

$$\begin{aligned}
\text{primary:} & \quad \langle 13 \rangle [32]; \\
\text{1st descendant:} & \quad \tilde{m}_1 \langle 13 \rangle [32], m_2 \langle 13 \rangle [32], m_3 \langle 13 \rangle [32], \tilde{m}_3 \langle 13 \rangle [32]; \\
\text{2nd descendant:} & \quad \tilde{m}_1 m_2 \langle 13 \rangle [32], \tilde{m}_1 m_3 \langle 13 \rangle [32], \tilde{m}_1 \tilde{m}_3 \langle 13 \rangle [32], m_2 m_3 \langle 13 \rangle [32], m_2 \tilde{m}_3 \langle 13 \rangle [32]; \\
\text{3rd descendant:} & \quad \tilde{m}_1 m_2 m_3 \langle 13 \rangle [32], \tilde{m}_1 m_2 \tilde{m}_3 \langle 13 \rangle [32]. \tag{2.27}
\end{aligned}$$

Similarly other descendant amplitudes can be obtained from other primary amplitudes in eq. (2.26).

2.2 Minimal Helicity-Chirality one-particle states

The massive momentum \mathbf{p} can always be decomposed to two massless momenta

$$\mathbf{p}_{\alpha\dot{\alpha}} = p_{\alpha\dot{\alpha}} + \eta_{\alpha\dot{\alpha}} = \lambda_{\alpha} \tilde{\lambda}_{\dot{\alpha}} + \eta_{\alpha} \tilde{\eta}_{\dot{\alpha}}, \tag{2.28}$$

and the massive spinor can be decomposed into two massless helicity spinors:

$$\begin{cases} \lambda_{\alpha}^I = -\lambda_{\alpha} \zeta^{-I} + \eta_{\alpha} \zeta^{+I}, \\ \tilde{\lambda}_{\dot{\alpha}}^I = \tilde{\lambda}_{\dot{\alpha}} \zeta^{+I} + \tilde{\eta}_{\dot{\alpha}} \zeta^{-I}, \end{cases} \tag{2.29}$$

where $\zeta^{\pm I}$ are the basis vectors of the $SU(2)$ little group space, satisfying $\varepsilon_{IJ} \zeta^{+I} \zeta^{-J} = 1$. The EOMs are then reduced to the following form,

$$p_{\alpha\dot{\alpha}} \tilde{\eta}^{\dot{\alpha}} = \tilde{m} \lambda_{\alpha}, \quad p_{\alpha\dot{\alpha}} \eta^{\alpha} = -m \tilde{\lambda}_{\dot{\alpha}}. \tag{2.30}$$

$$\eta_{\alpha\dot{\alpha}} \tilde{\lambda}^{\dot{\alpha}} = \tilde{m} \eta_{\alpha}, \quad \eta_{\alpha\dot{\alpha}} \lambda^{\alpha} = -m \tilde{\eta}_{\dot{\alpha}}. \tag{2.31}$$

The high energy decomposition induces a reduction of the extended little group $SU(2) \times ISO(2)$ to its subgroup $U(1)_w \times U(1)_z$. Here, $U(1)_w$ is associated with the generator J^3 and the helicity quantum number h while $U(1)_z$ corresponds to the generator D_- and the transversality t . The particle state is described by three quantum numbers: spin s , helicity h and transversality t , corresponding to representations in the extended Little group $SU(2) \times ISO(2)$. The single-particle state with the quantum numbers is $|s, h, t\rangle$, corresponding to the generators $[(J)^2, J^3, D_-]$. The generators of $SU(2)$ are

$$J^3 = \frac{1}{2} \left[\left(\eta_{\alpha} \frac{\partial}{\partial \eta_{\alpha}} + \tilde{\lambda}_{\dot{\alpha}} \frac{\partial}{\partial \tilde{\lambda}_{\dot{\alpha}}} \right) - \left(\lambda_{\alpha} \frac{\partial}{\partial \lambda_{\alpha}} + \tilde{\eta}_{\dot{\alpha}} \frac{\partial}{\partial \tilde{\eta}_{\dot{\alpha}}} \right) \right], \tag{2.32}$$

$$J^+ = -\eta_{\alpha} \frac{\partial}{\partial \lambda_{\alpha}} + \tilde{\lambda}_{\dot{\alpha}} \frac{\partial}{\partial \tilde{\eta}_{\dot{\alpha}}}, \tag{2.33}$$

$$J^- = -\lambda_{\alpha} \frac{\partial}{\partial \eta_{\alpha}} + \tilde{\eta}_{\dot{\alpha}} \frac{\partial}{\partial \tilde{\lambda}_{\dot{\alpha}}}, \tag{2.34}$$

and their action on a particle state yields

$$\begin{aligned} J^3|s, h, t\rangle &= h|s, h, t\rangle, \\ J^+|s, h, t\rangle &= (s(s+1) - h(h+1))|s, h+1, t\rangle, \\ J^-|s, h, t\rangle &= (s(s+1) - h(h-1))|s, h-1, t\rangle. \end{aligned} \quad (2.35)$$

Therefore, J^\pm act as ladder operators for the $SU(2)$ group.

Meanwhile, the additional little group $ISO(2)$ corresponds to the transversality t . Its generators are

$$D_- = \frac{1}{2} \left[\left(\tilde{\lambda}_{\dot{\alpha}} \frac{\partial}{\partial \tilde{\lambda}_{\dot{\alpha}}} + \tilde{\eta}_{\dot{\alpha}} \frac{\partial}{\partial \tilde{\eta}_{\dot{\alpha}}} \right) - \left(\lambda_{\alpha} \frac{\partial}{\partial \lambda_{\alpha}} + \eta_{\alpha} \frac{\partial}{\partial \eta_{\alpha}} \right) \right], \quad (2.36)$$

$$m = \lambda^{\alpha} \eta_{\alpha}, \quad (2.37)$$

$$\tilde{m} = \tilde{\lambda}^{\dot{\alpha}} \tilde{\eta}_{\dot{\alpha}}, \quad (2.38)$$

and they act as

$$\begin{aligned} D_-|s, h, t\rangle &= t|s, h, t\rangle, \\ m|s, h, t\rangle &= \mathbf{m}|s, h, t-1\rangle, \\ \tilde{m}|s, h, t\rangle &= \mathbf{m}|s, h, t+1\rangle. \end{aligned} \quad (2.39)$$

Here, \mathbf{m} is introduced on the right-hand side to ensure that the states $|s, h, t \pm 1\rangle$ have the same mass dimension as $|s, h, t\rangle$. Therefore, m and \tilde{m} serve as ladder operators for the $ISO(2)$ group. With the ladder operators J^\pm, m, \tilde{m} , the subgroup can be recovered with $U(1)_w \times U(1)_z \rightarrow SU(2) \times ISO(2)$.

This construction establishes the *helicity-chirality formalism*, which enables simultaneous tracking of both helicity and chirality information in the high-energy expansion of a massive particles. In this work, we focus on the massive representations that correspond directly to massless states. This would select the *minimal helicity-chirality* (MHC) representations, satisfying the *helicity-transversality unification*. In the high energy limit, $U(1)_w \times U(1)_z$ are unified into one $U(1)_w$, indicating that the massive spinors with both the transversality and the helicity quantum numbers should be unified into the massless one with only the helicity quantum number.

The energy scaling behaviors of the large-component spinors $(\lambda, \tilde{\lambda})$ and small-component spinors $(\eta, \tilde{\eta})$, gives

$$\begin{aligned} \lambda_{\alpha} &\sim \sqrt{E}, & \tilde{\lambda}_{\dot{\alpha}} &\sim \sqrt{E}, \\ \tilde{m}\eta_{\alpha} &\sim \frac{\mathbf{m}^2}{\sqrt{E}}, & m\tilde{\eta}_{\dot{\alpha}} &\sim \frac{\mathbf{m}^2}{\sqrt{E}}, \end{aligned} \quad (2.40)$$

where \mathbf{m} is the absolute value of mass spurions m and \tilde{m} . For the massive spinors, the primary and descendant representations gives the following decomposed states

$$\begin{array}{c|cc} & h = -\frac{1}{2} & h = +\frac{1}{2} \\ \hline t = -\frac{1}{2} & \lambda_{\alpha}, m\tilde{\eta}_{\dot{\alpha}} & \eta_{\alpha}, m\tilde{\lambda}_{\dot{\alpha}} \\ t = +\frac{1}{2} & \tilde{\eta}_{\dot{\alpha}}, \tilde{m}\lambda_{\alpha} & \tilde{\lambda}_{\dot{\alpha}}, \tilde{m}\eta_{\alpha} \end{array} \quad (2.41)$$

In the MHC formalism, the condition $h = t$ is imposed. Thus among all the above massless states, the MHC spinors are selected to be

	$c = -\frac{1}{2}$	$c = +\frac{1}{2}$
primary	$\lambda_\alpha (h = t = -\frac{1}{2})$	$\tilde{\lambda}_{\dot{\alpha}} (h = t = +\frac{1}{2})$
descendant	$\tilde{m}\eta_\alpha (h = t = +\frac{1}{2})$	$m\tilde{\eta}_{\dot{\alpha}} (h = t = -\frac{1}{2})$

(2.42)

They can be related by applying J^- and m , or J^+ and \tilde{m} . Therefore, the composite ladder operator is utilized

$$mJ^-, \quad \tilde{m}J^+. \quad (2.43)$$

to change the helicity h and transversality t simultaneously. These operators acting on the spinors gives the chirality flips

	$c = -\frac{1}{2}$	$c = +\frac{1}{2}$
$h = -\frac{1}{2}$	λ_α	$m\tilde{\eta}_{\dot{\alpha}}$
$h = +\frac{1}{2}$	$\tilde{m}J^+ \downarrow \uparrow mJ^-$	$\tilde{m}J^+ \downarrow \uparrow mJ^-$

(2.44)

Let us use diagram to illustrate the chirality flip. For the primary state with $c = h = +\frac{1}{2}$, acting with mJ^- yields the corresponding descendant state with $h = -\frac{1}{2}$,

$$\bullet \xleftarrow{\quad} + = \tilde{\lambda}_{\dot{\alpha}} \xrightarrow{mJ^-} \bullet \xleftarrow{\quad} - = m\tilde{\eta}_{\dot{\alpha}}. \quad (2.45)$$

Further action of mJ^- annihilates this state, consistent with the condition $|h| \leq s$. For the primary state with $c = h = -\frac{1}{2}$, we can act with $\tilde{m}J^+$ and obtain a similar descendant state ² with $h = +\frac{1}{2}$

$$\bullet \xleftarrow{\quad} - = \lambda_\alpha \xrightarrow{\tilde{m}J^+} \bullet \xleftarrow{\quad} - = \tilde{m}\eta_\alpha \quad (2.47)$$

Starting from a particle state $|s, h = t\rangle$, applying these operators ensures the state continues to satisfy $h = t$. By acting with them on external or internal particle lines, we can generate all relevant structures from a single MHC state. Similar to the fermion case, we could also obtain the MHC particle states for the vector boson

	$c = -1$	$c = 0$	$c = +1$
$h = t = -1$	$\lambda_{\alpha_1}\lambda_{\alpha_2}$	$m\lambda_{\alpha_1}\tilde{\eta}_{\dot{\alpha}}$	$m^2\tilde{\eta}_{\dot{\alpha}_1}\tilde{\eta}_{\dot{\alpha}_2}$
$h = t = 0$	$\tilde{m}\lambda_{\alpha_1}\eta_{\alpha_2}$	$\tilde{\lambda}_{\dot{\alpha}}\lambda_\alpha$ $m\tilde{m}\eta_\alpha\tilde{\eta}_{\dot{\alpha}}$	$m\tilde{\lambda}_{\dot{\alpha}_1}\tilde{\eta}_{\dot{\alpha}_2}$
$h = t = +1$	$\tilde{m}^2\eta_{\alpha_1}\eta_{\alpha_2}$	$\tilde{m}\tilde{\lambda}_{\dot{\alpha}}\eta_\alpha$	$\tilde{\lambda}_{\dot{\alpha}_1}\tilde{\lambda}_{\dot{\alpha}_2}$

(2.48)

²In Ref. [56], we have introduced a slash and a cross to denote respectively the action of spurion masses m, \tilde{m} and ladder operators J^\pm :

$$\left\{ \begin{array}{l} \bullet \xleftarrow{\quad} + = J^- \circ \tilde{\lambda}_{\dot{\alpha}} \\ \bullet \xleftarrow{\quad} - = m \circ \tilde{\lambda}_{\dot{\alpha}} \end{array} \right. \rightarrow \bullet \xleftarrow{\quad} - = mJ^- \circ \tilde{\lambda}_{\dot{\alpha}}. \quad (2.46)$$

In the present work, only the combinations mJ^- and $\tilde{m}J^+$ are used to convert MHC particle states. Therefore, we will omit the slash and simply employ the cross to represent descendant MHC states in this paper.

This can be reorganized by the primary and descendant states

	$c = -1$	$c = 0$	$c = +1$
primary	$\lambda_{\alpha_1} \lambda_{\alpha_2} (h = t = -1)$	$\tilde{\lambda}_{\dot{\alpha}} \lambda_{\alpha} (h = t = 0)$	$\tilde{\lambda}_{\dot{\alpha}_1} \tilde{\lambda}_{\dot{\alpha}_2} (h = t = +1)$
1st descendant	$\tilde{m} \lambda_{\alpha_1} \eta_{\alpha_2} (h = t = 0)$	$m \lambda_{\alpha} \tilde{\eta}_{\dot{\alpha}} (h = t = -1)$ $\tilde{m} \tilde{\lambda}_{\dot{\alpha}} \eta_{\alpha} (h = t = +1)$	$m \tilde{\lambda}_{\dot{\alpha}_1} \tilde{\eta}_{\dot{\alpha}_2} (h = t = 0)$
second descendant	$\tilde{m}^2 \eta_{\alpha_1} \eta_{\alpha_2} (h = t = +1)$	$m \tilde{m} \eta_{\alpha} \tilde{\eta}_{\dot{\alpha}} (h = t = 0)$	$m^2 \tilde{\eta}_{\dot{\alpha}_1} \tilde{\eta}_{\dot{\alpha}_2} (h = t = -1)$

(2.49)

In particular, Let us look at the vector boson with the chirality $c = 0$. If the vector boson is the massive gauge boson, it should recover the transverse gauge boson for $h = t = \pm 1$ and the Goldstone boson for $h = t = 0$, in the massless limit:

- For the massless spin-1 particle, the only zero helicity state is the derivative of massless scalar $\partial_{\mu} \phi$, which can be recognize to be the Goldstone boson. Thus the $\tilde{\lambda}_{\dot{\alpha}} \lambda_{\alpha}$ should be matched to the zero helicity massless spin-1 state

$$\partial_{\alpha, \dot{\alpha}} \phi \equiv \lambda_{\alpha} \tilde{\lambda}_{\dot{\alpha}}, \quad (2.50)$$

which denotes a massless Goldstone boson. It couples to the conserved current.

- For the massive gauge boson with $h = \pm 1$, its massless limit should recover the massless gauge boson. For positive polarization, the transverse massive gauge boson can be deformed as follows

$$\tilde{m} \eta_{\alpha} \tilde{\lambda}_{\dot{\alpha}} = \mathbf{m}^2 \frac{\eta_{\alpha} \tilde{\lambda}_{\dot{\alpha}}}{\langle \eta \lambda \rangle}. \quad (2.51)$$

On the other hand, the massless gauge boson has two helicity states, with the polarization vectors

$$A_{\alpha\dot{\alpha}}^+ : \frac{\xi_{\alpha} \tilde{\lambda}_{\dot{\alpha}}}{\langle \xi \lambda \rangle}, \quad A_{\alpha\dot{\alpha}}^- : -\frac{\lambda_{\alpha} \tilde{\xi}_{\dot{\alpha}}}{[\tilde{\lambda} \tilde{\xi}]} \quad (2.52)$$

where superscript \pm denotes the helicity of the gauge boson. The reference spinor ξ can be interpreted as fixing the light-cone gauge condition $A^{\mu} \xi_{\mu} = 0$. By taking ξ to be η , these two massless helicity states are identified as

$$A_{\alpha\dot{\alpha}}^+ : \frac{\eta_{\alpha} \tilde{\lambda}_{\dot{\alpha}}}{\langle \eta \lambda \rangle}, \quad A_{\alpha\dot{\alpha}}^- : -\frac{\lambda_{\alpha} \tilde{\eta}_{\dot{\alpha}}}{[\tilde{\lambda} \tilde{\eta}]} \quad (2.53)$$

Therefore, the transverse massive gauge boson state can be identified as the massless gauge boson in the light cone gauge.

Let us organize all the MHC states using the ladder operators. We begin with a primary MHC state composed solely of λ and $\tilde{\lambda}$, and then apply mJ^- or $\tilde{m}J^+$ to generate descendant MHC states

$$\text{primary} \xrightarrow{mJ^-, \tilde{m}J^+} \text{1st descendant} \xrightarrow{mJ^-, \tilde{m}J^+} \dots \quad (2.54)$$

After applying these operations $2s$ times, we obtain all MHC states, as shown in Fig. 1. In such representations, both h -flip and m -flip occur when we apply J^- and m , or J^+ and \tilde{m} , to the primary states. These two types of operations are interchangeable because the commutators satisfy $[m, J^\pm] = [\tilde{m}, J^\pm] = 0$. For example, applying either mJ^- or J^-m to the state $(s, h, t) = (\frac{1}{2}, +\frac{1}{2}, +\frac{1}{2})$ yields the same result. Although both operations lead to the same physical state, we adopt the convention of using the first type of operation (i.e. mJ^- or $\tilde{m}J^+$) to represent states with the chirality flips.

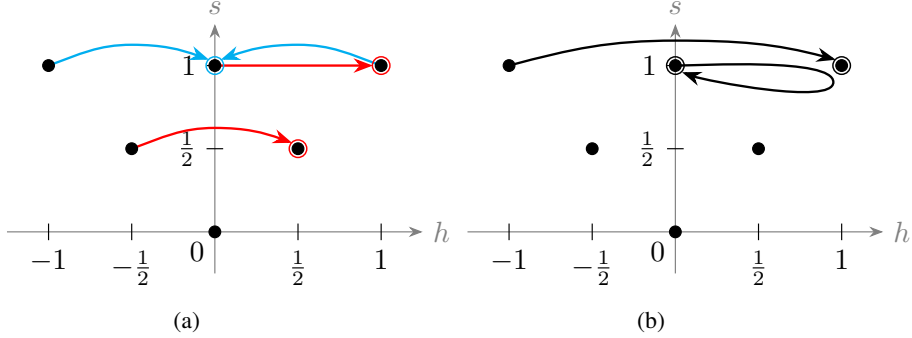


Figure 1: Illustration of the ladder operators mJ^- and $\tilde{m}J^+$ acting on the particle state. Diagram (a) shows a single application of the ladder operators for spin-0, spin-1/2, and spin-1 particles. Diagram (b) shows the result of two successive applications.

Let us organize the ladder operations of the primary and descendant particle states. To maintain the extended Little group (ELG) covariance, we will utilize the normalized ladder operators $\frac{m}{\mathbf{m}}J^\pm$, which would maintain the energy power of different states.

1. **primary \rightarrow descendant:** We begin with a primary state whose chirality equals its helicity, $c = h$. Acting with ladder operators generates descendant states with $c \neq h$. Scalar particles have no descendant states, so we first consider fermions. For the primary state with $c = h = +\frac{1}{2}$, acting with $\frac{m}{\mathbf{m}}J^-$ yields the corresponding descendant state with $h = -\frac{1}{2}$,

$$\bullet \xleftarrow{\text{---}} + = \tilde{\lambda}_{\dot{\alpha}} \quad \xrightarrow{\frac{m}{\mathbf{m}}J^-} \bullet \xleftarrow{\text{---}} \times - = \frac{m}{\mathbf{m}}\tilde{\eta}_{\dot{\alpha}}. \quad (2.55)$$

Further action of $\frac{m}{\mathbf{m}}J^-$ annihilates this state, consistent with the condition $|h| \leq s$. For the primary state with $c = h = -\frac{1}{2}$, we can act with $\frac{m}{\mathbf{m}}J^+$ and obtain a similar descendant state with $h = +\frac{1}{2}$ (and opposite color).

For vector states, we first consider the primary state with $c = h = +1$. Acting once and twice with the ladder operator gives the 1st and 2nd descendant states with $|c - h| = 1$ and 2, respectively:

$$\bullet \xleftarrow{\text{wavy}} + = \tilde{\lambda}_{\dot{\alpha}_1} \tilde{\lambda}_{\dot{\alpha}_2} \quad \xrightarrow{\frac{m}{\mathbf{m}}J^-} \bullet \xleftarrow{\text{wavy}} \times 0 = 2\frac{m}{\mathbf{m}}\tilde{\eta}_{(\dot{\alpha}_1} \tilde{\lambda}_{\dot{\alpha}_2)}, \quad (2.56)$$

$$\bullet \xleftarrow{\text{wavy}} + = \tilde{\lambda}_{\dot{\alpha}_1} \tilde{\lambda}_{\dot{\alpha}_2} \quad \xrightarrow{(\frac{m}{\mathbf{m}}J^-)^2} \bullet \xleftarrow{\text{wavy}} \times \times - = 2\frac{m^2}{\mathbf{m}^2}\tilde{\eta}_{\dot{\alpha}_1} \tilde{\eta}_{\dot{\alpha}_2}. \quad (2.57)$$

Here the factor 2 arises from Clebsch–Gordan coefficients as shown in Eq. (2.35). It should be dropped when transforming the scattering amplitude into different helicity amplitudes. The primary state with $c = h = -1$ gives analogous results with opposite helicity and color. For the primary state with $c = h = 0$, the situation is slightly different. Acting with ladder operators yields two distinct 1st descendant states with $|c - h| = 1$:

$$\begin{aligned}
 \bullet \text{---} \text{---} \text{---} 0 &= \lambda_\alpha \tilde{\lambda}_{\dot{\alpha}} \xrightarrow{\frac{\tilde{m}}{m} J^+} \bullet \text{---} \text{---} \text{---} + = \frac{\tilde{m}}{m} \eta_\alpha \tilde{\lambda}_{\dot{\alpha}}, \\
 \bullet \text{---} \text{---} \text{---} 0 &= \lambda_\alpha \tilde{\lambda}_{\dot{\alpha}} \xrightarrow{\frac{m}{\tilde{m}} J^-} \bullet \text{---} \text{---} \text{---} - = \frac{m}{\tilde{m}} \lambda_\alpha \tilde{\eta}_{\dot{\alpha}}.
 \end{aligned} \tag{2.58}$$

In this case, the 2nd descendant state has the same helicity as the primary state. Therefore, we act with both ladder operators $\frac{\tilde{m}}{m} J^+$ and $\frac{m}{\tilde{m}} J^-$ to obtain

$$\bullet \text{---} \text{---} \text{---} 0 = \lambda_\alpha \tilde{\lambda}_\alpha \xrightarrow{\frac{\tilde{m}}{m} J^+ \frac{m}{\tilde{m}} J^-} \bullet \text{---} \text{---} \text{---} 0 + \bullet \text{---} \times \text{---} \times \text{---} 0 = \lambda_\alpha \tilde{\lambda}_\alpha + \frac{m\tilde{m}}{m^2} \eta_\alpha \tilde{\eta}_\alpha. \quad (2.59)$$

The result contains both the primary and the 2nd descendant state. Acting the two ladder operators in the opposite order, $\frac{m}{m} J^- \frac{\tilde{m}}{m} J^+$, gives the same result.

2. **descendant \rightarrow primary**: Conversely, we can apply ladder operators on descendant states to recover primary states. For a 1st descendant state, one action suffices:

$$\begin{aligned}
 \bullet \xrightarrow{\text{blue}} \times \quad - &= \frac{m}{\mathbf{m}} \tilde{\eta}_{\dot{\alpha}} \quad \xrightarrow{\frac{\tilde{m}}{\mathbf{m}} J^+} \bullet \xleftarrow{\text{blue}} \quad + = \tilde{\lambda}_{\dot{\alpha}}, \\
 \bullet \xrightarrow{\text{blue}} \times \quad 0 &= \frac{m}{\mathbf{m}} \tilde{\eta}_{(\dot{\alpha}_1} \tilde{\lambda}_{\dot{\alpha}_2)} \quad \xrightarrow{\frac{\tilde{m}}{\mathbf{m}} J^+} \bullet \xrightarrow{\text{blue}} \quad + = \tilde{\lambda}_{\dot{\alpha}_1} \tilde{\lambda}_{\dot{\alpha}_2}, \\
 \bullet \xrightarrow{\text{orange}} \times \quad + &= \frac{\tilde{m}}{\mathbf{m}} \eta_{\alpha} \tilde{\lambda}_{\dot{\alpha}} \quad \xrightarrow{\frac{m}{\mathbf{m}} J^-} \bullet \xrightarrow{\text{orange}} \quad 0 = \lambda_{\alpha} \tilde{\lambda}_{\dot{\alpha}}, \\
 \bullet \xrightarrow{\text{orange}} \times \quad - &= \frac{m}{\mathbf{m}} \lambda_{\alpha} \tilde{\eta}_{\dot{\alpha}} \quad \xrightarrow{\frac{\tilde{m}}{\mathbf{m}} J^+} \bullet \xrightarrow{\text{orange}} \quad 0 = \lambda_{\alpha} \tilde{\lambda}_{\dot{\alpha}}.
 \end{aligned} \tag{2.60}$$

For a 2nd descendant state, two actions are required,

For states with $c = 0$, the descendant and primary appear together.

3. **descendant** → **descendant**: A fermion of given chirality c has only one kind of descendant state, so conversion between descendant states is not needed. For vector states, let $h^{1\text{st}}$ and $h^{2\text{nd}}$ denote the helicity of the 1st and 2nd descendant states. When $h^{1\text{st}} > h^{2\text{nd}}$, we can act with $\frac{m}{m} J^-$

on the 1st descendant state to obtain the 2nd one:

$$\begin{aligned}
 \bullet \text{---} \text{---} \text{---} \text{---} + &= \frac{\tilde{m}}{m} \eta_\alpha \tilde{\lambda}_{\dot{\alpha}} \xrightarrow{\frac{\tilde{m}}{m} J^-} \begin{cases} \bullet \text{---} \text{---} \text{---} \text{---} 0 = \lambda_\alpha \tilde{\lambda}_{\dot{\alpha}}, \\ \bullet \text{---} \text{---} \text{---} \text{---} 0 = \frac{m\tilde{m}}{m^2} \eta_\alpha \tilde{\eta}_{\dot{\alpha}}, \end{cases} \\
 \bullet \text{---} \text{---} \text{---} \text{---} 0 &= \frac{m}{m} \tilde{\eta}_{(\dot{\alpha}_1} \tilde{\lambda}_{\dot{\alpha}_2)} \xrightarrow{\frac{\tilde{m}}{m} J^+} \bullet \text{---} \text{---} \text{---} \text{---} - = \frac{m^2}{m^2} \tilde{\eta}_{\dot{\alpha}_1} \tilde{\eta}_{\dot{\alpha}_2}.
 \end{aligned} \tag{2.62}$$

In the first line, the primary and 2nd descendant states for $c = 0$ still appear together. Conversely, acting with $\frac{\tilde{m}}{m} J^+$ on the 2nd descendant state yields the 1st one:

$$\begin{aligned}
 \bullet \text{---} \text{---} \text{---} \text{---} 0 &= \frac{m\tilde{m}}{m^2} \eta_\alpha \tilde{\eta}_{\dot{\alpha}} \xrightarrow{\frac{\tilde{m}}{m} J^+} \bullet \text{---} \text{---} \text{---} \text{---} + = \frac{\tilde{m}}{m} \eta_\alpha \tilde{\lambda}_{\dot{\alpha}}, \\
 \bullet \text{---} \text{---} \text{---} \text{---} - &= \frac{m^2}{m^2} \tilde{\eta}_{\dot{\alpha}_1} \tilde{\eta}_{\dot{\alpha}_2} \xrightarrow{\frac{\tilde{m}}{m} J^+} \bullet \text{---} \text{---} \text{---} \text{---} 0 = 2 \frac{m}{m} \tilde{\eta}_{(\dot{\alpha}_1} \tilde{\lambda}_{\dot{\alpha}_2)}.
 \end{aligned} \tag{2.63}$$

For the case $h^{1\text{st}} < h^{2\text{nd}}$, analogous results follow by exchanging the roles of $\frac{\tilde{m}}{m} J^+$ and $\frac{m}{m} J^-$.

Finally, let us summarize the MHC states for particle with spin up to one. For spins $s = 0, \frac{1}{2}, 1$, the primary states are the same as the massless ones, while all the descendant states are obtained from the chirality flip, marked as cross sign. Diagrammatically, the resulting states can be listed as follow

	primary	1-st descendant	2-nd descendant
spin-0			
spin- $\frac{1}{2}$		$\xrightarrow{\tilde{m}J^+}$	
		$\xrightarrow{mJ^-}$	
spin-1		$\xrightarrow{\tilde{m}J^+}$	$\xrightarrow{\tilde{m}J^+}$
		$\xrightarrow{\tilde{m}J^+}$	$\xrightarrow{mJ^-}$
		$\xrightarrow{mJ^-}$	$\xrightarrow{mJ^-}$

(2.64)

where the color labels the chirality, and the number on the right labels the helicity. The difference between chirality and transversality is that chirality is also related to particle and anti-particle while transversality is not.

2.3 MHC 2-point currents

Having established the MHC one-particle states for particles of different spins, we now proceed to construct two-particle states. Given that a single particle transforms under the Lorentz representation $[t, j_1, j_2]$, the two-particle states are found in the representations obtained from the tensor product:

$$[t, j_1, j_2]_1 \otimes [t, j_1, j_2]_2 = \sum [t, j_1, j_2]_{12}. \tag{2.65}$$

In this work, we focus specifically on the $(\frac{1}{2}, \frac{1}{2})$ Lorentz representation, in which the two-particle structure—the current—plays a central role in analyzing amplitude deformations. We define the MHC two-point current as ³

$$\mathbf{J}^{\dot{\alpha}\alpha}(1,2). \quad (2.66)$$

This object is a two-particle structure transforming in the $(\frac{1}{2}, \frac{1}{2})$ representation.

Following the logic of the MHC state expansion, the full MHC current can be expanded into a series of components of increasing descendant order:

$$\mathbf{J} = [\mathbf{J}]_0 + [\mathbf{J}]_1 + [\mathbf{J}]_2 + \dots \quad (2.67)$$

These components are classified as follows:

$$\begin{aligned} \text{primary current : } & [\mathbf{J}]_0, \\ \text{1st descendant current : } & [\mathbf{J}]_1, \\ \text{2nd descendant current : } & [\mathbf{J}]_2, \\ & \vdots \end{aligned} \quad (2.68)$$

The primary current $[\mathbf{J}]_0$ contains only primary particle states, whereas the descendant currents incorporate descendant particle states.

Analogous to the construction of MHC states, descendant currents are derived by repeatedly applying the ladder operators mJ^- or $\tilde{m}J^+$ to the primary states. Applying one such operator to a specific particle flips its helicity and yields the corresponding first descendant current; successive applications generate higher descendants:

$$\begin{aligned} [\mathbf{J}]_1 &= mJ^- \circ [\mathbf{J}]_0 + \tilde{m}J^+ \circ [\mathbf{J}]_0, \\ [\mathbf{J}]_2 &= (mJ^-)^2 \circ [\mathbf{J}]_0 + (\tilde{m}J^+ mJ^-) \circ [\mathbf{J}]_0 + (\tilde{m}J^+)^2 \circ [\mathbf{J}]_0, \\ & \vdots \end{aligned} \quad (2.69)$$

We note that, depending on the spins s_1 and s_2 of the particles in the current, the MHC expansion terminates at the $2(s_1 + s_2)$ -th descendant current.

FF current We first consider the *FF* current, constructed from the tensor product of two fermion MHC states. Because the ladder operator can be applied at most twice, the MHC expansion for this current terminates at the second descendant level. We begin with the primary current $[\mathbf{J}]_0$. For clarity, we decompose it into distinct helicity components:

$$[\mathbf{J}]_0 = \sum_{h_1, h_2} \left[\mathbf{J} \left(1^{h_1}, 2^{h_2} \right) \right]_0, \quad (2.70)$$

³The massive current is generally defined as $\mathbf{J}_{\alpha\dot{\alpha}}(1, 2, \dots, N) = \langle \Omega | \mathcal{O}_{\alpha\dot{\alpha}} | \{1, 2, \dots, N\} \rangle$, which is an N -point form factor in the $(\frac{1}{2}, \frac{1}{2})$ Lorentz representation, characterized by the spin and transversality of each particle.

where h_1 and h_2 denote the helicities of particles 1 and 2. For the FF primary current, there are two helicity components: $(-1/2, +1/2)$ and $(+1/2, -1/2)$, while other helicity components do not correspond to the current $\mathbf{J}^{\dot{\alpha}\alpha}$, in the $(\frac{1}{2}, \frac{1}{2})$ representation. Explicitly, they are given by

$$(-\frac{1}{2}, +\frac{1}{2}) : \quad [\mathbf{J}(1^-, 2^+)]_0 = -c_1 |2]^\dot{\alpha} \langle 1|^\alpha, \quad (2.71)$$

$$(+\frac{1}{2}, -\frac{1}{2}) : \quad [\mathbf{J}(1^+, 2^-)]_0 = -c_2 |1]^\alpha \langle 2|^\dot{\alpha}, \quad (2.72)$$

where the superscripts \pm indicate helicity $\pm 1/2$, and c_1, c_2 are dependent coefficients.

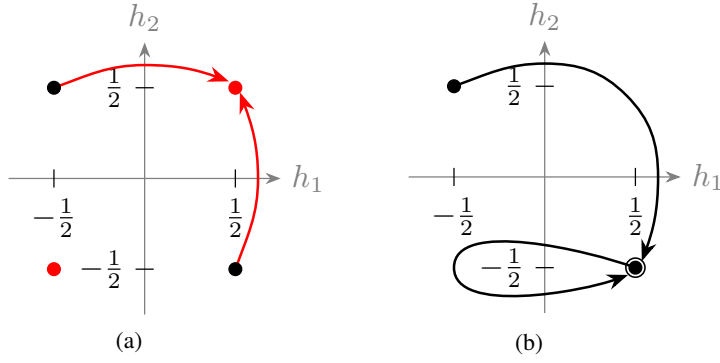


Figure 2: Illustration of the ladder operators mJ^- and $\tilde{m}J^+$ acting on the FF current, denoted by the helicity of the two particles in the current. On the left (a), the two black dots denote the two primary currents $[\mathbf{J}(1^-, 2^+)]_0$ and $[\mathbf{J}(1^+, 2^-)]_0$, while two red dots denote the two descendant currents $[\mathbf{J}(1^+, 2^+)]_1$ and $[\mathbf{J}(1^-, 2^-)]_1$. On the right (b), the second descendant current is obtained from the two primary currents.

As shown in Fig. 2a, each primary current with helicity $(\mp\frac{1}{2}, \pm\frac{1}{2})$ can be transformed via ladder operators into a first descendant current of uniform helicity, $(+\frac{1}{2}, +\frac{1}{2})$ or $(-\frac{1}{2}, -\frac{1}{2})$:

$$\begin{aligned} [\mathbf{J}(1^+, 2^+)]_1 &= \tilde{m}_2 J_2^+ \circ [\mathbf{J}(1^+, 2^-)]_0 + \tilde{m}_1 J_1^+ \circ [\mathbf{J}(1^-, 2^+)]_0, \\ [\mathbf{J}(1^-, 2^-)]_1 &= m_1 J_1^- \circ [\mathbf{J}(1^+, 2^-)]_0 + m_2 J_2^- \circ [\mathbf{J}(1^-, 2^+)]_0. \end{aligned} \quad (2.73)$$

Substituting the explicit forms from Eq. (2.71) yields the explicit first descendant currents:

$$(+\frac{1}{2}, +\frac{1}{2}) : \quad [\mathbf{J}(1^+, 2^+)]_1 = c_1 \tilde{m}_1 |2]^\dot{\alpha} \langle \eta_1|^\alpha + c_2 \tilde{m}_2 |1]^\alpha \langle \eta_2|^\dot{\alpha}, \quad (2.74)$$

$$(-\frac{1}{2}, -\frac{1}{2}) : \quad [\mathbf{J}(1^-, 2^-)]_1 = -c_1 m_2 |\eta_2]^\dot{\alpha} \langle 1|^\alpha - c_2 m_1 |\eta_1]^\alpha \langle 2|^\dot{\alpha}. \quad (2.75)$$

The coefficients c_1 and c_2 allow each term to be traced back to its specific primary current origin.

As illustrated in Fig. 2b. Applying two ladder operators converts the primary currents with helicity $(\pm\frac{1}{2}, \mp\frac{1}{2})$ into second descendant currents with the opposite helicity configuration, $(\mp\frac{1}{2}, \pm\frac{1}{2})$:

$$\begin{aligned} [\mathbf{J}(1^+, 2^-)]_2 &= m_2 J_2^- \tilde{m}_1 J_1^+ \circ [\mathbf{J}(1^-, 2^+)]_0, \\ [\mathbf{J}(1^-, 2^+)]_2 &= m_1 J_1^- \tilde{m}_2 J_2^+ \circ [\mathbf{J}(1^+, 2^-)]_0. \end{aligned} \quad (2.76)$$

In this case, each resulting component receives contributions from only one primary current. Evaluating these expressions gives the second descendant currents:

$$\left(+\frac{1}{2}, -\frac{1}{2}\right) : \quad [\mathbf{J}(1^+, 2^-)]_2 = c_1 \tilde{m}_1 m_2 |\eta_2|^{\dot{\alpha}} \langle \eta_1 |^\alpha, \quad (2.77)$$

$$\left(-\frac{1}{2}, +\frac{1}{2}\right) : \quad [\mathbf{J}(1^-, 2^+)]_2 = c_2 m_1 \tilde{m}_2 |\eta_1|^{\dot{\alpha}} \langle \eta_2 |^\alpha. \quad (2.78)$$

Thus, all MHC current components for the *FF* case have been systematically derived.

VS current We next consider the *VS* current, where particle 1 is a vector boson and particle 2 is a scalar boson. In this case, there is a single primary current, corresponding to the helicity configuration $(0, 0)$:

$$[\mathbf{J}(1^0, 2^0)]_0 = -|1|^{\dot{\alpha}} \langle 1 |^\alpha, \quad (2.79)$$

Given that the primary current contains only one helicity component, we omit an explicit coefficient here for simplicity.

Applying the ladder operators to this primary current generates two first descendant currents with helicity configurations $(\pm 1, 0)$:

$$[\mathbf{J}(1^0, 2^0)]_0 \xrightarrow{m_1 J_1^-} [\mathbf{J}(1^-, 2^0)]_1 = -m_1 |\eta_1|^{\dot{\alpha}} \langle 1 |^\alpha, \quad (2.80)$$

$$[\mathbf{J}(1^0, 2^0)]_0 \xrightarrow{\tilde{m}_1 J_1^+} [\mathbf{J}(1^+, 2^0)]_1 = \tilde{m}_1 |1|^{\dot{\alpha}} \langle \eta_1 |^\alpha. \quad (2.81)$$

Applying a second ladder flip returns the system to the $(0, 0)$ helicity configuration, producing the second descendant current:

$$[\mathbf{J}(1^0, 2^0)]_2 = m_1 \tilde{m}_1 |\eta_1|^{\dot{\alpha}} \langle \eta_1 |^\alpha. \quad (2.82)$$

Since no contributions exist beyond $[\mathbf{J}]_2$ for the *VS* current, we have now systematically derived all MHC current components in this case.

VV current Finally, we analyze the *VV* current. Its primary component consists of four independent helicity configurations: $(\pm 1, 0)$ and $(0, \pm 1)$. These are expressed as

$$[\mathbf{J}(1^+, 2^0)]_0 = -c_1 [12] |1|^{\dot{\alpha}} \langle 2 |^\alpha, \quad (2.83)$$

$$[\mathbf{J}(1^-, 2^0)]_0 = -c_2 \langle 12 | |2|^{\dot{\alpha}} \langle 1 |^\alpha, \quad (2.84)$$

$$[\mathbf{J}(1^0, 2^+)]_0 = -c_3 [12] |2|^{\dot{\alpha}} \langle 1 |^\alpha, \quad (2.85)$$

$$[\mathbf{J}(1^0, 2^-)]_0 = -c_4 \langle 12 | |1|^{\dot{\alpha}} \langle 2 |^\alpha, \quad (2.86)$$

where c_i ($i = 1, \dots, 4$) are independent the coefficients. All the primary currents are conserved currents.

Applying ladder operators to these primary configurations yields five helicity components of the first descendant current: $(\pm 1, \pm 1)$, $(\pm 1, \mp 1)$, and $(0, 0)$. As illustrated in Fig. 3a, the $(0, 0)$ component

(represented by a cyan dot) receives contributions from all four primary currents. Each of the other helicity components (marked by red dots) receives contributions from two distinct primary currents. The resulting 1st descendant currents are

$$[\mathbf{J}(1^+, 2^+)]_1 = c_1 \tilde{m}_2 [12] |1]^\alpha \langle \eta_2 |^\alpha + c_3 \tilde{m}_1 [12] |2]^\alpha \langle \eta_1 |^\alpha, \quad (2.87)$$

$$[\mathbf{J}(1^+, 2^-)]_1 = -c_1 m_2 [1\eta_2] |1]^\alpha \langle 2 |^\alpha + c_4 \tilde{m}_1 \langle \eta_1 2 | |1]^\alpha \langle 2 |^\alpha, \quad (2.88)$$

$$[\mathbf{J}(1^-, 2^+)]_1 = c_2 \tilde{m}_2 \langle 1\eta_2 | |2]^\alpha \langle 1 |^\alpha - c_3 m_1 [\eta_1 2] |2]^\alpha \langle 1 |^\alpha, \quad (2.89)$$

$$[\mathbf{J}(1^-, 2^-)]_1 = -c_2 m_2 \langle 12 | | \eta_2]^\alpha \langle 1 |^\alpha + c_4 m_1 \langle 12 | | \eta_1]^\alpha \langle 2 |^\alpha, \quad (2.90)$$

$$\begin{aligned} [\mathbf{J}(1^0, 2^0)]_1 = & -c_1 m_1 ([\eta_1 2] |1]^\alpha \langle 2 |^\alpha + [12] | \eta_1]^\alpha \langle 2 |^\alpha) \\ & + c_2 \tilde{m}_1 (\langle \eta_1 2 | |2]^\alpha \langle 1 |^\alpha + \langle 12 | |2]^\alpha \langle \eta_1 |^\alpha) \\ & - c_3 m_2 ([1\eta_2] | |2]^\alpha \langle 1 |^\alpha + [12] | \eta_2]^\alpha \langle 1 |^\alpha) \\ & + c_4 \tilde{m}_2 (\langle 1\eta_2 | |1]^\alpha \langle 2 |^\alpha + \langle 12 | |1]^\alpha \langle \eta_2 |^\alpha). \end{aligned} \quad (2.91)$$

Here all the currents with $(\pm 1, \mp 1)$, and $(0, 0)$ are conserved currents. For the helicity $(\pm 1, \pm 1)$, only one linear combinations of each helicity currents are conserved

$$\begin{aligned} [\mathbf{J}(1^-, 2^-)]_1 &= -\frac{1}{\tilde{m}_2} \langle 12 | | \eta_2]^\alpha \langle 1 |^\alpha - \frac{1}{\tilde{m}_1} \langle 12 | | \eta_1]^\alpha \langle 2 |^\alpha, \\ [\mathbf{J}(1^+, 2^+)]_1 &= \frac{1}{m_2} [12] |1]^\alpha \langle \eta_2 |^\alpha + \frac{1}{m_1} [12] |2]^\alpha \langle \eta_1 |^\alpha, \end{aligned} \quad (2.92)$$

while another combinations are not conserved.

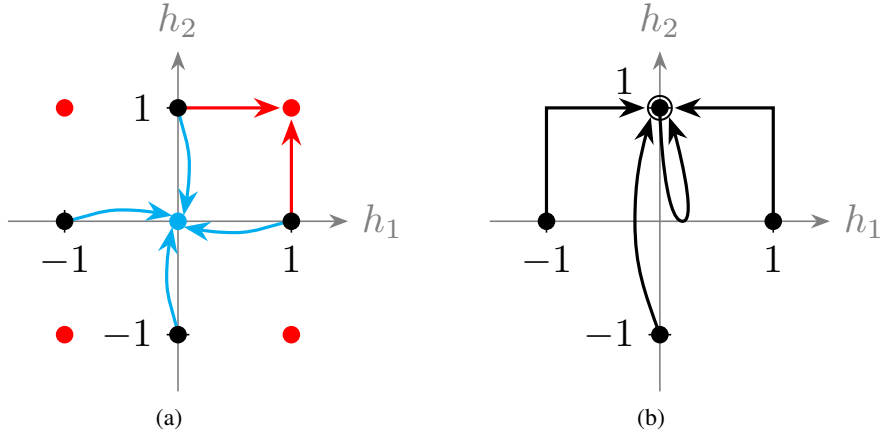


Figure 3: Illustration of the ladder operators mJ^- and $\tilde{m}J^+$ acting on the VV current. Black dots represent the primary current $[J]_0$. Diagram (a) shows the flip from $[J]_0$ to the 1st descendant current $[J]_1$, indicated by red and cyan dots. Diagram (b) shows the flip from $[J]_0$ to the 2nd descendant current $[J]_2$, which occupies the same position as one of the $[J]_0$ currents, represented by a black dot with a circle.

Applying two ladder flips generates the second descendant currents, which return to the helicity configurations $(\pm 1, 0)$ and $(0, \pm 1)$. As shown in Fig. 3b, each of these components receives contributions from all four primary currents:

$$\begin{aligned} [\mathbf{J}(1^+, 2^0)]_2 = & c_1 \tilde{m}_2 m_2 [1\eta_2] |1\rangle^{\dot{\alpha}} \langle \eta_2|^\alpha - c_2 \tilde{m}_1^2 \langle \eta_1 2\rangle |2\rangle^{\dot{\alpha}} \langle \eta_1|^\alpha \\ & + c_3 \tilde{m}_1 m_2 ([1\eta_2] |2\rangle^{\dot{\alpha}} \langle \eta_1|^\alpha + [12] |\eta_2\rangle^{\dot{\alpha}} \langle \eta_1|^\alpha) \\ & - c_4 \tilde{m}_1 \tilde{m}_2 (\langle \eta_1 \eta_2\rangle |1\rangle^{\dot{\alpha}} \langle 2|^\alpha + \langle \eta_1 2\rangle |1\rangle^{\dot{\alpha}} \langle \eta_2|^\alpha), \end{aligned} \quad (2.93)$$

$$\begin{aligned} [\mathbf{J}(1^-, 2^0)]_2 = & -c_1 m_1^2 [\eta_1 2\rangle | \eta_1] \langle 2|^\alpha + c_2 \tilde{m}_2 m_2 \langle 1\eta_2\rangle | \eta_2] \langle 1|^\alpha \\ & - c_3 m_1 m_2 ([\eta_1 \eta_2] |2\rangle^{\dot{\alpha}} \langle 1|^\alpha + [\eta_1 2\rangle | \eta_2] \langle 1|^\alpha) \\ & + c_4 m_1 \tilde{m}_2 (\langle 1\eta_2\rangle | \eta_1] \langle 2|^\alpha + \langle 1\eta_2\rangle | \eta_1] \langle 2|^\alpha), \end{aligned} \quad (2.94)$$

$$\begin{aligned} [\mathbf{J}(1^0, 2^+)]_2 = & c_1 m_1 \tilde{m}_2 ([\eta_1 2\rangle |1\rangle^{\dot{\alpha}} \langle \eta_2|^\alpha + [12] |\eta_1] \langle \eta_2|^\alpha) \\ & - c_2 m_1 m_2 (\langle \eta_1 \eta_2\rangle |2\rangle^{\dot{\alpha}} \langle 1|^\alpha + \langle 1\eta_2\rangle |2\rangle^{\dot{\alpha}} \langle \eta_1|^\alpha) \\ & + c_3 \tilde{m}_1 m_1 [\eta_1 2\rangle |2\rangle^{\dot{\alpha}} \langle \eta_1|^\alpha - c_4 \tilde{m}_2^2 \langle 1\eta_2\rangle |1\rangle^{\dot{\alpha}} \langle \eta_2|^\alpha, \end{aligned} \quad (2.95)$$

$$\begin{aligned} [\mathbf{J}(1^0, 2^-)]_2 = & -c_1 m_1 m_2 ([\eta_1 \eta_2] |1\rangle^{\dot{\alpha}} \langle 2|^\alpha + [1\eta_2] |\eta_1] \langle 2|^\alpha) \\ & + c_2 \tilde{m}_1 m_2 (\langle \eta_1 2\rangle | \eta_2] \langle 1|^\alpha + \langle 12\rangle | \eta_2] \langle \eta_1|^\alpha) \\ & - c_3 m_2^2 [1\eta_2] |\eta_2] \langle 1|^\alpha + c_4 \tilde{m}_1^2 \langle \eta_1 2\rangle | \eta_1] \langle 2|^\alpha, \end{aligned} \quad (2.96)$$

where all the 2nd descendant currents are not conserved currents.

The VV current expansion also contains higher-order contributions $[\mathbf{J}]_3$ and $[\mathbf{J}]_4$, obtained by applying the ladder operators three and four times, respectively. However, these higher-order terms do not contribute to the leading-order massless-massive matching and are therefore not discussed further in this analysis.

2.4 MHC 3-point amplitudes

Beginning with three-particle states, we focus on the MHC amplitudes, which belong to the $(0, 0)$ Lorentz representation. This can be obtained by the high-energy expansion of massive three-point amplitude $\mathbf{M}(\mathbf{1}^{s_1}, \mathbf{2}^{s_2}, \mathbf{3}^{s_3})$. In this expansion, the full amplitude, characterized by spins (s_1, s_2, s_3) , decomposes into a sum of helicity-chirality components $\mathcal{M}^{\mathcal{H}, \mathcal{T}}$ according to Eq. (2.29), and then select the terms that satisfy the chirality-helicity unification

$$\mathbf{M}(\mathbf{1}^{s_1}, \mathbf{2}^{s_2}, \mathbf{3}^{s_3}) \xrightarrow{MHC} \sum_{\mathcal{T}=\mathcal{H}} \mathcal{M}^{\mathcal{H}, \mathcal{T}} = \sum_{l=0}^{2s} [\mathcal{M}^{\mathcal{T}=\mathcal{H}}]_l \sim \sum_{l=0}^{2s} \underbrace{\mathbf{m}^{s-1+l}}_{\text{coefficient}} \times \underbrace{E^s \left(\frac{\mathbf{m}^2}{E} \right)^l}_{\text{spinor structure}}, \quad (2.97)$$

where $\mathcal{H} = (h_1, h_2, h_3)$ denotes the helicity configuration and $\mathcal{T} = (t_1, t_2, t_3)$ the corresponding transversality. Here $[\mathcal{M}^{\mathcal{T}=\mathcal{H}}]_l$ denotes the component of order l in the high-energy expansion, and $s = s_1 + s_2 + s_3$ is the total spin. The number of terms is determined by s . By analogy with the classification of particle states, we refer to these structures as primary and descendant MHC amplitudes.

These components are classified as follows:

$$\begin{aligned}
\text{primary amplitude : } & \mathcal{M}^{\text{pri}} = [\mathcal{M}]_0, \\
\text{1st descendant amplitude : } & \mathcal{M}^{\text{1st}} = [\mathcal{M}]_1, \\
\text{2nd descendant amplitudes : } & \mathcal{M}^{\text{2nd}} = [\mathcal{M}]_2, \\
& \vdots
\end{aligned} \tag{2.98}$$

The primary amplitude $[\mathcal{M}]_0$ contains only primary particle states, whereas the descendant currents incorporate descendant particle states.

To illustrate this expansion, we examine the FFV massive amplitude $\langle 13 \rangle [32]$, which can be decomposed into $2 \times 2 \times 3 = 12$ helicity categories. The FFV amplitude consists of five terms

$$\mathcal{M}(FFV) = [\mathcal{M}]_0 + [\mathcal{M}]_1 + [\mathcal{M}]_2 + [\mathcal{M}]_3 + [\mathcal{M}]_4, \tag{2.99}$$

where all the primary and descendant amplitudes are

order	amplitude			
primary $[\mathcal{M}]_0$	$(-\frac{1}{2}, +\frac{1}{2}, 0): \langle 13 \rangle [32]$			
1st des. $[\mathcal{M}]_1$	$(+\frac{1}{2}, +\frac{1}{2}, 0)$ $-\tilde{m}_1 \langle \eta_1 3 \rangle [32]$	$(-\frac{1}{2}, -\frac{1}{2}, 0)$ $m_2 \langle 13 \rangle [3 \eta_2]$	$(-\frac{1}{2}, +\frac{1}{2}, +1)$ $-m_3 \langle 1 \eta_3 \rangle [32]$	$(-\frac{1}{2}, +\frac{1}{2}, -1)$ $\tilde{m}_3 \langle 13 \rangle [\eta_3 2]$
2nd des. $[\mathcal{M}]_2$	$(-\frac{1}{2}, +\frac{1}{2}, 0)$ $-\tilde{m}_1 \langle \eta_1 3 \rangle [32]$	$(+\frac{1}{2}, -\frac{1}{2}, 0)$ $m_2 \langle 13 \rangle [3 \eta_2]$	$(\pm \frac{1}{2}, \pm \frac{1}{2}, \pm 1)$ $-m_3 \langle 1 \eta_3 \rangle [32]$	$(\pm \frac{1}{2}, \pm \frac{1}{2}, \mp 1)$ $\tilde{m}_3 \langle 13 \rangle [\eta_3 2]$
3rd des. $[\mathcal{M}]_3$	$(+\frac{1}{2}, +\frac{1}{2}, 0)$ $-\tilde{m}_1 \langle \eta_1 3 \rangle [32]$	$(-\frac{1}{2}, -\frac{1}{2}, 0)$ $m_2 \langle 13 \rangle [3 \eta_2]$	$(+\frac{1}{2}, -\frac{1}{2}, +1)$ $-m_3 \langle 1 \eta_3 \rangle [32]$	$(+\frac{1}{2}, -\frac{1}{2}, -1)$ $\tilde{m}_3 \langle 13 \rangle [\eta_3 2]$
4th des. $[\mathcal{M}]_4$	$(+\frac{1}{2}, -\frac{1}{2}, 0): \tilde{m}_1 m_2 m_3 \tilde{m}_3 \langle \eta_1 \eta_3 \rangle [\eta_3 \eta_2]$			

The amplitudes would only expand up to the 4th descendant order.

Extended Little Group Covariance Analogous to the construction of MHC states, first start with the primary amplitude, and then descendant ones are derived by repeatedly applying the ladder operators mJ^- or $\tilde{m}J^+$ to the primary one. Applying one such operator to a specific particle flips its helicity and yields the corresponding first descendant ones; successive applications generate higher descendants:

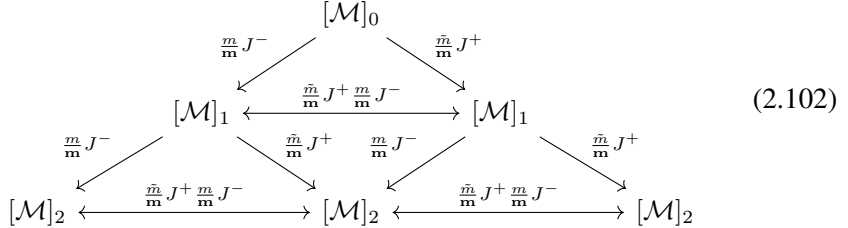
$$\begin{aligned}
[\mathcal{M}]_1 &= mJ^- \circ [\mathcal{M}]_0 + \tilde{m}J^+ \circ [\mathcal{M}]_0, \\
[\mathcal{M}]_2 &= (mJ^-)^2 \circ [\mathcal{M}]_0 + (\tilde{m}J^+ mJ^-) \circ [\mathcal{M}]_0 + (\tilde{m}J^+)^2 \circ [\mathcal{M}]_0, \\
& \vdots
\end{aligned} \tag{2.101}$$

We note that, depending on the spins s_1 and s_2 of the particles in the amplitude, the MHC expansion terminates at the $2(s_1 + s_2 + s_3)$ -th descendant amplitudes.

All the MHC amplitudes can be obtained by applying the ladder operator to the primary one. We note that all the MHC amplitudes should have the extended Little group covariance. We utilize the

$\frac{m}{m}J^-$ and $\frac{\tilde{m}}{m}J^+$ to precisely obtain the ELG covariant form. Starting from a primary amplitude with total helicity h^{pri} , this action can be illustrated as follows

$$\text{total helicity} \quad h^{\text{pri}} - 2 \quad h^{\text{pri}} - 1 \quad h^{\text{pri}} \quad h^{\text{pri}} + 1 \quad h^{\text{pri}} + 2$$



If the primary amplitude involve in the vector boson, the MHC amplitudes can also be identified to combination of the two-particle currents and vector boson states, derived in previous subsection

$$[\mathcal{M}]_{\text{Leading}} = \mathbb{J} \cdot \mathbb{A}. \quad (2.103)$$

In the following, we will start from the primary MHC amplitudes, obtained by simply unbolding the massive amplitudes, and then use the ladder operators to determine the descendant ones, each decomposed into two-particle MHC current and MHC vector boson order by order.

FFV amplitudes The first example is the *FFV* amplitudes. The the primary and descendant amplitudes can be decomposed into two-particle MHC current and MHC vector boson order by order,

order	amplitude	\mathbb{J}	\mathbb{A}
primary	$\langle 13 \rangle [23]$	$ 2\rangle^\alpha \langle 1 ^\alpha$	$ 3\rangle_\alpha [3 _\alpha$
1st descendant	$\tilde{m}_1 \langle \eta_1 13 \rangle [23]$	$\tilde{m}_1 2\rangle^\alpha \langle \eta_1 ^\alpha$	$ 3\rangle_\alpha [3 _\alpha$
	$m_2 \langle 13 \rangle [\eta_2 3]$	$m_2 \eta_2\rangle^\alpha \langle 1 ^\alpha$	
	$m_3 \langle 13 \rangle [\eta_3 2]$	$ 2\rangle^\alpha \langle 1 ^\alpha$	$m_3 \eta_3\rangle_\alpha [3 _\alpha$
	$\tilde{m}_3 \langle 1 \eta_3 \rangle [32]$		$\tilde{m}_3 3\rangle_\alpha [\eta_3 _\alpha$
2nd descendant	$\tilde{m}_1 m_3 \langle \eta_1 3 \rangle [\eta_3 2]$	$\tilde{m}_1 2\rangle^\alpha \langle \eta_1 ^\alpha$	$m_3 3\rangle_\alpha [\eta_3 _\alpha$
	$\tilde{m}_1 m_2 \langle \eta_1 3 \rangle [3 \eta_2]$	$\tilde{m}_1 m_2 \eta_2\rangle^\alpha \langle \eta_1 ^\alpha$	$ 3\rangle_\alpha [3 _\alpha$
	\vdots	\vdots	\vdots

In the following only the primary and first descendant MHC amplitudes are needed, and all other descendant amplitudes can be neglected.

For the *FFV* amplitude, the primary amplitudes are obtained by simply unbolding the *FFV* massive amplitudes. The primary amplitudes fall into two helicity categories with total helicity $h = 0$,

$$h = 0 : \quad (-\frac{1}{2}, +\frac{1}{2}, 0), \quad (+\frac{1}{2}, -\frac{1}{2}, 0). \quad (2.105)$$

The corresponding amplitude are

$$\langle 13 \rangle [32] = 1^- \xrightarrow{\text{red}} \begin{smallmatrix} 2^+ \\ \text{wavy} \\ 3^0 \end{smallmatrix}, \quad [13] \langle 32 \rangle = 1^+ \xleftarrow{\text{blue}} \begin{smallmatrix} 2^- \\ \text{wavy} \\ 3^0 \end{smallmatrix}. \quad (2.106)$$

These are vanishing structures because they contain both $\langle ij \rangle$ and $[ij]$. Due to momentum conservation $\sum p_i = 0$, we have $\lambda_1 \propto \lambda_2 \propto \lambda_3$ or $\tilde{\lambda}_1 \propto \tilde{\lambda}_2 \propto \tilde{\lambda}_3$, which implies that any MHC amplitude involving both $\langle ij \rangle$ and $[ij]$ must vanish.

These vanishing primary amplitudes correspond to the combination between a primary *FF* current $[\mathbf{J}]_0$ and a primary vector state $[\mathbf{A}]_0$.

$$\begin{aligned} \langle 13 \rangle [32] &= [\mathbf{J}(1^{-\frac{1}{2}}, 2^{+\frac{1}{2}})]_0 \cdot [\mathbf{A}(3^0)]_0, \\ [13] \langle 32 \rangle &= [\mathbf{J}(1^{+\frac{1}{2}}, 2^{-\frac{1}{2}})]_0 \cdot [\mathbf{A}(3^0)]_0, \end{aligned} \quad (2.107)$$

where the primary currents are

$$[\mathbf{J}(1^{-\frac{1}{2}}, 2^{+\frac{1}{2}})]_0 = |2\rangle^{\dot{\alpha}} \langle 1|^{\alpha}, \quad [\mathbf{J}(1^{+\frac{1}{2}}, 2^{-\frac{1}{2}})]_0 = |1\rangle^{\dot{\alpha}} \langle 2|^{\alpha}. \quad (2.108)$$

These currents correspond to the Noether current of massless fermion, $\bar{\psi} \gamma^{\mu} \psi$. They satisfy the conserved current condition

$$\partial \cdot [\mathbf{J}(1^{-\frac{1}{2}}, 2^{+\frac{1}{2}})]_0 = \langle 1|1+2|2 \rangle = 0, \quad \partial \cdot [\mathbf{J}(1^{+\frac{1}{2}}, 2^{-\frac{1}{2}})]_0 = \langle 2|1+2|1 \rangle = 0. \quad (2.109)$$

Thus the conserved current condition is closely associated with the vanishing MHC amplitudes.

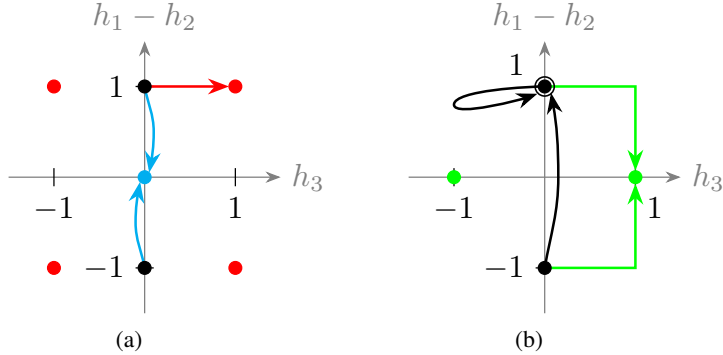


Figure 4: Illustration of the ladder operators mJ^- and $\tilde{m}J^+$ acting on the *FFV* amplitude. The black dots represent the primary amplitudes. Diagram (a) shows the flip from the primary amplitude to its 1st descendant, indicated by red and cyan dots. Diagram (b) shows the flip from primary amplitude to its 2nd, represented by a green dot and a circled black dot.

Then we can apply the ladder operator to the primary amplitude, as shown in Fig. 4a and 4b, and obtain the 1st descendant amplitudes, which have six helicity categories,

$$\begin{aligned} h = +1 : \quad & (+\frac{1}{2}, +\frac{1}{2}, 0), (+\frac{1}{2}, -\frac{1}{2}, +1), (-\frac{1}{2}, +\frac{1}{2}, +1), \\ h = -1 : \quad & (-\frac{1}{2}, -\frac{1}{2}, 0), (+\frac{1}{2}, -\frac{1}{2}, -1), (-\frac{1}{2}, +\frac{1}{2}, -1). \end{aligned} \quad (2.110)$$

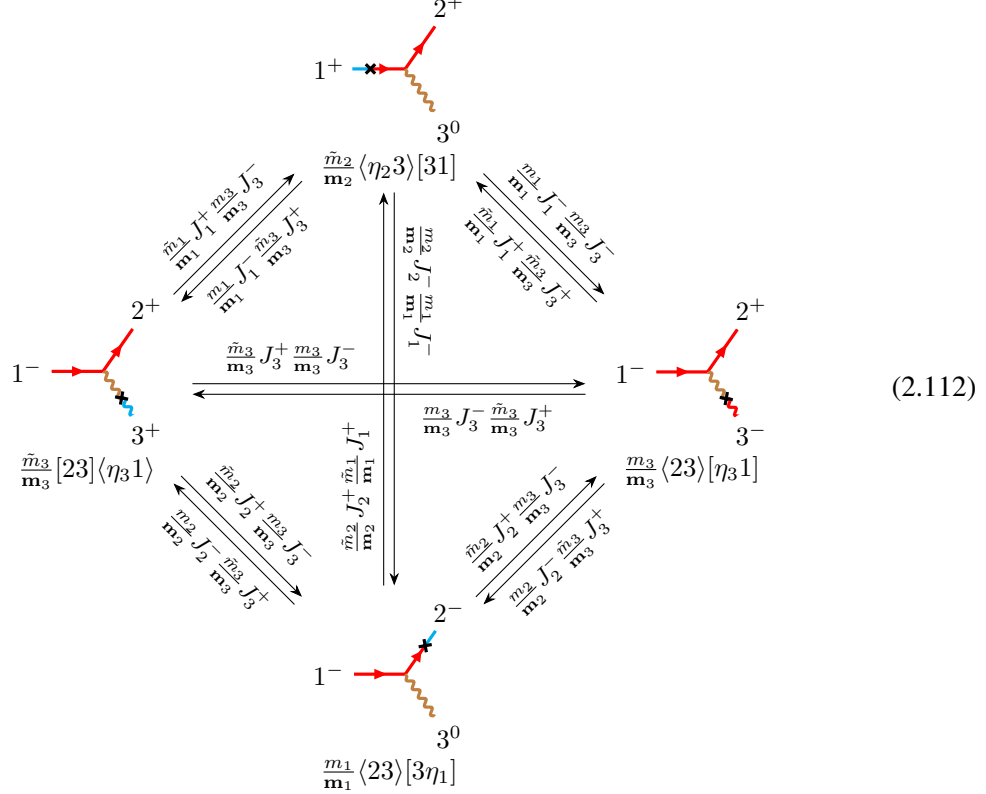
They satisfy the condition $h = \pm 1$, so the 1st descendant amplitude can provide the leading contribution. As examples, we consider two typical helicity categories: $(-\frac{1}{2}, +\frac{1}{2}, +1)$ with one transverse vector, and $(+\frac{1}{2}, +\frac{1}{2}, 0)$ with zero transverse vectors. Their corresponding amplitudes are

$$\begin{aligned} (-\frac{1}{2}, +\frac{1}{2}, +1) : \quad & \tilde{m}_3[23]\langle\eta_3 1\rangle = 1^- \text{ (diagram 1)}, \\ & \text{ (diagram 1) is a wavy line with a red arrow pointing up, ending in a cross, with labels } 2^+ \text{ and } 3^+ \text{ above it.} \\ (+\frac{1}{2}, +\frac{1}{2}, 0) : \quad & \tilde{m}_1[23]\langle 3\eta_1 \rangle = 1^+ \text{ (diagram 2)}, \quad \tilde{m}_2\langle\eta_2 3\rangle[31] = 1^+ \text{ (diagram 3)}, \\ & \text{ (diagram 2) is a wavy line with a red arrow pointing up, ending in a cross, with labels } 2^+ \text{ and } 3^0 \text{ above it.} \\ & \text{ (diagram 3) is a wavy line with a red arrow pointing up, ending in a cross, with labels } 2^+ \text{ and } 3^0 \text{ below it.} \end{aligned} \quad (2.111)$$

Others can be similarly obtained.

Note that the above leading MHC amplitudes does not have extended little group covariance. To recover the extended little group covariance, let us apply the normalized ladder operator, which would

relate the four amplitudes.



Similarly, this method can be used to obtain higher-order descendant amplitudes.

FFS & SSS Amplitudes For the *FFS* amplitude, the primary MHC amplitudes has two helicity categories

$$\begin{aligned} h = -1 : & \quad \left(-\frac{1}{2}, -\frac{1}{2}, 0\right), \\ h = +1 : & \quad \left(+\frac{1}{2}, +\frac{1}{2}, 0\right), \end{aligned} \quad (2.113)$$

They satisfy the condition $h = \pm 1$. The corresponding primary amplitude are

$$\begin{aligned} \left(-\frac{1}{2}, -\frac{1}{2}, 0\right) : \quad & \langle 12 \rangle = 1^- \text{ (blue line)} \rightarrow 2^- \text{ (red line)}, \\ & \qquad \qquad \qquad 3^0 \text{ (dashed line)}, \\ \left(+\frac{1}{2}, +\frac{1}{2}, 0\right) : \quad & [12] = 1^+ \text{ (blue line)} \rightarrow 2^+ \text{ (red line)}, \\ & \qquad \qquad \qquad 3^0 \text{ (dashed line)}. \end{aligned} \quad (2.114)$$

They do not vanish, they consist of λ or $\tilde{\lambda}$ only. Thus, the priamry *FFS* amplitude gives the leading contributions.

For the SSS amplitude, it only has one helicity category $(0,0,0)$. The primary MHC amplitude corresponds to the trivial Lorentz structure

$$(0,0,0) : \quad 1 = 1^0 \text{---} \begin{array}{c} 2^0 \\ \diagup \\ \diagdown \\ 3^0 \end{array} . \quad (2.115)$$

It gives the leading contribution obviously.

VVS amplitudes For the VVS amplitude, the primary amplitude has only one helicity category,

$$h = 0 : \quad (0,0,0). \quad (2.116)$$

The corresponding amplitude is given by

$$(0,0,0) : \quad \langle 12 \rangle [21] = 1^0 \text{---} \begin{array}{c} 2^0 \\ \diagup \\ \diagdown \\ 3^0 \end{array} \quad (2.117)$$

This amplitude vanishes due to the simultaneous presence of $\langle 12 \rangle$ and $[21]$.

Applying the ladder operator to the primary VVS amplitude yields the first descendant amplitudes, which fall into four helicity categories,

$$\begin{aligned} h = +1 : & \quad (-1,0,0), (0,-1,0), \\ h = -1 : & \quad (+1,0,0), (0,+1,0). \end{aligned} \quad (2.118)$$

Since these satisfy $h = \pm 1$, the corresponding amplitudes are leading contributions:

$$\begin{aligned} m_1 \langle 12 \rangle [2\eta_1] &= 1^- \text{---} \begin{array}{c} 2^0 \\ \diagup \\ \diagdown \\ 3^0 \end{array}, \quad -\tilde{m}_1 \langle \eta_1 2 \rangle [21] = 1^+ \text{---} \begin{array}{c} 2^0 \\ \diagup \\ \diagdown \\ 3^0 \end{array}, \\ m_2 \langle 12 \rangle [\eta_2 1] &= 1^0 \text{---} \begin{array}{c} 2^- \\ \diagup \\ \diagdown \\ 3^0 \end{array}, \quad -\tilde{m}_2 \langle 1 \eta_2 \rangle [21] = 1^0 \text{---} \begin{array}{c} 2^+ \\ \diagup \\ \diagdown \\ 3^0 \end{array}. \end{aligned} \quad (2.119)$$

For the VVS amplitude, the primary amplitude has only one helicity category,

$$h = 0 : \quad (0,0,0). \quad (2.120)$$

The corresponding amplitude is given by

$$(0,0,0) : \quad \langle 12 \rangle [21] = 1^0 \text{ (wavy line)} \quad 2^0 \text{ (dashed line)} \quad 3^0 \text{ (dashed line)} . \quad (2.121)$$

This amplitude vanishes due to the simultaneous presence of $\langle 12 \rangle$ and $[21]$. The vanishing primary amplitude can also be expressed as a coupling of the form $[\mathbf{J}]_0 \cdot [\mathbf{A}]_0$. There are two equivalent ways to perform the decomposition:

$$\langle 12 \rangle [21] = [\mathbf{J}(2^0, 3^0)]_0 \cdot [\mathbf{A}(1^0)]_0 = [\mathbf{J}(1^0, 3^0)]_0 \cdot [\mathbf{A}(2^0)]_0, \quad (2.122)$$

where the primary *VS* current $[\mathbf{J}]_0$ is defined as

$$\begin{aligned} [\mathbf{J}(2^0, 3^0)]_0 &= |2]^\alpha \langle 2|^\alpha, \\ [\mathbf{J}(1^0, 3^0)]_0 &= |1]^\alpha \langle 1|^\alpha. \end{aligned} \quad (2.123)$$

This current is conserved and can be interpreted as the Noether current for a massless scalar boson, $\phi^*(D^\mu \phi) - (D^\mu \phi) \phi$ ⁴.

Applying the ladder operator to the primary *VVS* amplitude yields the first descendant amplitudes, which fall into four helicity categories,

$$\begin{aligned} h = +1 : & \quad (-1, 0, 0), (0, -1, 0), \\ h = -1 : & \quad (+1, 0, 0), (0, +1, 0). \end{aligned} \quad (2.124)$$

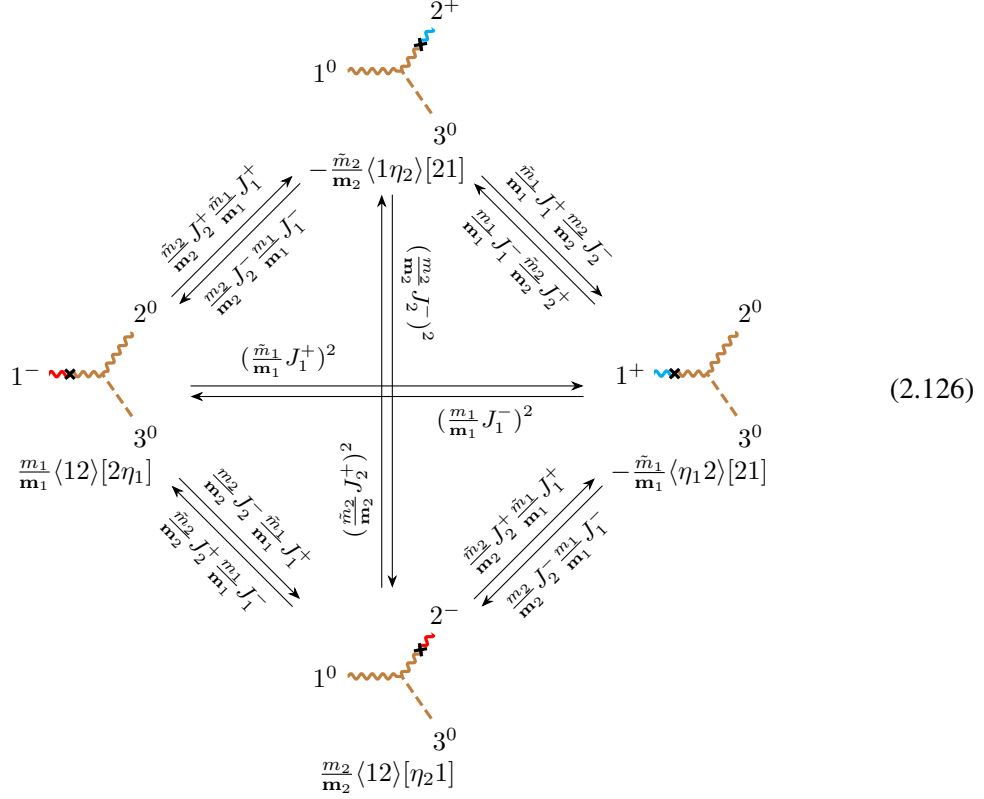
Since these satisfy $h = \pm 1$, the corresponding amplitudes are leading contributions:

$$\begin{aligned} m_1 \langle 12 \rangle [2\eta_1] &= 1^- \text{ (wavy line)} \quad 2^0 \text{ (dashed line)} \quad 3^0 \text{ (dashed line)}, \quad -\tilde{m}_1 \langle \eta_1 2 \rangle [21] = 1^+ \text{ (wavy line)} \quad 2^0 \text{ (dashed line)} \quad 3^0 \text{ (dashed line)}, \\ m_2 \langle 12 \rangle [\eta_2 1] &= 1^0 \text{ (wavy line)} \quad 2^- \text{ (dashed line)} \quad 3^0 \text{ (dashed line)}, \quad -\tilde{m}_2 \langle 1 \eta_2 \rangle [21] = 1^0 \text{ (wavy line)} \quad 2^+ \text{ (dashed line)} \quad 3^0 \text{ (dashed line)}. \end{aligned} \quad (2.125)$$

For the *VVS* case, we can also apply the ladder operators to relate the descendants of the same order, recovering the extended little group covariance. For the four 1st descendant amplitudes, we

⁴Strictly speaking, the Noether current $\phi^*(D^\mu \phi) - (D^\mu \phi^*) \phi$ corresponds to the spinor structure $\frac{1}{2}(|2]^\alpha \langle 2|^\alpha - |3]^\alpha \langle 3|^\alpha)$, which is not identical to the primary MHC current $[\mathbf{J}]_0$. However, when coupled to a vector $[\mathbf{A}]_0$, the two become equivalent: $[\mathbf{J}]_0 \cdot [\mathbf{A}]_0 = \langle 12 \rangle [21] = \frac{1}{2}(\langle 12 \rangle [21] - \langle 13 \rangle [31])$.

have



The higher-order descendant amplitudes can be obtained in a similar way.

VVV amplitudes For the VVV amplitude, given the six massive amplitudes, the primary amplitudes fall into six helicity categories⁵, classified by the total helicity h ,

$$\begin{aligned} h = -1 : & \quad (-1, 0, 0), (0, -1, 0), (0, 0, -1), \\ h = +1 : & \quad (+1, 0, 0), (0, +1, 0), (0, 0, +1). \end{aligned} \quad (2.127)$$

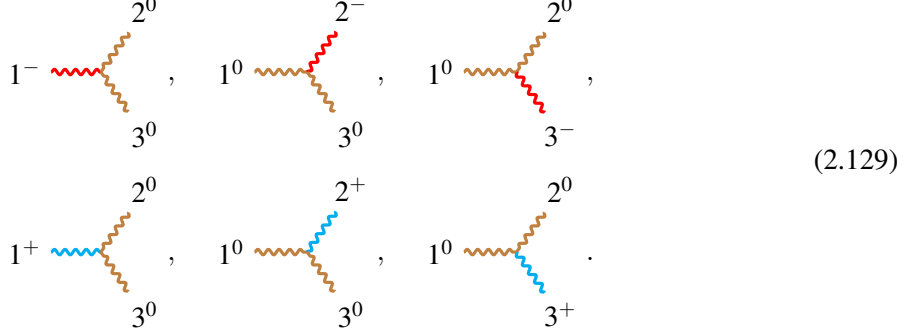
The corresponding amplitudes are

$$\begin{aligned} & \langle 12 \rangle [23] \langle 31 \rangle, \quad \langle 12 \rangle \langle 23 \rangle [31], \quad [12] \langle 23 \rangle \langle 31 \rangle, \\ & [12] \langle 23 \rangle [31], \quad [12] [23] \langle 31 \rangle, \quad \langle 12 \rangle [23] [31]. \end{aligned} \quad (2.128)$$

Although these primary amplitudes carry total helicity $h = \pm 1$, they vanish because each contains both angle and square brackets $\langle ij \rangle$ and $[ij]$. Diagrammatically, these vanishing primary amplitudes

⁵There are another two helicity categories $(-1, -1, -1)$ and $(+1, +1, +1)$ for primary amplitudes, belonging to the EFT operators.

can be represented as



Each primary VVV amplitude can be expressed in two equivalent ways as the current form $[\mathbf{J}]_0 \cdot [\mathbf{A}]_0$. For the helicity category $(-1, 0, 0)$:

$$\langle 12 \rangle [23] \langle 31 \rangle = [\mathbf{J}(1^{-1}, 3^0)]_0 \cdot [\mathbf{A}(2^0)]_0 = [\mathbf{J}(1^{-1}, 2^0)]_0 \cdot [\mathbf{A}(3^0)]_0, \quad (2.130)$$

where the primary VV current $[\mathbf{J}]_0$ is conserved current and defined as

$$\begin{aligned} [\mathbf{J}(1^{-1}, 2^0)]_0 &= -\langle 12 \rangle |2] \dot{\alpha} \langle 1|^\alpha, \\ [\mathbf{J}(1^0, 2^-)]_0 &= -\langle 12 \rangle |1] \dot{\alpha} \langle 2|^\alpha, \\ [\mathbf{J}(1^+, 2^0)]_0 &= -[12] |1] \dot{\alpha} \langle 2|^\alpha, \\ [\mathbf{J}(1^0, 2^+)]_0 &= -[12] |2] \dot{\alpha} \langle 1|^\alpha. \end{aligned} \quad (2.131)$$

For the 1st descendant MHC amplitudes, there are thirteen helicity categories,

$$\begin{aligned} h = +2 : & \quad (+1, +1, 0), \quad (0, +1, +1), \quad (+1, 0, +1), \\ h = 0 : & \quad (\pm 1, \mp 1, 0), \quad (0, \pm 1, \mp 1), \quad (\pm 1, 0, \mp 1), \quad (0, 0, 0), \\ h = -2 : & \quad (-1, -1, 0), \quad (0, -1, -1), \quad (-1, 0, -1). \end{aligned} \quad (2.132)$$

These do not satisfy the condition $h = \pm 1$, so the 1st descendant VVV amplitude do not correspond to the massless amplitude in the SM, and they should either vanish or belong to the EFT category. Among the 1st descendant currents, the helicity- $(\pm \mp)$ currents are all conserved

$$[\mathbf{J}(1^+, 2^-)]_1 = -c_1 m_2 [1 \eta_2] |1] \dot{\alpha} \langle 2|^\alpha + c_4 \tilde{m}_1 \langle \eta_1 2] |1] \dot{\alpha} \langle 2|^\alpha, \quad (2.133)$$

$$[\mathbf{J}(1^-, 2^+)]_1 = c_2 \tilde{m}_2 \langle 1 \eta_2] |2] \dot{\alpha} \langle 1|^\alpha - c_3 m_1 [\eta_1 2] |2] \dot{\alpha} \langle 1|^\alpha, \quad (2.134)$$

corresponding to the $F_{\mu\nu} A^\nu$ (and $\tilde{F}_{\mu\nu} A^\nu$) Noether current. While the helicity- $(\pm \pm)$ currents, in contrast,

$$[\mathbf{J}(1^+, 2^+)]_1 = c_1 \tilde{m}_2 [12] |1] \dot{\alpha} \langle \eta_2|^\alpha + c_3 \tilde{m}_1 [12] |2] \dot{\alpha} \langle \eta_1|^\alpha, \quad (2.135)$$

$$[\mathbf{J}(1^-, 2^-)]_1 = -c_2 m_2 \langle 12] | \eta_2] \dot{\alpha} \langle 1|^\alpha + -c_4 m_1 \langle 12] | \eta_1] \dot{\alpha} \langle 2|^\alpha, \quad (2.136)$$

lead to either the $F_{\mu\nu} A^\nu$ Noether current or non-conserved ones.

We classify them into three cases, in which only in the first case some combination of amplitudes are non-vanishing EFT ones, and all other are vanishing:

- First consider the helicity categories with $h = \pm 2$, which have two transverse vectors of the same helicity. In this case, certain combinations of amplitudes vanish, but another non-vanishing combination belongs to the EFT amplitudes. For example, the helicity $(-1, -1, 0)$ includes two terms,

$$(-1, -1, 0) : m_2 \langle 12 \rangle [\eta_2 3] \langle 31 \rangle = 1^- \text{ (red wavy line)} \text{ (orange wavy line)} \text{ (blue cross)} \text{ (orange wavy line)} \text{ (red wavy line)} , m_1 \langle 12 \rangle \langle 23 \rangle [3\eta_1] = 1^- \text{ (red wavy line)} \text{ (orange wavy line)} \text{ (blue cross)} \text{ (orange wavy line)} \text{ (red wavy line)} . \quad (2.137)$$

Each of the two terms can be identified as $[\mathbf{J}]_1 \cdot [\mathbf{A}]_0$, while together they can be identified as $[\mathbf{J}]_0 \cdot [\mathbf{A}]_1$:

$$[\mathbf{J}(1^{-1}, 2^{-1})]_1 \cdot [\mathbf{A}(3^0)]_0 = c_1 m_2 \langle 12 \rangle [\eta_2 3] \langle 31 \rangle + c_2 m_1 \langle 12 \rangle \langle 23 \rangle [3\eta_1] , \quad (2.138)$$

where c_i are coefficients. Although the two terms are individually non-zero, their sum can vanish

$$\frac{1}{\mathbf{m}_2^2} m_2 \langle 12 \rangle [\eta_2 3] \langle 31 \rangle + \frac{1}{\mathbf{m}_1^2} m_1 \langle 12 \rangle \langle 23 \rangle [3\eta_1] = 0. \quad (2.139)$$

Hence, the 1st descendant current $[\mathbf{J}(1^{-1}, 2^{-1})]_1$ is conserved only if takes the form

$$[\mathbf{J}(1^{-1}, 2^{-1})]_1 = -\frac{1}{\mathbf{m}_2^2} m_2 \langle 12 \rangle [\eta_2]^\alpha \langle 1 |^\alpha - \frac{1}{\mathbf{m}_1^2} m_1 \langle 12 \rangle [\eta_1]^\alpha \langle 2 |^\alpha . \quad (2.140)$$

For the other helicity category with $h = \pm 2$, each category corresponds to one such conserved current.

- For helicity categories with $h = 0$, there are two cases, and in both cases, the amplitudes vanish. We consider the helicity categories with two transverse vector of opposite helicity. For example, the helicity $(-1, +1, 0)$ includes two terms,

$$(-1, +1, 0) : \tilde{m}_2 \langle 1\eta_2 \rangle [23] \langle 31 \rangle = 1^- \text{ (red wavy line)} \text{ (orange wavy line)} \text{ (blue cross)} \text{ (orange wavy line)} \text{ (red wavy line)} , m_1 [\eta_1 2] [23] \langle 31 \rangle = 1^- \text{ (red wavy line)} \text{ (orange wavy line)} \text{ (blue cross)} \text{ (orange wavy line)} \text{ (red wavy line)} , \quad (2.141)$$

which are derived by acting ladder operators on the primary amplitudes with helicities $(-1, +1, 0)$ and $(+1, -1, 0)$. We identify these two terms as the coupling $[\mathbf{J}]_1 \cdot [\mathbf{A}]_0$:

$$[\mathbf{J}(1^{+1}, 2^{-1})]_1 \cdot [\mathbf{A}(3^0)]_0 = c_1 \tilde{m}_2 \langle 1\eta_2 \rangle [23] \langle 31 \rangle + c_2 m_1 [\eta_1 2] [23] \langle 31 \rangle , \quad (2.142)$$

Both terms contain $[23]$ and $\langle 31 \rangle$, and thus vanish individually.

$$\tilde{m}_2 \langle 1\eta_2 \rangle [23] \langle 31 \rangle = m_1 [\eta_1 2] [23] \langle 31 \rangle = 0. \quad (2.143)$$

Therefore, the current $[\mathbf{J}(1^{+1}, 2^{-1})]_1$ is conserved, with no constraints on the coefficients c_1 and c_2 . The same holds for currents in other helicity categories with $h = \pm 2$.

- Finally we consider the helicity $(0, 0, 0)$. It has six terms,

$$\begin{aligned}
(0,0,0) : \tilde{m}_1(\langle \eta_1 2 \rangle [23] \langle 31 \rangle + \langle 12 \rangle [23] \langle 3 \eta_1 \rangle) &= 1^0 \text{ (diagram 1)} , \\
\tilde{m}_2(\langle 1 \eta_2 \rangle \langle 23 \rangle [31] + \langle 12 \rangle \langle \eta_2 3 \rangle [31]) &= 1^0 \text{ (diagram 2)} , \\
\tilde{m}_3([\eta_2 1] \langle 23 \rangle \langle 31 \rangle + [12] \langle 23 \rangle \langle \eta_3 1 \rangle) &= 1^0 \text{ (diagram 3)} , \\
m_1([\eta_1 2] \langle 23 \rangle \langle 31 \rangle + [12] \langle 23 \rangle \langle 3 \eta_1 \rangle) &= 1^0 \text{ (diagram 4)} , \\
m_2([1 \eta_2] [23] \langle 31 \rangle + [12] [\eta_2 3] \langle 31 \rangle) &= 1^0 \text{ (diagram 5)} , \\
m_3(\langle 12 \rangle [2 \eta_3] [31] + \langle 12 \rangle [23] [\eta_3 1]) &= 1^0 \text{ (diagram 6)} .
\end{aligned} \tag{2.144}$$

If we identify particle 3 as the vector $[\mathbf{A}]_0$, there are four terms can compose coupling $[\mathbf{J}]_1 \cdot [\mathbf{A}]_0$,

$$\begin{aligned}
[\mathbf{J}(1^0, 2^0)]_1 \cdot [\mathbf{A}(3^0)]_0 = & c_1 \tilde{m}_1 (\langle \eta_1 2 \rangle [23] \langle 31 \rangle + \langle 12 \rangle [23] \langle 3 \eta_1 \rangle) \\
& + c_2 \tilde{m}_2 (\langle 1 \eta_2 \rangle \langle 23 \rangle [31] + \langle 12 \rangle \langle \eta_2 3 \rangle [31]) \\
& + c_3 m_1 ([\eta_1 2] \langle 23 \rangle [31] + [12] \langle 23 \rangle [3 \eta_1]) \\
& + c_4 m_2 ([1 \eta_2] [23] \langle 31 \rangle + [12] [\eta_2 3] \langle 31 \rangle),
\end{aligned} \tag{2.145}$$

These terms contain $[ij]$ and $\langle ij \rangle$ simultaneously, and thus vanish individually. Therefore, the current $[J(1^0, 2^0)]_1$ is also conserved, with no constraints on the four coefficients.

For 2nd descendant MHC amplitudes, it has twelve helicity categories,

$$\begin{aligned}
h = +1 : \quad & (-1, +1, +1), \quad (+1, -1, +1), \quad (+1, +1, -1), \\
& (0, 0, +1), \quad (0, +1, 0), \quad (+1, 0, 0), \\
h = -1 : \quad & (-1, -1, +1), \quad (+1, -1, -1), \quad (-1, +1, -1), \\
& (0, 0, -1), \quad (0, -1, 0), \quad (-1, 0, 0),
\end{aligned} \tag{2.146}$$

They satisfy the condition $h = \pm 1$, and one can verify that the MHC amplitudes do not vanish. Therefore, the leading VVV contribution arises from 2nd descendant MHC amplitudes. Due to the large number of such amplitudes, we restrict our consideration to two typical helicity categories $(+1, +1, -1)$ and $(-1, 0, 0)$, which has three and one transverse vector bosons. The other helicity categories can be obtained in a similar way, whose diagram can be derived by change color and location of mass insertion. The two typical helicity categories have

- For the $(+1, +1, -1)$ helicity category, the only amplitudes are the $[\mathbf{J}]_1 \cdot [\mathbf{A}]_1$ case, since the currents belong to $(\pm 1, \pm 1)$ or $(\pm 1, \mp 1)$. The amplitudes are constructed by $[\mathbf{J}(1^+, 2^+)]_1 \cdot [\mathbf{A}(3^-)]_1$ or $[\mathbf{J}(1^+, 2^-)]_1 \cdot [\mathbf{A}(3^+)]_1$. Note that $[\mathbf{J}(1^+, 2^-)]_1$ are all conserved current, while $[\mathbf{J}(1^+, 2^+)]_1$ are partially conserved. The non-conserved combination would give rise to the descendant EFT amplitudes. While all other amplitudes with the conserved currents give rise to the leading SM amplitudes. First the three conserved currents give

Then the conserved current combination gives

$$[\mathbf{J}(1^-, 2^-)]_1 \cdot [\mathbf{A}(3^+)]_1 = \frac{\tilde{m}_3}{\tilde{m}_2} \langle 12 \rangle [3\eta_2] \langle 1\eta_3 \rangle + \frac{\tilde{m}_3}{\tilde{m}_1} \langle 12 \rangle [3\eta_1] \langle 2\eta_3 \rangle$$



$$= 1^- \text{ (red wavy line)} + 1^- \text{ (red wavy line)} . \quad (2.148)$$

- For the $(-1, 0, 0)$ helicity category, there are three kinds of current structures: $[\mathbf{J}(1^-, 2^0)]_2 \cdot [\mathbf{A}(3^0)]_0$, $[\mathbf{J}(1^-, 2^0)]_0 \cdot [\mathbf{A}(3^0)]_2$, $[\mathbf{J}(2^0, 3^0)]_1 \cdot [\mathbf{A}(1^-)]_1$. For the $[\mathbf{J}]_1 \cdot [\mathbf{A}]_1$ case, $[\mathbf{J}(2^0, 3^0)]_1$ is the conserved current, which gives

$$[\mathbf{J}(2^0,3^0)]_1 \cdot [\mathbf{A}(1^-)]_1 = -c_{31}m_1\tilde{m}_3(\langle\eta_32\rangle[\eta_12]\langle31\rangle + \langle32\rangle[\eta_12]\langle\eta_31\rangle)$$

$$\begin{aligned}
& -c_{32}m_1\tilde{m}_2(\langle 3\eta_2\rangle[\eta_13]\langle 21\rangle + \langle 32\rangle[\eta_13]\langle\eta_21\rangle) \\
& +c_{33}m_1m_3([\eta_32][\eta_13]\langle 21\rangle + [32][\eta_1\eta_3]\langle 21\rangle) \\
& +c_{34}m_1m_2([3\eta_2][\eta_12]\langle 31\rangle + [32][\eta_1\eta_2]\langle 31\rangle). \quad (2.149)
\end{aligned}$$

Note that the MHC amplitudes contains both the leading SM amplitudes and 1st descendant EFT amplitudes. For the $[J(1^-, 2^0)]_2 \cdot [A(3^0)]_0$, there is no conserved current. Thus the amplitudes should belong to either the leading SM one or 1st descendant EFT amplitudes.

$$\begin{aligned}
& [\mathbf{J}(1^-, 2^0)]_2 \cdot [\mathbf{A}(3^0)]_0 + [\mathbf{J}(1^-, 3^0)]_2 \cdot [\mathbf{A}(2^0)]_0 \\
&= -c_1 \langle 1|\eta_2 \rangle [\eta_2 3] \langle 3|1 \rangle - c_2 m_1 \tilde{m}_2 (\langle 1|\eta_2 \rangle \langle 23| [3|\eta_1] + \langle 12\rangle \langle \eta_2 3| [3|\eta_1]) \\
&+ c_3 m_1^2 [\eta_1 2] \langle 23| [3|\eta_1] + c_4 m_1 m_2 ([\eta_1|\eta_2] [23] \langle 3|1 \rangle + [\eta_1 2] [\eta_2 3] \langle 3|1 \rangle) \\
&- c_5 \langle 1|\eta_3 \rangle [\eta_3 2] \langle 2|1 \rangle - c_6 m_1 \tilde{m}_3 (\langle 1|\eta_3 \rangle \langle 32| [2|\eta_1] + \langle 13\rangle \langle \eta_3 2| [2|\eta_1]) \\
&+ c_7 m_1^2 [\eta_1 3] \langle 32| [2|\eta_1] + c_8 m_1 m_3 ([\eta_1|\eta_3] [32] \langle 2|1 \rangle + [\eta_1 3] [\eta_3 2] \langle 2|1 \rangle). \quad (2.150)
\end{aligned}$$

For $[\mathbf{J}(1^-, 2^0)]_0 \cdot [\mathbf{A}(3^0)]_2$, $[\mathbf{J}(1^-, 2^0)]_0$ is the conserved current, which would contribute to the leading SM amplitudes and descendant EFT amplitudes. Finally let us select the seven MHC amplitudes which contribute to the SM

$$-m_1\tilde{m}_3[\eta_12]\langle 2\eta_3\rangle\langle 31\rangle = 1^- \text{ (diagram 1)} \quad , \quad -m_1\tilde{m}_2\langle 12\rangle\langle\eta_23\rangle[3\eta_1] = 1^- \text{ (diagram 2)} \quad ,$$

(2.151)

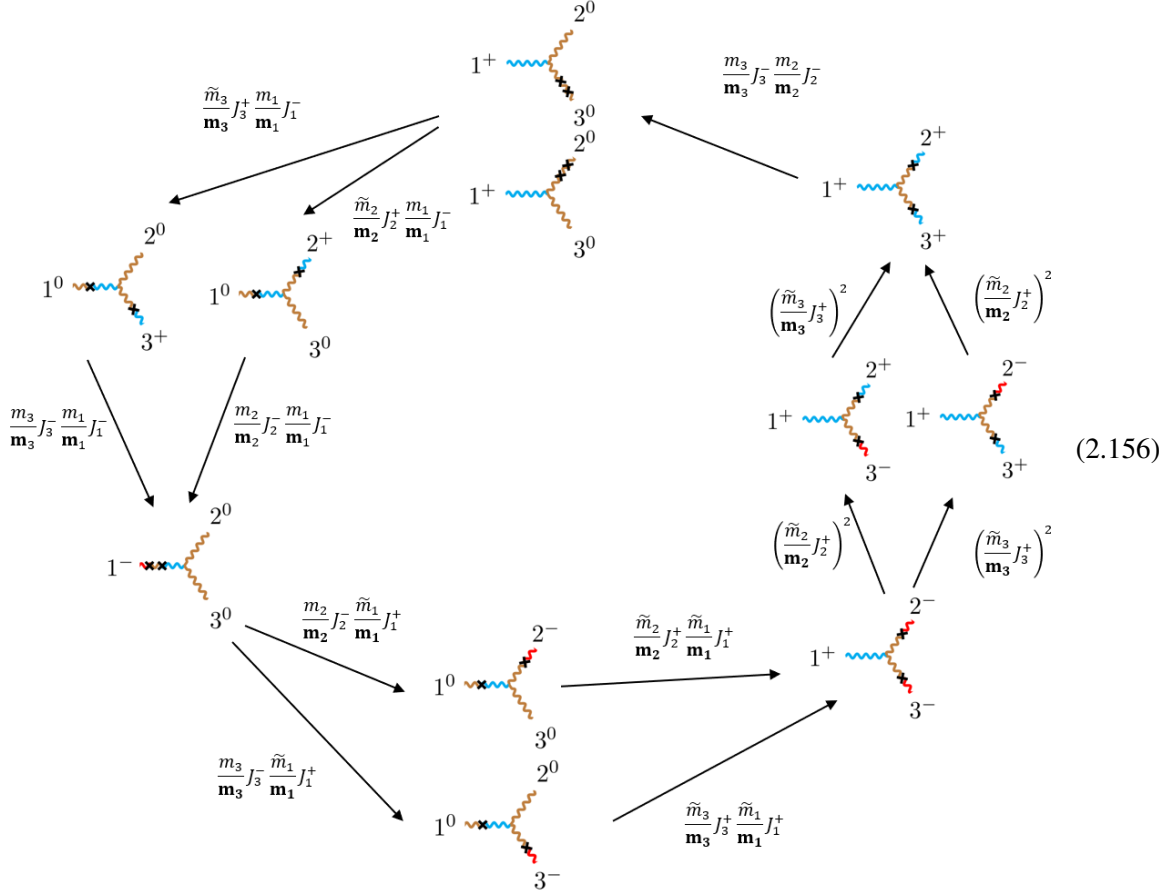
$$-m_3\tilde{m}_3\langle 12\rangle[2\eta_3]\langle\eta_31\rangle = 1^- \text{ (diagram 1)}, \quad -m_2\tilde{m}_2\langle 1\eta_2\rangle[\eta_23]\langle 31\rangle = 1^- \text{ (diagram 2)},$$

(2.152)

$$m_1 m_2 ([\eta_1 2][\eta_2 3]\langle 31 \rangle + [\eta_1 \eta_2][23]\langle 31 \rangle) = 1 - \text{wavy line}^{\text{blue}} \text{ with } \begin{matrix} 2^0 \\ \text{+} \\ 3^0 \end{matrix} , \quad (2.154)$$

$$m_1^2[\eta_1 2]\langle 23\rangle[3\eta_1] = 1^- \text{ (red wavy line)} \text{ (blue wavy line)} \text{ (orange wavy line)} \quad . \quad (2.155)$$

The VVV descendant amplitudes at the same order can also be related through the ladder operators. Given the large number of terms in the VVV amplitude, we only list for conciseness all leading (2nd descendant) diagrams originating from a primary amplitude, without showing their corresponding analytic expressions:



3 The 3-point Amplitude Matching For SM Amplitudes

In previous section, both the 3-point massless and massive amplitudes are determined by the little group scaling and extended little group covariance. The primary MHC amplitudes are obtained from the massive amplitudes, and all the descendant MHC ones are followed by action of the ladder operators. In this section, we will discuss the gauge structures of the massless and massive amplitudes, and then match the SM massless and massive amplitudes via the MHC amplitude deformation.

3.1 Massless and massive 3-point SM amplitudes

In the unbroken phase of the renormalizable SM, massless amplitudes are required to satisfy the dimensional constraint $\dim [\mathcal{A}(1, \dots, n)] = 4 - n$. This imposes a constraint on the coupling constant \mathcal{G} ,

$$\dim \mathcal{G} = 1 - |h_1 + h_2 + h_3|. \quad (3.1)$$

In the massless SM, the 3-point coupling constant should be 0, indicating the total helicity of the 3-pt massless amplitude is constrained to

$$h_1 + h_2 + h_3 = \pm 1. \quad (3.2)$$

This determines the total helicity for the 3-pt amplitude in the SM. Therefore, the amplitudes such as $(h_1, h_2, h_3) = (+\frac{1}{2}, -\frac{1}{2}, 0), (+1, -1, 0)$ or $(0, 0, 0)$ are forbidden. Therefore, the massless amplitudes in the SM belong to the *SSSS*, *VVV*, *FFS*, *FFV* and *VSS* categories, while the *VVS* one is excluded.

The 3-point massless amplitudes contains the group structure in the unbroken phase. Here the notation of the group indices are

unbroken phase	gauge boson	fermion	scalar boson
index	I	\hat{i}	i
upper index value	$W^I = \{W^1, W^2, W^3\}; B$	$\{u_L, d_L\}, \{v_L, e_L\}; u_R, d_R, e_R$	$\{\phi^+, \phi^0\}$
lower index value	-	$\{\bar{u}_L, \bar{d}_L\}, \{\bar{v}_L, \bar{e}_L\}; \bar{u}_R, \bar{d}_R, \bar{e}_R$	$\{\phi^-, \phi^{0*}\}$

(3.3)

where i represents the $SU(2)_W$ fundamental indices, denoting the first or second component of H_i ; \hat{i} stands for the reducible representation for fermion, including both $SU(2)_W$ -doublets $\{u_L, d_L\}, \{v_L, e_L\}$ and $SU(2)_W$ -singlets u_R, d_R, e_R . The upper index and lower index represent particle and anti-particle separately. For simplicity, here we only consider one generation of fermions.

For 3-pt amplitude, the group structure should have three indices, labeling a covariant tensor under the $SU(2)_W \times U(1)$ group. There are four types of 3-pt massless amplitude, and we can define their coefficient to be

$$FFS: \quad 7 \times 7 \times 2 \text{ tensors} \quad (Y^{i_3})_{\hat{i}_2}^{\hat{i}_1}, (\tilde{Y}^{i_3})_{\hat{i}_2}^{\hat{i}_1}, (Y_{i_3})_{\hat{i}_2}^{\hat{i}_1}, (\tilde{Y}_{i_3})_{\hat{i}_2}^{\hat{i}_1}, \quad (3.4)$$

$$FFV: \quad 7 \times 7 \times 4 \text{ tensor} \quad (T_f^{I_3})_{\hat{i}_2}^{\hat{i}_1}, (\tilde{T}_f^{I_3})_{\hat{i}_2}^{\hat{i}_1}, \quad (3.5)$$

$$VSS: \quad 4 \times 2 \times 2 \text{ tensor} \quad (T_s^{I_1})_{i_3}^{i_2}, \quad (3.6)$$

$$VVV: \quad 4 \times 4 \times 4 \text{ tensor} \quad f^{I_1 I_2 I_3}. \quad (3.7)$$

Massless VVV The electroweak $SU(2)$ Yang-Mills theory has the following 3-pt amplitude

$$\begin{array}{c} 2^{-1, I_2} \\ \swarrow \\ 3^{+1, I_3} \\ \searrow \\ 1^{-1, I_1} \end{array} = \mathcal{A}(1^{-1, I_1}, 2^{-1, I_2}, 3^{+1, I_3}) = f^{I_1 I_2 I_3} \frac{\langle 12 \rangle^3}{\langle 23 \rangle \langle 31 \rangle}, \quad (3.8)$$

where all three indices are fixed and the coupling takes the form

$$f^{W^I W^J W^K} = -i\sqrt{2}g\epsilon^{IJK}. \quad (3.9)$$

where ϵ^{IJK} is the Levi-Civita tensor. The $U(1)$ structure with the B boson does not participate in the gauge boson self interaction. In the off-shell Lagrangian description, the 3-vertex is an off-shell

non-gauge invariant object, and thus the contact quartic $VVVV$ is fully determined from the off-shell non-gauge invariant VVV to ensure the off-shell gauge invariance of the Lagrangian. On the other hand, in the on-shell method, since the 3-point on-shell amplitude is gauge invariant, there is no need to add contact 4-pt amplitudes.

Massless VSS The unbroken SM contains the scalar QED theory, in which the 3-point VSS amplitudes take the form

$$\begin{array}{c}
 2_{i_2}^0 \\
 \diagdown \quad \diagup \\
 \text{---} \quad 3^{0,i_3} \\
 \text{---} \quad \diagup \quad \diagdown \\
 1^{-1,I_1} \\
 \end{array} = \mathcal{A}(1^{-1,I_1}, 2_{i_2}^0, 3^{0,i_3}) = (T_s^{I_1})_{i_3}^{i_2} \frac{\langle 12 \rangle \langle 31 \rangle}{\langle 23 \rangle}, \quad (3.10)$$

where I_1 denote (B, W^I) , and i_2, i_3 denotes (h^+, h^0) . The coupling structures are

$$(T_s^B)_{i_3}^{i_2} = -\sqrt{2}g' \begin{pmatrix} Y_{\phi^+} & 0 \\ 0 & Y_{\phi^0} \end{pmatrix}, \quad (T_s^{W^I})_{i_3}^{i_2} = -\frac{g}{\sqrt{2}} \begin{pmatrix} \sigma^I \end{pmatrix}, \quad (3.11)$$

where the hypercharge for scalar boson is $Y_{\phi^+} = Y_{\phi^0} = \frac{1}{2}$. Note that again the contact quartic $VVSS$ is not needed because the gauge invariance of the 3-pt amplitudes in the on-shell method.

Massless FFV Of course, the SM contains the gauge fermion couplings. We consider two massless amplitudes with opposite helicity for the fermion and antifermion with helicity $(\mp \frac{1}{2}, \pm \frac{1}{2}, +1)$

$$\begin{array}{c}
 2_{\hat{i}_2}^{+1/2} \\
 \diagdown \quad \diagup \\
 \text{---} \quad 3^{+1,I_3} \\
 \text{---} \quad \diagup \quad \diagdown \\
 1^{-1/2,\hat{i}_1} \rightarrow \text{---} \\
 \text{---} \quad \diagup \quad \diagdown \\
 2_{\hat{i}_2}^{-1/2} \\
 \text{---} \quad 3^{+1,I_3} \\
 \end{array} = \mathcal{A}(1^{-\frac{1}{2},\hat{i}_1}, 2_{\hat{i}_2}^{+\frac{1}{2}}, 3^{+1,I_3}) = (\tilde{T}_f^{I_3})_{\hat{i}_2}^{\hat{i}_1} \frac{[23]^2}{[12]}, \quad (3.12)$$

where \tilde{T}_f denotes the coupling for the right-handed current, and T_f for left-handed current. T_f represents the coefficients of $\frac{\langle 23 \rangle^2}{\langle 12 \rangle}, \frac{[13]^2}{[12]}$, and \tilde{T}_f represents the ones of $\frac{\langle 13 \rangle^2}{\langle 12 \rangle}, \frac{[23]^2}{[12]}$.

For W^I boson, the two diagonal blocks are

$$\begin{aligned}
 (T_f^{W^I})_{\hat{i}_2}^{\hat{i}_1} &= -\frac{g}{\sqrt{2}} \begin{pmatrix} \sigma^I & \\ & \sigma^I \end{pmatrix}, \quad \hat{i}_1 = u_L, d_L, v_L, e_L, \quad \hat{i}_2 = \bar{u}_L, \bar{d}_L, \bar{v}_L, \bar{e}_L, \\
 (\tilde{T}_f^{W^I})_{\hat{i}_2}^{\hat{i}_1} &= \begin{pmatrix} 0 & \\ & 0 & \\ & & 0 \end{pmatrix}, \quad \hat{i}_1 = u_R, d_R, e_R, \quad \hat{i}_2 = \bar{u}_R, \bar{d}_R, \bar{e}_R,
 \end{aligned} \quad (3.13)$$

where g is the $SU(2)_W$ coupling constant, and σ^I are the Pauli matrices acting as $SU(2)_W$ generators. For B boson, we have

$$(T_f^B)_{\hat{i}_2}^{\hat{i}_1} = -\sqrt{2}g' \begin{pmatrix} Y_{u_L} & & \\ & Y_{d_L} & \\ & & Y_{v_L} \\ & & & Y_{e_L} \end{pmatrix}, \quad (\tilde{T}_f^B)_{\hat{i}_2}^{\hat{i}_1} = -\sqrt{2}g' \begin{pmatrix} Y_{u_R} & & \\ & Y_{d_R} & \\ & & Y_{e_R} \end{pmatrix}, \quad (3.14)$$

where g' is $U(1)_Y$ coupling constant. In the SM, the hypercharge Y of $U(1)_Y$ group is set by

$$\begin{aligned} Y_{u_L} = Y_{d_L} &= \frac{1}{6}, & Y_{u_R} &= \frac{2}{3}, & Y_{d_R} &= -\frac{1}{3}, \\ Y_{e_L} = Y_{v_L} &= -\frac{1}{2}, & Y_{e_R} &= -1. \end{aligned} \quad (3.15)$$

Massless FFS The SM contains the scalar Yukawa interactions, and their amplitudes take the form

$$1^{-1/2, \hat{i}_1} \xrightarrow{\begin{array}{c} \nearrow \\ \searrow \end{array}} \begin{matrix} 2_{\hat{i}_2}^{-1/2} \\ = Y_{\hat{i}_2}^{\hat{i}_1 i_3} \langle 12 \rangle, \end{matrix} \quad 1^{+1/2, \hat{i}_1} \xrightarrow{\begin{array}{c} \nearrow \\ \searrow \end{array}} \begin{matrix} 2_{\hat{i}_2}^{+1/2} \\ = \tilde{Y}_{\hat{i}_2}^{\hat{i}_1 i_3} [12]. \end{matrix} \quad (3.16)$$

Here Y and \tilde{Y} represents the coefficients of $\langle 12 \rangle$ and $[12]$, respectively. The two Yukawa matrices are

$$Y_{\hat{i}_2}^{\hat{i}_1 i_3} = - \begin{pmatrix} \mathcal{Y}^{(u)} \delta_{\phi^0}^{i_3} & 0 & 0 \\ \mathcal{Y}^{(u)} \delta_{\phi^+}^{i_3} & 0 & 0 \\ 0 & 0 & 0 \\ 0 & 0 & 0 \end{pmatrix}, \quad \hat{i}_1 = u_L, d_L, v_L, e_L \quad \hat{i}_2 = \bar{u}_R, \bar{d}_R, \bar{e}_R, \quad (3.17)$$

$$\tilde{Y}_{\hat{i}_2}^{\hat{i}_1 i_3} = - \begin{pmatrix} 0 & 0 & 0 & 0 \\ \mathcal{Y}^{(d)} \delta_{\phi^+}^{i_3} & \mathcal{Y}^{(d)} \delta_{\phi^0}^{i_3} & 0 & 0 \\ 0 & 0 & \mathcal{Y}^{(e)} \delta_{\phi^+}^{i_3} & \mathcal{Y}^{(e)} \delta_{\phi^0}^{i_3} \end{pmatrix}, \quad \hat{i}_1 = u_R, d_R, e_R, \quad \hat{i}_2 = \bar{u}_L, \bar{d}_L, \bar{e}_L, \quad (3.18)$$

where $i_3 = \phi^+, \phi^0$ and $\mathcal{Y}^{(f)}$ denotes the Yukawa coupling for fermion f . There is no right-handed neutrino in the SM, so we do not have a coupling like $\mathcal{Y}^{(v)}$ and the above blocks are not square matrices. Similarly we have

$$Y_{\hat{i}_2 i_3}^{\hat{i}_1} = - \begin{pmatrix} 0 & \mathcal{Y}^{(d)} \delta_{i_3}^{\phi^-} & 0 \\ 0 & \mathcal{Y}^{(d)} \delta_{i_3}^{\phi^0} & 0 \\ 0 & 0 & \mathcal{Y}^{(e)} \delta_{i_3}^{\phi^-} \\ 0 & 0 & \mathcal{Y}^{(e)} \delta_{i_3}^{\phi^0} \end{pmatrix}, \quad \tilde{Y}_{\hat{i}_2 i_3}^{\hat{i}_1} = - \begin{pmatrix} \mathcal{Y}^{(u)} \delta_{i_3}^{\phi^0} & \mathcal{Y}^{(u)} \delta_{i_3}^{\phi^-} & 0 & 0 \\ 0 & 0 & 0 & 0 \\ 0 & 0 & 0 & 0 \end{pmatrix}. \quad (3.19)$$

Massless SSSS Finally the SM contains the single 4-point amplitudes, the $\lambda\phi^4$ amplitude

$$\begin{array}{c}
 2_{i_2}^0 \\
 \vdots \\
 1_{i_1}^0 \cdots + - 3^{0,i_3} \\
 \vdots \\
 4^{0,i_4}
 \end{array} = \mathcal{A}(1_{i_1}^0, 2_{i_2}^0, 3^{0,i_3}, 4^{0,i_4}) = -4\lambda\delta_{i_3}^{(i_1}\delta_{i_4}^{i_2)}.
 \quad (3.20)$$

Massive 3-point SM Amplitudes After spontaneously symmetry breaking, we use the indices \mathbf{I} , $\hat{\mathbf{i}}$ and h to label vector boson, fermion and scalar boson. Their possible values are

broken phase	vector boson	fermion	scalar boson	
index	\mathbf{I}	$\hat{\mathbf{i}}$	h	
upper index value	$\{W^+, W^-, Z, A\}$	$\{u, d; v, e\}$	$\{h\}$	
lower index value	-	$\{\bar{u}, \bar{d}; \bar{v}, \bar{e}\}$	-	

(3.21)

Similarly the massive 3-point AHH amplitudes are summarized. In the broken phase, identify the gauge structure and we should obtain the following results

$$\begin{array}{c}
 2_q^{1/2, \mathbf{i}_2} \\
 \nearrow \\
 1_{p\mathbf{i}_1}^{1/2} \\
 \cdots \\
 \mathbf{3}^{0,h}
 \end{array} = \mathcal{M}(\mathbf{1}_{i_1}^{1/2}, 2^{1/2, \mathbf{i}_2}, \mathbf{3}^{0,h}) = y_{\mathbf{i}_2}^{\mathbf{i}_1} \langle \mathbf{12} \rangle + y_{\mathbf{i}_2}^{\mathbf{i}_1} [\mathbf{12}], \quad (3.22)$$

$$\begin{array}{c}
 2_q^{1/2, \mathbf{i}_2} \\
 \nearrow \\
 1_{p\mathbf{i}_1}^{1/2} \\
 \cdots \\
 \mathbf{3}^{1, \mathbf{i}_3}
 \end{array} = \mathcal{M}(\mathbf{1}_{i_1}^{1/2}, 2^{1/2, \mathbf{i}_2}, \mathbf{3}^{1, \mathbf{i}_3}) = (X_1^{\mathbf{i}_3})_{\hat{\mathbf{i}}_2}^{\mathbf{i}_1} \frac{\langle \mathbf{13} \rangle [\mathbf{23}]}{\mathbf{m}_3} + (X_2^{\mathbf{i}_3})_{\hat{\mathbf{i}}_2}^{\mathbf{i}_1} \frac{\langle \mathbf{23} \rangle [\mathbf{13}]}{\mathbf{m}_3}, \quad (3.23)$$

$$\begin{array}{c}
 \mathbf{2}^{1, \mathbf{i}_2} \\
 \nearrow \\
 1^{1, \mathbf{i}_1} \\
 \cdots \\
 \mathbf{3}^{1, \mathbf{i}_3}
 \end{array} = \mathcal{M}(\mathbf{1}^{1, \mathbf{i}_1}, \mathbf{2}^{1, \mathbf{i}_2}, \mathbf{3}^{1, \mathbf{i}_3}) \\
 = \mathbf{f}^{\mathbf{I}_1 \mathbf{I}_2 \mathbf{I}_3} \left(\frac{[\mathbf{12}] \langle \mathbf{23} \rangle \langle \mathbf{31} \rangle}{\mathbf{m}_1 \mathbf{m}_2} + \frac{[\mathbf{12}] [\mathbf{23}] \langle \mathbf{31} \rangle}{\mathbf{m}_1 \mathbf{m}_3} + \frac{[\mathbf{12}] \langle \mathbf{23} \rangle [\mathbf{31}]}{\mathbf{m}_2 \mathbf{m}_3} \right) \\
 + \mathbf{f}^{\mathbf{I}_1 \mathbf{I}_2 \mathbf{I}_3} \left(\frac{\langle \mathbf{12} \rangle [\mathbf{23}] [\mathbf{31}]}{\mathbf{m}_1 \mathbf{m}_2} + \frac{\langle \mathbf{12} \rangle \langle \mathbf{23} \rangle [\mathbf{31}]}{\mathbf{m}_1 \mathbf{m}_3} + \frac{\langle \mathbf{12} \rangle [\mathbf{23}] \langle \mathbf{31} \rangle}{\mathbf{m}_2 \mathbf{m}_3} \right), \quad (3.24)$$

$$\begin{array}{c}
\textbf{2}^{1,\mathbf{I}_2} \\
\backslash \\
\textbf{3}^{0,h} \\
\backslash \\
\textbf{1}^{1,\mathbf{I}_1}
\end{array} = \mathcal{M}(\textbf{1}^{1,\mathbf{I}_1}, \textbf{2}^{1,\mathbf{I}_2}, \textbf{3}^{0,h}) = \mathbf{g}^{\mathbf{I}_1\mathbf{I}_2} \frac{\langle 12 \rangle [12]}{\mathbf{m}_1 \mathbf{m}_2}, \quad (3.25)$$

$$\begin{array}{c}
\textbf{2}^{0,h} \\
\backslash \\
\textbf{3}^{0,h} \\
\backslash \\
\textbf{1}^{0,h}
\end{array} = \mathcal{M}(\textbf{1}^{0,h}, \textbf{2}^{0,h}, \textbf{3}^{0,h}) = \lambda_3, \quad (3.26)$$

$$\begin{array}{c}
\textbf{2}^{0,h} \\
| \\
\textbf{1}^{0,h} \quad \textbf{3}^{0,h} \\
| \\
\textbf{4}^{0,h}
\end{array} = \mathcal{M}(\textbf{1}^{0,h}, \textbf{2}^{0,h}, \textbf{3}^{0,h}, \textbf{4}^{0,h}) = \lambda_4, \quad (3.27)$$

Unlike the massless amplitudes, here all the couplings are to be determined.

3.2 3-point matching from MHC amplitude deformation

Given the massless and massive amplitudes, let us perform their matching by identifying the helicity-transversality unification at the amplitude level. Note that all the helicity categories of the massless amplitudes are identified by the condition $h_1 + h_2 + h_3 = \pm 1$:

Massless	$h_1 + h_2 + h_3 = 1$	$h_1 + h_2 + h_3 = -1$	
	(h_1, h_2, h_3) Lorentz structures	(h_1, h_2, h_3) Lorentz structures	
FFV	$(-\frac{1}{2}, +\frac{1}{2}, +1)$	$\frac{[23]^2}{[12]}$	$(-\frac{1}{2}, +\frac{1}{2}, -1)$
FFS	$(+\frac{1}{2}, +\frac{1}{2}, 0)$	$[12]$	$(-\frac{1}{2}, -\frac{1}{2}, 0)$
VVV	$(+1, +1, -1)$	$\frac{[12]^3}{[23][31]}$	$(-1, -1, +1)$
VSS	$(+1, 0, 0)$	$\frac{[12][31]}{[23]}$	$(-1, 0, 0)$

(3.28)

The only exception in the SM is SSS , which corresponds to the 4-point massless amplitude. On the other hand, simply unbolding the massive amplitudes gives the following helicity categories

Primary MHC	$h_1 + h_2 + h_3$	$h_1 + h_2 + h_3$	
	(h_1, h_2, h_3) Lorentz structures	(h_1, h_2, h_3) Lorentz structures	
FFV	$(-\frac{1}{2}, +\frac{1}{2}, 0)$	$\langle 13 \rangle [32]$	$(+\frac{1}{2}, -\frac{1}{2}, 0)$
FFS	$(+\frac{1}{2}, +\frac{1}{2}, 0)$	$[12]$	$(-\frac{1}{2}, -\frac{1}{2}, 0)$
VVV	$(-1, 0, 0)$	$\langle 12 \rangle [23] \langle 31 \rangle$	$(+1, 0, 0)$
	$(0, -1, 0)$	$\langle 12 \rangle \langle 23 \rangle [31]$	$(0, +1, 0)$
	$(0, 0, -1)$	$[12] \langle 23 \rangle \langle 31 \rangle$	$(0, 0, +1)$
VSS	$(0, 0, 0)$	$\langle 12 \rangle [21]$	

(3.29)

Comparing the helicity structures, we note that the helicity does not match except the *FFS* structure. This agrees with the results from the previous section, that all the primary MHC amplitudes except the *FFS* vanish due to conserved currents. Therefore, we expect for those vanishing primary case the matching should be the first non-vanishing descendant amplitudes, named as the leading MHC amplitudes.

For a massive amplitude with spins (s_1, s_2, s_3) , all massless amplitudes with $|h_i| \leq s_i$ can contribute to the massive structure. The leading MHC amplitude receive the contribution from 3-pt massless amplitude, so the corresponding helicity category must satisfy $h_1 + h_2 + h_3 = \pm 1$. To obtain the leading MHC amplitudes, let us start from the primary helicity categories in the SM, and check the total helicity

$$h = h_1 + h_2 + h_3. \quad (3.30)$$

If they satisfy $h = \pm 1$ and they do not vanishes, we identify these primary amplitude is leading. Otherwise, we will use the ladder operator to obtain the descendant MHC amplitudes with total helicity $h + 1$ or $h - 1$, until we find the amplitudes with total helicity ± 1 , as the leading contribution. For convenience, we define the *helicity class* as the set of helicity categories sharing the same number of transverse vector bosons, denoted as n_T . In the SM, the helicity classes for all 3-pt massive amplitudes are

Leading MHC	helicity class	helicity category	
SSS	$n_T = 0$	$(0, 0, 0)$	
FFS	$n_T = 0$	$(\pm \frac{1}{2}, \pm \frac{1}{2}, 0)$	
FFV	$n_T = 0$	$(\pm \frac{1}{2}, \pm \frac{1}{2}, 0)$	(3.31)
	$n_T = 1$	$(\pm \frac{1}{2}, \mp \frac{1}{2}, +1), (\pm \frac{1}{2}, \mp \frac{1}{2}, -1)$	
VVS	$n_T = 1$	$(\pm 1, 0, 0), (0, \pm 1, 0)$	
VVV	$n_T = 1$	$(\pm 1, 0, 0), (0, \pm 1, 0), (0, 0, \pm 1)$	
	$n_T = 3$	$(\pm 1, \mp 1, \mp 1), (\mp 1, \pm 1, \mp 1), (\mp 1, \mp 1, \pm 1)$	

Notice that the leading MHC *FFV* would contain massless *FFS* structures, and the leading *VVV* also contains *VSS* structures. In the following we will match the massless amplitudes with the leading MHC ones.

1. FFS & SSS For the *FFS* amplitude, the primary MHC amplitudes has two helicity categories

$$\begin{aligned} h = -1 : & \quad (-\frac{1}{2}, -\frac{1}{2}, 0), \\ h = +1 : & \quad (+\frac{1}{2}, +\frac{1}{2}, 0), \end{aligned} \quad (3.32)$$

They satisfy the condition $h = \pm 1$. Since the primary amplitude is non-vanishing and thus there is no conserved current, the matching is quite simple

$$\begin{aligned}
 (-\frac{1}{2}, -\frac{1}{2}, 0) : \quad & \langle 12 \rangle = 1^- \xrightarrow{\text{red}} \begin{array}{c} 2^- \\ \diagup \text{blue} \\ \diagdown \text{brown} \end{array} , \\
 (+\frac{1}{2}, +\frac{1}{2}, 0) : \quad & [12] = 1^+ \xrightarrow{\text{blue}} \begin{array}{c} 2^+ \\ \diagup \text{red} \\ \diagdown \text{brown} \end{array} . \tag{3.33}
 \end{aligned}$$

For the SSS amplitude, it only has one helicity category $(0,0,0)$. The primary MHC amplitude is non-vanishing and thus the matching is also simple

$$(0,0,0) : \quad 1 = 1^0 \xrightarrow{\quad} \begin{array}{c} 2^0 \\ \diagup \quad \diagdown \\ \quad \quad \quad \end{array} \quad . \quad (3.34)$$

2. FFV From the MHC leading amplitudes

$$\begin{aligned}
\left(+\frac{1}{2}, +\frac{1}{2}, 0\right) : & \quad \tilde{m}_1[23]\langle 3\eta_1 \rangle, \quad \tilde{m}_2\langle \eta_2 3 \rangle[31], \\
\left(-\frac{1}{2}, -\frac{1}{2}, 0\right) : & \quad m_2[\eta_2 3]\langle 31 \rangle, \quad m_1\langle 23 \rangle[3\eta_1], \\
\left(-\frac{1}{2}, +\frac{1}{2}, +1\right) : & \quad \tilde{m}_3[23]\langle \eta_3 1 \rangle, \quad \left(-\frac{1}{2}, +\frac{1}{2}, -1\right) : \quad m_3[2\eta_3]\langle 31 \rangle \\
\left(+\frac{1}{2}, -\frac{1}{2}, +1\right) : & \quad \tilde{m}_3\langle 2\eta_3 \rangle[31], \quad \left(+\frac{1}{2}, -\frac{1}{2}, -1\right) : \quad m_3\langle 23 \rangle[\eta_3 1],
\end{aligned} \tag{3.35}$$

Therefore, the 1st descendant amplitudes can be expressed in the following two forms

helicity	current form	diagram	
$(-\frac{1}{2}, +\frac{1}{2}, +1)$	$[\mathbf{J}(1^{-\frac{1}{2}}, 2^{+\frac{1}{2}})]_0 \cdot [\mathbf{A}(3^+)]_1$		
$(+\frac{1}{2}, +\frac{1}{2}, 0)$	$[\mathbf{J}(1^{+\frac{1}{2}}, 2^{+\frac{1}{2}})]_1 \cdot [\mathbf{A}(3^0)]_0$		(3.36)

Note that the last line contains two MHC amplitudes, since the descendant current $[\mathbf{J}(1^{+1/2}, 2^{+1/2})]_1$ consists of two terms. Similarly, MHC amplitudes in other helicity categories can also be rewritten as $[\mathbf{J}]_1 \cdot [\mathbf{A}]_0$ or $[\mathbf{J}]_0 \cdot [\mathbf{A}]_1$.

Gauge Deformation: For the massless FFV amplitude with helicity $(-\frac{1}{2}, +\frac{1}{2}, +1)$, we should flip particle 3. Diagrammatically, we have

$$1^- \xrightarrow{\text{wavy line}} 2^+ \quad \Rightarrow \quad [\mathbf{J}^{-+}]_0 \cdot [\mathbf{A}^+]_1 = 1^- \xrightarrow{\text{red line}} 2^+ \quad . \quad (3.37)$$

Applying the gauge deformation, the massless amplitude match to

$$\frac{[23]^2}{[12]} \xrightarrow{\text{Gauge}} \frac{\tilde{m}_3 \langle 1 \eta_3 \rangle [23]}{\mathbf{m}_3^2}. \quad (3.38)$$

Goldstone Deformation: When we match the Goldstone boson to a symmetric vector boson, we should flip the chirality of particles in the current. For massless *FFS* amplitude with helicity $(-\frac{1}{2}, -\frac{1}{2}, 0)$, particle 3 is a Goldstone boson, so we can only flip particle 1 or 2 in the current \mathbb{J} . In this case, one massless diagram corresponds to two MHC diagrams

$$1^- \xrightarrow{\text{---}} \begin{array}{c} 2^- \\ \diagup \quad \diagdown \\ \diagdown \quad \diagup \end{array} \quad = \langle 12 \rangle \rightarrow [\mathbf{J}^{--}]_1 \cdot [\mathbf{A}^0]_0 = \quad 1^- \xrightarrow{\text{---}} \begin{array}{c} 2^- \\ \diagup \quad \diagdown \\ \diagdown \quad \diagup \end{array} \quad = m_2 \langle 13 \rangle [3\eta_2], \quad (3.39)$$

Thus, applying Goldstone deformation can give two MHC terms

$$[12] \xrightarrow{\text{Goldstone}} -b_1 \frac{\tilde{m}_1 \langle \eta_1 3 \rangle [32]}{\mathbf{m}_1^2} - b_2 \frac{\tilde{m}_2 [13] \langle 3 \eta_2 \rangle}{\mathbf{m}_2^2}, \quad (3.40)$$

where $b_1 + b_2 = 1$.

Finally taking the little group covariance, we obtain the AHH formalism.

3. VVS The primary amplitude is also vanishing and thus the leading MHC amplitudes are

$$\begin{aligned} (-1,0,0) : \quad m_1 \langle 12 \rangle [2\eta_1], \quad & (+1,0,0) : \quad -\tilde{m}_1 \langle \eta_1 2 \rangle [21], \\ (0,-1,0) : \quad m_2 \langle 12 \rangle [\eta_2 1], \quad & (0,+1,0) : \quad -\tilde{m}_2 \langle 1 \eta_2 \rangle [21]. \end{aligned} \quad (3.41)$$

Therefore the massless amplitudes belong to the same helicity, and the diagrammatic matching is straightforward.

These can also be rewritten in terms of MHC currents and vector states. For each helicity, two decomposition forms remain available. As an example, consider the helicity category $(-1, 0, 0)$:

helicity	current form	diagram	
$(-1, 0, 0)$	$\begin{aligned} & [\mathbf{J}(2^0, 3^0)]_0 \cdot [\mathbf{A}(1^-)]_1 \\ & [\mathbf{J}(1^{-1}, 3^0)]_1 \cdot [\mathbf{A}(1^0)]_0 \end{aligned}$		(3.42)

Amplitudes for other helicities can similarly be rewritten as $[\mathbf{J}]_1 \cdot [\mathbf{A}]_0$ or $[\mathbf{J}]_0 \cdot [\mathbf{A}]_1$. In analogy with the FFV case, the 1st descendant current $[\mathbf{J}]_1$ is not conserved.

From the first MHC amplitude, the massless matching has

$$\begin{array}{c} 2^0 \\ \diagup \quad \diagdown \\ 1^- \text{ wavy line} \quad 3^0 \end{array} = \frac{\langle 12 \rangle \langle 31 \rangle}{\langle 23 \rangle} \rightarrow \begin{array}{c} 2^0 \\ \diagup \quad \diagdown \\ 1^- \text{ wavy line} \quad 3^0 \end{array} = m_1 \langle 12 \rangle [2\eta_1], \quad (3.43)$$

4. VVV To apply the matching procedure, the first step is analyzing the MHC amplitudes. The primary amplitudes are vanishing, the 1st descendant amplitudes are either vanishing or belong to the EFT amplitude, and thus the leading amplitudes should be the 2nd descendant amplitudes with the following helicity categories:

$$\begin{aligned} & (\pm, \pm, \mp), (\pm, \mp, \pm), (\mp, \pm, \pm), \\ & (\pm, 0, 0), (0, \pm, 0), (0, 0, \pm). \end{aligned} \quad (3.44)$$

Let us separate the leading matching into two different categories. The first category is the matching from massless VVV to massive VVV amplitudes. As shown in eq. (2.147), a massless VVV diagram corresponds to three MHC diagrams. Because the massless amplitude has exchange symmetry, it is more convenient to treat the combination of MHC diagrams as the matching object. For helicity $(+1, +1, -1)$, we can consider the exchange symmetry between particles 1 and 2, so the matching yields two cases:

$$\begin{array}{c} 2^+ \\ \diagup \quad \diagdown \\ 1^+ \text{ wavy line} \quad 3^- \end{array} = \frac{[12]^3}{[23][31]} \rightarrow \left\{ \begin{array}{c} 1^+ \text{ wavy line} \quad 2^+ \\ \diagup \quad \diagdown \\ 3^- \quad 2^+ \\ + \quad 1^+ \text{ wavy line} \quad 2^+ \\ \diagup \quad \diagdown \\ 3^- \quad 3^- \end{array} \right. , \quad (3.45)$$

In this case, any two of the above 2nd descendant amplitudes can be identified as a massive

current $[\mathbf{J}]_1$ that couples to a vector $[\mathbf{A}]_1$:

current form	diagram	
$[\mathbf{J}(1^+, 2^+)]_1 \cdot [\mathbf{A}(3^-)]_1$		
$[\mathbf{J}(1^+, 3^-)]_1 \cdot [\mathbf{A}(2^+)]_1$		(3.46)
$[\mathbf{J}(2^+, 3^-)]_1 \cdot [\mathbf{A}(1^+)]_1$		

where $[\mathbf{J}]_1$ is the conserved current we previously derived from the vanishing 1st descendant MHC amplitudes.⁶

After amplitude deformation, we obtain the matching results as

massless	massive amplitude	

The second category is the matching from the massless VSS amplitude to massive VVV ampli-

⁶There are also non-conserved $[\mathbf{J}]_1$ currents which contribute to the EFT amplitudes. Here we identify that $[\mathbf{J}(1^\pm, 2^\pm)]_1$ contribute to the SM amplitudes while $[\mathbf{J}(1^\pm, 2^\mp)]_1$ contribute to the EFT amplitudes.

tudes. According to exchange symmetry of two scalar boson, there are four cases

$$\begin{aligned}
 & \text{Diagram: } 1^- \text{ (red wavy line)} \text{ and } 3^0 \text{ (dashed line)} \text{ exchange } 2^0 \text{ (orange wavy line).} \\
 & \text{Equation: } \frac{\langle 12 \rangle \langle 31 \rangle}{\langle 23 \rangle} \rightarrow \left\{ \begin{array}{l} \text{Diagram: } 1^- \text{ (red wavy line)} \text{ and } 3^0 \text{ (dashed line)} \text{ exchange } 2^0 \text{ (orange wavy line).} \\ + \text{ Diagram: } 1^- \text{ (red wavy line)} \text{ and } 3^0 \text{ (dashed line)} \text{ exchange } 2^0 \text{ (orange wavy line).} \\ + \text{ Diagram: } 1^- \text{ (red wavy line)} \text{ and } 3^0 \text{ (dashed line)} \text{ exchange } 2^0 \text{ (orange wavy line).} \\ + \text{ Diagram: } 1^- \text{ (red wavy line)} \text{ and } 3^0 \text{ (dashed line)} \text{ exchange } 2^0 \text{ (orange wavy line).} \end{array} \right. , \quad (3.48)
 \end{aligned}$$

In this case, we can identify several 2nd descendant amplitudes as the coupling $[\mathbf{J}]_0 \cdot [\mathbf{A}]_2$, $[\mathbf{J}]_1 \cdot$

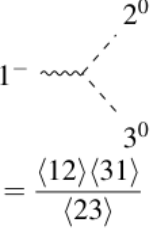
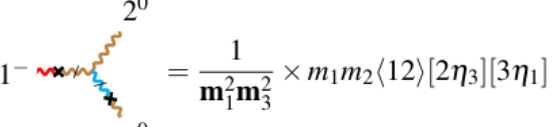
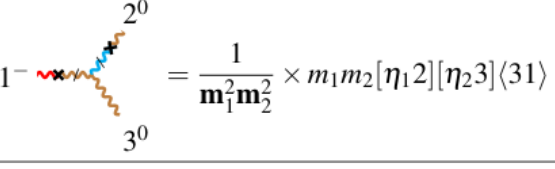
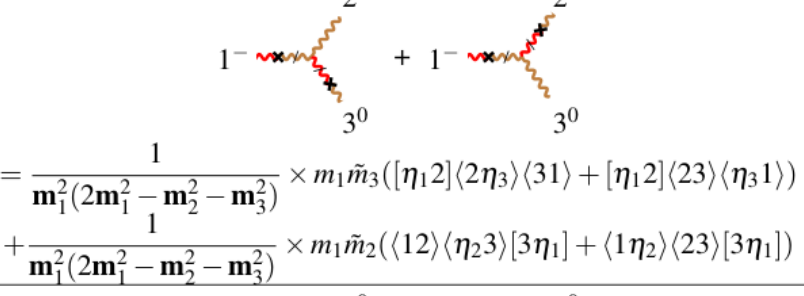
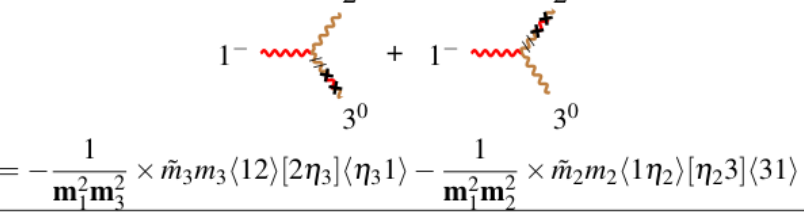
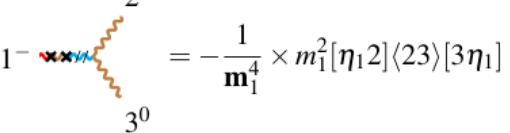
$[\mathbf{A}]_1$ or $[\mathbf{J}]_2 \cdot [\mathbf{A}]_0$:

current form	diagram
$[\mathbf{J}(1^-, 2^0)]_2 \cdot [\mathbf{A}(3^0)]_0$	
$[\mathbf{J}(1^-, 3^0)]_2 \cdot [\mathbf{A}(2^0)]_0$	
$[\mathbf{J}(1^-, 2^0)]_0 \cdot [\mathbf{A}(3^0)]_2$	
$[\mathbf{J}(1^-, 3^0)]_0 \cdot [\mathbf{A}(2^0)]_2$	
$[\mathbf{J}(2^0, 3^0)]_1 \cdot [\mathbf{A}(1^-)]_1$	

(3.49)

Here $[\mathbf{J}]_2$ is not conserved and is absent from the primary and first-descendant VVV amplitudes. Determining the current form of each diagram will help us analyze the leading matching in a later subsection.

The above matching result is summarized in the following table,

massless	massive diagram
	
	
	
	
	

(3.50)

Finally taking the little group covariance, we obtain the AHH formalism

$$\begin{aligned}
 \mathbf{M}(\mathbf{1}^1, \mathbf{2}^1, \mathbf{3}^1) = & c_1 \left(\frac{[12]\langle 23 \rangle \langle 31 \rangle}{\mathbf{m}_1 \mathbf{m}_2} + \frac{[12][23]\langle 31 \rangle}{\mathbf{m}_1 \mathbf{m}_3} + \frac{[12]\langle 23 \rangle [31]}{\mathbf{m}_2 \mathbf{m}_3} \right) \\
 & + c_2 \left(\frac{\langle 12 \rangle [23][31]}{\mathbf{m}_1 \mathbf{m}_2} + \frac{\langle 12 \rangle \langle 23 \rangle [31]}{\mathbf{m}_1 \mathbf{m}_3} + \frac{\langle 12 \rangle [23]\langle 31 \rangle}{\mathbf{m}_2 \mathbf{m}_3} \right),
 \end{aligned} \tag{3.51}$$

where c_i should be determined by the UV physics from the massless amplitudes.

3.3 Matching results for SM amplitudes

The amplitude deformation from massless to leading MHC amplitudes provides the matching for the Lorentz structure. In this subsection, we would perform the matching for group structure. The group

structure for the massless and massive amplitude are given in the first subsection. Now let us address how the indices changes from the unbroken to broken phase through the transformation matrices. There are four types of transformation matrices, summarized as follows

$$\begin{array}{cccc}
\text{unbroken} & \text{scalar } i & \text{gauge boson } I & \text{fermion } \hat{i} \\
\downarrow & \downarrow \mathcal{U}_i^h, \mathcal{U}^{ih} & \downarrow \mathcal{U}_i^I, \mathcal{U}^{I\bar{I}} & \downarrow \Omega_{\hat{i}}^{\hat{i}}, \Omega_{\hat{i}}^{\hat{i}} \\
\text{broken} & \text{Higgs } h & \text{massive vector } \mathbf{I} & \text{fermion } \hat{\mathbf{i}}
\end{array} \quad (3.52)$$

Note that for $S \rightarrow V$ and $S \rightarrow S$ cases, there are two kinds of transformation matrices, from the Higgs mechanism.

We classify four types of transformation matrices between massless and massive states in the SM:

- $S \rightarrow S$ and $S \rightarrow V$ transitions:

We use the matrices \mathcal{U} to match massless scalar to massive Higgs boson and the vector boson. The projector \mathcal{U} applies to the Higgs field. On one hand, the Higgs field matches the massive scalar field h via the projector \mathcal{U}^h ,

$$\mathcal{U}^{ih} = \mathcal{U}_i^h = \begin{pmatrix} 0 \\ \frac{1}{\sqrt{2}} \end{pmatrix}. \quad (3.53)$$

Here, the complex scalars ϕ^0 or ϕ^{0*} possesses 2 DOF, while the real Higgs boson h has 1 DOF. This leads to a factor of $\frac{1}{\sqrt{2}}$.

On the other hand, the Higgs field matches the massive vector fields because of the Higgs mechanism. Since of the charge conservation, the projections on the Higgs field and its hermitian conjugate are different,

$$\mathcal{U}^{I\bar{I}} = \begin{pmatrix} \mathcal{U}^{1W^-} & \mathcal{U}^{1Z} \\ \mathcal{U}^{2W^-} & \mathcal{U}^{2Z} \end{pmatrix} = \begin{pmatrix} \sqrt{2} & \\ & 1 \end{pmatrix}, \quad \mathcal{U}_I^I = \begin{pmatrix} \mathcal{U}_1^{W^+} & \mathcal{U}_1^Z \\ \mathcal{U}_2^{W^+} & \mathcal{U}_2^Z \end{pmatrix} = - \begin{pmatrix} \sqrt{2} & \\ & 1 \end{pmatrix}. \quad (3.54)$$

The factor $\sqrt{2}$ reflects the DOF difference between the complex scalar ϕ^\pm and the longitudinal modes of the massive W^\pm boson. For the neutral sector, matching the complex ϕ^0 to the real Z boson modifies the factor to $\sqrt{2} \times 1/\sqrt{2} = 1$.

- $F \rightarrow F$ and $V \rightarrow V$ transitions:

The conversion between massless and massive fermion is described by matrices $\Omega^{\hat{\mathbf{i}}}$ and $\Omega_{\hat{i}}^{\hat{\mathbf{i}}}$. Since there is only one generation, we do not consider the mixing of fermion. Here Ω is diagonal and thus trivial

$$\Omega_{\hat{i}}^{\hat{i}} = \Omega_{\hat{i}}^i = \begin{pmatrix} 1 & & & \\ & 1 & & \\ & & 1 & \\ & & & 1 \end{pmatrix}, \quad (3.55)$$

The 4×4 square matrix $O^{\mathbf{I}}$ maps massless gauge bosons (W^1, W^2, W^3, B) to massive vectors W^+, W^-, Z, γ , incorporating the gauge boson mixing. Under the symmetry breaking $SU(2)_W \times U(1)_Y \rightarrow U(1)_{\text{em}}$, the transformation matrices are

$$O^{\mathbf{I}} = O_I^{\mathbf{I}} = \begin{pmatrix} \frac{1}{\sqrt{2}} & \frac{1}{\sqrt{2}} \\ \frac{i}{\sqrt{2}} & -\frac{i}{\sqrt{2}} \\ & \cos \theta_W & \sin \theta_W \\ & -\sin \theta_W & \cos \theta_W \end{pmatrix}, \quad (3.56)$$

where θ_W is the Weinberg angle, and

$$\cos \theta_W = \frac{g}{\sqrt{g^2 + g'^2}}, \quad \sin \theta_W = \frac{g'}{\sqrt{g^2 + g'^2}}. \quad (3.57)$$

Using this strategy, we determine all massive coefficients for 3-pt amplitudes and establish the relation between massless and massive coefficient.

1. SSS and SSSS: This is the simplest case. the $\lambda \phi^4$ amplitude takes the form

$$\mathcal{A}^{\text{ct}}(1^0, 2^0, 3^0, 4^0) = -4\lambda \delta_{i_3}^{(i_1} \delta_{i_4}^{i_2)}. \quad (3.58)$$

where the superscript 0 indicates the helicity of massless scalars. Then match to SSSS is trivial and take VEV ν to match to the massive SSS amplitude

$$\mathbf{M}(\mathbf{1}^0, \mathbf{2}^0, \mathbf{3}^0) = -6\lambda \nu, \quad (3.59)$$

where the superscript 0 now denotes the spin of massive scalars.

2. FFS: The massless Yukawa amplitudes take the form,

$$\begin{aligned} \mathcal{A}(1^{-\frac{1}{2}}, 2^{-\frac{1}{2}}, 3^0) &= Y_{\hat{i}_2}^{\hat{i}_1 i_3} \langle 12 \rangle, \\ \mathcal{A}(1^{+\frac{1}{2}}, 2^{+\frac{1}{2}}, 3^0) &= \tilde{Y}_{\hat{i}_2 i_3}^{\hat{i}_1} [12], \end{aligned} \quad (3.60)$$

where Y and \tilde{Y} represent the massless matrices. To match the massless FFS amplitude to the massive one, we utilize the transformation matrices Ω and \mathcal{U} acting on the massless couplings Y and \tilde{Y} , and they become the massive couplings y and y' as follows,

$$\begin{aligned} Y_{\hat{i}_2}^{\hat{i}_1 i_3} \times \Omega_{\hat{i}_1}^{\hat{i}_1} \Omega_{\hat{i}_2}^{\hat{i}_2} \mathcal{U}_{i_3}^h + Y_{i_2 i_3}^{\hat{i}_1} \times \Omega_{\hat{i}_1}^{\hat{i}_1} \Omega_{\hat{i}_2}^{\hat{i}_2} \mathcal{U}^{i_3 h} &\Rightarrow y_{\hat{i}_2}^{\hat{i}_1}, \\ \tilde{Y}_{\hat{i}_2}^{\hat{i}_1 i_3} \times \Omega_{\hat{i}_1}^{\hat{i}_1} \Omega_{\hat{i}_2}^{\hat{i}_2} \mathcal{U}_{i_3}^h + \tilde{Y}_{i_2 i_3}^{\hat{i}_1} \times \Omega_{\hat{i}_1}^{\hat{i}_1} \Omega_{\hat{i}_2}^{\hat{i}_2} \mathcal{U}^{i_3 h} &\Rightarrow y_{\hat{i}_2}^{\hat{i}_1}. \end{aligned} \quad (3.61)$$

Here the index for massive Higgs boson is suppressed for simplicity. By bolding the massless spinors, we obtain the massive FFS amplitude

$$\mathbf{M}(\mathbf{1}^{1/2}, \mathbf{2}^{1/2}, \mathbf{3}^0) = y_{\hat{i}_2}^{\hat{i}_1} \langle \mathbf{12} \rangle + y_{\hat{i}_2}^{\hat{i}_1} [\mathbf{12}]. \quad (3.62)$$

The non-zero values of the massive coefficients y and y' are given by

$$\begin{aligned} y_{\bar{u}}^u &= y'_{\bar{u}} = \frac{1}{\sqrt{2}} y^{(u)}, \\ y_{\bar{d}}^d &= y'_{\bar{d}} = \frac{1}{\sqrt{2}} y^{(d)}, \\ y_{\bar{e}}^e &= y'_{\bar{e}} = \frac{1}{\sqrt{2}} y^{(e)}. \end{aligned} \quad (3.63)$$

The result agrees with the Yukawa matrix for massive fermions in the single-flavor case.

3. FFV: In this case, both massless FFS and FFV match to the massive FFV . Because of the little group covariance, we can take only one massless FFV to perform the matching, and the massless FFS matching is implicitly taken. Here we consider two massless amplitudes with opposite helicity for the fermion and anti-fermion $(\mp\frac{1}{2}, \pm\frac{1}{2}, +1)$. The deformation tells

$$\begin{aligned} \mathcal{A}(1^{-\frac{1}{2}}, 2^{+\frac{1}{2}}, 3^{+1}) &= (\tilde{T}_f^{I_3})_{\hat{i}_2}^{\hat{i}_1} \frac{[23]^2}{[12]} \rightarrow (\tilde{T}_f^{I_3})_{\hat{i}_2}^{\hat{i}_1} \frac{[23]\langle 1\eta_3 \rangle}{m_3}, \\ \mathcal{A}(1^{+\frac{1}{2}}, 2^{-\frac{1}{2}}, 3^{+1}) &= (T_f^{I_3})_{\hat{i}_2}^{\hat{i}_1} \frac{[13]^2}{[12]} \rightarrow -(T_f^{I_3})_{\hat{i}_2}^{\hat{i}_1} \frac{[13]\langle 2\eta_3 \rangle}{m_3}, \end{aligned} \quad (3.64)$$

where \tilde{T}_f denotes the coupling for the right-handed current, and T_f for the left-handed current. Applying the transformation matrices O and Ω to convert massless particles to massive ones, we obtain the massive coefficients X_1 and X_2 :

$$\begin{aligned} (T_f^{I_3})_{\hat{i}_2}^{\hat{i}_1} \times O^{I_3} \mathbf{I}_3 \Omega_{\hat{i}_1}^{\hat{i}_1} \Omega_{\hat{i}_2}^{\hat{i}_2} &\Rightarrow (X_1^{\mathbf{I}_3})_{\hat{i}_2}^{\hat{i}_1}, \\ (\tilde{T}_f^{I_3})_{\hat{i}_2}^{\hat{i}_1} \times O^{I_3} \mathbf{I}_3 \Omega_{\hat{i}_1}^{\hat{i}_1} \Omega_{\hat{i}_2}^{\hat{i}_2} &\Rightarrow (X_2^{\mathbf{I}_3})_{\hat{i}_2}^{\hat{i}_1}. \end{aligned} \quad (3.65)$$

By bolding the massless spinors, we obtain the massive amplitudes

$$\mathbf{M}(\mathbf{1}^{1/2}, \mathbf{2}^{1/2}, \mathbf{3}^1) = \sqrt{2}(X_1^{\mathbf{I}_3})_{\hat{i}_2}^{\hat{i}_1} \frac{\langle 13 \rangle [23]}{\mathbf{m}_3} + \sqrt{2}(X_2^{\mathbf{I}_3})_{\hat{i}_2}^{\hat{i}_1} \frac{\langle 23 \rangle [13]}{\mathbf{m}_3}. \quad (3.66)$$

Here for the charged vector boson $\mathbf{I}_3 = W^\pm$, only X_1 exists,

$$\begin{aligned} (X_1^{W^+})_{\bar{u}}^d &= (X_1^{W^+})_{\bar{e}}^v = \frac{e}{\sqrt{2} \sin \theta_W}, \\ (X_1^{W^-})_{\bar{d}}^u &= (X_1^{W^-})_{\bar{v}}^e = \frac{e}{\sqrt{2} \sin \theta_W}, \\ (X_2^{W^\pm})_{\hat{i}_2}^{\hat{i}_1} &= 0, \end{aligned} \quad (3.67)$$

where $e = g \sin \theta_W$ is the coupling of $U(1)_{\text{em}}$. This describes the coupling between the W boson and the charged current. For the neutral vector boson $\mathbf{I}_3 = Z$, both coefficients contribute, with X_1 and X_2

taking different values:

$$\begin{aligned}
(X_1^Z)_{\bar{u}}^u &= \frac{e}{2} \left(\frac{1}{3} \tan \theta_W - \cot \theta_W \right), & (X_1^Z)_{\bar{d}}^d &= \frac{e}{2} \left(\frac{1}{3} \tan \theta_W + \cot \theta_W \right), \\
(X_1^Z)_{\bar{v}}^v &= \frac{e}{2} (-\tan \theta_W - \cot \theta_W), & (X_1^Z)_{\bar{e}}^e &= \frac{e}{2} (-\tan \theta_W + \cot \theta_W), \\
(X_2^Z)_{\bar{u}}^u &= \frac{2e}{3} \tan \theta_W, & (X_2^Z)_{\bar{d}}^d &= -\frac{e}{2} \tan \theta_W, \\
(X_2^Z)_{\bar{e}}^e &= -e \tan \theta_W.
\end{aligned} \tag{3.68}$$

For the photon $\mathbf{I}_3 = A$, the two coefficients X_1 and X_2 are identical:

$$(X_1^A)_{\bar{u}}^u = (X_2^A)_{\bar{u}}^u = -\frac{2}{3}e, \quad (X_1^A)_{\bar{d}}^d = (X_2^A)_{\bar{d}}^d = \frac{1}{3}e, \quad (X_1^A)_{\bar{e}}^e = (X_2^A)_{\bar{e}}^e = e. \tag{3.69}$$

4. VVS: In this case, a single massless VSS amplitude with helicity category $(-1, 0, 0)$ is sufficient,

$$\mathcal{A}(1^{-1}, 2^0, 3^0) = (T_s^{I_1})_{i_3}^{i_2} \frac{\langle 12 \rangle \langle 31 \rangle}{\langle 23 \rangle} \rightarrow \frac{[\eta_1 2] \langle 12 \rangle}{\tilde{m}_1}, \tag{3.70}$$

The massless coefficient T_s maps to the massive coupling \mathbf{g} via

$$(T_s^{I_1})_{i_3}^{i_2} O^{I_1 \mathbf{I}_1} \mathcal{U}_{i_2}^{I_2} \mathcal{U}_{i_3}^{i_3 h} - (T_s^{I_1})_{i_2}^{i_3} O^{I_1 \mathbf{I}_1} \mathcal{U}^{i_2 \mathbf{I}_2} \mathcal{U}_{i_3}^h \Rightarrow \mathbf{g}^{\mathbf{I}_1 \mathbf{I}_2}. \tag{3.71}$$

Bolding the massless spinors, we obtain the massive amplitude

$$\mathbf{M}(\mathbf{1}^1, \mathbf{2}^1, \mathbf{3}^0) = \mathbf{g}^{\mathbf{I}_1 \mathbf{I}_2} \frac{\langle 12 \rangle [12]}{\mathbf{m}_1}, \tag{3.72}$$

where we enforce $\mathbf{m}_1 = \mathbf{m}_2$ for consistency. The non-vanishing components of the massive coupling \mathbf{g} are

$$\mathbf{g}^{W^+ W^-} = \mathbf{g}^{W^- W^+} = g, \quad \mathbf{g}^{ZZ} = \frac{g}{\cos \theta_W}. \tag{3.73}$$

5. VVV: Similar to the FFV case, the matching can be taken from only the massless VVV amplitudes to their massive counterparts, and the matching from massless VSS to massive VVV can be recovered by the little group covariance. Note that, one massless VVV amplitude cannot account for all massive terms. We select two massless amplitudes with opposite helicities in the matching procedure. Specifically, we choose:

$$\begin{aligned}
\mathcal{A}(1^{+1}, 2^{+1}, 3^{-1}) &= f^{I_1 I_2 I_3} \frac{[12]^3}{[23][31]}, \\
\mathcal{A}(1^{-1}, 2^{-1}, 3^{+1}) &= f^{I_1 I_2 I_3} \frac{\langle 12 \rangle^3}{\langle 23 \rangle \langle 31 \rangle}.
\end{aligned} \tag{3.74}$$

Each massless amplitude admits two distinct deformations to the MHC amplitude, which gives equal contributions with the factor $\frac{1}{2}$. The massless deformation thus yields

$$\begin{aligned}
f^{I_1 I_2 I_3} \frac{[12]^3}{[23][31]} &\rightarrow \frac{1}{2} f^{I_1 I_2 I_3} \frac{[12] \langle \eta_2 3 \rangle \langle 3 \eta_1 \rangle}{m_1 m_2} + \frac{1}{2} f^{I_1 I_2 I_3} \left(\frac{[12][2\eta_3] \langle 3 \eta_1 \rangle}{m_1 \tilde{m}_3} + \frac{[12] \langle \eta_2 3 \rangle [\eta_3 1]}{m_2 \tilde{m}_3} \right), \\
f^{I_1 I_2 I_3} \frac{\langle 12 \rangle^3}{\langle 23 \rangle \langle 31 \rangle} &\rightarrow \frac{1}{2} f^{I_1 I_2 I_3} \frac{\langle 12 \rangle [\eta_2 3] \langle 3 \eta_1 \rangle}{\tilde{m}_1 \tilde{m}_2} + \frac{1}{2} f^{I_1 I_2 I_3} \left(\frac{\langle 12 \rangle \langle 2 \eta_3 \rangle \langle 3 \eta_1 \rangle}{\tilde{m}_1 m_3} + \frac{\langle 12 \rangle [\eta_2 3] \langle \eta_3 1 \rangle}{\tilde{m}_2 m_3} \right).
\end{aligned} \tag{3.75}$$

The massless coefficient f maps to the massive coupling \mathbf{f} via

$$\frac{1}{2} f^{I_1 I_2 I_3} O^{I_1 \mathbf{I}_1} O^{I_2 \mathbf{I}_2} O^{I_3 \mathbf{I}_3} \Rightarrow \mathbf{f}^{\mathbf{I}_1 \mathbf{I}_2 \mathbf{I}_3}. \quad (3.76)$$

Summing both contributions and restoring $SU(2)_{\text{LG}}$ covariance yields the complete massive VVV amplitude

$$\begin{aligned} \mathbf{M}(\mathbf{1}^1, \mathbf{2}^1, \mathbf{3}^1) = & \mathbf{f}^{\mathbf{I}_1 \mathbf{I}_2 \mathbf{I}_3} \left(\frac{[12]\langle 23 \rangle \langle 31 \rangle}{\mathbf{m}_1 \mathbf{m}_2} + \frac{[12][23]\langle 31 \rangle}{\mathbf{m}_1 \mathbf{m}_3} + \frac{[12]\langle 23 \rangle [31]}{\mathbf{m}_2 \mathbf{m}_3} \right) \\ & + \mathbf{f}^{\mathbf{I}_1 \mathbf{I}_2 \mathbf{I}_3} \left(\frac{\langle 12 \rangle [23][31]}{\mathbf{m}_1 \mathbf{m}_2} + \frac{\langle 12 \rangle \langle 23 \rangle [31]}{\mathbf{m}_1 \mathbf{m}_3} + \frac{\langle 12 \rangle [23]\langle 31 \rangle}{\mathbf{m}_2 \mathbf{m}_3} \right), \end{aligned} \quad (3.77)$$

where all terms share the same massive coefficient. In analogy to the massless case, $\mathbf{f}^{\mathbf{I}_1 \mathbf{I}_2 \mathbf{I}_3}$ is totally antisymmetric. Substituting the relevant particle types, we obtain the non-zero values,

$\mathbf{I}_1 \mathbf{I}_2 \mathbf{I}_3$	$\mathbf{f}^{\mathbf{I}_1 \mathbf{I}_2 \mathbf{I}_3}$
$W^+ W^- Z$	
$W^- Z W^+$	$\frac{1}{2} g \cos \theta_W$
$Z W^+ W^-$	
$W^- W^+ Z$	
$W^+ Z W^-$	$-\frac{1}{2} g \cos \theta_W$
$Z W^- W^+$	

4 MHC Amplitude Bootstrapping and 4-point Contact MHC amplitudes

In the previous section, the 3-pt MHC amplitudes are the necessary ingredients to build the massless-massive 3-point amplitude correspondence in the SM. In order to describe the higher-point amplitudes, one can suitably glue the 3-pt amplitudes together, which is based on the following properties of the singularity structure of scattering amplitudes with the total $\delta^{(4)}$ -momentum conservation stripped out:

- Analyticity: the singularities are restricted to only having poles and branch points;
- Locality: the singularities are further restricted to having only simple poles and branch cuts;
- Unitarity: when approaching the singularities, one or more particles go on-shell and the amplitude factorizes into lower-point amplitudes.

In the factorization limit, the amplitudes are decomposed into a product of sub-amplitudes corresponding to two distinct processes. This factorization property places stringent conditions on the simple pole structure of the massless amplitude

$$\lim_{P^2 \rightarrow 0} P^2 \mathcal{M} = M^L \times M^R, \quad (4.1)$$

where P^2 is the on-shell propagator of the immediate massless particle, and the M^L and M^R are sub-amplitudes.

For the massive amplitudes, the pole structure is different from the massless ones, which has only one simple pole structure $1/p^2$. The massive pole structure with propagator momentum \mathbf{P} takes the form $\mathbf{P}^2 - \mathbf{m}^2$. Since the MHC amplitudes decompose massive structure into large and small components, the propagator momentum should also be expanded as $\mathbf{P} = P + \eta$. Therefore, the massive pole structure decomposes as

$$\mathbf{P}^2 - \mathbf{m}^2 = P^2 + (2P \cdot \eta - \mathbf{m}^2) + \eta^2. \quad (4.2)$$

This gives three contributions at different orders. Thus, a 4-point MHC amplitude \mathcal{M}_4 with such a pole structure should have the form

$$\mathcal{M}_4 \sim \frac{N}{P^2} + \frac{N}{P^2} \frac{2P \cdot \eta - \mathbf{m}^2}{P^2} + \frac{N}{P^2} \left(\frac{(2P \cdot \eta - \mathbf{m}^2)^2}{P^4} + \frac{\eta^2}{P^2} \right) + \dots, \quad (4.3)$$

where $N = M^L \times M^R$ is the numerator, with the M^L and M^R are massive sub-amplitudes. This expansion is infinite due to the propagator. For higher-point amplitudes, each massive pole will have a corresponding expansion.

The term P^2 corresponds to a massless pole. To isolate this contribution in the MHC amplitude, we take the limit

$$\lim_{\substack{2P \cdot \eta \rightarrow \mathbf{m}^2 \\ \eta^2 \rightarrow 0}} \mathcal{M}_4 \sim \frac{M^L \times M^R}{P^2}, \quad (4.4)$$

which extracts the single-pole term, and M^L and M^R are 3-pt MHC sub-amplitudes. Using the gluing technique, we can obtain this term by further taking the limit $P^2 \rightarrow 0$, leading to

$$\lim_{P^2 \rightarrow 0} \lim_{\substack{2P \cdot \eta \rightarrow \mathbf{m}^2 \\ \eta^2 \rightarrow 0}} P^2 \mathcal{M}_4 = \sum_{h_P} M^L \times M^R, \quad (4.5)$$

where h_P is the helicity of the on-shell propagator. Once the single-pole term is obtained, the higher-order terms in eq. (4.3) can be systematically derived by expanding the massive pole $\mathbf{P}^2 - \mathbf{m}^2$.

4.1 Gluing 3-point MHC amplitudes: $u\bar{d} \rightarrow Wh$ as example

In this subsection, let us consider the massive $u\bar{d}Wh$ amplitude to illustrate the gluing technique. This amplitude has twelve helicity categories:

$$\begin{aligned} & (\pm \frac{1}{2}, \pm \frac{1}{2}, +1, 0), \quad (\pm \frac{1}{2}, \pm \frac{1}{2}, 0, 0), \quad (\pm \frac{1}{2}, \pm \frac{1}{2}, -1, 0), \\ & (\pm \frac{1}{2}, \mp \frac{1}{2}, +1, 0), \quad (\pm \frac{1}{2}, \mp \frac{1}{2}, 0, 0), \quad (\pm \frac{1}{2}, \mp \frac{1}{2}, -1, 0). \end{aligned} \quad (4.6)$$

In what follows, we choose $(+\frac{1}{2}, -\frac{1}{2}, +1, 0)$ to show the gluing procedure, and the other helicity categories can be obtained in a similar way. The amplitude has three channel

$$\mathcal{M}(1^{+\frac{1}{2}}, 2^{-\frac{1}{2}}, 3^{+1}, 4^0) = \mathcal{M}_{(12)} + \mathcal{M}_{(13)} + \mathcal{M}_{(14)}. \quad (4.7)$$

The term $\mathcal{M}_{(ij)}$ corresponds to the term with single pole $P_{ij} = p_i + p_j$. Let us consider them one by one.

(14)-channel We first consider the (14) channel, where the internal line corresponds to a u quark propagator. The relevant 3-pt sub-amplitudes are

$$\begin{array}{c}
 \text{1}^- \quad \text{4}^0 \\
 \text{---} \quad \text{---} \\
 \text{1}^- \quad \text{4}^0 \\
 \text{---} \quad \text{---} \\
 \text{2}^+ \quad \text{3}^- \\
 \end{array}
 = y_u^u \langle 1P_{14} \rangle, \quad (4.8)$$

$$\begin{array}{c}
 \text{1}^- \quad \text{4}^0 \\
 \text{---} \quad \text{---} \\
 \text{1}^- \quad \text{4}^0 \\
 \text{---} \quad \text{---} \\
 \text{2}^+ \quad \text{3}^- \\
 \end{array}
 = y_u^u \frac{m_1}{\mathbf{m}_1} \frac{m_{14}}{\mathbf{m}_{14}} [\eta_1 \eta_{14}], \quad (4.9)$$

$$\begin{array}{c}
 \text{1}^- \quad \text{4}^0 \\
 \text{---} \quad \text{---} \\
 \text{1}^- \quad \text{4}^0 \\
 \text{---} \quad \text{---} \\
 \text{2}^+ \quad \text{3}^- \\
 \end{array}
 = -\sqrt{2} (X_1^{W^-})_d^u \frac{\tilde{m}_3}{\mathbf{m}_3} \frac{\tilde{m}_{14}}{\mathbf{m}_{14}} \frac{[2\eta_3] \langle 3\eta_{14} \rangle}{\mathbf{m}_3}, \quad (4.10)$$

where $P_{14} \equiv p_1 + p_4$, $\eta_{14} \equiv \eta_1 + \eta_4$, and particle P is taken to be the internal fermion. The first line and second lines correspond to the $u\bar{u}h$ amplitude, while the third line corresponds to the $u\bar{d}W^-$ amplitude.

In the factorized limit, we sum over helicities of internal particle. When a particle line with a chirality flip is glued to one without chirality flip, two helicity combinations contribute to one propagator

$$\left\{ \begin{array}{l} \bullet \text{---} P^- \quad P^+ \text{---} \times \bullet = \tilde{m} \eta_\alpha \times \lambda^\beta \\ \bullet \text{---} \times \text{---} P^+ \quad P^- \text{---} \bullet = -\lambda_\alpha \times \tilde{m} \eta_\beta \end{array} \right. \Rightarrow \bullet \text{---} \times \text{---} \bullet = \mathbf{m}^2 \epsilon_{\alpha\beta}. \quad (4.11)$$

The resulting structure is for the propagator, which carries zero helicity and transversality, and its chirality-flip nature is encoded in the Levi-Civita tensor $\epsilon_{\alpha\beta}$. Using this method, we glue the 3-pt sub-amplitudes from eq. (4.8) and (4.10) to obtain

$$\begin{array}{c}
 \text{1}^- \quad \text{4}^0 \\
 \text{---} \quad \text{---} \\
 \text{1}^- \quad \text{4}^0 \\
 \text{---} \quad \text{---} \\
 \text{2}^+ \quad \text{3}^- \\
 \end{array}
 \Rightarrow -\sqrt{2} y_u^u (X_1^{W^-})_d^u \frac{\tilde{m}_3}{\mathbf{m}_3^2} \mathbf{m}_{14} \langle 13 \rangle [\eta_3 2], \quad (4.12)$$

where \mathbf{m}_{14} is the u quark mass. It exhibit a different power of \mathbf{m}_{14} from eq. (4.11), due to a $1/\mathbf{m}_{14}$ factor in the 3-point sub-amplitude.

If we glue two particle lines both without chirality flips or both with chirality flips, we obtain the internal fermion in other two orders

$$\begin{array}{l}
 \bullet \text{---} P^+ \quad P^- \text{---} \bullet = \tilde{\lambda}_{\dot{\alpha}} \times \lambda_\beta \quad \Rightarrow \quad \bullet \text{---} \bullet = P_{\beta\dot{\alpha}}, \\
 \bullet \text{---} \times \text{---} P^+ \quad P^- \text{---} \times \bullet = m \tilde{\eta}_{\dot{\alpha}} \times \tilde{m} \eta_\beta \quad \Rightarrow \quad \bullet \text{---} \times \text{---} \times \bullet = \mathbf{m}^2 \eta_{\beta\dot{\alpha}}. \end{array} \quad (4.13)$$

In the right-hand side of the second line, the glued internal line is shown without color change for convenience, since two chirality flips on a fermion do not produce a Levi-Civita tensor, making it equivalent to the non-flip representation. These correspond to the 3-pt sub-amplitudes given in eqs. (4.9) and (4.10). Gluing them, we obtain

$$\begin{array}{c}
 \text{Diagram 1: } \begin{array}{c} 1^- \\ 2^+ \\ 1^- \\ 2^+ \end{array} \xrightarrow{\text{glue}} \begin{array}{c} 4^0 \\ 3^- \\ 4^0 \\ 3^- \end{array} \Rightarrow \sqrt{2} y_{\bar{u}}^u (X_1^{W^-})_d^u \frac{\tilde{m}_3}{\mathbf{m}_3^2} \frac{m_1}{\mathbf{m}_1} [\eta_1 | P_{14} | 3 \rangle [\eta_3 2], \\
 \text{Diagram 2: } \begin{array}{c} 1^- \\ 2^+ \\ 1^- \\ 2^+ \end{array} \xrightarrow{\text{glue}} \begin{array}{c} 4^0 \\ 3^- \\ 4^0 \\ 3^- \end{array} \Rightarrow \sqrt{2} y_{\bar{u}}^u (X_1^{W^-})_d^u \frac{\tilde{m}_3}{\mathbf{m}_3^2} \frac{m_1}{\mathbf{m}_1} [\eta_1 | \eta_{14} | 3 \rangle [\eta_3 2].
 \end{array} \quad (4.14)$$

After accounting for the $1/\mathbf{m}$ factors in the 3-pt sub-amplitudes, neither of these results contain a factor of \mathbf{m}_{14} . Summing over contributions from all three diagrams and restoring the denominator, the final result takes the form

$$\mathcal{M}_t = \sqrt{2} y_{\bar{u}}^u (X_1^{W^-})_d^u \frac{\tilde{m}_3}{\mathbf{m}_3^2} \frac{\mathbf{m}_{14} \langle 13 \rangle [\eta_3 2]}{s_{14}} + \sqrt{2} y_{\bar{u}}^u (X_1^{W^-})_d^u \frac{\tilde{m}_3}{\mathbf{m}_3^2} \frac{m_1}{\mathbf{m}_1} \frac{[\eta_1 | P_{14} + \eta_{14} | 3 \rangle [\eta_3 2]}{s_{14}}, \quad (4.15)$$

where the massless pole is given by $s_{14} = P_{14}^2$.

(13)-channel We now turn to the (13) channel, where the internal line also corresponds to a d quark propagator. In this case, we glue the $d\bar{d}h$ and $u\bar{d}W^-$ amplitudes. The gluing results are

$$\begin{array}{c}
 \text{Diagram 1: } \begin{array}{c} 1^- \\ 2^+ \\ 1^- \\ 2^+ \end{array} \xrightarrow{\text{glue}} \begin{array}{c} 3^- \\ 4^0 \\ 3^- \\ 4^0 \end{array} \Rightarrow \sqrt{2} (X_1^{W^-})_{\bar{d}}^u y_d^u \frac{\tilde{m}_3}{\mathbf{m}_3} \mathbf{m}_{13} \langle 13 \rangle [\eta_3 2], \\
 \text{Diagram 2: } \begin{array}{c} 1^- \\ 2^+ \\ 1^- \\ 2^+ \end{array} \xrightarrow{\text{glue}} \begin{array}{c} 3^- \\ 4^0 \\ 3^- \\ 4^0 \end{array} \Rightarrow \sqrt{2} (X_1^{W^-})_{\bar{d}}^u y_d^u \frac{\tilde{m}_3}{\mathbf{m}_3^2} \frac{\tilde{m}_2}{\mathbf{m}_2} \langle 1 \eta_3 \rangle [3 | P_{13} | \eta_2 \rangle,
 \end{array} \quad (4.16)$$

$$\begin{array}{c}
 \text{Diagram 3: } \begin{array}{c} 1^- \\ 2^+ \\ 1^- \\ 2^+ \end{array} \xrightarrow{\text{glue}} \begin{array}{c} 3^- \\ 4^0 \\ 3^- \\ 4^0 \end{array} \downarrow J_{13}^+ J_{13}^- \Rightarrow \sqrt{2} (X_1^{W^-})_{\bar{d}}^u y_d^u \frac{\tilde{m}_3}{\mathbf{m}_3^2} \frac{\tilde{m}_2}{\mathbf{m}_2} \langle 1 \eta_3 \rangle [3 | \eta_{13} | \eta_2 \rangle.
 \end{array} \quad (4.17)$$

$$\begin{array}{c}
 \text{Diagram 4: } \begin{array}{c} 1^- \\ 2^+ \\ 1^- \\ 2^+ \end{array} \xrightarrow{\text{glue}} \begin{array}{c} 3^- \\ 4^0 \\ 3^- \\ 4^0 \end{array} \Rightarrow \sqrt{2} (X_1^{W^-})_{\bar{d}}^u y_d^u \frac{\tilde{m}_3}{\mathbf{m}_3^2} \frac{\tilde{m}_2}{\mathbf{m}_2} \langle 1 \eta_3 \rangle [3 | \eta_{13} | \eta_2 \rangle.
 \end{array} \quad (4.18)$$

The results in last two lines can be related by the operator $J_{13}^+ J_{13}^-$. Here the first diagram corresponds to a chirality flip on the internal line, while the second and third diagrams involve no chirality flip. These diagrams are structurally similar to those in the (12) channel, but with particles 3 and 4 exchanged.

Summing the three contributions and including the propagator denominator, the (13)-channel amplitude is given by

$$\mathcal{M}_{(13)} = \sqrt{2}(X_1^{W^-})_{\bar{d}y'd}^u \frac{\tilde{m}_3}{\mathbf{m}_3^2} \frac{\mathbf{m}_{13} \langle 13 \rangle [\eta_3 2]}{s_{13}} + \sqrt{2}(X_1^{W^-})_{\bar{d}y'd}^u \frac{\tilde{m}_3}{\mathbf{m}_3^2} \frac{\tilde{m}_2}{\mathbf{m}_2} \frac{\langle 1 \eta_3 \rangle [3 | P_{13} + \eta_{13} | \eta_2 \rangle}{s_{13}}. \quad (4.19)$$

(12)-channel The final contribution comes from the (12) channel, where the internal particle is a W boson. Here, we glue two particle lines with zero, one, or two chirality flips to form the internal vector boson in several different orders:

$$\bullet \text{~~~~~} P^0 \text{~~~~~} P^0 \text{~~~~~} \bullet = \frac{1}{2} \tilde{\lambda}_{\dot{\alpha}} \lambda_{\alpha} \times \tilde{\lambda}_{\dot{\beta}} \lambda_{\beta}, \quad (4.20)$$

$$\left\{ \begin{array}{l} \bullet \text{~~~~~} P^+ \text{~~~~~} P^- \text{~~~~~} \bullet = -m \tilde{\eta}_{\dot{\alpha}} \lambda_{\alpha} \times \tilde{\lambda}_{\dot{\beta}} \tilde{m} \eta_{\beta}, \\ \bullet \text{~~~~~} P^- \text{~~~~~} P^0 \text{~~~~~} \bullet = -\tilde{\lambda}_{\dot{\alpha}} \tilde{m} \eta_{\alpha} \times m \tilde{\eta}_{\dot{\beta}} \lambda_{\beta}, \\ \bullet \text{~~~~~} P^0 \text{~~~~~} P^0 \text{~~~~~} \bullet = +\frac{1}{2} m \tilde{\eta}_{\dot{\alpha}} \tilde{m} \eta_{\alpha} \times \tilde{\lambda}_{\dot{\beta}} \lambda_{\beta}, \\ \bullet \text{~~~~~} P^0 \text{~~~~~} P^0 \text{~~~~~} \bullet = +\frac{1}{2} \tilde{\lambda}_{\dot{\alpha}} \lambda_{\alpha} \times m \tilde{\eta}_{\dot{\beta}} \tilde{m} \eta_{\beta}, \end{array} \right. \quad (4.21)$$

$$\bullet \text{~~~~~} P^0 \text{~~~~~} P^0 \text{~~~~~} \bullet = \frac{1}{2} m \tilde{\eta}_{\dot{\alpha}} \tilde{m} \eta_{\alpha} \times m \tilde{\eta}_{\dot{\beta}} \tilde{m} \eta_{\beta}, \quad (4.22)$$

When we glue two external diagrams with helicity \pm , the resulting internal diagram has multiple representations. since $m\tilde{m} = \tilde{m}m$, their effects are quite similar we will use the same color to represent different diagrams, like the following

$$\bullet \text{~~~~~} \text{red} \text{~~~~~} \text{red} \text{~~~~~} \bullet = \bullet \text{~~~~~} \text{blue} \text{~~~~~} \text{blue} \text{~~~~~} \bullet. \quad (4.23)$$

Using this notation, we obtain the following three kinds of propagators

$$\bullet \text{~~~~~} \bullet = \frac{1}{2} p_{\alpha\dot{\alpha}} p_{\beta\dot{\beta}}, \quad (4.24)$$

$$\bullet \text{~~~~~} \bullet = \mathbf{m}^4 \epsilon_{\alpha\beta} \epsilon_{\alpha\dot{\beta}} - \mathbf{m}^2 \frac{1}{2} p_{\alpha\dot{\alpha}} \eta_{\beta\dot{\beta}} - \mathbf{m}^2 \frac{1}{2} \eta_{\alpha\dot{\alpha}} p_{\beta\dot{\beta}}, \quad (4.25)$$

$$\bullet \text{~~~~~} \bullet = \frac{1}{2} \mathbf{m}^4 \eta_{\alpha\dot{\alpha}} \eta_{\beta\dot{\beta}}. \quad (4.26)$$

Using these rules, we glue the W^+W^-h and $u\bar{d}W^-$ sub-amplitudes to obtain the three contributions



$$\Rightarrow \langle 1 | P_{12} | 2 \rangle [\eta_3 | P_{12} | 3 \rangle, \quad (4.27)$$

$\downarrow J_{12}^+ J_{12}^- \text{ & add } \mathbf{m}^2 \text{ contribution}$

$$\Rightarrow -2\mathbf{m}_{12}^2 \langle 13 | 2\eta_3 \rangle + \langle 1 | P_{12} | 2 \rangle [\eta_3 | \eta_{12} | 3 \rangle + \langle 1 | \eta_{12} | 2 \rangle [\eta_3 | P_{12} | 3 \rangle], \quad (4.28)$$

$\downarrow J_{12}^+ J_{12}^-$

$$\Rightarrow \langle 1 | \eta_{12} | 2 \rangle [\eta_3 | \eta_{12} | 3 \rangle, \quad (4.29)$$

where \mathbf{m}_{12} is the physical mass of the internal W boson. These three contributions can be related by the operator $J_{12}^+ J_{12}^-$. This extra term is proportional to the square of the internal particle mass, \mathbf{m}^2 . All these contributions share the same coefficient $(X_1^{W^-})_d^u \mathbf{g}^{W^+ W^-}$ from the two 3-pt sub-amplitudes.

After restoring the denominator s_{12} and summing over three contributions in this channel, we obtain

$$\mathcal{M}_{(12)} = \sqrt{2} (X_1^{W^-})_d^u \mathbf{g}^{W^+ W^-} \frac{-2\mathbf{m}_{12}^2 \langle 13 | 2\eta_3 \rangle + \langle 1 | P_{12} + \eta_{12} | 2 \rangle [\eta_3 | P_{12} + \eta_{12} | 3 \rangle]}{s_{12}}. \quad (4.30)$$

Ladder operator applied to internal particle In above calculation, we note that while the external particles are in the same order, while the propagator belongs to different order. Therefore, once the leading-order propagator is known, all the sub-leading order propagators should be obtained by the ladder operator.

We note that the MHC internal particles are obtained by gluing two external particle states with opposite helicity. Therefore, they always have total helicity 0. In this case, we must apply the ladder operator twice, defined as

$$\frac{m}{\mathbf{m}} J^- \frac{\tilde{m}}{\mathbf{m}} J^+ = J^- J^+, \quad (4.31)$$

which does not change the helicity.

For an internal fermion, acting with $J^- J^+$ on the primary internal particle state yields both the primary and descendant states,

$$\bullet \rightarrow \bullet = p_{\alpha\beta} \quad \xrightarrow{J^- J^+} \quad \left\{ \begin{array}{l} \bullet \rightarrow \bullet = p_{\alpha\beta}, \\ \bullet \rightarrow \times \rightarrow \bullet = \eta_{\alpha\beta}. \end{array} \right. \quad (4.32)$$

Conversely, the primary internal state can also be obtained from the descendant state by acting with $J^- J^+$.

For a vector state, acting with $J^- J^+$ generates all particle states. Starting from a given primary internal vector state, one and two applications yield:

$$\begin{aligned}
 \bullet \text{---} \text{wavy line} \bullet &= p_{(\dot{\alpha}_1} p_{\dot{\alpha}_2)}^{(\beta_1 \beta_2)} \xrightarrow{J^- J^+} \begin{cases} \bullet \text{---} \text{wavy line} \bullet = p_{(\dot{\alpha}_1} p_{\dot{\alpha}_2)}^{(\beta_1 \beta_2)}, \\ \bullet \text{---} \text{crossed wavy line} \bullet = p_{(\dot{\alpha}_1} \eta_{\dot{\alpha}_2)}^{(\beta_1 \beta_2)}, \end{cases} \\
 \bullet \text{---} \text{wavy line} \bullet &= p_{(\dot{\alpha}_1} p_{\dot{\alpha}_2)}^{(\beta_1 \beta_2)} \xrightarrow{(J^- J^+)^2} \begin{cases} \bullet \text{---} \text{crossed wavy line} \bullet = p_{(\dot{\alpha}_1} \eta_{\dot{\alpha}_2)}^{(\beta_1 \beta_2)}, \\ \bullet \text{---} \text{crossed wavy line} \bullet = \eta_{(\dot{\alpha}_1} \eta_{\dot{\alpha}_2)}^{(\beta_1 \beta_2)}. \end{cases}
 \end{aligned} \tag{4.33}$$

Starting from a 1st or 2nd descendant state, one or two applications of $J^- J^+$ similarly produce all states.

Other internal states can be obtained analogously by acting with $J^- J^+$, with one exception: the internal vector state represented by a brown line. In this case, a term $\mathbf{m}^2 \epsilon_{\alpha\beta} \epsilon_{\dot{\alpha}\dot{\beta}}$ appearing in the 1st descendant state cannot be generated by $J^- J^+$ and must be inserted by hand:

$$\bullet \text{---} \text{brown line} \bullet = p_{\alpha\dot{\alpha}} p_{\beta\dot{\beta}} \xrightarrow[\text{add } \mathbf{m}^2 \epsilon^2]{J^- J^+} \begin{cases} \bullet \text{---} \text{brown line} \bullet = p_{\alpha\dot{\alpha}} p_{\beta\dot{\beta}}, \\ \bullet \text{---} \text{crossed brown line} \bullet = \mathbf{m}^2 \epsilon_{\alpha\beta} \epsilon_{\dot{\alpha}\dot{\beta}} - p_{\alpha\dot{\alpha}} \eta_{\beta\dot{\beta}} - \eta_{\alpha\dot{\alpha}} p_{\beta\dot{\beta}}, \end{cases} \tag{4.34}$$

$$\bullet \text{---} \text{brown line} \bullet = p_{\alpha\dot{\alpha}} p_{\beta\dot{\beta}} \xrightarrow[\text{add } \mathbf{m}^2 \epsilon^2]{J^- J^+} \begin{cases} \bullet \text{---} \text{crossed brown line} \bullet = \mathbf{m}^4 \epsilon_{\alpha\beta} \epsilon_{\dot{\alpha}\dot{\beta}} - \mathbf{m}^2 p_{\alpha\dot{\alpha}} \eta_{\beta\dot{\beta}} - \mathbf{m}^2 \eta_{\alpha\dot{\alpha}} p_{\beta\dot{\beta}}, \\ \bullet \text{---} \text{crossed brown line} \bullet = \mathbf{m}^4 \eta_{\alpha\dot{\alpha}} \eta_{\beta\dot{\beta}}. \end{cases} \tag{4.35}$$

total amplitude From the above ladder operator action, we can only calculate the leading MHC amplitude by gluing the leading 3-point amplitudes, and then apply the ladder operator to obtain the full MHC results. Summing over the contributions in all three channels, the leading MHC amplitudes read

$$\begin{aligned}
 & \text{Diagram 1: } 1^- \text{---} \text{wavy line} \text{---} 4^0 + 1^- \text{---} \text{wavy line} \text{---} 3^- + 1^- \text{---} \text{wavy line} \text{---} 3^- + 1^- \text{---} \text{wavy line} \text{---} 4^0 \\
 &= \sqrt{2} y_{\bar{u}}^u (X_1^{W^-})_d^u \frac{\tilde{m}_3}{\mathbf{m}_3^2} \frac{m_1}{\mathbf{m}_1} [\eta_1 | P_{14} | 3] [\eta_3 | 2] + \sqrt{2} (X_1^{W^-})_d^u y_d^d \frac{\tilde{m}_3}{\mathbf{m}_3} \mathbf{m}_{13} \langle 13 | [\eta_3 | 2] \\
 & \quad + \sqrt{2} (X_1^{W^-})_d^u y_d^d \frac{\tilde{m}_3}{\mathbf{m}_3^2} \frac{\tilde{m}_2}{\mathbf{m}_2} \langle 1 | \eta_3 \rangle [3 | P_{13} | \eta_2] + \langle 1 | P_{12} | 2] [\eta_3 | P_{12} | 3]. \tag{4.36}
 \end{aligned}$$

Add the sub-leading propagator contributions using the ladder operators and add single pole structure, we obtain the total amplitude:

$$\begin{aligned}
 \mathcal{M}(1^{+\frac{1}{2}}, 2^{-\frac{1}{2}}, 3^{+1}, 4^0) &= \sqrt{2} y_{\bar{u}}^u (X_1^{W^-})_d^u \frac{\tilde{m}_3}{\mathbf{m}_3^2} \frac{\mathbf{m}_{14} \langle 13 \rangle [\eta_3 | 2]}{s_{14}} + \sqrt{2} y_{\bar{u}}^u (X_1^{W^-})_d^u \frac{\tilde{m}_3}{\mathbf{m}_3^2} \frac{m_1 [\eta_1 | P_{14} + \eta_{14} | 3] [\eta_3 | 2]}{s_{14}} \\
 & \quad + \sqrt{2} (X_1^{W^-})_d^u y_d^d \frac{\tilde{m}_3}{\mathbf{m}_3^2} \frac{\mathbf{m}_{13} \langle 13 \rangle [\eta_3 | 2]}{s_{13}} + \sqrt{2} (X_1^{W^-})_d^u y_d^d \frac{\tilde{m}_3}{\mathbf{m}_3^2} \frac{\tilde{m}_2 \langle 1 | \eta_3 \rangle [3 | P_{13} + \eta_{13} | \eta_2]}{s_{13}} \\
 & \quad + \sqrt{2} (X_1^{W^-})_d^u \mathbf{g}^{W^+ W^-} \frac{-2 \mathbf{m}_{12}^2 \langle 13 \rangle [2 | \eta_3] + \langle 1 | P_{12} + \eta_{12} | 2] [\eta_3 | P_{12} + \eta_{12} | 3]}{s_{12}}. \tag{4.37}
 \end{aligned}$$

The same procedure can be applied to the MHC amplitudes involving in pure gauge sector, such as the $WW \rightarrow hh$ amplitude. Similar to the $u\bar{d} \rightarrow Wh$ amplitudes, the $WW \rightarrow hh$ amplitude has the same topologies

$$\mathcal{M} = \underbrace{\mathcal{M}_{(12)} + \mathcal{M}_{(13)} + \mathcal{M}_{(14)}}_{\mathcal{M}_f} . \quad (4.38)$$

Using the gluing technique, each channel amplitudes can be constructed. For each channel, the corresponding internal particle and sub-amplitudes are

channel	sub-amplitudes	internal particle
(12)-channel	$WWh \times hhh$	h
(13)-channel		
(14)-channel	$WWh \times WWh$	W

This shows that we can use two types of 3-point amplitudes, WWh and hhh , to construct the $WWhh$ amplitude. However, the result does not match the correct amplitudes, and we will show a 4-point contact MHC amplitude is needed for $WW \rightarrow hh$, while the amplitude $u\bar{d} \rightarrow Wh$ does not need any 4-pt contact amplitude.

4.2 Massless and MHC amplitudes in light-cone gauge

From the 3-point massless-MHC amplitude matching, we learned that a MHC amplitude should be deformed from massless amplitudes. For the 3-point MHC amplitudes involving in gauge boson A , it should be matched from massless amplitudes in the light-cone gauge. We expect a 4-point MHC amplitude should be equivalent to the massless amplitudes in the light-cone gauge. Let us first investigate the on-shell massless amplitudes in two different ways: gauge-independent description, and gauge-dependent (light-cone gauge) description.

In a renormalizable pure gauge theory, all physical information is encoded in the three-point vertices. Four-point vertices are required only to ensure the gauge invariance of the complete scattering amplitude. There exist three distinct conceptual descriptions of scattering amplitudes, distinguished by their treatment of on-shell/off-shell states and gauge (in)dependence:

- *Off-shell Feynman rule description*: The standard Feynman rules yield off-shell vertices that are not individually gauge invariant. For example, in the Yang-Mills theory, although the cubic term $A^2 \partial A$ captures the information needed for the amplitudes, the quartic term A^4 is needed for the requirements of the off-shell gauge invariance of the Lagrangian.
- *On-shell Gauge invariant description*: In the on-shell description, the scattering amplitude are written entirely in terms of massless spinors $|p]$ and $|p\rangle$. Different from the Feynman rule description, the 3-point on-shell amplitude is gauge invariant, for example, the 3-point VVV amplitudes are

$$A(+1, +1, -1) = \frac{[12]^3}{[23][31]}, \quad A(-1, -1, +1) = \frac{\langle 12 \rangle^3}{\langle 23 \rangle \langle 31 \rangle}, \quad (4.40)$$

and thus the 4-point $VVVV$ amplitude is not needed since the 4-point $VVVV$ contains no new on-shell information. Therefore, two 3-point VVV amplitudes are bootstrapped to obtain the four-gluon scattering amplitude, which can be written as

$$\mathcal{A}[1^-, 2^-, 3^+, 4^+] = \frac{\langle 12 \rangle^2 [34]^2}{s_{12}s_{14}}. \quad (4.41)$$

The form of this 4-pt amplitude is quite compact and the pole structure is obscure, since each s , t , u channel is not separable.

- *On-shell Gauge dependence description:* For a massless amplitude involving in gauge boson A , the gauge boson state is described using the Lorentz $(\frac{1}{2}, \frac{1}{2})$ representation

$$A_{\alpha\dot{\alpha}}^+ : \frac{\xi_\alpha \tilde{\lambda}_{\dot{\alpha}}}{\langle \xi \lambda \rangle}, \quad A_{\alpha\dot{\alpha}}^- : -\frac{\lambda_\alpha \tilde{\xi}_{\dot{\alpha}}}{[\tilde{\lambda} \tilde{\xi}]}.$$
(4.42)

Here ξ and $\tilde{\xi}$ are reference spinors introduced to construct the $(\frac{1}{2}, \frac{1}{2})$ representation. These spinors correspond to the reference vector n in the light-cone gauge,

$$n \cdot A^\pm \equiv \xi^\alpha \tilde{\xi}^\dot{\alpha} A_{\alpha\dot{\alpha}}^\pm = 0. \quad (4.43)$$

In this description, although the amplitude is on-shell, the 3-point amplitude, made on-shell by complex momenta, is gauge dependent due to the reference spinor ξ , and thus the 4-point contact amplitude is needed to ensure the gauge dependence. This is quite similar to the Feynman rule description. However, there are also differences: the propagator is put to on-shell by factorization, while the propagator is off-shell in the Feynman rule description.

Since the on-shell gauge-independent description has already been discussed in literature, we now focus on the gauge-dependent description for comparison. As an example, we consider scalar QED in this language. In this theory, there exists a two-particle current J , which also transforms as a $(\frac{1}{2}, \frac{1}{2})$ representation:

$$J^{\alpha\dot{\alpha}} = p_1^{\alpha\dot{\alpha}} - p_2^{\alpha\dot{\alpha}}. \quad (4.44)$$

This corresponds to the Noether current of scalar field, $\phi^* D_\mu \phi - D_\mu \phi^* \phi$. Thus, the 3-pt massless amplitude can be written as the coupling of this current to the gauge boson,

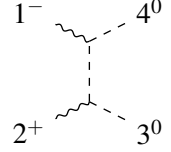
$$\mathcal{A}(1^0, 2^0, 3^\pm) = J \cdot A^\pm, \quad (4.45)$$

where the superscripts denote the helicity. Thus in scalar QED, the two 3-pt amplitudes with different helicity are

$$\begin{aligned}
& \text{Diagram 1: } 1^0 \text{---} \text{[wavy line]}^2 \text{---} 3^- = \mathcal{A}(1^0, 2^0, 3^-) = \frac{e}{\sqrt{2}} \frac{\langle \xi_3 | 1 - 2 | 3 \rangle}{\langle \xi_3 | 3 \rangle}, \\
& \text{Diagram 2: } 1^0 \text{---} \text{[wavy line]}^2 \text{---} 3^+ = \mathcal{A}(1^0, 2^0, 3^+) = \frac{e}{\sqrt{2}} \frac{\langle 3 | 1 - 2 | \xi_3 \rangle}{[3 | \xi_3]}, \tag{4.46}
\end{aligned}$$

where e is the coupling constant in scalar QED.

Then we consider the 4-pt amplitude in scalar QED. We now examine a $\gamma\gamma\phi\phi^*$ amplitude, which is similar to the massless $WWHH^\dagger$ amplitude. The massless $\gamma\gamma\phi\phi^*$ amplitude in helicity $(-1, +1, 0, 0)$ receives contributions from the (13)-channel, the (14)-channel, and a contact term. For the (14)-channel, the amplitude can be obtained by gluing two 3-pt amplitudes,

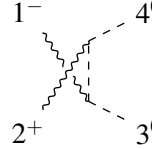


$$= \mathcal{A}(1^-, 4^0, -P_{14}^0) \times \frac{1}{s_{14}} \times \mathcal{A}(P_{14}^0, 2^+, 3^0). \quad (4.47)$$

Substituting Eq. (4.46) with appropriate relabeling gives

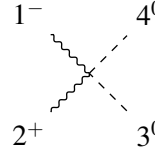
$$\frac{e}{\sqrt{2}} \frac{\langle \xi_1 | 4 + P_{14} | 1 \rangle}{\langle \xi_1 | 1 \rangle} \times \frac{1}{s_{14}} \times \frac{e}{\sqrt{2}} \frac{\langle 2 | 3 + P_{13} | \xi_2 \rangle}{[3 \xi_3]} = 2e^2 \frac{\langle \xi_1 | 4 | 1 \rangle \langle 2 | 3 | \xi_2 \rangle}{s_{14} \langle \xi_1 | 1 \rangle [2 \xi_2]}. \quad (4.48)$$

Similarly, the (13)-channel gives



$$= 2e^2 \frac{-\langle \xi_1 | 3 | 1 \rangle \langle 2 | 4 | \xi_2 \rangle}{s_{13} \langle \xi_1 | 1 \rangle [2 \xi_2]}. \quad (4.49)$$

These two contributions depend on the gauge parameters $|\xi_1\rangle$ and $|\xi_2\rangle$. To obtain a gauge-invariant amplitude, we must include a contact term,



$$= -2e^2 \frac{\langle \xi_1 | 2 | 1 \xi_2 \rangle}{\langle \xi_1 | 1 \rangle [2 \xi_2]}. \quad (4.50)$$

Combining all three contributions, we obtain the total amplitude for $\phi^*\phi \rightarrow \gamma\gamma$,

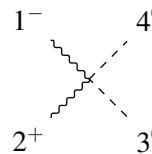
$$\mathcal{A}(1^-, 2^+, 3, 4) = \frac{2e^2}{\langle \xi_1 | 1 \rangle [2 \xi_2]} \left(\frac{\langle \eta_1 | 4 | 1 \rangle \langle 2 | 3 | \eta_2 \rangle}{s_{14}} + \frac{\langle \eta_1 | 3 | 1 \rangle \langle 2 | 4 | \eta_2 \rangle}{s_{13}} - \langle \eta_1 | 2 | 1 \eta_2 \rangle \right). \quad (4.51)$$

One can check that this amplitude is independent of the gauge choice. After some algebra, it simplifies to

$$\mathcal{A}(1^-, 2^+, 3^0, 4^0) = \frac{e^2}{2} \frac{\langle 1 | 3 - 4 | 2 \rangle^2}{s_{13} s_{14}}. \quad (4.52)$$

The spurious poles $\langle \xi_1 | 1 \rangle$ and $[2 \xi_2]$ cancel in the final expression. On the other hand, the physical pole structure is not so transparent as the gauge-dependent description.

Similar to the 3-point amplitude matching, the massless contact $VVSS$ amplitude



$$= \frac{\langle \xi_1 | 2 | 1 \xi_2 \rangle}{\langle \xi_1 | 1 \rangle [2 \xi_2]} \quad (4.53)$$

should match to the contact $VVSS$ MHC amplitudes, where we ignore the overall coefficient for now. Taking the gauge $\xi_i = \eta_i$, we have the MHC amplitude

$$\begin{array}{ccc}
 + & 0 & \\
 \diagup & & \diagdown \\
 \text{---} & & \text{---} \\
 - & 0 &
 \end{array} = \frac{\langle \eta_1 2 | 1 \eta_2 \rangle}{m_1 \tilde{m}_2}, \quad (4.54)$$

which contains the gauge dependence. Similarly we should obtain other MHC $VVSS$ amplitudes in other helicity categories, by the ladder operators $\frac{m}{m} J^-$ and $\frac{\tilde{m}}{m} J^+$. Inversely using the ladder operators, the primary $VVSS$ amplitude is obtained to be

$$\begin{array}{ccc}
 1^0 & 4^0 & \\
 \diagup & & \diagdown \\
 \text{---} & & \text{---} \\
 2^0 & 3^0 &
 \end{array} = \frac{\langle 12 \rangle [21]}{\mathbf{m}_1 \mathbf{m}_2}. \quad (4.55)$$

Unlike the 3-point primary MHC amplitude involving the gauge boson, this primary MHC amplitude is non-vanishing. Thus there exists $VVSS$ contact amplitude in the light cone gauge. To make sure the $WW \rightarrow hh$ amplitude gauge invariant, the contact amplitude is needed.

4.3 Contact 4-point MHC amplitudes

Similar to the 3-point MHC primary and descendant amplitudes, let us classify all the contact 4-point MHC primary amplitudes and obtain the descendant 4-point contact amplitudes in the SM.

From massless-massive correspondence, the 4-point primary MHC amplitudes should be matched from the 4-point massless amplitudes. If the massless amplitudes with certain helicity belong to the EFT category, we would classify them to be the EFT MHC amplitudes. Otherwise, it would be the 4-point contact MHC amplitudes in the SM. The classification is as follows

Primary MHC	helicity class	helicity category	amplitudes
SSSS	$n_T = 0$	$(0, 0, 0, 0)$	1
FFSS, FFVS FFVV, FFFF	$n_T \geq 0$	EFT	-
VVSS	$n_T = 0$	$(0, 0, 0, 0)$	$\langle 12 \rangle [21]$
	$n_T > 0$	EFT	-
VVVS	$n_T \geq 0$	EFT	-
VVVV	$n_T = 0$	$(0, 0, 0, 0)$	$(\langle 12 \rangle [21] \langle 34 \rangle [34] + \text{cycle})$
	$n_T > 0$	EFT	-
higher-point		All belong to EFT	-

Here all the 4-point contact amplitudes involving in fermions belong to the EFT categories. Only the $(0, 0, 0, 0)$ helicity categories of the SSSS, VVSS, and VVVV are the SM amplitudes, in which all the

vector bosons in the amplitudes should be the Goldstone boson. All others should be the EFT primary amplitudes, or the descendant amplitudes in the SM or EFT. For example, $(+1, -1, 0, 0)$ of the VVSS amplitude is either the descendant amplitude obtained from $(0, 0, 0, 0)$ by ladder operators, or the EFT one.

Analogous to the construction of 3-point MHC amplitudes, after obtaining the 4-point primary amplitudes, the descendant amplitudes are derived by repeatedly applying the ladder operators mJ^- or $\tilde{m}J^+$ to the primary amplitudes. Applying one such operator to a specific particle flips its helicity and yields the corresponding first descendant current; successive applications generate higher descendants:

$$\begin{aligned} [\mathcal{M}]_1 &= mJ^- \circ [\mathcal{M}]_0 + \tilde{m}J^+ \circ [\mathcal{M}]_0, \\ [\mathcal{M}]_2 &= (mJ^-)^2 \circ [\mathcal{M}]_0 + (\tilde{m}J^+ mJ^-) \circ [\mathcal{M}]_0 + (\tilde{m}J^+)^2 \circ [\mathcal{M}]_0, \\ &\vdots \end{aligned} \quad (4.57)$$

There are two equivalent ways to obtain the 4-point MHC contact amplitudes:

- Starting from one MHC amplitude, we can apply the ladder operators $\frac{\tilde{m}}{m}J^+$ and $\frac{m}{\tilde{m}}J^+$ to obtain any other MHC amplitude. First obtain the primary amplitudes with all gauge bosons identified as the Goldstone boson, then use ladder operator to obtain all the descendant ones. In this way, the Lorentz structure is systematically obtained, and the gauge structure is matched from the massless ones.
- First obtain the descendant ones with all the transverse gauge boson, then use ladder operator to obtain others including the primary one. In this way, it is easier to implement the gauge structure from the massless UV SM.

Note again the primary 4-point contact amplitudes are non-vanishing, unlike the 3-point amplitudes due to the momentum conservation. In the following we will use both ways to obtain the matched gauge structures.

VVSS Contact Amplitudes Consider the $WWhh$ MHC contact amplitude. In the SM, the possible helicity categories for the corresponding primary and descendant amplitudes are as follows:

amplitude		helicity
primary		(0000)
descendant	1st	$(\pm 000), (0 \pm 00)$
	2nd	$(0000), (\pm \mp 00), (\pm \pm 00)$
	3rd	$(\pm 000), (0 \pm 00)$
	4th	(0000)

(4.58)

Primary \leftrightarrow Descendant

We first take the primary amplitude as the starting point. By repeatedly acting with ladder operators, we can obtain all descendant amplitudes as follows:

$$\text{primary} \quad \xrightarrow{\frac{\tilde{m}}{m}J^+ \circ \frac{m}{\tilde{m}}J^-} \quad \text{1st descendant} \quad \xrightarrow{\frac{\tilde{m}}{m}J^+ \circ \frac{m}{\tilde{m}}J^-} \quad \text{2nd descendant} \quad \rightarrow \quad \dots \quad (4.59)$$

This shows that by acting with k ladder operators, we obtain the k -th descendant amplitude. For the $WWhh$ amplitude, the primary MHC amplitude has helicity (0000). Applying a ladder operator flips the helicity and yields the 1st descendant amplitude with (+000):

$$\begin{array}{ccc} \text{Diagram: } & = \frac{\langle 12 \rangle [12]}{\mathbf{m}_1 \mathbf{m}_2} & \text{Diagram: } = \frac{\langle \eta_1 2 \rangle [12]}{m_1 \mathbf{m}_2} \\ \begin{array}{c} \text{0} \\ \text{0} \\ \text{0} \\ \text{0} \end{array} & \xrightarrow{\frac{\tilde{m}_1}{m_1} J_1^+} & \begin{array}{c} + \\ \text{0} \\ \text{0} \\ \text{0} \end{array} \end{array} \quad (4.60)$$

Other 1st descendant amplitudes can be obtained by acting on the primary amplitude with $\frac{\tilde{m}_2}{m_2} J_2^+$, $\frac{m_1}{\mathbf{m}_1} J_1^-$, or $\frac{m_2}{\mathbf{m}_2} J_2^-$. Continuing to apply ladder operators to the 1st descendant amplitude with (+000), we obtain the 2nd descendant amplitudes with (+-00) and (0000),

$$\begin{array}{ccc} \text{Diagram: } & \rightarrow \left\{ \begin{array}{l} \frac{m_2}{\mathbf{m}_2} J_2^- \\ \frac{m_1}{\mathbf{m}_1} J_1^- \end{array} \right. & \begin{array}{c} + \\ \text{0} \\ \text{0} \\ \text{0} \end{array} = \frac{\langle \eta_1 2 \rangle [1\eta_2]}{m_1 \tilde{m}_2}, \\ & \left. \begin{array}{l} + \\ \text{0} \\ \text{0} \\ \text{0} \end{array} \right. & = \frac{\langle \eta_1 2 \rangle [\eta_1 2]}{\mathbf{m}_1 \mathbf{m}_2}. \end{array} \quad (4.61)$$

Because there are vector bosons, the helicity of a 2nd descendant amplitude can be the same as that of the primary amplitude, as seen in the second line.

Conversely, we can start from a higher-order descendant amplitude, apply ladder operators to obtain lower-order descendant amplitudes, and finally reach the primary amplitude. Compared with the previous case, we now use the opposite ladder operators:

$$\begin{array}{ccc} \text{Diagram: } & \xrightarrow{\frac{\tilde{m}_1}{m_1} J_1^+} & \text{Diagram: } \xrightarrow{\frac{m_2}{\mathbf{m}_2} J_2^+} \text{Diagram: } \\ \begin{array}{c} + \\ \text{0} \\ \text{0} \\ \text{0} \end{array} & & \begin{array}{c} + \\ \text{0} \\ \text{0} \\ \text{0} \end{array} & \begin{array}{c} 0 \\ \text{0} \\ \text{0} \\ \text{0} \end{array} \end{array} \quad (4.62)$$

Descendant \leftrightarrow Descendant

We now consider conversion between descendant amplitudes. First, we examine conversion within the same order. In most cases, descendant amplitudes of the same order belong to different helicity categories, so we can use ladder operators to flip helicities and obtain different descendant amplitudes. For the 1st descendant of the $WWhh$ amplitude, starting from helicity (+000), we can

obtain the other three 1st descendant amplitudes:

$$\begin{array}{c}
 \text{Diagram: } \begin{array}{c} + \\ \diagup \text{wavy} \\ \diagdown \text{dashed} \end{array} \quad 0 \quad 0 \\
 = \frac{\langle \eta_1 2 \rangle [12]}{m_1 m_2}
 \end{array} \rightarrow \left\{ \begin{array}{l}
 \begin{array}{c} \frac{m_1}{m_1} J_1^- \frac{\tilde{m}_1}{m_1} J_1^+ \\
 \rightarrow \end{array} \quad \begin{array}{c} - \\ \diagup \text{wavy} \\ \diagdown \text{dashed} \end{array} \quad 0 \\
 = \frac{\langle 12 \rangle [\eta_1 2]}{\tilde{m}_1 m_2}, \\
 \begin{array}{c} \frac{m_2}{m_2} J_2^- \frac{\tilde{m}_1}{m_1} J_1^+ \\
 \rightarrow \end{array} \quad \begin{array}{c} 0 \\ \diagup \text{wavy} \\ \diagdown \text{dashed} \end{array} \quad 0 \\
 = \frac{\langle 12 \rangle [1 \eta_2]}{m_1 \tilde{m}_2}, \\
 \begin{array}{c} \frac{\tilde{m}_2}{m_2} J_2^+ \frac{m_1}{m_1} J_1^+ \\
 \rightarrow \end{array} \quad \begin{array}{c} - \\ \diagup \text{wavy} \\ \diagdown \text{dashed} \end{array} \quad 0 \\
 = \frac{\langle \eta_1 2 \rangle [12]}{m_1 m_2}.
 \end{array} \right. \quad (4.63)$$

For the 2nd descendant amplitudes, we can also use ladder operators to flip helicity. Starting from $(+ - 00)$, we obtain the 2nd descendant amplitudes with helicity $(- + 00)$ and (0000) :

$$\begin{array}{c}
 \text{Diagram: } \begin{array}{c} + \\ \diagup \text{wavy} \\ \diagdown \text{dashed} \end{array} \quad 0 \quad 0 \\
 = \frac{\langle \eta_1 2 \rangle [1 \eta_2]}{m_1 \tilde{m}_2}
 \end{array} \rightarrow \left\{ \begin{array}{l}
 \begin{array}{c} \frac{m_1}{m_1} J_1^- \frac{\tilde{m}_2}{m_2} J_2^+ \\
 \rightarrow \end{array} \quad \begin{array}{c} 0 \\ \diagup \text{wavy} \\ \diagdown \text{dashed} \end{array} \quad 0 \quad 0 \quad 0 \\
 = \frac{\langle \eta_1 2 \rangle [\eta_1 2]}{m_1 m_2} + \frac{\langle 1 \eta_2 \rangle [1 \eta_2]}{m_1 m_2}, \\
 \begin{array}{c} \frac{m_2}{m_2} J_2^- \frac{\tilde{m}_1}{m_1} J_1^+ \\
 \rightarrow \end{array} \quad \begin{array}{c} - \\ \diagup \text{wavy} \\ \diagdown \text{dashed} \end{array} \quad 0 \quad 0 \quad 0 \\
 = \frac{\langle 1 \eta_2 \rangle [\eta_1 2]}{\tilde{m}_1 m_2}.
 \end{array} \right. \quad (4.64)$$

The helicity $(\pm \pm 00)$ can be obtained similarly. Note that the helicity (0000) corresponds to two distinct descendant amplitudes. Starting from one (0000) amplitude, we need four ladder operators to convert it into the other:

$$\begin{array}{c}
 \text{Diagram: } \begin{array}{c} 0 \\ \diagup \text{wavy} \\ \diagdown \text{dashed} \end{array} \quad 0 \quad 0 \\
 = \frac{\langle \eta_1 2 \rangle [\eta_1 2]}{m_1 m_2}
 \end{array} \quad \begin{array}{c} \frac{\tilde{m}_1}{m_1} J_1^+ \frac{m_1}{m_1} J_1^- \frac{\tilde{m}_2}{m_2} J_2^+ \frac{m_2}{m_2} J_2^- \\
 \rightarrow \end{array} \quad \begin{array}{c} 0 \\ \diagup \text{wavy} \\ \diagdown \text{dashed} \end{array} \quad 0 \quad 0 \\
 = \frac{\langle 1 \eta_2 \rangle [1 \eta_2]}{m_1 m_2}. \quad (4.65)$$

This situation only occurs in amplitudes with two or more vector bosons.

To convert between descendant amplitudes of different orders, we can first use ladder operators to increase or decrease the order, and then convert between amplitudes of the same order to reach the target amplitude.

VVSS Contact Amplitudes by Massless-Massive Matching Although the above ladder operator is quite convenient, but it can not give the exact coefficient inherited from the UV massless contact amplitudes. Now we take the second way to obtain the VVSS contact amplitudes.

The VVSS massless contact amplitude in the SM has the similar structure as in scalar QED, which we have derived in the light-cone gauge. Replace the coefficient by the gauge structure of $SU(2)_W \times U(1)_Y$, we have

$$\begin{array}{ccccc}
 & 1^+ & & 4^0 & \\
 & \swarrow & \searrow & & \\
 & 2^- & & 3^0 & \\
 \end{array} = \begin{pmatrix} (T_s^{I_2} T_s^{I_1})_{i_4}^{i_3} + (T_s^{I_1} T_s^{I_2})_{i_4}^{i_3} \\ (T_s^{I_2} T_s^{I_1})_{i_3}^{i_4} + (T_s^{I_1} T_s^{I_2})_{i_3}^{i_4} \end{pmatrix} \frac{\langle \xi_1 2 \rangle [1 \xi_2]}{2 \langle \xi_1 1 \rangle [2 \xi_2]}, \quad (4.66)$$

where $(T_s^{I_2} T_s^{I_1})_{i_4}^{i_3} \equiv (T_s^{I_1})_j^{i_3} (T_s^{I_2})_{i_4}^j$ is the contraction of two 3-pt coefficients. The coefficients in two rows corresponds to the particle type $WWHH^\dagger$ and $WWH^\dagger H$. Multiplying with the transformation matrices, the coefficient becomes

$$\begin{pmatrix} (T_s^{I_2} T_s^{I_1})_{i_4}^{i_3} + (T_s^{I_1} T_s^{I_2})_{i_4}^{i_3} \\ (T_s^{I_2} T_s^{I_1})_{i_3}^{i_4} + (T_s^{I_1} T_s^{I_2})_{i_3}^{i_4} \end{pmatrix}^T \begin{pmatrix} O^{I_1 W^+} O^{I_2 W^-} \mathcal{U}_{i_3}^h \mathcal{U}_{i_4}^{i_3} \\ O^{I_1 W^+} O^{I_2 W^-} \mathcal{U}_{h i_3}^h \mathcal{U}_h^{i_4} \end{pmatrix} = \mathbf{g}^{\mathbf{I}_1 \mathbf{J}} \mathbf{g}^{\mathbf{J} \mathbf{I}_2}. \quad (4.67)$$

Taking the gauge $\xi_i = \eta_i$, we obtain the MHC contact amplitude

$$\begin{array}{ccccc}
 & + & & 0 & \\
 & \swarrow & \searrow & & \\
 & - & & 0 & \\
 \end{array} = \mathbf{g}^{\mathbf{I}_1 \mathbf{J}} \mathbf{g}^{\mathbf{J} \mathbf{I}_2} \frac{\langle \eta_1 2 \rangle [1 \eta_2]}{2 m_1 \tilde{m}_2}. \quad (4.68)$$

This is a descendant amplitude in helicity $(+ - 00)$. Note that, in the same helicity category, there is no following primary amplitude in the SM

$$\begin{array}{ccccc}
 & 1^+ & & 4^0 & \\
 & \swarrow & \searrow & & \\
 & 2^- & & 3^0 & \\
 \end{array} . \quad (4.69)$$

Then we can use ladder operators to obtain the MHC contact amplitude in other helicity. We first consider the contact amplitude with both longitudinal and transverse vectors, which can be obtained by acting one ladder operator $\frac{m}{m} J^-$ and $\frac{\tilde{m}}{m} J^+$. For helicity $(+000)$, we obtain the descendant amplitude

as below

$$\mathbf{g}^{\mathbf{I}_1 \mathbf{J}_1} \mathbf{g}^{\mathbf{J}_2} \frac{\langle \eta_1 2 \rangle [1 \eta_2]}{2m_1 \tilde{m}_2} \xrightarrow{\frac{\tilde{m}_2}{m_2} J_2^+} \left\{ \begin{array}{l} \text{1}^+ \quad \text{4}^0 \\ \text{2}^0 \quad \text{3}^0 \\ \text{1}^+ \quad \text{4}^0 \\ \text{2}^0 \quad \text{3}^0 \end{array} \right. = \mathbf{g}^{\mathbf{I}_1 \mathbf{J}_1} \mathbf{g}^{\mathbf{J}_2} \frac{\langle \eta_1 2 \rangle [21]}{2m_1 \mathbf{m}_2}, \\
 = \mathbf{g}^{\mathbf{I}_1 \mathbf{J}_1} \mathbf{g}^{\mathbf{J}_2} \frac{\langle \eta_1 \eta_2 \rangle [\eta_2 1]}{m_1 \mathbf{m}_2}.
 \end{math>
 (4.70)$$

Then we consider the longitudinal contact amplitude, which should be obtained by applying the two ladder operators $m_1 J_1^-$ and $\tilde{m}_2 J_2^+$,

$$+ \quad \text{0} \quad 1^0 \quad 4^0 \quad 1^0 \quad 4^0 \quad 1^0 \quad 4^0 \quad 1^0 \quad 4^0 \\
 + \quad \text{0} \quad 2^0 \quad 3^0 \quad 2^0 \quad 3^0 \quad 2^0 \quad 3^0 \quad 2^0 \quad 3^0 \quad . \\
 - \quad \text{0} \quad 2^0 \quad 3^0 \quad 2^0 \quad 3^0 \quad 2^0 \quad 3^0 \quad 2^0 \quad 3^0
 \end{math>
 (4.71)$$

The primary and descendant amplitudes in helicity (0000) are given together. The corresponding amplitude expression is

$$\mathbf{g}^{\mathbf{I}_1 \mathbf{J}_1} \mathbf{g}^{\mathbf{J}_2} \frac{\langle \eta_1 2 \rangle [1 \eta_2]}{2m_1 \tilde{m}_2} \rightarrow \mathbf{g}^{\mathbf{I}_1 \mathbf{J}_1} \mathbf{g}^{\mathbf{J}_2} \left(\frac{\langle 12 \rangle [12]}{2\mathbf{m}_1 \mathbf{m}_2} - \frac{m_1 \tilde{m}_1 \langle \eta_1 2 \rangle [\eta_1 2]}{2\mathbf{m}_1^3 \mathbf{m}_2} - \frac{m_2 \tilde{m}_2 \langle 1 \eta_2 \rangle [1 \eta_2]}{2\mathbf{m}_1 \mathbf{m}_2^3} + \frac{m_1 \tilde{m}_1 m_2 \tilde{m}_2 \langle \eta_1 \eta_2 \rangle [\eta_1 \eta_2]}{2\mathbf{m}_1^3 \mathbf{m}_2^3} \right).
 \end{math>
 (4.72)$$

The first term corresponds to the primary $VVSS$ amplitude. Unlike in the 3-pt case, this 4-pt primary contact amplitude is non-vanishing and must therefore have an UV origin. This origin can be traced to the electroweak chiral Lagrangian $\text{tr}[(D_\mu U)(D^\mu U)^\dagger]$. In this framework, the scalar field U is expressed in an exponential parameterization involving both the Goldstone bosons π and the Higgs boson h :

$$U = \exp \left[i \frac{\sqrt{2}}{v} \begin{pmatrix} \pi^0 & \pi^- \\ \pi^+ & \pi^0 \end{pmatrix} \right] \begin{pmatrix} 0 \\ \frac{v+h}{\sqrt{2}} \end{pmatrix}.
 \end{math>
 (4.73)$$

Here π differs from the field ϕ used in linear parameterizations. Expanding the chiral Lagrangian yields

$$\text{tr}[(D_\mu U)(D^\mu U)^\dagger] = \frac{1}{v^2} (\partial_\mu \pi^-)(\partial^\mu \pi^+) h^2 + \dots,
 \end{math>
 (4.74)$$

which contains a coupling proportional to $1/v^2$ that is absent in the linear realization. We can therefore establish a correspondence between this non-linearly realized UV theory and the primary $VVSS$

amplitude:

$$\begin{array}{c} 1^0 \\ \diagup \quad \diagdown \\ 2^0 \quad 3^0 \\ \diagdown \quad \diagup \end{array} \quad 4^0 = \frac{1}{v^2} \langle 12 \rangle [12] \quad \rightarrow \quad
 \begin{array}{c} 1^0 \\ \text{wavy} \quad \text{dashed} \\ \diagup \quad \diagdown \\ 2^0 \quad 3^0 \\ \diagdown \quad \diagup \end{array} \quad 4^0 = \mathbf{g}^{\mathbf{I}_1 \mathbf{J}} \mathbf{g}^{\mathbf{J} \mathbf{I}_2} \frac{\langle 12 \rangle [12]}{2 \mathbf{m}_1 \mathbf{m}_2}. \quad (4.75)$$

Note that this UV does not exist in the unbroken linear SM, and thus must vanish in the massless-massive matching due to a cancellation between contact and factorized $(0,0,0,0)$ amplitudes ⁷. This vanishing can also be explained by the conserved current, which provides an alternative method for obtaining the MHC contact amplitude. This derivation is given in Appendix B.

Among these MHC terms in helicity (0000), two descendant amplitudes whose diagram has two cross can be matched from the 4-pt massless amplitude. Let us consider the matching from massless four-scalar amplitude to the W^+W^-hh amplitude. In this case, the massless contact amplitude cannot match to the MHC contact amplitude only, we must include the contribution from the massless factorized amplitude. Therefore, we should consider the full massless amplitude, which has four contributions:

$$\begin{array}{ccc}
 1^0 & & 4^0 \\
 \backslash & \diagup & \diagdown \\
 & \text{~~~~~} & \\
 \diagup & & \diagdown \\
 2^0 & & 3^0
 \end{array} : \quad \begin{pmatrix} -(T_s^J)_{i_1}^{i_1} (T_s^J)_{i_3}^{i_3} \\ (T_s^J)_{i_2}^{i_1} (T_s^J)_{i_3}^{i_4} \end{pmatrix} \frac{s_{13} - s_{14}}{2s_{12}}, \quad (4.79)$$

⁷In addition to the contact primary amplitude in the (0000) helicity category, there exists a factorized primary amplitude for the same helicity, which also originates from this chiral Lagrangian. In the (13)-channel, we have



$$= \frac{1}{v^2} \frac{\langle 13 \rangle [13] \langle 24 \rangle [24]}{s_{13}}. \quad (4.76)$$

The full factorized amplitude includes this term and the corresponding (14)-channel contribution, which is obtained by exchanging particles 3 and 4. Both the factorized and contact primary amplitudes scale as $\frac{E^2}{v^2}$, so their presence can violate the tree-level unitarity. To avoid such unitarity violation, a cancellation between them must occur:

$$\begin{array}{c} \text{Diagram 1} \\ \text{Diagram 2} \\ \text{Diagram 3} \end{array} + \begin{array}{c} \text{Diagram 4} \\ \text{Diagram 5} \\ \text{Diagram 6} \end{array} + \begin{array}{c} \text{Diagram 7} \\ \text{Diagram 8} \\ \text{Diagram 9} \end{array} = \frac{1}{v^2} \left(\frac{\langle 13 \rangle [13] \langle 24 \rangle [24]}{s_{13}} + \frac{\langle 14 \rangle [14] \langle 23 \rangle [23]}{s_{14}} + \langle 12 \rangle [12] \right) = 0. \quad (4.77)$$

Note that only the (0000)-helicity primary amplitude has mass dimension 4. Primary MHC amplitudes in other helicity categories than the (0000) one, such as

$$1^+ \quad \quad \quad 4^0 \\ \text{---} \quad \quad \quad \text{---} \\ 2^- \quad \quad \quad 3^0 \quad , \quad \quad \quad (4.78)$$

belong to the massive EFT.

$$: \quad \begin{pmatrix} -(T_s^J)_{i_4}^{i_1} (T_s^J)_{i_2}^{i_3} \\ 0 \end{pmatrix} \frac{s_{13} - s_{12}}{2s_{14}}, \quad (4.80)$$

$$: \quad \begin{pmatrix} 0 \\ -(T_s^J)_{i_3}^{i_1} (T_s^J)_{i_2}^{i_4} \end{pmatrix} \frac{s_{14} - s_{12}}{2s_{13}}, \quad (4.81)$$

$$: \quad - \begin{pmatrix} \delta_{i_2}^{(i_1} \delta_{i_4}^{i_3)} \\ \delta_{i_2}^{(i_1} \delta_{i_3}^{i_4)} \end{pmatrix} 4\lambda, \quad (4.82)$$

where the two rows of coefficients correspond to the particle types $HH^\dagger HH^\dagger$ and $HH^\dagger H^\dagger H$. After multiplying with the transformation matrix, the massless coefficients of the four contributions become

$$\begin{pmatrix} -(T_s^J)_{i_2}^{i_1} (T_s^J)_{i_4}^{i_3} & -(T_s^J)_{i_4}^{i_1} (T_s^J)_{i_2}^{i_3} \\ (T_s^J)_{i_2}^{i_1} (T_s^J)_{i_3}^{i_4} & 0 \end{pmatrix} \begin{pmatrix} 0 \\ \delta_{i_2}^{(i_1} \delta_{i_4}^{i_3)} \end{pmatrix}^T \begin{pmatrix} \mathcal{U}_{i_1}^{W^+} \mathcal{U}_{i_2}^{W^-} \mathcal{U}_{i_3}^h \mathcal{U}_{i_4}^{i_4 h} \\ \mathcal{U}_{i_1}^{W^+} \mathcal{U}_{i_2}^{W^-} \mathcal{U}_{i_3}^{h i_3} \mathcal{U}_{i_4}^{i_4} \end{pmatrix} = \begin{pmatrix} 0 \\ g^2 \\ g^2 \\ -\lambda \end{pmatrix}. \quad (4.83)$$

The amplitude now becomes

$$g^2 \frac{s_{13} - s_{12}}{2s_{14}} + g^2 \frac{s_{14} - s_{12}}{2s_{13}} + 4\lambda. \quad (4.84)$$

The last term corresponds to the contact amplitude from the $\lambda\phi^4$ interaction. To match the MHC contact amplitude, we must combine contributions from gauge interactions and the $\lambda\phi^4$ interaction. This mixing can be achieved through an amplitude deformation where the factorized terms satisfy the Goldstone behavior for particles 1 and 2:

$$-g^2 \frac{s_{12}}{s_{14}} - g^2 \frac{s_{12}}{s_{13}} + g^2 + 4\lambda, \quad (4.85)$$

The last two terms have no pole structure and can therefore mix. To produce the MHC contact terms $\langle \eta_1 2 \rangle [\eta_1 2]$ and $\langle 1 \eta_2 \rangle [1 \eta_2]$, we convert the coupling constants into mass squares

$$g^2 = \frac{g^2}{2\mathbf{m}_W^2} (\mathbf{m}_1^2 + \mathbf{m}_2^2) = \frac{g^2}{2\mathbf{m}_W^2} [(p_1 + \eta_1 + p_2 + \eta_2)^2 - 2p_1 \cdot \eta_2 - 2\eta_1 \cdot p_2], \quad (4.86)$$

$$\lambda = \frac{\lambda}{2\mathbf{m}_h^2} (\mathbf{m}_3^2 + \mathbf{m}_4^2) = \frac{\lambda}{2\mathbf{m}_h^2} [(p_3 + \eta_4 + p_4 + \eta_3)^2 - 2p_3 \cdot \eta_4 - 2\eta_3 \cdot p_4].$$

It shows that the g^2 alone does not exactly reproduce the MHC contact term, but a cancellation involving λ makes it possible. This requires momentum conservation $p_1 + \eta_1 + p_2 + \eta_2 = -p_3 - \eta_3 - p_4 - \eta_4$ and the following relation between UV couplings and IR masses:

$$\frac{g^2}{2\mathbf{m}_W^2} = \frac{4\lambda}{\mathbf{m}_h^2}, \quad (4.87)$$

Under this condition, the amplitude in Eq. (4.85) can be further decomposed as

$$\begin{aligned} \text{gauge interaction : } & -g^2 \frac{s_{12}}{s_{14}} - g^2 \frac{s_{12}}{s_{13}} + \frac{g^2}{2\mathbf{m}_W^2} (\mathbf{m}_1^2 + \mathbf{m}_2^2), \\ \lambda \phi^4 \text{ interaction : } & 12\lambda + \frac{8\lambda}{\mathbf{m}_h^2} (p_3 \cdot \eta_4 + \eta_3 \cdot p_3) - \frac{4\lambda}{\mathbf{m}_h^2} (p_3 + \eta_3 + p_4 + \eta_4)^2. \end{aligned} \quad (4.88)$$

The last terms in both lines contribute to the MHC contact term, as illustrated in figure 5.

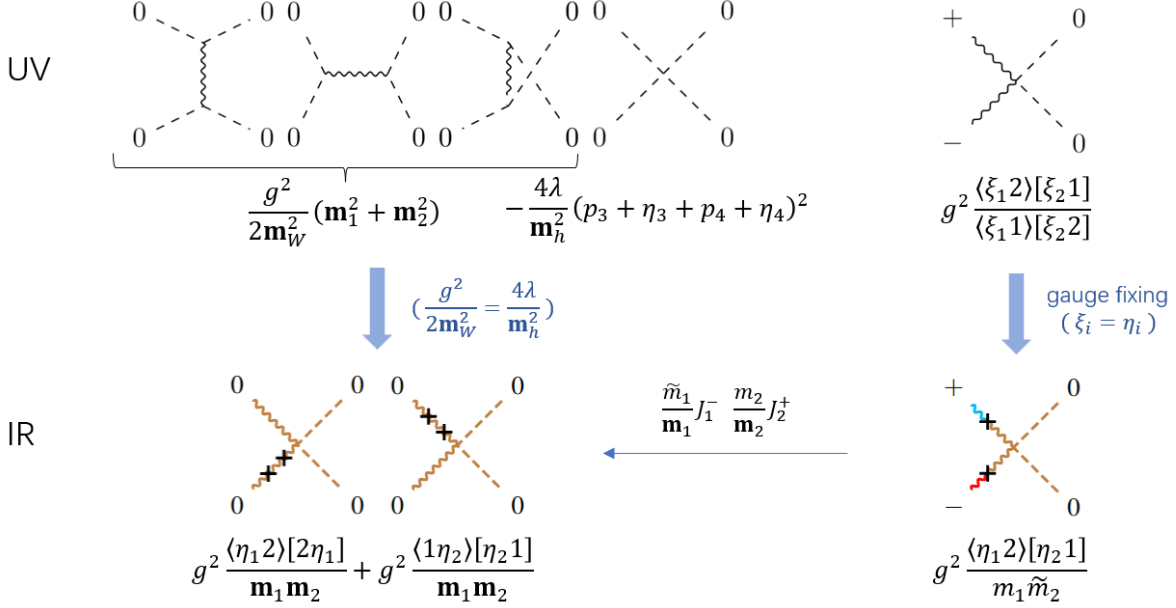


Figure 5: The diagrammatic matching for the contact $W^+ W^- hh$ amplitude in two helicities, related by the ladder operator.

Restore the $SU(2)$ little group covariance, we can derive the AHH contact amplitude,

$$\begin{array}{c} 1 \\ \diagup \\ \diagdown \\ 2 \end{array} \quad \begin{array}{c} 4 \\ \diagup \\ \diagdown \\ 3 \end{array} = \frac{\mathbf{g}^{W^+ W^-} \mathbf{g}^{W^+ W^-}}{\mathbf{m}_W^2} \langle \mathbf{12} | \mathbf{21} \rangle. \quad (4.89)$$

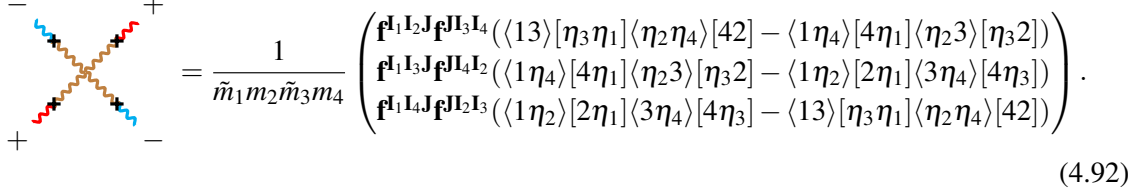
VVVV Contact Amplitudes In analogy to the VVSS case, we can write down the massless contact VVVV amplitude in the light-cone gauge,

$$\begin{array}{c} 1^- \\ \diagup \\ \diagdown \\ 2^+ \end{array} \quad \begin{array}{c} 4^+ \\ \diagup \\ \diagdown \\ 3^- \end{array} = \frac{1}{[\xi_1 1] \langle 2 \xi_2 | \xi_3 3 \rangle \langle 4 \xi_4]} \left(\begin{array}{l} f^{I_1 I_2 J} f^{J I_3 I_4} (\langle 13 \rangle [\xi_3 \xi_1] \langle \xi_2 \xi_4] [42] - \langle 1 \xi_4 \rangle [4 \xi_1] \langle \xi_2 3 \rangle [\xi_3 2]) \\ f^{I_1 I_3 J} f^{J I_4 I_2} (\langle 1 \xi_4 \rangle [4 \xi_1] \langle \xi_2 3 \rangle [\xi_3 2] - \langle 1 \xi_2 \rangle [2 \xi_1] \langle 3 \xi_4 \rangle [4 \xi_3]) \\ f^{I_1 I_4 J} f^{J I_2 I_3} (\langle 1 \xi_2 \rangle [2 \xi_1] \langle 3 \xi_4 \rangle [4 \xi_3] - \langle 13 \rangle [\xi_3 \xi_1] \langle \xi_2 \xi_4] [42]) \end{array} \right). \quad (4.90)$$

Multiplying with the transformation matices, the coefficient becomes

$$\begin{pmatrix} f^{I_1 I_2 J} f^{J I_3 I_4} \\ f^{I_1 I_3 J} f^{J I_4 I_2} \\ f^{I_1 I_4 J} f^{J I_2 I_3} \end{pmatrix} O^{I_1 \mathbf{I}_1} O^{I_2 \mathbf{I}_2} O^{I_3 \mathbf{I}_3} O^{I_4 \mathbf{I}_4} = \begin{pmatrix} \mathbf{f}^{I_1 \mathbf{I}_2 \mathbf{J}} \mathbf{f}^{J \mathbf{I}_3 \mathbf{I}_4} \\ \mathbf{f}^{I_1 \mathbf{I}_3 \mathbf{J}} \mathbf{f}^{J \mathbf{I}_4 \mathbf{I}_2} \\ \mathbf{f}^{I_1 \mathbf{I}_4 \mathbf{J}} \mathbf{f}^{J \mathbf{I}_2 \mathbf{I}_3} \end{pmatrix}. \quad (4.91)$$

Taking the gauge $\xi_i = \eta_i$, we have

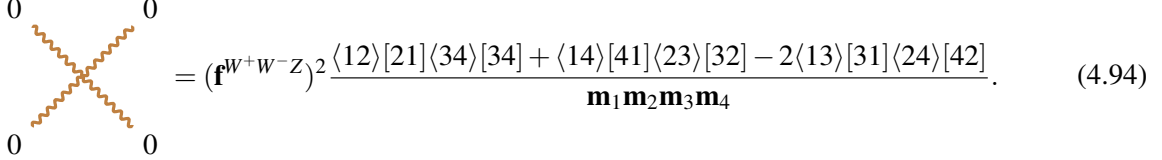


$$= \frac{1}{\tilde{m}_1 m_2 \tilde{m}_3 m_4} \left(\begin{array}{l} \mathbf{f}^{I_1 \mathbf{I}_2 \mathbf{J}} \mathbf{f}^{J \mathbf{I}_3 \mathbf{I}_4} (\langle 13 \rangle [\eta_3 \eta_1] \langle \eta_2 \eta_4 \rangle [42] - \langle 1 \eta_4 \rangle [4 \eta_1] \langle \eta_2 3 \rangle [\eta_3 2]) \\ \mathbf{f}^{I_1 \mathbf{I}_3 \mathbf{J}} \mathbf{f}^{J \mathbf{I}_4 \mathbf{I}_2} (\langle 1 \eta_4 \rangle [4 \eta_1] \langle \eta_2 3 \rangle [\eta_3 2] - \langle 1 \eta_2 \rangle [2 \eta_1] \langle 3 \eta_4 \rangle [4 \eta_3]) \\ \mathbf{f}^{I_1 \mathbf{I}_4 \mathbf{J}} \mathbf{f}^{J \mathbf{I}_2 \mathbf{I}_3} (\langle 1 \eta_2 \rangle [2 \eta_1] \langle 3 \eta_4 \rangle [4 \eta_3] - \langle 13 \rangle [\eta_3 \eta_1] \langle \eta_2 \eta_4 \rangle [42]) \end{array} \right). \quad (4.92)$$

In the SM, the massive particle type can be W^\pm and Z boson. For example, we can choose $\mathbf{I}_1 = \mathbf{I}_3 = W^+$ and $\mathbf{I}_2 = \mathbf{I}_4 = W^-$, the amplitude will reduce to

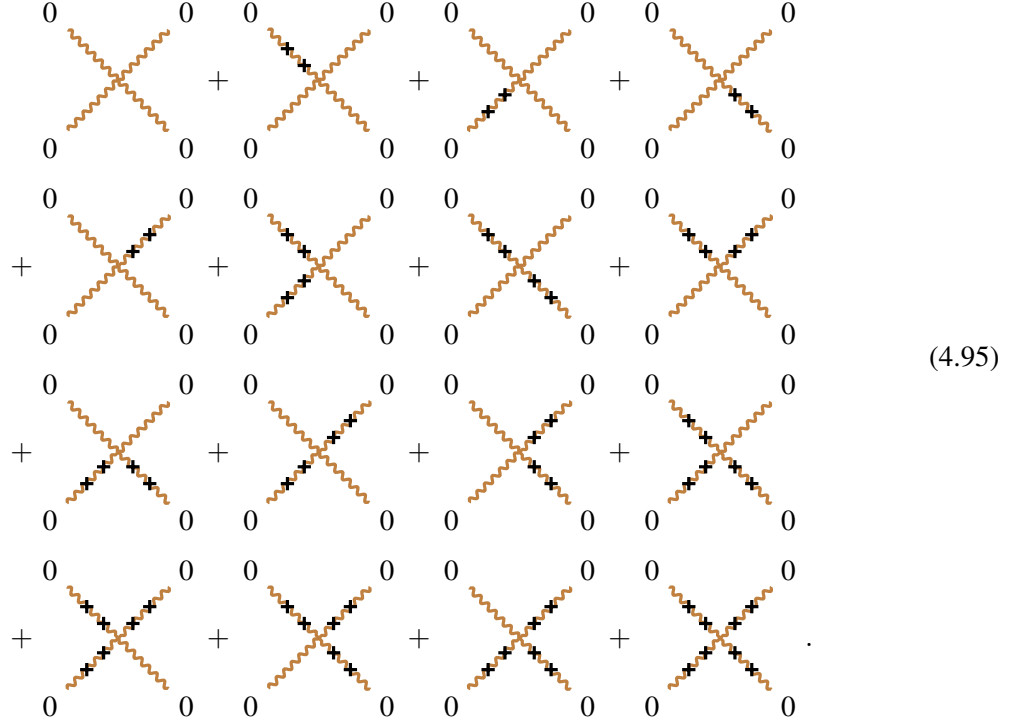
$$\frac{\mathbf{f}^{W^+ W^- Z} \mathbf{f}^{Z W^+ W^-} (\langle 1 \eta_2 \rangle [2 \eta_1] \langle 3 \eta_4 \rangle [4 \eta_3] + \langle 1 \eta_4 \rangle [4 \eta_1] \langle \eta_2 3 \rangle [\eta_3 2] - 2 \langle 13 \rangle [\eta_3 \eta_1] \langle \eta_2 \eta_4 \rangle [42])}{\tilde{m}_1 m_2 \tilde{m}_3 m_4}. \quad (4.93)$$

Reversely using the ladder operator, we recover the primary amplitude



$$= (\mathbf{f}^{W^+ W^- Z})^2 \frac{(\langle 12 \rangle [21] \langle 34 \rangle [34] + \langle 14 \rangle [41] \langle 23 \rangle [32] - 2 \langle 13 \rangle [31] \langle 24 \rangle [42])}{\mathbf{m}_1 \mathbf{m}_2 \mathbf{m}_3 \mathbf{m}_4}. \quad (4.94)$$

The subleading order contribution in this helicity category is also determined.



$$+ \quad + \quad +$$

$$+ \quad + \quad +$$

$$+ \quad + \quad +$$

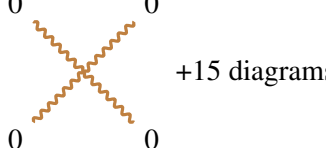
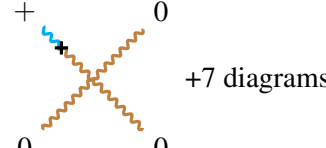
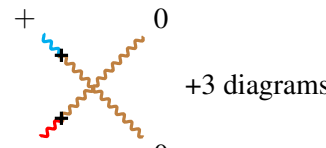
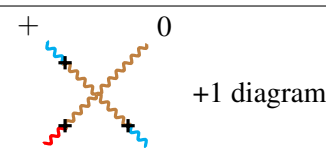
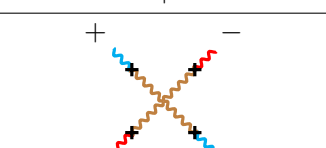
$$+ \quad + \quad +$$

$$. \quad (4.95)$$

The corresponding amplitude is

$$\begin{aligned}
& \frac{(\mathbf{f}^{W^+W^-Z})^2}{\mathbf{m}_1\mathbf{m}_2\mathbf{m}_3\mathbf{m}_4} \times \left((\langle 12 \rangle [21] - \langle \eta_1 2 \rangle [2\eta_1] - \langle 1\eta_2 \rangle [\eta_2 1] + \langle \eta_1 \eta_2 \rangle [\eta_2 \eta_1]) \right. \\
& \quad \times (\langle 34 \rangle [43] - \langle \eta_3 4 \rangle [4\eta_3] - \langle 3\eta_4 \rangle [\eta_4 3] + \langle \eta_3 \eta_4 \rangle [\eta_4 \eta_3]) \\
& \quad + (\langle 14 \rangle [41] - \langle \eta_1 4 \rangle [4\eta_1] - \langle 1\eta_4 \rangle [\eta_4 1] + \langle \eta_1 \eta_4 \rangle [\eta_4 \eta_1]) \\
& \quad \times (\langle 23 \rangle [32] - \langle \eta_2 3 \rangle [3\eta_2] - \langle 2\eta_3 \rangle [\eta_3 2] + \langle \eta_2 \eta_3 \rangle [\eta_3 \eta_2]) \\
& \quad + (\langle 13 \rangle [31] - \langle \eta_1 3 \rangle [3\eta_1] - \langle 1\eta_3 \rangle [\eta_3 1] + \langle \eta_1 \eta_3 \rangle [\eta_3 \eta_1]) \\
& \quad \left. \times (\langle 24 \rangle [42] - \langle \eta_2 4 \rangle [4\eta_2] - \langle 2\eta_4 \rangle [\eta_4 2] + \langle \eta_2 \eta_4 \rangle [\eta_4 \eta_2]) \right). \tag{4.96}
\end{aligned}$$

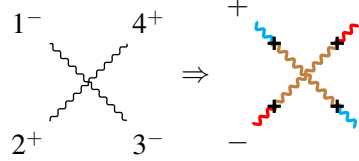
Using the extended little group covariance, we can determine the contact term in all helicity categories. Since it has many diagrams, we only list the leading term in some typical helicity categories,

helicity category	diagrams	amplitude
$(0,0,0,0)$		$\frac{(\mathbf{f}^{W^+W^-Z})^2}{\mathbf{m}_1\mathbf{m}_2\mathbf{m}_3\mathbf{m}_4} \times (\langle 12 \rangle [21] \langle 34 \rangle [34] + \langle 14 \rangle [41] \langle 23 \rangle [32] - 2\langle 13 \rangle [31] \langle 24 \rangle [42]) + 15 \text{ terms}$
$(+,0,0,0)$		$\frac{(\mathbf{f}^{W^+W^-Z})^2}{\mathbf{m}_1\mathbf{m}_2\mathbf{m}_3\mathbf{m}_4} \times (\langle \eta_1 2 \rangle [21] \langle 34 \rangle [34] + \langle \eta_1 4 \rangle [41] \langle 23 \rangle [32] - 2\langle \eta_1 3 \rangle [31] \langle 24 \rangle [42]) + 7 \text{ terms}$
$(+,-,0,0)$		$\frac{(\mathbf{f}^{W^+W^-Z})^2}{\mathbf{m}_1\tilde{\mathbf{m}}_2\mathbf{m}_3\mathbf{m}_4} \times (\langle \eta_1 2 \rangle [\eta_2 1] \langle 34 \rangle [34] + \langle \eta_1 4 \rangle [41] \langle 23 \rangle [3\eta_2] - 2\langle \eta_1 3 \rangle [31] \langle 24 \rangle [4\eta_2]) + 3 \text{ terms}$
$(+,-,+0)$		$\frac{(\mathbf{f}^{W^+W^-Z})^2}{\mathbf{m}_1\tilde{\mathbf{m}}_2\mathbf{m}_3\mathbf{m}_4} \times (\langle \eta_1 2 \rangle [\eta_2 1] \langle \eta_3 4 \rangle [34] + \langle \eta_1 4 \rangle [41] \langle 2\eta_3 \rangle [3\eta_2] - 2\langle \eta_1 \eta_3 \rangle [31] \langle 24 \rangle [4\eta_2]) + 1 \text{ term}$
$(+,-,+,-)$		$\frac{(\mathbf{f}^{W^+W^-Z})^2}{\mathbf{m}_1\tilde{\mathbf{m}}_2\mathbf{m}_3\tilde{\mathbf{m}}_4} \times (\langle \eta_1 2 \rangle [\eta_2 1] \langle \eta_3 4 \rangle [3\eta_4] + \langle \eta_1 4 \rangle [\eta_4 1] \langle 2\eta_3 \rangle [3\eta_2] - 2\langle \eta_1 \eta_3 \rangle [31] \langle 24 \rangle [\eta_4 \eta_2])$

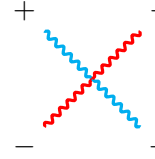
(4.97)

Note for each helicity category, there exist several diagrams with increasing double chirality flip, until reaching eight chirality flips for each diagram. Furthermore, the primary and up-to-third descendant diagrams do not contribute to the SM due to unitarity cancellation, and only starting from the 4th

descendant contact amplitude, there is a massless-massive matching in the SM, such as

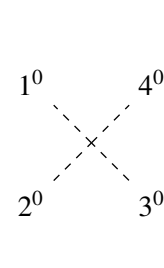

(4.98)

Again, all other primary amplitude than the $(0, 0, 0, 0)$ helicity category, such as


(4.99)

belong to EFT.

SSSS contact amplitude The massless amplitude is

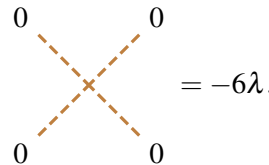


$$= -4\lambda \begin{pmatrix} \delta_{i_3}^{(i_1} \delta_{i_4)}^{i_2)} \\ \delta_{i_2}^{(i_1} \delta_{i_4)}^{i_3)} \\ \delta_{i_2}^{(i_1} \delta_{i_4)}^{i_4)} \\ \delta_{i_1}^{(i_2} \delta_{i_3)}^{i_4)} \\ \delta_{i_1}^{(i_2} \delta_{i_4)}^{i_4)} \\ \delta_{i_1}^{(i_3} \delta_{i_2)}^{i_4)} \end{pmatrix}.$$
(4.100)

Multiplying with the transformation matrices, the coefficient becomes

$$-4\lambda \begin{pmatrix} \delta_{i_3}^{(i_1} \delta_{i_4)}^{i_2)} \\ \delta_{i_2}^{(i_1} \delta_{i_4)}^{i_3)} \\ \delta_{i_2}^{(i_1} \delta_{i_4)}^{i_4)} \\ \delta_{i_1}^{(i_2} \delta_{i_3)}^{i_4)} \\ \delta_{i_1}^{(i_2} \delta_{i_4)}^{i_4)} \\ \delta_{i_1}^{(i_3} \delta_{i_2)}^{i_4)} \end{pmatrix}^T \begin{pmatrix} \mathcal{U}_{i_1}^h \mathcal{U}_{i_2}^h \mathcal{U}_{i_3}^h \mathcal{U}_{i_4}^h \\ \mathcal{U}_{i_1}^h \mathcal{U}_{i_2}^h \mathcal{U}_{i_3}^h \mathcal{U}_{i_4}^h \end{pmatrix} = -6\lambda.$$
(4.101)

Therefore, the massive contact amplitude is


(4.102)

5 Constructive Amplitudes in 3 Ways: $WW \rightarrow hh$ as Example

In this section, we will perform systematic construction of higher-point MHC amplitudes from the contact MHC amplitudes in the SM. Two kinds of on-shell constructive methods, the bootstrap, and the recursive relation, are proposed for the massless amplitude construction. We will show that both methods can be generalized to the MHC amplitudes and the AHH massive amplitudes.

The building blocks for such construction are the contact MHC amplitudes in the light-cone gauge, containing both the 3-point MHC amplitudes and 4-point contact MHC amplitudes⁸. Therefore in the bootstrap method, the 4-point amplitudes, would have four contributions

$$\mathcal{M} = \mathcal{M}_{(12)} + \mathcal{M}_{(13)} + \mathcal{M}_{(14)} + \mathcal{M}_{\text{ct}}. \quad (5.1)$$

The first three terms can be obtained by gluing 3-pt amplitudes, while the last contact term is given in previous section. Note that in this section, only leading MHC amplitudes are needed for bootstrap and BCFW construction.

In this section, we will show how to construct higher-point massive amplitudes in three different ways using the same process $WW \rightarrow hh$ in the SM:

- MHC bootstrap: list all relevant 3-point leading MHC amplitudes and 4-point contact MHC amplitudes, then glue them to obtain 4-point factorized amplitudes. Different from the previous section, we can use the leading MHC contact amplitudes to determine the leading higher point MHC amplitudes, and all sub-leading one can be neglected.
- AHH bootstrap: list all relevant 3-point AHH amplitudes and 4-point contact AHH amplitudes, then glue them to obtain 4-point factorized AHH amplitudes.
- MHC recursion: list only the 3-point leading MHC amplitudes in the light-cone gauge, then use BCFW recursive relation to obtain 4-point leading factorized amplitudes. Note that compare to the massless BCFW, now we can avoid the $\lambda\phi^4$ interaction in the BCFW construction for the MHC amplitudes due to the little group covariance.

5.1 Bootstrapping MHC amplitudes

For the MHC amplitudes $WW \rightarrow hh$, because of little group covariance, we can focus on one helicity category, such as $(+, -, 0, 0)$. Once the result for such helicity is obtained, other helicity categories can be obtained by extended little group covariance.

First let us list the relevant 3-pt amplitudes at the leading order. The 3-pt leading MHC amplitudes are

$$1^+ \quad 4^0 \quad P^0 = g^{W^+W^-} \frac{\langle \eta_1 P_{14} \rangle [P_{14} 1]}{m_1}, \quad (5.2)$$

⁸In the SM, there is no need to introduce 5-point contact MHC amplitudes and higher, all belonging to EFT, to obtain higher-point factorized MHC amplitudes.

$$2^- \quad 3^- \quad P^0 = \mathbf{g}^{W^+W^-} \frac{\langle 2P_{14} \rangle [P_{14}\eta_2]}{\tilde{m}_2}. \quad (5.3)$$

These building blocks can be glued to 4-pt amplitudes in three channels. For the (14)-channel, the internal particle is a W boson. Gluing these two WWh amplitude we can get

$$1^+ \quad 4^0 = (\mathbf{g}^{W^+W^-})^2 \frac{\langle \eta_1 | P_{14} | 1 \rangle \langle 2 | P_{14} | \eta_2 \rangle}{s_{14} m_1 \tilde{m}_2}. \quad (5.4)$$

Similarly, we can obtain the contribution of (13)-channel,

$$1^+ \quad 4^0 = (\mathbf{g}^{W^+W^-})^2 \frac{\langle \eta_1 | P_{13} | 1 \rangle \langle 2 | P_{13} | \eta_2 \rangle}{s_{13} m_1 \tilde{m}_2}. \quad (5.5)$$

It is equivalent to exchange particles 3 and 4 to the result of (14)-channel. For (12)-channel, the internal particle is a Higgs boson. We glue WWh and hh amplitude and obtain

$$1^+ \quad 4^0 = \frac{\mathbf{g}^{W^+W^-} \lambda_3}{\mathbf{m}_W^2} \frac{[12] \langle 21 \rangle}{s_{12} m_1 \tilde{m}_2}. \quad (5.6)$$

The contact term is already derived as

$$1^+ \quad 4^0 = (\mathbf{g}^{W^+W^-})^2 \frac{\langle \eta_1 2 \rangle [\eta_2 1]}{m_1 \tilde{m}_2}. \quad (5.7)$$

Combining all these contributions, we obtain

$$\begin{aligned} & (\mathbf{g}^{W^+W^-})^2 \frac{\langle \eta_1 | P_{14} | 1 \rangle \langle 2 | P_{14} | \eta_2 \rangle}{s_{14} m_1 \tilde{m}_2} - (\mathbf{g}^{W^+W^-})^2 \frac{\langle \eta_1 | P_{13} | 1 \rangle \langle 2 | P_{13} | \eta_2 \rangle}{s_{13} m_1 \tilde{m}_2} \\ & + \frac{\mathbf{g}^{W^+W^-} \lambda_3}{\mathbf{m}_W^2} \frac{\langle \eta_1 2 \rangle [\eta_2 1]}{s_{12} m_1 \tilde{m}_2} + (\mathbf{g}^{W^+W^-})^2 \frac{\langle \eta_1 2 \rangle [\eta_2 1]}{m_1 \tilde{m}_2}. \end{aligned} \quad (5.8)$$

There are other contributions from the subleading diagrams with more cross on the internal line. They can be obtained by acting J^+J^- on the particle line, which we introduced in subsection 4.1. For (13)- and (14)-channel, the result is equalvalent to the replacement $p_{\dot{\alpha}_2}^{\beta_1} p_{\dot{\alpha}_1}^{\dot{\beta}_2} \rightarrow -2\mathbf{m}^2 \delta_{\dot{\alpha}_1}^{\beta_1} \delta_{\dot{\alpha}_2}^{\dot{\beta}_2} + (p + \eta)_{\dot{\alpha}_2}^{\beta_1} (p + \eta)_{\dot{\alpha}_1}^{\dot{\beta}_2}$.

Finally, we derive the total $WWhh$ amplitude,

$$\begin{aligned} \mathcal{M}(1^{+1}, 2^{-1}, 3^0, 4^0) &= (\mathbf{g}^{W^+W^-})^2 \frac{-2\mathbf{m}^2 \langle \eta_1 2 \rangle [\eta_2 1] + \langle \eta_1 | P_{14} + \eta_{14} | 1 \rangle \langle 2 | P_{14} + \eta_{14} | \eta_2 \rangle}{s_{14} m_1 \tilde{m}_2} \\ &\quad (\mathbf{g}^{W^+W^-})^2 \frac{-2\mathbf{m}^2 \langle \eta_1 2 \rangle [\eta_2 1] + \langle \eta_1 | P_{13} + \eta_{13} | 1 \rangle \langle 2 | P_{13} + \eta_{13} | \eta_2 \rangle}{s_{13} m_1 \tilde{m}_2} \\ &\quad + \frac{\mathbf{g}^{W^+W^-} \lambda_3}{\mathbf{m}_W^2} \frac{\langle \eta_1 2 \rangle [\eta_2 1]}{s_{12} m_1 \tilde{m}_2} + (\mathbf{g}^{W^+W^-})^2 \frac{\langle \eta_1 2 \rangle [\eta_2 1]}{m_1 \tilde{m}_2}. \end{aligned} \quad (5.9)$$

The other 4-pt MHC amplitude can be obtained in a similar way. For instance, the four-vector scattering amplitude is provided in Appendix C. In the SM, the MHC amplitude with more than four external particles do not have new contact term, so we can always glue the lower-point amplitude to construct the any-point MHC amplitude.

5.2 Bootstrapping AHH amplitudes

Similar bootstrap can be applied to the AHH amplitudes. In this case, the building blocks are the 3-pt and 4-pt contact AHH amplitudes, which are obtained by bolding the 3-pt and 4-pt contact MHC amplitudes. The difference from literature is that the 4-pt contact AHH amplitudes should be added in the bootstrap.

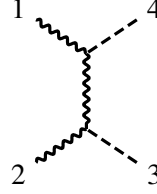
We again take the $WWhh$ amplitude as an example to illustrate the bootstrap procedure. The relevant 3-pt contact amplitudes are

$$\begin{aligned} \text{Diagram: } & \text{A vertex with three external lines. The top line is a wavy line labeled '1' with superscript '2'. The left line is a dashed line labeled '1' with superscript '3'. The right line is a dashed line labeled '3' with superscript '2'.} \\ & = \mathbf{M}(\mathbf{1}^1, \mathbf{2}^1, \mathbf{3}^1) = \frac{\mathbf{g}^{W^+W^-}}{\mathbf{m}_W} \langle \mathbf{1} \mathbf{2} \rangle [\mathbf{2} \mathbf{1}], \\ \text{Diagram: } & \text{A vertex with three external lines. The top line is a dashed line labeled '1' with superscript '2'. The left line is a dashed line labeled '1' with superscript '3'. The right line is a dashed line labeled '3' with superscript '2'.} \\ & = \mathbf{M}(\mathbf{1}^0, \mathbf{2}^0, \mathbf{3}^0) = \lambda_3, \end{aligned} \quad (5.10)$$

where the superscript represents the particle spin.

The factorized contributions, which correspond to the (12)-, (13)- and (14)-channels, are obtained by gluing two 3-pt AHH amplitudes. We first consider the (14)-channel, in which the internal particle

is a W boson. In this case, we glue two WWh amplitudes,



$$= \frac{\mathbf{M}(\mathbf{1}^1, \mathbf{4}^0, -\mathbf{P}_{14}^1) \otimes \mathbf{M}(\mathbf{P}_{14}^1, \mathbf{2}^1, \mathbf{3}^0)}{\mathbf{P}_{14}^2 - \mathbf{m}_W^2}, \quad (5.11)$$

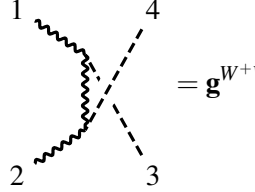
where \otimes denotes the contraction of little group indices of two external particles \mathbf{P}_{14} and $-\mathbf{P}_{14}$. Writing the little group indices explicitly, this contraction gives

$$|\mathbf{P}|^{\dot{\alpha}} \langle \mathbf{P} \rangle_{\alpha} \otimes |\mathbf{P}|_{\dot{\beta}} \langle \mathbf{P} \rangle^{\beta} = |\mathbf{P}|^{\dot{\alpha}(I_1} \langle \mathbf{P} \rangle_{\alpha}^{I_2)} \times |\mathbf{P}|_{\dot{\beta}I_1}^{\beta} \langle \mathbf{P} \rangle_{I_2}^{\beta} = \mathbf{m}^2 \delta_{\dot{\beta}}^{\dot{\alpha}} \delta_{\alpha}^{\beta} - \frac{1}{2} \mathbf{P}^{\dot{\alpha}\beta} \mathbf{P}_{\alpha\dot{\beta}}. \quad (5.12)$$

Thus, the (14)-channel amplitude should be

$$\begin{aligned} & \frac{\mathbf{g}^{W^+W^-} \mathbf{g}^{W^+W^-}}{\mathbf{m}_W^2} \langle \mathbf{1} \mathbf{P}_{14} \rangle [\mathbf{P}_{14} 1] \otimes \langle \mathbf{2} \mathbf{P}_{14} \rangle [\mathbf{P}_{14} 2] \\ &= \frac{\mathbf{g}^{W^+W^-} \mathbf{g}^{W^+W^-}}{2\mathbf{m}_W^2} \frac{2\mathbf{m}_W^2 \langle \mathbf{12} \rangle [\mathbf{21}] - \langle \mathbf{1} \mathbf{P}_{14} | \mathbf{1} \rangle \langle \mathbf{2} | \mathbf{P}_{14} | \mathbf{2}]}{\mathbf{P}_{14}^2 - \mathbf{m}_W^2}. \end{aligned} \quad (5.13)$$

Similarly, the (13)-channel amplitude is



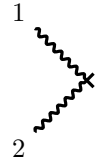
$$= \mathbf{g}^{W^+W^-} \mathbf{g}^{W^+W^-} \frac{2\mathbf{m}_W^2 \langle \mathbf{12} \rangle [\mathbf{21}] - \langle \mathbf{1} | \mathbf{P}_{13} | \mathbf{1} \rangle \langle \mathbf{2} | \mathbf{P}_{13} | \mathbf{2}]}{\mathbf{P}_{13}^2 - \mathbf{m}_W^2}. \quad (5.14)$$

In the (12)-channel we glue a WWh amplitude with an hh amplitude. Here the internal particle is a massive scalar, which carries no little group spinor indices. Thus we have



$$= \frac{\mathbf{g}^{W^+W^-} \lambda_3}{\mathbf{m}_W^2} \frac{[\mathbf{12}] \langle \mathbf{21} \rangle}{\mathbf{P}_{12}^2 - \mathbf{m}_h^2}. \quad (5.15)$$

The final ingredient is the 4-pt contact amplitude,



$$= \frac{\mathbf{g}^{W^+W^-} \mathbf{g}^{W^+W^-}}{2\mathbf{m}_W^2} \langle \mathbf{12} \rangle [\mathbf{21}]. \quad (5.16)$$

Putting everything together, we obtain the total AHH amplitude,

$$\begin{aligned}
\mathbf{M}(1,2,3,4) = & -\frac{\mathbf{g}^{W^+W^-} \mathbf{g}^{W^+W^-}}{2\mathbf{m}_W^2} \frac{2\mathbf{m}_W^2 \langle \mathbf{12} \rangle [\mathbf{21}] - \langle \mathbf{1} | \mathbf{P}_{14} | \mathbf{1} \rangle \langle \mathbf{2} | \mathbf{P}_{14} | \mathbf{2} \rangle}{\mathbf{P}_{14}^2 - \mathbf{m}_W^2} \\
& -\frac{\mathbf{g}^{W^+W^-} \mathbf{g}^{W^+W^-}}{2\mathbf{m}_W^2} \frac{2\mathbf{m}_W^2 \langle \mathbf{12} \rangle [\mathbf{21}] - \langle \mathbf{1} | \mathbf{P}_{13} | \mathbf{1} \rangle \langle \mathbf{2} | \mathbf{P}_{13} | \mathbf{2} \rangle}{\mathbf{P}_{13}^2 - \mathbf{m}_W^2} \\
& -\frac{\mathbf{g}^{W^+W^-} \lambda_3}{\mathbf{m}_W^2} \frac{\langle \mathbf{12} \rangle [\mathbf{21}]}{\mathbf{P}_{12}^2 - \mathbf{m}_h^2} - \frac{\mathbf{g}^{W^+W^-} \mathbf{g}^{W^+W^-}}{2\mathbf{m}_W^2} \langle \mathbf{12} \rangle [\mathbf{21}].
\end{aligned} \tag{5.17}$$

5.3 MHC recursive construction

In addition to the bootstrap method, MHC amplitudes can also be constructed using recursion relations. In Ref. [24, 55], the authors introduced the All-Line Transverse (ALT) shift, which defines different momentum shifts for transverse and longitudinal mode of the spin-1 particles, and thus allows the recursive construction of AHH massive amplitudes. In the AHH amplitudes, different momentum shift for different mode seems strange. On the other hand, it becomes quite natural to consider different shift in the MHC amplitudes for different transversality. Here, we extend this approach to a variant form suitable for the MHC formalism. In the following, we will use the variant ALT shift to construct the $WWhh$ amplitude.

In the variant ALT shift, all external particle spinors are shifted by a complex parameter z . The specific shift for each particle depends on its helicity h . For a particle i with helicity $h \neq 0$,

$$(h > 0) : |\hat{i}\rangle = |i\rangle + zc_i|\eta_i\rangle, \quad (h < 0) : |\hat{i}\rangle = |i\rangle + zc_i|\eta_i\rangle, \tag{5.18}$$

where c_i is a coefficient ensuring momentum conservation. These coefficients will not appear in the final expression of a correctly constructed amplitude. These shifts leave the fermion and transverse vector states unchanged, consistent with the original ALT shift. The difference lies in the shift for the particle with helicity $h = 0$,

$$(h = 0) : |\hat{i}\rangle = |i\rangle + zc_i|\eta_i\rangle \quad \text{or} \quad |\hat{i}\rangle = |i\rangle + zc_i|\eta_i\rangle. \tag{5.19}$$

Unlike the original ALT shift, we do not require the longitudinal vector states to remain unchanged. Therefore, the scope of application for the variant ALT shift differs: when an MHC amplitude involves a vector boson, we will only consider shifts for the helicity categories where the vector boson is transverse.

As an example, for the $WWhh$ amplitude, we consider helicity categories where both W bosons are transversely polarized, such as $(+ - 00)$. A possible variant ALT shift is:

$$\begin{aligned}
|\hat{1}\rangle &= |1\rangle + zc_1|\eta_1\rangle, \\
|\hat{2}\rangle &= |2\rangle + zc_2|\eta_2\rangle, \\
|\hat{3}\rangle &= |3\rangle + z\frac{c_3}{2}|\eta_3\rangle, \\
|\hat{4}\rangle &= |4\rangle + z\frac{c_4}{2}|\eta_4\rangle.
\end{aligned} \tag{5.20}$$

Under this shift, the momentum of each external particle becomes

$$\hat{p}_i = p_i + zq_i, \quad i = 1, 2, 3, 4, \quad (5.21)$$

where

$$\begin{aligned} q_1 &= c_1|1]\langle\eta_1|, & q_2 &= c_2|\eta_2]\langle 2|, \\ q_3 &= c_3|3]\langle\eta_3|, & q_4 &= c_4|4]\langle\eta_4|, \end{aligned} \quad (5.22)$$

and the q_i satisfy momentum conservation

$$q_1 + q_2 + q_3 + q_4 = 0. \quad (5.23)$$

In the MHC formalism, the momentum of internal particles is also decomposed into the large and small components. For an internal particle in the 4-pt amplitude, the large component is $P_{ij} \equiv (p_i + p_j)$ and the small component is $\eta_{ij} \equiv (\eta_i + \eta_j)$. Under the variant ALT shift, only the large component momentum is shifted,

$$\hat{P}_{ij} = \hat{P}_{ij} + z\hat{Q}_{ij}, \quad (5.24)$$

$$\hat{\eta}_{ij} = \eta_{ij}, \quad (5.25)$$

where $Q_{1i} \equiv q_1 + q_i$. The pole structure of the MHC amplitude consists of P_{1i}^2 for $i = 2, 3, 4$, which do not include η_{1i} . When a given pole goes on-shell, $\hat{P}_{1i}^2 = 0$, the shift parameter z takes two solutions:

$$\hat{P}_{1i}^2 = 0 \quad \rightarrow \quad z_{1i}^\pm = \frac{1}{Q_{1i}^2} (-P_{1i} \cdot Q_{1i} \pm \sqrt{(P_{1i} \cdot Q_{1i})^2 - P_{1i}^2 Q_{1i}^2}). \quad (5.26)$$

Using these solutions, the shifted pole structure can be written as

$$\frac{1}{\hat{P}_{1i}^2} = \frac{1}{P_{1i}^2} \frac{z_{1i}^+ z_{1i}^-}{(z - z_{1i}^+)(z - z_{1i}^-)}. \quad (5.27)$$

Therefore, the MHC amplitude can be calculated from the residue of the shifted amplitude $\hat{\mathcal{M}}(z)$. By Cauchy's residue theorem, the physical amplitude $\hat{\mathcal{M}}(0)$ is determined by the other residues in the complex z -plane,

$$\hat{\mathcal{M}}(0) = \frac{1}{2\pi i} \oint \frac{\hat{\mathcal{M}}(z)}{z} = \sum_{i=2,3,4} \left(\text{Res}_{z=z_{1i}^-} \frac{\hat{\mathcal{M}}(z)}{z} + \text{Res}_{z=z_{1i}^+} \frac{\hat{\mathcal{M}}(z)}{z} \right) + B_\infty, \quad (5.28)$$

where $\text{Res}_{z=z_{1i}^\pm}$ denotes the residue at finite z , and B_∞ denotes the residue at infinity.

The existence of B_∞ depends on the large- z behavior of the amplitude. In the large- z limit, a general amplitude $\hat{\mathcal{M}}(z)$ scales as z^γ . If $\gamma < 0$, then $B_\infty = 0$. In a renormalizable gauge theory, $B_\infty = 0$ can be ensured by using the Ward identity to analyze the large- z behavior of the scattering amplitude. As an example, consider the $WWhh$ amplitude, which must have the form

$$\mathcal{M}(WWhh) \sim \frac{\epsilon^2(P^2 + P\eta + \eta^2)}{P^2} + \epsilon^2, \quad (5.29)$$

where ε is the polarization vector. The first term corresponds to a factorized term with pole structure $\frac{1}{P^2}$, while the second term corresponds to a contact term. Here P^2 , $P\eta$ and η^2 in the numerator should not be interpreted as inner products of momenta, but rather as direct products. In the large- z limit, \hat{P} is shifted while $\hat{\eta}$ and the polarization vector $\hat{\varepsilon}$ remain unchanged. Therefore, the naive large- z behavior of the $WWhh$ amplitude is

$$\lim_{z \rightarrow \infty} \hat{\mathcal{M}}(z) \sim \left(\frac{\hat{\varepsilon}^2 \hat{P}^2}{\hat{P}^2} + \hat{\varepsilon}^2 \right) \sim z^0. \quad (5.30)$$

This behavior can be further suppressed by consider hidden gauge symmetry. Note that an amplitude involving vector boson can be decomposed as a polarization vector ε contracted with a structure Γ . As shown in Eq. (5.22), the polarization vector is proportional to the shift momentum q , so we have

$$\hat{\mathcal{M}} = \hat{\varepsilon} \cdot \hat{\Gamma} \sim q \cdot \hat{\Gamma}. \quad (5.31)$$

In the large- z limit, the shifted amplitude can be viewed as the amplitude in the high-energy limit, where gauge symmetry is restored, allowing us to use the Ward identity. It states that replacing the polarization vector with the shifted momentum $\hat{p} = p + zq$ makes the amplitude vanish:

$$(p + zq) \cdot \hat{\Gamma} = 0 \quad \rightarrow \quad q \cdot \Gamma = -\frac{1}{z} p \cdot \Gamma. \quad (5.32)$$

This implies we substitute $q \rightarrow -\frac{1}{z} p$ to imporve the large- z behavior. After applying the Ward identity, the large- z behavior of the $WWhh$ amplitude become z^{-1} . Thus, the residue at infinity vanishes, $B_\infty = 0$.

The finite- z residues factorize into products of subamplitudes \mathcal{M}_L and \mathcal{M}_R . Using Eq. (5.27), this factorization can be expressed as

$$\begin{aligned} \text{Res}_{z^+} \frac{\hat{\mathcal{M}}(z)}{z} &= - \sum_h \frac{1}{P^2} \frac{z^-}{z^+ - z^-} \left(\hat{\mathcal{M}}_L(\dots, \hat{P}^h) \times \hat{\mathcal{M}}_R(P^{-h}, \dots) \right) \Big|_{z=z^+}, \\ \text{Res}_{z^-} \frac{\hat{\mathcal{M}}(z)}{z} &= \sum_h \frac{1}{\hat{P}^2} \frac{z^+}{z^+ - z^-} \left(\hat{\mathcal{M}}_L(\dots, \hat{P}^h) \times \hat{\mathcal{M}}_R(P^{-h}, \dots) \right) \Big|_{z=z^+}, \end{aligned} \quad (5.33)$$

where \hat{P} represents the on-shell internal particle and h denotes its helicity. For convenience, the subscript $1i$ is omitted. It shows that higher-point MHC amplitudes can be calculated from lower-point ones, providing a recursive construction.

Now we return to the $WWhh$ amplitude with helicity $(+-00)$ and use the recursive construction to compute it. The product of two subamplitudes \mathcal{M}_L and \mathcal{M}_R can be treated similarly to the gluing technique, yielding the shifted factorized amplitude without pole structure. For (13) and (14)-channel,

we can obtain the numerator of shifted leading amplitude,

$$\begin{aligned}
 \hat{1}^+ & \quad \hat{4}^0 \\
 \hat{2}^- & \quad \hat{3}^0 \\
 1^+ & \quad 4^0 \\
 2^- & \quad 3^0
 \end{aligned}
 = \frac{\mathbf{g}^{W^+W^-} \mathbf{g}^{W^+W^-}}{2} \frac{\langle \eta_1 | \hat{P}_{14} | 1 \rangle \langle 2 | \hat{P}_{14} | \eta_2 \rangle}{\tilde{m}_1 m_2}, \\
 = \frac{\mathbf{g}^{W^+W^-} \mathbf{g}^{W^+W^-}}{2} \frac{\langle \eta_1 | \hat{P}_{13} | 1 \rangle \langle 2 | \hat{P}_{13} | \eta_2 \rangle}{\tilde{m}_1 m_2}.
 \end{aligned} \tag{5.34}$$

Since the variant ALT shift does not change the external particle states, we only need to consider the shifted internal particle state for these two diagrams. In general, we write the internal state as $\hat{P}_{\alpha\dot{\alpha}}\hat{P}_{\beta\dot{\beta}}$. Using Eq. (5.33) but neglecting the pole structure, the sum of two contributions gives

$$\begin{aligned}
 \bullet \text{---} \bullet & \Rightarrow -\frac{z^-}{z^+ - z^-} \hat{P}_{\alpha\dot{\alpha}}\hat{P}_{\beta\dot{\beta}} \Big|_{z=z^+} + \frac{z^+}{z^+ - z^-} \hat{P}_{\alpha\dot{\alpha}}\hat{P}_{\beta\dot{\beta}} \Big|_{z=z^-} \\
 & = -\frac{z^-}{z^+ - z^-} (P + z^+ Q)_{\alpha\dot{\alpha}} (P + z^+ Q)_{\beta\dot{\beta}} + \frac{z^+}{z^+ - z^-} (P + z^- Q)_{\alpha\dot{\alpha}} (P + z^- Q)_{\beta\dot{\beta}} \\
 & = P_{\alpha\dot{\alpha}} P_{\beta\dot{\beta}} + z^+ z^- Q_{\alpha\dot{\alpha}} Q_{\beta\dot{\beta}} = P_{\alpha\dot{\alpha}} P_{\beta\dot{\beta}} + \frac{P^2}{Q^2} Q_{\alpha\dot{\alpha}} Q_{\beta\dot{\beta}}.
 \end{aligned} \tag{5.35}$$

The last term $Q_{\alpha\dot{\alpha}} Q_{\beta\dot{\beta}}$ contributes to the contact term, and the value of z^\pm is given in eq. (5.26). Only the quadratic term in z^\pm survive, as the linear terms cancel when combining the residues at z^+ and z^- .

Combining the leading contributions from the (13)- and (14)-channels and restoring the pole structure, we have

$$\begin{aligned}
 & \mathbf{g}^{W^+W^-} \mathbf{g}^{W^+W^-} \left(\frac{\langle \eta_1 | P_{14} | 1 \rangle \langle 2 | P_{14} | \eta_2 \rangle}{P_{14}^2 \tilde{m}_1 m_2} + \frac{\langle \eta_1 | Q_{14} | 1 \rangle \langle 2 | Q_{14} | \eta_2 \rangle}{Q_{14}^2 \tilde{m}_1 m_2} \right) + (3 \leftrightarrow 4) \\
 & = \mathbf{g}^{W^+W^-} \mathbf{g}^{W^+W^-} \left(\frac{\langle \eta_1 | P_{14} | 1 \rangle \langle 2 | P_{14} | \eta_2 \rangle}{P_{14}^2 \tilde{m}_1 m_2} + \frac{q_2 \cdot q_4}{c_1 c_2} \right) + (3 \leftrightarrow 4) \\
 & = \mathbf{g}^{W^+W^-} \mathbf{g}^{W^+W^-} \left(\frac{\langle \eta_1 | P_{14} | 1 \rangle \langle 2 | P_{14} | \eta_2 \rangle}{P_{14}^2 \tilde{m}_1 m_2} + \frac{\langle \eta_1 | P_{14} | 1 \rangle \langle 2 | P_{14} | \eta_2 \rangle}{P_{14}^2 \tilde{m}_1 m_2} + \frac{\langle \eta_1 | 2 \rangle \langle \eta_2 | 1 \rangle}{\tilde{m}_1 m_2} \right).
 \end{aligned} \tag{5.36}$$

The last term is the contact term for the $WWhh$ amplitude. Here we use the fact that the shift momenta q_1 and q_2 are proportional to the transverse polarization vectors, as shown in eq. (5.22).

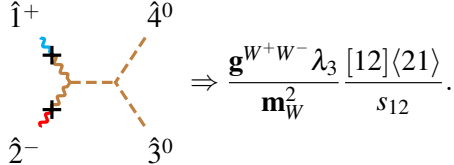
For contributions involving subleading internal structures, their shift does not contribute to the

contact amplitude. This can be verified by examining the following two shifted internal states:

$$\begin{aligned}
\bullet \text{---} \text{---} \text{---} \text{---} \bullet &\Rightarrow -\frac{z^-}{z^+ - z^-} (2\mathbf{m}^4 \epsilon_{\alpha\beta} \epsilon_{\dot{\alpha}\dot{\beta}} - \mathbf{m}^2 \hat{P}_{\alpha\dot{\alpha}} \hat{\eta}_{\beta\dot{\beta}} - \mathbf{m}^2 \hat{\eta}_{\alpha\dot{\alpha}} \hat{P}_{\beta\dot{\beta}}) \Big|_{z=z^+} \\
&\quad + \frac{z^+}{z^+ - z^-} (2\mathbf{m}^4 \epsilon_{\alpha\beta} \epsilon_{\dot{\alpha}\dot{\beta}} - \mathbf{m}^2 \hat{P}_{\alpha\dot{\alpha}} \hat{\eta}_{\beta\dot{\beta}} - \mathbf{m}^2 \hat{\eta}_{\alpha\dot{\alpha}} \hat{P}_{\beta\dot{\beta}}) \Big|_{z=z^-} \\
&= 2\mathbf{m}^4 \epsilon_{\alpha\beta} \epsilon_{\dot{\alpha}\dot{\beta}} - \mathbf{m}^2 P_{\alpha\dot{\alpha}} \eta_{\beta\dot{\beta}} - \mathbf{m}^2 \eta_{\alpha\dot{\alpha}} P_{\beta\dot{\beta}}, \\
\bullet \text{---} \text{---} \text{---} \text{---} \bullet &\Rightarrow -\frac{z^-}{z^+ - z^-} \mathbf{m}^4 \hat{\eta}_{\alpha\dot{\alpha}} \hat{\eta}_{\beta\dot{\beta}} \Big|_{z=z^+} + \frac{z^+}{z^+ - z^-} \mathbf{m}^4 \hat{\eta}_{\alpha\dot{\alpha}} \hat{\eta}_{\beta\dot{\beta}} \Big|_{z=z^-} = \mathbf{m}^4 \eta_{\alpha\dot{\alpha}} \eta_{\beta\dot{\beta}}.
\end{aligned} \tag{5.37}$$

Both results coincide with the corresponding unshifted internal states, because they contain no quadratic terms in z^\pm .

For the (12)-channel, the internal particle is a Higgs boson. Its contribution also equals the unshifted gluing result:



$$\Rightarrow \frac{\mathbf{g}^{W^+W^-} \lambda_3 [12]\langle 21 \rangle}{\mathbf{m}_W^2 s_{12}}. \tag{5.38}$$

Combining contributions from all channels, we can use the ladder operators to generate the sub-leading amplitudes. The final result of the total amplitude is

$$\begin{aligned}
\mathcal{M} = & -\frac{\mathbf{g}^{W^+W^-} \mathbf{g}^{W^+W^-}}{2} \frac{2\mathbf{m}^2 \langle \eta_1 2 \rangle [\eta_2 1] - \langle \eta_1 | P_{14} + \eta_{14} | 1 \rangle \langle 2 | P_{14} + \eta_{14} | \eta_2 \rangle}{s_{14} \tilde{m}_1 m_2} \\
& - \frac{\mathbf{g}^{W^+W^-} \mathbf{g}^{W^+W^-}}{2} \frac{2\mathbf{m}^2 \langle \eta_1 2 \rangle [\eta_2 1] - \langle \eta_1 | P_{13} + \eta_{13} | 1 \rangle \langle 2 | P_{13} + \eta_{13} | \eta_2 \rangle}{s_{13} \tilde{m}_1 m_2} \\
& - \frac{\mathbf{g}^{W^+W^-} \lambda_3}{\mathbf{m}_W} \frac{\langle \eta_1 2 \rangle [\eta_2 1]}{s_{12} \tilde{m}_1 m_2} - \frac{\mathbf{g}^{W^+W^-} \mathbf{g}^{W^+W^-}}{2} \frac{\langle \eta_1 2 \rangle [\eta_2 1]}{\tilde{m}_1 m_2}.
\end{aligned} \tag{5.39}$$

6 Massless-Massive Matching at Leading and Sub-leading Orders

In previous sections, since the contact 3-pt and 4-pt MHC amplitudes, are in the light-cone gauge, all the construction of higher-point amplitudes are in the light-cone gauge. In this section, we present an alternative way of constructing higher point amplitudes in the gauge-invariant way.

In this case, the higher-point massless amplitudes are first constructed, then match to the same point massive amplitudes. Let us still use $WW \rightarrow hh$ as example. Different from the previous sections, the 4-point massless $WWhh$ amplitudes is constructed by the massless bootstrap method in a gauge-invariant way, and then deform the gauge-invariant massless amplitudes to the MHC amplitudes, which is in the light-cone gauge with pole separation. This is essentially the matching procedure between massless and massive amplitudes for 4-point amplitudes.

For an n -point massive amplitude with spin category $\mathcal{S} = (s_1, \dots, s_n)$, it can be decomposed into a sum of MHC amplitudes

$$\mathbf{M}(\mathbf{1}^{s_1}, \mathbf{2}^{s_2}, \dots, \mathbf{n}^{s_n}) \xrightarrow{\text{MHC}} \mathcal{M} \equiv \sum_{\mathcal{T}=\mathcal{H}} \mathcal{M}^{\mathcal{H}, \mathcal{T}}. \tag{6.1}$$

In the high-energy regime $E \gg v$, these MHC amplitudes can be expanded as

$$\mathcal{M} = \sum_l [\mathcal{M}]_l \sim E^{4-n} \left(\frac{v}{E}\right)^l. \quad (6.2)$$

There is another expansion, which decomposes the amplitude into a primary part and descendant parts:

$$\mathcal{M} = \mathcal{M}^{\text{pri}} + \sum_k \mathcal{M}^{k\text{-th}}, \quad (6.3)$$

where \mathcal{M}^{pri} denotes the primary amplitude and $\mathcal{M}^{k\text{-th}}$ the k -th descendant.

The relation between these two expansions differs for 3-point and higher-point amplitudes:

- For a 3-point amplitude with total spin s , the two expansions are equivalent: all primary amplitudes have the same power counting. We can establish a one-to-one correspondence:

$$\begin{aligned} [\mathcal{M}]_{-s+1} &= \mathcal{M}^{\text{pri}}, \\ [\mathcal{M}]_{-s+2} &= \mathcal{M}^{1\text{st}}, \\ &\vdots \\ [\mathcal{M}]_{s+1} &= \mathcal{M}^{k_{\max}\text{-th}}. \end{aligned} \quad (6.4)$$

- For higher-point amplitudes, internal particles also possess spin, which must be considered. Consequently, primary amplitudes with different internal particles can exhibit different power counting. This means a one-to-one correspondence cannot be established for the full amplitude. Instead, we must decompose the amplitude into distinct channels,

$$\mathcal{M} = \sum_{\mathcal{I}} \mathcal{M}_{\mathcal{S}_{\mathcal{I}}}, \quad (6.5)$$

where \mathcal{I} labels the channel and $\mathcal{S}_{\mathcal{I}}$ denotes the spin category of the internal particles. For each channel \mathcal{I} , the primary and descendant amplitudes scale as

$$\begin{aligned} \mathcal{M}_{\mathcal{S}_{\mathcal{I}}}^{\text{pri}} &\sim v^{4-n} \left(\frac{v}{E}\right)^{-s-2s_{\mathcal{I}}+2n_{\mathcal{I}}}, \\ \mathcal{M}_{\mathcal{S}_{\mathcal{I}}}^{k\text{-th}} &\sim v^{4-n} \left(\frac{v}{E}\right)^{k-s-2s_{\mathcal{I}}+2n_{\mathcal{I}}}, \end{aligned} \quad (6.6)$$

where s is the total spin of external particles, while $n_{\mathcal{I}}$ and $s_{\mathcal{I}}$ are number and total spin of internal particles. Pole-expansion contributions are not considered here.

To illustrate the latter case, consider the 4-point W^+W^-hh amplitude, which has total external spin $s = 2$. It receives three types of contributions with different $s_{\mathcal{I}}$ and $n_{\mathcal{I}}$:

channel	internal particle	$s_{\mathcal{I}}$	$n_{\mathcal{I}}$	k_{\max}	power counting	
					primary	highest order
(13)- and (14)-channel	W boson	1	1	8	$\left(\frac{E}{v}\right)^2$	$\left(\frac{v}{E}\right)^{-6}$
(12)-channel	Higgs boson	0	1	4	1	$\left(\frac{E}{v}\right)^{-4}$
contact term	-	0	0	4	$\left(\frac{E}{v}\right)^2$	$\left(\frac{E}{v}\right)^{-2}$

Here k_{\max} is the highest order of descendant amplitudes in each channel. The table shows that primary amplitudes from different channels do not share the same power counting; they belong to $[\mathcal{M}]_{-2}$ and $[\mathcal{M}]_0$. Thus we can relate $[\mathcal{M}]_l$ to the primary/descendant amplitude of each channel:

$$\begin{aligned}
[\mathcal{M}]_{-2} &= \mathcal{M}_W^{\text{pri}} + \mathcal{M}_{\text{ct}}^{\text{pri}}, \\
[\mathcal{M}]_{-1} &= \mathcal{M}_W^{\text{1st}} + \mathcal{M}_{\text{ct}}^{\text{1st}}, \\
[\mathcal{M}]_0 &= \mathcal{M}_W^{\text{2nd}} + \mathcal{M}_{\text{ct}}^{\text{2nd}} + \mathcal{M}_h^{\text{pri}}, \\
&\vdots \\
[\mathcal{M}]_6 &= \mathcal{M}_W^{\text{8th}},
\end{aligned} \tag{6.8}$$

where subscripts W, h and ct refer to channels with an internal W boson, an internal Higgs boson, and the contact term.

An $(n+l)$ -point massless amplitude \mathcal{A}_{n+l} scales as E^{4-n-l} , so $[\mathcal{M}]_l$ should correspond to such a massless amplitude. This establishes a correspondence between an MHC amplitude with helicity $\mathcal{H} = (h_1, \dots, h_n)$ and a corresponding massless amplitude:

$$[\mathcal{M}]_l \Rightarrow \mathcal{A}_{n+l}^{\mathcal{H}^l}, \quad l \geq 0, \tag{6.9}$$

where $\mathcal{H}^l = (h_1, \dots, h_n; \overbrace{0, \dots, 0}^l)$ is the helicity category for the massless amplitude, in containing l extra scalar bosons among the external particles. Now it is the time to reconsider the helicity information on both sides of the matching.

First consider the MHC side. The general procedure is to identify the helicity of the primary amplitude, denoted $\mathcal{H}^{\text{pri}} = h^{\text{pri}} i$. For any other helicity category, we define the helicity difference h_d relative to the primary amplitude,

$$h_d = \sum_i |h_i^{\text{pri}} - h_i^{k\text{-th}}|. \tag{6.10}$$

The k -th descendant amplitudes then only correspond to helicity categories with $h_d \leq k$, and h_d must have the same parity as k . Explicitly,

$$\begin{aligned}
\mathcal{M}^{\text{pri}} : \quad &h_d = 0, \\
\mathcal{M}^{\text{1st}} : \quad &h_d = 1, \\
\mathcal{M}^{\text{2nd}} : \quad &h_d = 2, 0, \\
\mathcal{M}^{\text{3rd}} : \quad &h_d = 3, 1, \\
\mathcal{M}^{\text{4th}} : \quad &h_d = 4, 2, 0, \\
&\vdots
\end{aligned} \tag{6.11}$$

Thus we find the helicity difference for MHC amplitude at each order. To see which helicity categories contribute for a given h_d , we can return to the $WWhh$ example. Here the primary amplitude for all

structures has helicity $\mathcal{H}^{\text{pri}} = (0, 0, 0, 0)$, so we find

$$\begin{aligned} h_d = 0 : & (0, 0, 0, 0), \\ h_d = 1 : & (\pm 1, 0, 0, 0), (0, \pm 1, 0, 0), \\ h_d = 2 : & (\pm 1, \pm 1, 0, 0), (\pm 1, \mp 1, 0, 0). \end{aligned} \quad (6.12)$$

Since the primary amplitude with an internal Higgs boson has a different order from the others, we can list the MHC amplitudes for different channels into a table to distinguish them:

$h_d \backslash l$	-2	-1	0	1	2	...
0	$\mathcal{M}_W^{\text{pri}}, \mathcal{M}_{\text{ct}}^{\text{pri}}$	-	$\mathcal{M}_W^{\text{2nd}}, \mathcal{M}_{\text{ct}}^{\text{2nd}}$ $\mathcal{M}_h^{\text{pri}}$		$\mathcal{M}_W^{\text{4th}}, \mathcal{M}_{\text{ct}}^{\text{4th}}$ $\mathcal{M}_h^{\text{2nd}}$	
1	-	$\mathcal{M}_W^{\text{1st}}, \mathcal{M}_{\text{ct}}^{\text{1st}}$	-	$\mathcal{M}_W^{\text{3rd}}, \mathcal{M}_{\text{ct}}^{\text{3rd}}$ $\mathcal{M}_h^{\text{1st}}$		
2	-	-	$\mathcal{M}_W^{\text{2nd}}, \mathcal{M}_{\text{ct}}^{\text{2nd}}$		$\mathcal{M}_W^{\text{4th}}, \mathcal{M}_{\text{ct}}^{\text{4th}}$ $\mathcal{M}_h^{\text{2nd}}$	

(6.13)

Entries in gray ($l < 0$) do not correspond to massless amplitudes with a linear realization of the scalar field in the SM.

Now consider the helicity category of the $(4+l)$ -point massless amplitude. To match the $WWhh$ amplitude, the helicity of first four massless particles are given in Eq. (6.12). Since the number of extra scalars is equal to the order l in Eq. (6.13), filling the massless amplitudes into an analogous table gives:

$h_d \backslash l$	0	1	2	...
0	$\mathcal{A}^{(0,0,0,0)}$		$\mathcal{A}^{(0,0,0,0,0)}$	
1		$v\mathcal{A}^{(\pm 1,0,0,0,0)}$ $v\mathcal{A}^{(0,\pm 1,0,0,0)}$		
2	$\mathcal{A}^{(\pm 1,\mp 1,0,0)}$		$v^2\mathcal{A}^{(\pm 1,\mp 1,0,0,0,0)}$ $v^2\mathcal{A}^{(\pm 1,\pm 1,0,0,0,0)}$	

(6.14)

The helicity matching between the MHC amplitude and the UV massless amplitude setup a framework for massless-massive correspondence. This correspondence allows us to reorganize the MHC amplitudes from a top-down matching perspective. We will start with the primary matching, and then discuss matching at sub-leading order.

6.1 Massless 4-point amplitudes: the gauge-invariant way

In this subsection, we will construct the 4-point massless amplitudes from the gauge-invariant 3-point massless amplitudes. The building blocks are 3-pt massless amplitudes in the SM, which are given in section 3. Let us briefly review how the recursive and BCFW methods are used for the SM massless amplitudes. The two methods show their own advantages in the SM amplitude construction.

The BCFW recursion relations [14, 15] is the most popular method to calculate the higher-point massless amplitudes in gauge theories, which is based on the analytic properties of scattering amplitudes. Consider a holomorphic function $\mathcal{A}(z)$, which is a complexification of the physical amplitude $\mathcal{A}(0)$ with a complex parameter z . Although the momenta become complex-valued, the momentum conservation and the on-shell condition are still valid. Therefore, the Cauchy's residue theorem show that

$$\mathcal{A}(0) = \frac{1}{2\pi i} \oint \frac{\mathcal{A}(z)}{z}, \quad (6.15)$$

where the poles in the complex plane correspond to the on-shell propagators except for the pole at origin, so $\mathcal{A}(0)$ can be derived from the sum of the residues. In the BCFW recursion relations, two momenta are shifted by to be shifted the complex parameter z (2-line shift).

This method is quite successful to applied to gauge theory, gravity and supersymmetric theory, but fail in the electroweak massless amplitudes. To show the problem, let us consider a theory includes scalar-QED and $\lambda\phi^4$ interaction, which is contained in the electroweak theory. The 4-scalar amplitude derived by the BCFW recursion relations and Feynman rules [5] are given seperately by

$$\begin{aligned} \mathcal{A}^{\text{BCFW}}(\varphi\varphi^*\varphi\varphi^*) &= \tilde{e}^2 \frac{\langle 13 \rangle^2 \langle 24 \rangle^2}{\langle 12 \rangle \langle 23 \rangle \langle 34 \rangle \langle 41 \rangle}, \\ \mathcal{A}^{\text{Feynman}}(\varphi\varphi^*\varphi\varphi^*) &= -\lambda + \tilde{e}^2 \left(1 + \frac{\langle 13 \rangle^2 \langle 24 \rangle^2}{\langle 12 \rangle \langle 23 \rangle \langle 34 \rangle \langle 41 \rangle} \right). \end{aligned} \quad (6.16)$$

Since the contact term $-\lambda + \tilde{e}^2$ don't have pole, it cannot be constructed by the simple recursion relations. Therefore, the 4-scalar amplitude should be an input to calculate the massless amplitudes with more than four legs. To calculate the general amplitudes, the generalizations [17, 19, 20, 59–61] of BCFW recursion relations were studied, which have more than two shifted momenta. For the SM, people found that the massless amplitudes are 3-line constructible [61]. However, when $n \geq 3$, the n -line shifts is not convenient to construct the amplitudes.

Therefore, another approach, known as the bootstrap method, is applied to construct higher-point amplitudes in the SM. The amplitude decomposes into a product of sub-amplitudes corresponding to two distinct processes with the simple pole structure in the massless amplitude

$$\lim_{P^2 \rightarrow 0} P^2 \mathcal{M} = M^L \times M^R, \quad (6.17)$$

where P^2 is the on-shell propagators of the immediate massless particle, and the M^L and M^R are sub-amplitudes. In this method, the final form of the factorized amplitudes should have the following form. The ansatz consists of the denominator D , the numerator N and the group tensor G

$$\mathcal{A} = \sum_i G_i \frac{N_i}{D_i}, \quad (6.18)$$

where G, D are known while N need to be determined. A reasonable ansatz should satisfy the following requirements:

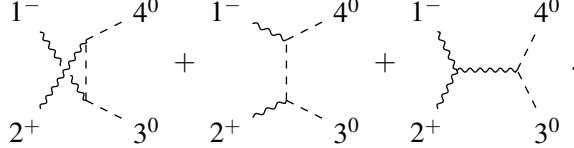
- The group tensor G usually form a group structure basis, and thus every group tensor appeared in the amplitude should be independent term.

- The denominator D represents the pole structure of the massless amplitudes and must has the form

$$D \equiv \prod_{ij\cdots} (p_i + p_j + \cdots)^2. \quad (6.19)$$

All the terms in the ansatz should correspond to diagrams. Depending on whether the group tensors are independent, the terms in the ansatz may or may not correspond one-to-one with these diagrams. In the following, we will discuss these two cases separately and show how the ansatz can be used to obtain the massless amplitudes. We will construct the primary massless amplitudes in the $(+, -, 0, 0)$ and $(0, 0, 0, 0)$ helicity categories, in the massless scalar QED and Yang-Mills theory.

$(-1, +1, 0, 0)$ helicity with non-independent group structure In the $WW \rightarrow hh$ amplitude, we choose the helicity category to be $(-1, +1, 0, 0)$. From the bootstrap, this 4-pt amplitude consists of the following three diagrams



$$. \quad (6.20)$$

In the three diagrams, we read the corresponding group tensors and denominators

$$\begin{aligned} G_1 &= (T_s^{I_2} T_s^{I_1})_{i_4}^{i_3}, & G_2 &= (T_s^{I_1} T_s^{I_2})_{i_4}^{i_3}, & G_3 &= f^{J_1 J_2} (T_s^J)_{i_4}^{i_3}, \\ D_1 &= s_{13}, & D_2 &= s_{14}, & D_3 &= s_{12}. \end{aligned} \quad (6.21)$$

One can verify the these three group tensors are not independent. They satisfy the linear following relation

$$G_1 - G_2 - G_3 = 0. \quad (6.22)$$

Let us choose two of them to get the ansatz and calculate the massless amplitude. Here we choose G_1, G_2 as an independent basis, in which case G_3 becomes a redundant group structure. The ansatz should therefore only contain the first two gauge tensors. Correspondingly, we define the new denominators D' to incorporate the pole structure s_{12} associated with the redundant gauge tensor G_3

$$D_1, D_2, D_3 \rightarrow \begin{cases} D'_1 = D_1 D_3 = s_{13} s_{12}, \\ D'_2 = D_2 D_3 = s_{14} s_{12}. \end{cases} \quad (6.23)$$

Therefore, the full ansatz for the $WWHH^\dagger$ amplitude can be written as

$$\mathcal{A}(1^{I_1}, 2^{I_2}, 3^{i_3}, 4_{i_4}) = (T_s^{I_2} T_s^{I_1})_{i_4}^{i_3} \frac{N_1}{s_{12} s_{13}} + (T_s^{I_1} T_s^{I_2})_{i_4}^{i_3} \frac{N_2}{s_{12} s_{14}}. \quad (6.24)$$

In the factorized limit, we have

$$\begin{aligned}
\lim_{P_{13}^2 \rightarrow 0} P_{13}^2 \mathcal{A} &= A^L(1^{-1,I_1}, 3_{i_3}^0, (P_{13})^{0,j}) \times A^R(2^{+1,I_2}, (-P_{13})_j^0, 4^{0,i_4}) \\
&= (T_s^{I_1})_j^{i_3} \frac{\langle 13 \rangle \langle P_{13} 1 \rangle}{\langle 3 P_{13} \rangle} \times (T_s^{I_2})_j^{i_4} \frac{[2(-P_{13})][42]}{[(-P_{13})4]} \\
&= (T_s^{I_2} T_s^{I_1})_{i_4}^{i_3} \langle 13 \rangle [32] \frac{[24]}{[14]} = (T_s^{I_2} T_s^{I_1})_{i_4}^{i_3} \langle 13 \rangle [32] \frac{[24] \langle 41 \rangle}{[14] \langle 41 \rangle} \\
&= (T_s^{I_2} T_s^{I_1})_{i_4}^{i_3} \frac{\langle 1|3|2 \rangle^2}{s_{12}}, \tag{6.25}
\end{aligned}$$

where we use $\langle \cdot P_{13} \rangle [(-P_{13}) \cdot] = -\langle \cdot | p_1 + p_3 | \cdot \rangle$ and momentum conservation. For N_1 , since $\langle 1|4|2 \rangle = -\langle 1|3|2 \rangle$, there is only one kinematic structure $\langle 1|3|2 \rangle^2$ and the coefficient is determined by Eq. (6.25). Another numerator N_2 can be derived by the limit $P_{14}^2 \rightarrow 0$.

Thus, we find the result of the massless $WWHH^\dagger$ amplitude in the gauge-invariant form

$$\mathcal{A}(1^{-1,I_1}, 2^{+1,I_2}, 3^{0,i_3}, 4_{i_4}^0) = (T_s^{I_2} T_s^{I_1})_{i_4}^{i_3} \frac{\langle 1|3|2 \rangle^2}{s_{12} s_{13}} + (T_s^{I_1} T_s^{I_2})_{i_4}^{i_3} \frac{\langle 1|3|2 \rangle^2}{s_{12} s_{14}}. \tag{6.26}$$

(0,0,0,0) helicity with independent group structure Let us consider the four-scalar amplitude with helicity category $(0,0,0,0)$, in which the external particles do not include gauge bosons. Using the bootstrap, the 4-point amplitude involves three diagrams,

$$\begin{array}{c} 1^0 \quad \quad \quad 4^0 \\ \backslash \quad \quad \quad \backslash \\ \text{---} \quad \quad \quad \text{---} \\ \text{---} \quad \quad \quad \text{---} \\ 2^0 \quad \quad \quad 3^0 \end{array} + \begin{array}{c} 1^0 \quad \quad \quad 4^0 \\ \backslash \quad \quad \quad \backslash \\ \text{---} \quad \quad \quad \text{---} \\ \text{---} \quad \quad \quad \text{---} \\ 2^0 \quad \quad \quad 3^0 \end{array} + \begin{array}{c} 1^0 \quad \quad \quad 4^0 \\ \backslash \quad \quad \quad \backslash \\ \text{---} \quad \quad \quad \text{---} \\ \text{---} \quad \quad \quad \text{---} \\ 2^0 \quad \quad \quad 3^0 \end{array}, \tag{6.27}$$

where the script 0 represent the helicity of the external particle. The corresponding group tensors and pole structures are given by:

$$\begin{aligned}
G_1 &= (T_s^J)_{i_2}^{i_1} (T_s^J)_{i_4}^{i_3}, & G_2 &= (T_s^J)_{i_4}^{i_1} (T_s^J)_{i_2}^{i_3}, & G_3 &= \lambda \delta_{i_2}^{(i_1} \delta_{i_4}^{i_3)}. \\
D_1 &= s_{12}, & D_2 &= s_{13}, & D_3 &= s_{14}. \tag{6.28}
\end{aligned}$$

The first two group tensors, G_1 and G_2 , are simply products of the group tensor from the VSS amplitude, denoted as T_s , while the last group tensor G_3 originates from the $\lambda \phi^4$ interaction. One can verify that G_1 , G_2 , and G_3 are independent. Therefore, the ansatz for the four-scalar amplitude can be written as

$$\mathcal{A}(1^{i_1}, 2_{i_2}, 3^{i_3}, 4_{i_4}) = (T_s^J)_{i_2}^{i_1} (T_s^J)_{i_4}^{i_3} \frac{N_1}{s_{12}} + (T_s^J)_{i_4}^{i_1} (T_s^J)_{i_2}^{i_3} \frac{N_2}{s_{14}} + \lambda \delta_{i_2}^{(i_1} \delta_{i_4}^{i_3)} N_3, \tag{6.29}$$

where $s_{ij} = (p_i + p_j)^2$ is the denominator.

To determine the expression for numerator N_i , we can consider the factorized limit, in which the corresponding propagator goes on-shell. Therefore, the unknown numerator can factorized into two lower-point amplitudes,

$$G_i N_i = \lim_{P^2 \rightarrow 0} P^2 \mathcal{A} = \sum_{hp} A^L \times A^R, \tag{6.30}$$

where P and h_P are the momentum and the helicity of the on-shell propagator, A^L and A^R are massless sub-amplitudes. The building blocks are the 3-pt and 4-scalar massless amplitudes, which are derived in section 3. In Ref. [36], the authors listed all possible kinematic structures for N . Then the coefficients can be determined by Eq. (6.30). For simplicity, we will not list all kinematic structure in this subsection. Instead, we will use other argument to find the correct result.

Return to the four-scalar amplitude. The unknown numerator N_1 can be obtained by the we use the the factorized limit $s_{12} \rightarrow 0$. We have

$$\begin{aligned} \lim_{P_{12}^2 \rightarrow 0} P_{12}^2 \mathcal{A} &= A^L \left((P_{12})^{-1,J}, 1^{0,i_1}, 2_{i_2}^0 \right) \times A^R \left((-P_{12})^{+1,J}, (-P_{12})_{i_3}^0, 4^{0,i_4} \right) \\ &= (T_s^J)_{i_2}^{i_1} \frac{\langle 1P_{12} \rangle \langle P_{12} 2 \rangle}{\langle 12 \rangle} \times (T_s^J)_{i_4}^{i_3} \frac{[3(-P_{12})][(-P_{12})4]}{[34]} \\ &= -(T_s^J)_{i_2}^{i_1} (T_s^J)_{i_4}^{i_3} \frac{\langle 1|P_{12}|3 \rangle \langle 2|P_{34}|4 \rangle + \langle 1|P_{12}|4 \rangle \langle 2|P_{34}|3 \rangle}{2\langle 12 \rangle [34]} \\ &= (T_s^J)_{i_2}^{i_1} (T_s^J)_{i_4}^{i_3} \frac{-[23]\langle 23 \rangle + [24]\langle 24 \rangle}{2}, \end{aligned} \quad (6.31)$$

where $P_{12} = p_1 + p_2$. In the second line, we should convert $\langle \cdot | P \rangle$ and $[P \cdot]$ to $\langle \cdot | P | \cdot \rangle$. There are two ways to convert them, but we don't find any constraint between the two ways. Therefore, we average the two ways in the third line to give the numerator $N_1 = \frac{1}{2}(-[23]\langle 23 \rangle + [24]\langle 24 \rangle)$. The other numerator N_2 can be computed similarly in the limit $P_{14}^2 \rightarrow 0$. The last $N_3 = -4$ are determined by Eq. (3.20).

Finally, we obtain the gauge-invariant four-scalar amplitude in the scalar QED

$$\mathcal{A}(1^{i_1}, 2_{i_2}, 3^{i_3}, 4_{i_4}) = -(T_s^J)_{i_2}^{i_1} (T_s^J)_{i_4}^{i_3} \frac{s_{13} - s_{14}}{2s_{12}} - (T_s^J)_{i_4}^{i_1} (T_s^J)_{i_2}^{i_3} \frac{s_{13} - s_{12}}{2s_{14}} - 4\lambda \delta_{i_2}^{(i_1} \delta_{i_4}^{i_3)}. \quad (6.32)$$

6.2 Scaling structure for MHC amplitudes

Having obtained the gauge-invariant massless amplitudes, we would perform amplitude deformation to obtain massless amplitudes in the light-cone gauge, in which the pole separation should also be done. To guide the amplitude deformation, the scaling behavior of the MHC amplitudes should be known. Let us examine the scaling structure of the massless and MHC amplitudes.

For a general massless amplitude, each term can be characterized by a spinor scaling structure of the form

$$\mathbb{A} = \mathbb{E}(\lambda, \tilde{\lambda}) \times \mathbb{I}(p) \times \mathbb{P}, \quad (6.33)$$

where \mathbb{E} represents the external scaling, which depends on all external particles; \mathbb{I} is the internal scaling, containing only massless momentum; and \mathbb{P} denotes the pole structure. This schematic form omits coefficients, particle labels, and spinor indices, thus providing a broad outline of the amplitude's scaling behavior.

To illustrate this, consider the $HHHH$ amplitude obtained in the previous subsection. One of its terms has the spinor behavior

$$\frac{\langle 1|3|2]^2}{s_{12}s_{13}} \rightarrow \begin{cases} \text{external scaling: } E(\lambda^2 \tilde{\lambda}^2) \sim \lambda_1 \tilde{\lambda}_2^2, \\ \text{internal scaling: } I(p^2) \sim p_3^2, \\ \text{pole scaling: } \mathbb{P}(p^{-4}) \sim \frac{1}{s_{12}s_{13}}. \end{cases} \quad (6.34)$$

Similarly, another term in the $HHHH$ amplitude exhibits the same scaling structure

$$\frac{\langle 1|3|2]^2}{s_{12}s_{14}} \sim \mathbb{E}(\lambda^2\tilde{\lambda}^2) \times \mathbb{I}(p^2) \times \mathbb{P}(p^{-4}). \quad (6.35)$$

In previous subsection, we also obtained the $WWHH$ amplitude. Its three terms display two distinct scaling behaviors

$$\begin{aligned} \frac{s_{13}-s_{14}}{2s_{12}}, \frac{s_{13}-s_{12}}{2s_{14}} &\sim \mathbb{E}(1) \times \mathbb{I}(p^2) \times \mathbb{P}(p^{-2}), \\ 1 &\sim \mathbb{E}(1) \times \mathbb{I}(1) \times \mathbb{P}(1). \end{aligned} \quad (6.36)$$

Similarly, for general MHC amplitudes, we can also define a scaling structure for each diagram,

$$\mathbb{M} = \mathbf{m}^a \times \underbrace{\mathbb{E} \times \mathbb{I}}_{\text{MHC diagram}} \times \mathbb{P}, \quad (6.37)$$

which consists of four parts

- The external scaling $\mathbb{E}(\tilde{\lambda}, \lambda, m\tilde{\eta}, m\eta)$ captures the spinor scaling behavior of all external particles. Here we list the external particle that will appear in the $WWhh$ amplitude

boson	scaling of external state		
scalar		$0 \sim 1$	-
vector		$0 \sim \tilde{\lambda}\lambda$	$\begin{aligned} &\bullet \text{---} \text{---} \text{---} \sim \lambda m\tilde{\eta} \\ &\bullet \text{---} \text{---} \text{---} \sim \tilde{\lambda}\tilde{m}\eta \end{aligned}$

- The internal scaling $\mathbb{I}(p, m\tilde{\eta}\eta)$ encodes the scaling information of internal particles. Here η is the momentum $\eta_{\alpha\alpha}$, which should not be mixing with the spinor η_α . For $WWhh$ amplitude, the internal particle can be only scalar or vector boson:

boson	scaling of internal state		
scalar		$\bullet \sim 1$	-
vector		$\bullet \sim p^2$	$\begin{aligned} &\bullet \text{---} \text{---} \text{---} \sim m\tilde{\eta}p\eta \\ &\bullet \text{---} \text{---} \text{---} \sim m^2\tilde{m}^2\eta^2 \end{aligned}$

- The pole scaling \mathbb{P} describes a universal scaling behavior of the pole structures, which does not depend strongly on the particle type. For the single-pole term, the pole scaling gives an infinite expansion

$$\mathbb{P}(p^{-2}) + \mathbb{P}(\eta p^{-3}) + \mathbb{P}(\eta^2 p^{-4}) + \dots \quad (6.40)$$

Combined with the internal scaling, it can be represented diagrammatically as

boson	scaling of internal state and pole structure		
scalar		$\bullet \text{---} \text{---} \text{---} \sim \mathbb{I}(1) \times \mathbb{P}(p^{-2})$	
vector		$\bullet \text{---} \text{---} \text{---} \sim \mathbb{I}(p^2) \times \mathbb{P}(p^{-2})$	

where each \otimes on a particle line denotes a subleading correction in the pole expansion. For convenience, we take one \otimes to represent a factor of order \mathbf{m}^2/E^2 in the expansion. Thus, it is of the same order as a cross term and always appears in pairs. For contact term, the pole scaling is trivial

$$\mathbb{P}(1). \quad (6.42)$$

- The last thing is a power of physical mass \mathbf{m} , which is used to make sure that the n -point amplitude satisfy the mass dimension $4 - n$.

For 3pt amplitudes, there are no internal particle and pole structures, so the scaling structure is simple

$$\begin{aligned} \text{primary : } & \mathbb{M}_3 = \mathbf{m}^{1-s_1-s_2-s_3} \mathbb{E}, \\ \text{k-th descendant : } & \mathbb{M}_3 = \mathbf{m}^{1-s_1-s_2-s_3-k} \mathbb{E}. \end{aligned} \quad (6.43)$$

For example, consider the VSS amplitude, we can list the scaling behavior for each order:

$$\begin{aligned} \text{primary : } & \text{Diagram: } \text{0 } \text{--- } \text{0 } \text{--- } \text{0 } \text{ (top)} \text{--- } \text{0 } \text{ (bottom)} \text{--- } \text{0 } \text{ (right)} \text{--- } \text{0 } \text{ (left)} \text{--- } \text{0 } \text{ (top)} \text{ (wavy line)} \sim \frac{1}{\mathbf{m}} \mathbb{E}(\tilde{\lambda}^2 \lambda^2), \\ \text{1st descendant : } & \text{Diagram: } \text{0 } \text{--- } \text{0 } \text{--- } \text{0 } \text{ (top)} \text{--- } \text{0 } \text{ (bottom)} \text{--- } \text{0 } \text{ (right)} \text{--- } \text{0 } \text{ (left)} \text{--- } \text{0 } \text{ (wavy line)} \sim \frac{1}{\mathbf{m}^2} \mathbb{E}(\tilde{\lambda} \lambda^2 m \tilde{\eta}), \quad + \text{Diagram: } \text{0 } \text{--- } \text{0 } \text{--- } \text{0 } \text{ (top)} \text{--- } \text{0 } \text{ (bottom)} \text{--- } \text{0 } \text{ (right)} \text{--- } \text{0 } \text{ (left)} \text{--- } \text{0 } \text{ (wavy line)} \sim \frac{1}{\mathbf{m}^2} \mathbb{E}(\tilde{\lambda}^2 \lambda \tilde{m} \eta), \\ \text{2nd descendant : } & \text{Diagram: } \text{0 } \text{--- } \text{0 } \text{--- } \text{0 } \text{ (top)} \text{--- } \text{0 } \text{ (bottom)} \text{--- } \text{0 } \text{ (right)} \text{--- } \text{0 } \text{ (left)} \text{--- } \text{0 } \text{ (wavy line)} \sim \frac{1}{\mathbf{m}^3} \mathbb{E}(\tilde{\lambda} \lambda \tilde{m} \eta m \tilde{\eta}). \end{aligned} \quad (6.44)$$

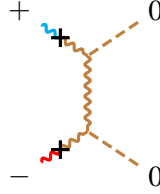
For the 2nd descendant, we list only amplitude with total helicity $h_1 + h_2 + h_3 = 0$, because it is enough for the $WWhh$ matching.

For SSS amplitude, the scaling is given by

$$\text{primary : } \text{0 } \text{--- } \text{0 } \text{--- } \text{0 } \text{ (top)} \text{--- } \text{0 } \text{ (bottom)} \text{--- } \text{0 } \text{ (right)} \text{--- } \text{0 } \text{ (left)} \sim \mathbf{m} \mathbb{E}(1). \quad (6.45)$$

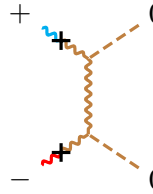
Then we can consider the scaling of the 4-pt amplitudes. For helicity category $(+1, -1, 0, 0)$, the

external and internal scaling can be obtained by multiplying the scaling of two 3-pt amplitudes,



$$: \frac{\mathbb{E}(\tilde{\lambda}\lambda^2 m\tilde{\eta})}{\mathbf{m}^2} \times \frac{\mathbb{E}(\tilde{\lambda}^2\lambda\tilde{m}\eta)}{\mathbf{m}^2} = \frac{\mathbb{E}(\tilde{\lambda}\lambda m\tilde{\eta}\tilde{m}\eta)}{\mathbf{m}^4} \times \mathbb{I}(p^2). \quad (6.46)$$

Combining with the pole structure, it gives



$$\sim \frac{1}{\mathbf{m}^4} \mathbb{E}(\tilde{\lambda}\lambda m\tilde{\eta}\tilde{m}\eta) \times \mathbb{I}(p^2) \times (\mathbb{P}(p^{-2}) + \mathbb{P}(\eta p^{-3}) + \dots). \quad (6.47)$$

The massless amplitude does not match all these MHC diagrams. To determine which MHC diagrams can be matched, we can carry out a power counting analysis. The massive amplitude involves two scales: the energy scale E and mass scale \mathbf{m} . In the high-energy regime $E \gg \mathbf{m}$, only terms scaling as $E^0 \mathbf{m}^0$ can be matched from 4-pt massless amplitude. The building blocks appearing in the scaling structure have the following power counting

$$\begin{aligned} \lambda, \tilde{\lambda} &\sim \sqrt{E}, \quad \tilde{m}\eta, m\tilde{\eta} \sim \frac{\mathbf{m}^2}{\sqrt{E}}, \\ p &\sim E, \quad \eta \sim \frac{\mathbf{m}^2}{E}. \end{aligned} \quad (6.48)$$

Using these, we can determine the power counting of eq. (6.50),

$$\begin{aligned} \frac{1}{\mathbf{m}^4} \mathbb{E}(\tilde{\lambda}\lambda m\tilde{\eta}\tilde{m}\eta) &\sim 1, \\ \mathbb{I}(p^2) &\sim E^2, \\ \mathbb{P}(p^{-2}) + \mathbb{P}(\eta p^{-3}) + \dots &\sim \frac{1}{E^2} + \frac{\mathbf{m}^2}{E^4} + \dots \end{aligned} \quad (6.49)$$

Therefore, only the leading term of the pole structure contributes at $E^0 \mathbf{m}^0$, which corresponds to

$$\frac{1}{\mathbf{m}^4} \mathbb{E}(\tilde{\lambda}\lambda m\tilde{\eta}\tilde{m}\eta) \times \mathbb{I}(p^2) \times \mathbb{P}(p^{-2}). \quad (6.50)$$

Similarly, we can derive the leading scaling of all MHC diagrams in helicity category $(+, -, 0, 0)$

and the corresponding power counting.

diagram	leading scaling	leading power counting
	$\frac{1}{m^4} \mathbb{E}(\tilde{\lambda} \lambda m \tilde{\eta} \tilde{m} \eta) \times \mathbb{I}(p^2) \times \mathbb{P}(p^{-2})$	1
	$\frac{1}{m^4} \mathbb{E}(\tilde{\lambda} \lambda m \tilde{\eta} \tilde{m} \eta) \times \mathbb{I}(1) \times \mathbb{P}(1)$	
	$\frac{1}{m^4} \mathbb{E}(\tilde{\lambda} \lambda m \tilde{\eta} \tilde{m} \eta) \times \mathbb{I}(p\eta) \times \mathbb{P}(p^{-2})$	$\frac{m^2}{E^2}$
	$\frac{1}{m^2} \mathbb{E}(\tilde{\lambda} \lambda m \tilde{\eta} \tilde{m} \eta) \times \mathbb{I}(1) \times \mathbb{P}(p^{-2})$	
	$\frac{1}{m^4} \mathbb{E}(\tilde{\lambda} \lambda m \tilde{\eta} \tilde{m} \eta) \times \mathbb{I}(\eta^2) \times \mathbb{P}(p^{-2})$	$\frac{m^4}{E^4}$

Since the 4-pt massless amplitude has power counting E^0 , so it can match to the first two MHC diagrams with leading power counting 1. The massless matching

$$\mathcal{A} \rightarrow + \text{ (diagram 1)} + + \text{ (diagram 2)} . \quad (6.52)$$

Similarly, we can obtain the MHC scaling for $(0,0,0,0)$ helicity category, and select the ones that have same power counting as 4-pt masselss amplitude.

For s_{13} and s_{14} channel, we have

$$\begin{aligned}
 & \text{Top Diagram: } \sim \frac{1}{\mathbf{m}^2} \mathbb{E}(\tilde{\lambda}^2 \lambda^2) \times \mathbb{I}(p^2) \times \mathbb{P}(\eta p^{-3}), \\
 & \text{Bottom Diagram: } \sim \frac{1}{\mathbf{m}^2} \mathbb{E}(\tilde{\lambda}^2 \lambda^2) \times \mathbb{I}(p\eta) \times \mathbb{P}(p^{-2}), \\
 & \text{Bottom Diagram with plus sign: } \sim \frac{1}{\mathbf{m}^4} \mathbb{E}(\tilde{\lambda} \lambda m \tilde{\eta} \tilde{m} \eta) \times \mathbb{I}(p^2) \times \mathbb{P}(p^{-2}).
 \end{aligned} \tag{6.53}$$

For s_{12} channel and contact term, we have

$$\begin{aligned}
 & \text{Top Diagram: } \sim \frac{1}{\mathbf{m}^4} \mathbb{E}(\tilde{\lambda} \lambda m \tilde{\eta} \tilde{m} \eta) \times \mathbb{I}(1) \times \mathbb{P}(1), \\
 & \text{Bottom Diagram with plus sign: } \sim \mathbb{E}(\tilde{\lambda}^2 \lambda^2) \times \mathbb{I}(1) \times \mathbb{P}(p^{-2}).
 \end{aligned} \tag{6.54}$$

The scaling change will guide us to perform the amplitude matching in the following discussion.

6.3 Amplitude deformation and pole separation

In this subsection, we match the massless amplitude to the MHC amplitude by amplitude deformation. This deformation has two steps. First match the coefficient, denoted as group tensor, from unbroken phase to the broken phase. Then we deform the massless amplitude in the gauge invariant form, to the massless amplitude in the light cone gauge, so the massless pole structure can match the MHC ones, which is guided by the analysis of scaling structure between massless and MHC amplitude. This pole matching will involve the cases of the pole separation and extraction, which will be discussed in detail with the example of W^+W^-hh matching.

helicity $(+, -, 0, 0)$ We first consider the helicity category $(+, -, 0, 0)$. The corresponding massless amplitude has been derived. Since both Higgs doublets H and H^\dagger can match to the massive Higgs

boson h , we need the following two amplitude expressions:

$$\begin{aligned}\mathcal{A}(1^{-1,I_1}, 2^{+1,I_2}, 3^{0,i_3}, 4_{i_4}^0) &= (T_s^{I_2} T_s^{I_1})_{i_4}^{i_3} \frac{[1|3|2\rangle[1|4|2\rangle}{s_{12}s_{13}} + (T_s^{I_1} T_s^{I_2})_{i_4}^{i_3} \frac{[1|3|2\rangle[1|4|2\rangle}{s_{12}s_{14}}, \\ \mathcal{A}(1^{-1,I_1}, 2^{+1,I_2}, 3_{i_3}^0, 4^{0,i_4}) &= (T_s^{I_2} T_s^{I_1})_{i_3}^{i_4} \frac{[1|3|2\rangle[1|4|2\rangle}{s_{12}s_{14}} + (T_s^{I_1} T_s^{I_2})_{i_3}^{i_4} \frac{[1|3|2\rangle[1|4|2\rangle}{s_{12}s_{13}}.\end{aligned}\quad (6.55)$$

These correspond to the $WWHH^\dagger$ and $WWH^\dagger H$ amplitudes.

The massless amplitude contains double poles, such as $s_{12}s_{13}$, which do not appear in the massive case. Therefore, we need to separate this multipole structure. This can be analyzed through scaling behavior. All terms in eq. (6.55) share the same scaling $\mathbb{E}(\lambda^2 \tilde{\lambda}^2) \times \mathbb{I}(p^2) \times \mathbb{P}(p^{-4})$, where the double pole structure is contained in $\mathbb{P}(p^{-4})$. To separate the poles, we must increase the power of the pole scaling from $\mathbb{P}(p^{-4})$ to something like $\mathbb{P}(p^{-2})$. However, this scaling cannot be changed directly as

$$\mathbb{E}(\lambda^2 \tilde{\lambda}^2) \times \mathbb{I}(p^2) \times \mathbb{P}(p^{-4}) \not\rightarrow \mathbb{E}(\lambda^2 \tilde{\lambda}^2) \times \mathbb{I}(1) \times \mathbb{P}(p^{-2}), \quad (6.56)$$

because the only spinor structure satisfying $\mathbb{E}(\lambda^2 \tilde{\lambda}^2) \times \mathbb{I}(1)$ is $\langle 11 \rangle [22] = 0$. A better way to achieve a sensible pole separation is to convert the massless scaling to the MHC scaling. Multiplying by $\frac{\langle \lambda \eta \rangle}{m} \frac{[\lambda \eta]}{\tilde{m}}$ transforms the massless scaling as follows,

$$\begin{aligned}\mathbb{E}(\lambda^2 \tilde{\lambda}^2) \times \mathbb{I}(p^2) \times \mathbb{P}(p^{-4}) &\xrightarrow{\frac{\langle \lambda \eta \rangle}{m} \frac{[\lambda \eta]}{\tilde{m}}} \frac{1}{\mathbf{m}^4} \mathbb{E}(\tilde{\lambda}^3 \lambda^3 m \tilde{\eta} \tilde{m} \eta) \times \mathbb{I}(p^2) \times \mathbb{P}(p^{-4}) \\ &\rightarrow \frac{1}{\mathbf{m}^4} \mathbb{E}(\tilde{\lambda} \lambda m \tilde{\eta} \tilde{m} \eta) \times \mathbb{I}(p^4) \times \mathbb{P}(p^{-4}) \\ &\xrightarrow{\text{pole isolation}} \frac{1}{\mathbf{m}^4} \mathbb{E}(\tilde{\lambda} \lambda m \tilde{\eta} \tilde{m} \eta) \times \mathbb{I}(p^2) \times \mathbb{P}(p^{-2}) + \frac{1}{\mathbf{m}^4} \mathbb{E}(\tilde{\lambda} \lambda m \tilde{\eta} \tilde{m} \eta) \times \mathbb{I}(1) \times \mathbb{P}(1).\end{aligned}\quad (6.57)$$

In the third line, part of the spinor scaling is transferred from the external scaling \mathbb{E} to the internal scaling \mathbb{I} , which acquires an inverse scaling relative to $\mathbb{P}(p^{-4})$. As a result, the pole separation yields not only a term with a single pole but also a contact term with no poles.

The corresponding amplitude deformation is given by

$$\begin{aligned}\frac{[1|3|2\rangle[1|4|2\rangle}{s_{12}s_{13}} &\xrightarrow{\frac{\langle \lambda \eta \rangle}{m} \frac{[\lambda \eta]}{\tilde{m}}} \frac{\langle \eta_1 1 \rangle [1|3|2\rangle[1|4|2\rangle[2\eta_2]}{\tilde{m}_1 m_2 s_{12}s_{13}} \\ &= \frac{\langle \eta_1 | 13|2\rangle[1|42|\eta_2]}{\tilde{m}_1 m_2 s_{12}s_{13}}.\end{aligned}\quad (6.58)$$

To isolate the pole structure, we can deform the numerator. By commuting the momenta in the spinor chains, we obtain

$$\begin{aligned}\langle \eta_1 | 13|2\rangle &= -\langle \eta_1 | 3|1\rangle\langle 12\rangle + s_{13}\langle \eta_1 2\rangle, \\ [1|42|\eta_2] &= -[12]\langle 2|4|\eta_2] + s_{24}[1\eta_2].\end{aligned}\quad (6.59)$$

Using this relation, we find

$$\begin{aligned}
\frac{[1|3|2][1|4|2]}{s_{12}s_{13}} &= \frac{(-\langle\eta_1|3|1]\langle12\rangle + s_{13}\langle\eta_12\rangle)(-[12]\langle2|4|\eta_2\rangle + s_{24}[1\eta_2])}{s_{12}s_{13}} \\
&= \frac{\langle\eta_1|2|1]\langle2|4|\eta_2\rangle - \langle\eta_1|3|1]\langle2|1|\eta_2\rangle + s_{13}\langle\eta_12\rangle[1\eta_2]}{s_{12}} \\
&\quad - \frac{\langle\eta_1|3|1]\langle2|4|\eta_2\rangle}{s_{13}} + \langle\eta_12\rangle[1\eta_2] \\
&= \frac{\langle\eta_1|2|1]\langle2|4-3|\eta_2\rangle - \langle\eta_1|3-4|1]\langle2|1|\eta_2\rangle + (s_{13}-s_{14})\langle\eta_12\rangle[1\eta_2]}{2s_{12}} \\
&\quad - \frac{\langle\eta_1|3|1]\langle2|4|\eta_2\rangle}{s_{13}} + \frac{1}{2}\langle\eta_12\rangle[1\eta_2].
\end{aligned} \tag{6.60}$$

In the last step, we require the spinor structure in the term containing the s_{12} pole to be proportional to $p_3 - p_4$, which ensures that the total angular momentum of this channel is 1.

Now the massless amplitudes reduce to a form containing at most one pole, which become the massless amplitudes in the light-cone gauge. Therefore, it can be decomposed into four channel contributions:

$$\begin{array}{c} 1^+ \\ \diagup \quad \diagdown \\ \text{wavy line} \quad \text{dashed line} \\ \diagdown \quad \diagup \\ 2^- \quad 3^0 \end{array} \quad : \quad \begin{pmatrix} (T_s^{I_2} T_s^{I_1})_{i_4}^{i_3} \\ (T_s^{I_1} T_s^{I_2})_{i_3}^{i_4} \end{pmatrix} \frac{-\langle\eta_1|3|1]\langle2|4|\eta_2\rangle}{s_{13}}, \tag{6.61}$$

$$\begin{array}{c} 1^+ \\ \diagup \quad \diagdown \\ \text{wavy line} \quad \text{dashed line} \\ \diagdown \quad \diagup \\ 2^- \quad 3^0 \end{array} \quad : \quad \begin{pmatrix} (T_s^{I_1} T_s^{I_2})_{i_4}^{i_3} \\ (T_s^{I_2} T_s^{I_1})_{i_3}^{i_4} \end{pmatrix} \frac{-\langle\eta_1|4|1]\langle2|3|\eta_2\rangle}{s_{14}}, \tag{6.62}$$

$$\begin{array}{c} 1^+ \\ \diagup \quad \diagdown \\ \text{wavy line} \quad \text{dashed line} \\ \diagdown \quad \diagup \\ 2^- \quad 3^0 \end{array} \quad : \quad \begin{pmatrix} (T_s^{I_2} T_s^{I_1})_{i_4}^{i_3} - (T_s^{I_1} T_s^{I_2})_{i_4}^{i_3} \\ (T_s^{I_1} T_s^{I_2})_{i_3}^{i_4} - (T_s^{I_2} T_s^{I_1})_{i_3}^{i_4} \end{pmatrix} \times \frac{\langle\eta_1|2|1]\langle2|4-3|\eta_2\rangle - \langle\eta_1|3-4|1]\langle2|1|\eta_2\rangle + (s_{13}-s_{14})\langle\eta_12\rangle[1\eta_2]}{2s_{12}}, \tag{6.63}$$

$$\begin{array}{c} 1^+ \\ \diagup \quad \diagdown \\ \text{wavy line} \quad \text{dashed line} \\ \diagdown \quad \diagup \\ 2^- \quad 3^0 \end{array} \quad : \quad \begin{pmatrix} (T_s^{I_2} T_s^{I_1})_{i_4}^{i_3} + (T_s^{I_1} T_s^{I_2})_{i_4}^{i_3} \\ (T_s^{I_2} T_s^{I_1})_{i_3}^{i_4} + (T_s^{I_1} T_s^{I_2})_{i_3}^{i_4} \end{pmatrix} \langle\eta_12\rangle[1\eta_2]. \tag{6.64}$$

Then we can match the massless light-cone gauge amplitude to the MHC amplitude. The conversion from unbroken-phase gauge tensors to broken ones is performed using two transformation matrices, \mathcal{T}_1 and \mathcal{T}_2 :

$$\mathcal{T}_1 = O^{I_1 W^+} O^{I_2 W^-} \mathcal{U}_{i_3}^h \mathcal{U}^{i_4 h}, \quad \mathcal{T}_2 = O^{I_1 W^+} O^{I_2 W^-} \mathcal{U}^{h i_3} \mathcal{U}_h^{i_4}. \tag{6.65}$$

These matrices convert the particle types from $WWHH^\dagger$ or $WWH^\dagger H$ to W^+W^-hh . The transformation shows that only half of the coefficients survive

$$\begin{aligned} (T_s^{I_2} T_s^{I_1})_{i_4}^{i_3} &\xrightarrow{\mathcal{T}_1} \frac{1}{2} g^2, & (T_s^{I_1} T_s^{I_2})_{i_4}^{i_3} &\xrightarrow{\mathcal{T}_1} 0, \\ (T_s^{I_2} T_s^{I_1})_{i_3}^{i_4} &\xrightarrow{\mathcal{T}_2} \frac{1}{2} g^2, & (T_s^{I_1} T_s^{I_2})_{i_3}^{i_4} &\xrightarrow{\mathcal{T}_2} 0. \end{aligned} \quad (6.66)$$

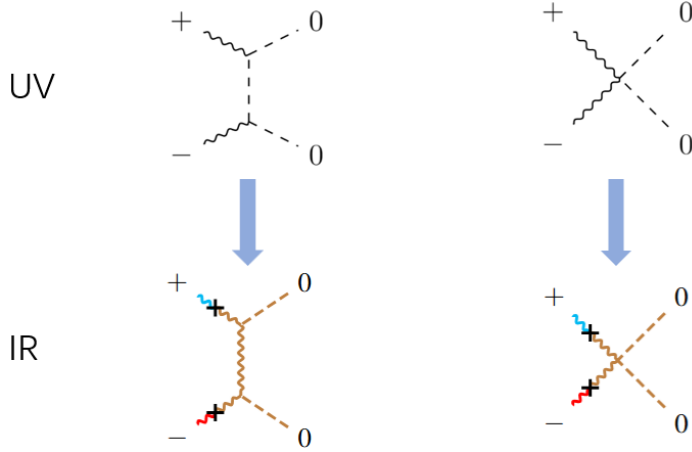


Figure 6: The diagrammatic matching for helicity category $(-1, +1, 0, 0)$ of W^+W^-hh amplitude.

Substituting these broken gauge structures into the massless amplitude establishes a matching between massless diagrams and MHC diagrams. As shown in Fig. 6, the diagrammatic correspondence is straightforward: the (13)-channel, (14)-channel and contact term in the massless amplitude match directly to their MHC counterparts.

Finally, we obtain the MHC amplitude for this helicity category

$$\begin{aligned} [\mathcal{M}(1^{+1}, 2^{-1}, 3^0, 4^0)]_0 &= \frac{1}{2} g^2 \frac{\langle \eta_1 | P_{14} | 1 \rangle \langle 2 | P_{14} | \eta_2 \rangle}{s_{14} \tilde{m}_1 m_2} + \frac{1}{2} g^2 \frac{\langle \eta_1 | P_{13} | 1 \rangle \langle 2 | P_{13} | \eta_2 \rangle}{s_{13} \tilde{m}_1 m_2} \\ &+ \frac{1}{2} g^2 \frac{\langle \eta_1 2 \rangle [\eta_2 1]}{\tilde{m}_1 m_2}. \end{aligned} \quad (6.67)$$

helicity (0,0,0,0) Then we consider $(0,0,0,0)$ helicity category. Similarly, in this case, we should also consider two amplitude expressions

$$\begin{aligned} \mathcal{A}(1^{i_1}, 2_{i_2}, 3^{i_3}, 4_{i_4}) &= -(T_s^J)_{i_2}^{i_1} (T_s^J)_{i_4}^{i_3} \frac{s_{13} - s_{14}}{2s_{12}} - (T_s^J)_{i_4}^{i_1} (T_s^J)_{i_2}^{i_3} \frac{s_{13} - s_{12}}{2s_{14}} - 4\lambda \delta_{i_2}^{(i_1} \delta_{i_4}^{i_3)}, \\ \mathcal{A}(1^{i_1}, 2_{i_2}, 3_{i_3}, 4^{i_4}) &= -(T_s^J)_{i_2}^{i_1} (T_s^J)_{i_3}^{i_4} \frac{s_{14} - s_{13}}{2s_{12}} - (T_s^J)_{i_3}^{i_1} (T_s^J)_{i_2}^{i_4} \frac{s_{14} - s_{12}}{2s_{13}} - 4\lambda \delta_{i_2}^{(i_1} \delta_{i_3}^{i_4)}. \end{aligned} \quad (6.68)$$

In this case, we do not need to separate pole structure. These massless amplitudes can be decomposed into four contributions:

$$\begin{array}{c} 1^0 \\ \backslash \quad \diagup \\ \text{---} \quad \text{---} \\ 2^0 \quad 3^0 \end{array} \quad : \quad \begin{pmatrix} -(T_s^J)_{i_2}^{i_1} (T_s^J)_{i_4}^{i_3} \\ (T_s^J)_{i_2}^{i_1} (T_s^J)_{i_3}^{i_4} \end{pmatrix} \frac{s_{13} - s_{14}}{2s_{12}}, \quad (6.69)$$

$$\begin{array}{c} 1^0 \\ \diagdown \quad \diagup \\ \text{---} \quad \text{---} \\ 2^0 \quad 3^0 \end{array} \quad : \quad \begin{pmatrix} -(T_s^J)_{i_4}^{i_1} (T_s^J)_{i_2}^{i_3} \\ 0 \end{pmatrix} \frac{s_{13} - s_{12}}{2s_{14}}, \quad (6.70)$$

$$\begin{array}{c} 1^0 \\ \diagup \quad \diagdown \\ \text{---} \quad \text{---} \\ 2^0 \quad 3^0 \end{array} \quad : \quad \begin{pmatrix} 0 \\ -(T_s^J)_{i_3}^{i_1} (T_s^J)_{i_2}^{i_4} \end{pmatrix} \frac{s_{14} - s_{12}}{2s_{13}}, \quad (6.71)$$

$$\begin{array}{c} 1^0 \\ \diagdown \quad \diagup \\ \text{---} \quad \text{---} \\ 2^0 \quad 3^0 \end{array} \quad : \quad - \begin{pmatrix} \delta_{i_2}^{(i_1} \delta_{i_4)}^{i_3)} \\ \delta_{i_2}^{(i_1} \delta_{i_3)}^{i_4)} \end{pmatrix} 4\lambda. \quad (6.72)$$

Then we multiply the transformation matrix \mathcal{T}_1 and \mathcal{T}_2 ,

$$\mathcal{T}_1 = \mathcal{U}_{i_1}^{W^+} \mathcal{U}_{i_2}^{W^-} \mathcal{U}_{i_3}^h \mathcal{U}_{i_4}^{i_4h}, \quad \mathcal{T}_2 = \mathcal{U}_{i_1}^{W^+} \mathcal{U}_{i_2}^{W^-} \mathcal{U}_{i_3}^{h i_3} \mathcal{U}_h^{i_4}. \quad (6.73)$$

The group tensors become

$$\begin{aligned}
 (T_s^J)_{i_2}^{i_1} (T_s^J)_{i_4}^{i_3} &\xrightarrow{\mathcal{T}_1} \frac{g^2}{2}, & (T_s^J)_{i_4}^{i_1} (T_s^J)_{i_2}^{i_3} &\xrightarrow{\mathcal{T}_1} -g^2, & \lambda \delta_{i_2}^{(i_1} \delta_{i_4)}^{i_3)} &\xrightarrow{\mathcal{T}_1} -\frac{1}{2}\lambda, \\
 (T_s^J)_{i_2}^{i_1} (T_s^J)_{i_3}^{i_4} &\xrightarrow{\mathcal{T}_2} \frac{g^2}{2}, & (T_s^J)_{i_3}^{i_1} (T_s^J)_{i_2}^{i_4} &\xrightarrow{\mathcal{T}_2} -g^2, & \lambda \delta_{i_2}^{(i_1} \delta_{i_3)}^{i_4)} &\xrightarrow{\mathcal{T}_2} -\frac{1}{2}\lambda.
 \end{aligned} \quad (6.74)$$

The amplitude now becomes

$$g^2 \frac{s_{13} - s_{12}}{2s_{14}} + g^2 \frac{s_{14} - s_{12}}{2s_{13}} + 4\lambda. \quad (6.75)$$

It shows the (12)-channel contribution vanishes.

As discussed in section 4.3, we can separate this amplitude expression into two contributions,

$$\begin{aligned}
 \text{matched factorized term :} \quad & -g^2 \frac{s_{12}}{s_{14}} - g^2 \frac{s_{12}}{s_{13}} + \frac{8\lambda}{\mathbf{m}_h^2} (p_3 \cdot \eta_4 + \eta_3 \cdot p_3)^2 + 12\lambda, \\
 \text{matched contact term :} \quad & \frac{g^2}{2\mathbf{m}_W^2} (\mathbf{m}_1^2 + \mathbf{m}_2^2) - \frac{4\lambda}{\mathbf{m}_h^2} (p_3 + \eta_3 + p_4 + \eta_4)^2.
 \end{aligned} \quad (6.76)$$

As shown in Fig. 7, these contributions belongs to different massless diagrams, and they will match to the following terms of the MHC amplitude

$$[\mathcal{M}]_0 = [\mathcal{M}_{(12)}]_0 + [\mathcal{M}_{(13)}]_0 + [\mathcal{M}_{(14)}]_0 + [\mathcal{M}_{\text{ct}}]_0. \quad (6.77)$$

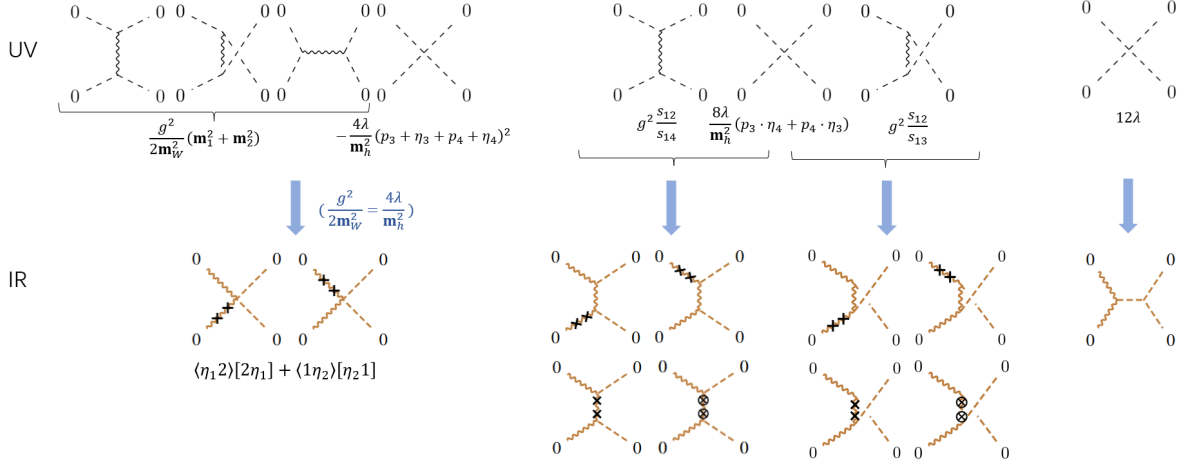


Figure 7: The diagrammatic matching for helicity category $(0,0,0,0)$ of W^+W^-hh amplitude.

They correspond to (12), (13), (14)-channel and contact amplitude separately.

- contact term: Using the condition $\frac{g^2}{2m_W^2} = \frac{4\lambda}{m_h^2}$, we can convert the amplitude in eq. (6.76) to the MHC contact term

$$[\mathcal{M}_{\text{ct}}]_0 = -\frac{g^2}{2}([1\eta_2]\langle\eta_2 1\rangle + [\eta_1 2]\langle 2\eta_1\rangle). \quad (6.78)$$

- (12)-channel: There is no term with the pole s_{12} now, so we need to extract a such pole from it. This extraction can be only applied to the term with no pole, which corresponds to the following scaling change

$$\mathbb{E}(1) \times \mathbb{I}(1) \times \mathbb{P}(1) \rightarrow \mathbb{E}(\tilde{\lambda}^2 \lambda^2) \times \mathbb{I}(1) \times \mathbb{P}(p^{-2}). \quad (6.79)$$

For the term with s_{13} and s_{14} pole, such extraction will give the double pole contribution, which is not we need. The corresponding amplitude deformation is

$$12\lambda \Rightarrow [\mathcal{M}_{(12)}]_0 = 12\lambda \frac{[12]\langle 21\rangle}{s_{12}}. \quad (6.80)$$

The term $(p_3 \cdot \eta_4 + \eta_3 \cdot p_3)^2$ also do not have pole, but it does not satisfy the scaling in eq. (6.79), so it will contribute to not (12)-channel, but (13) and (14)-channels.

- (13) and (14)-channel: These two channels include more diagrams than the former contributions. Analyze each scaling change can give the corresponding amplitude deformation is possible, but here we can use a more convenient method. It is to use the amplitude expression in helicity $(+1, -1, 0, 0)$, and use the extended little group covariance to convert them into helicity $(0, 0, 0, 0)$. The result of (13)-channel is

$$[\mathcal{M}_{(13)}]_0 = \frac{g^2}{2} \left(\frac{[13]\langle 31\rangle([2\eta_4]\langle\eta_4 2\rangle - [\eta_2 4]\langle 4\eta_2\rangle) + ([1\eta_3]\langle\eta_3 1\rangle - [\eta_1 3]\langle 3\eta_1\rangle)[24]\langle 42\rangle}{\mathbf{m}_1 \mathbf{m}_2 s_{13}} \right. \\ \left. + \frac{2\mathbf{m}_W^2[12]\langle 21\rangle}{\mathbf{m}_1 \mathbf{m}_2 s_{13}} - \frac{[13]\langle 31\rangle[24]\langle 42\rangle}{s_{13} \mathbf{m}_1 \mathbf{m}_2} \frac{2p_1 \cdot \eta_3 + 2p_3 \cdot \eta_1 + \mathbf{m}_1^2 + \mathbf{m}_3^2 - \mathbf{m}_W^2}{s_{13}} \right). \quad (6.81)$$

The (14)-channel can be obtained by exchange particles 3 and 4.

Combining these contribution, the total amplitude is

$$\begin{aligned}
[\mathcal{M}]_0 = & \frac{g^2}{2} \left(\frac{[13]\langle 31 \rangle ([2\eta_4]\langle \eta_4 2 \rangle - [\eta_2 4]\langle 4\eta_2 \rangle) + ([1\eta_3]\langle \eta_3 1 \rangle - [\eta_1 3]\langle 3\eta_1 \rangle)[24]\langle 42 \rangle}{\mathbf{m}_1 \mathbf{m}_2 s_{13}} \right. \\
& + \frac{2\mathbf{m}_W^2 [12]\langle 21 \rangle}{\mathbf{m}_1 \mathbf{m}_2 s_{13}} - \frac{[13]\langle 31 \rangle [24]\langle 42 \rangle}{s_{13} \mathbf{m}_1 \mathbf{m}_2} \frac{2p_1 \cdot \eta_3 + 2p_3 \cdot \eta_1 + \mathbf{m}_1^2 + \mathbf{m}_3^2 - \mathbf{m}_W^2}{s_{13}} \Big) \\
& + \frac{g^2}{2} \left(\frac{[14]\langle 41 \rangle ([2\eta_3]\langle \eta_3 2 \rangle - [\eta_2 3]\langle 3\eta_2 \rangle) + ([1\eta_4]\langle \eta_4 1 \rangle - [\eta_1 4]\langle 4\eta_1 \rangle)[23]\langle 32 \rangle}{\mathbf{m}_1 \mathbf{m}_2 s_{14}} \right. \\
& + \frac{2\mathbf{m}_W^2 [12]\langle 21 \rangle}{\mathbf{m}_1 \mathbf{m}_2 s_{14}} - \frac{[14]\langle 41 \rangle [23]\langle 32 \rangle}{s_{14} \mathbf{m}_1 \mathbf{m}_2} \frac{2p_1 \cdot \eta_4 + 2p_4 \cdot \eta_1 + \mathbf{m}_1^2 + \mathbf{m}_4^2 - \mathbf{m}_W^2}{s_{14}} \Big) \\
& + 12\lambda \frac{[12]\langle 21 \rangle}{s_{12}} - \frac{g^2}{2} ([1\eta_2]\langle \eta_2 1 \rangle + [\eta_1 2]\langle 2\eta_1 \rangle).
\end{aligned} \tag{6.82}$$

Matching Results for Unitarized Amplitudes Now we have derived the MHC amplitude from massless amplitudes in the two helicity category $(+, -, 0, 0)$ and $(0, 0, 0, 0)$. Restore the $SU(2)$ little group covariance, these matching result can simply gives the AHH amplitude.

In $(+, -, 0, 0)$, we can rewrite the gauge coupling to massive coefficient as $g^2 \rightarrow (\mathbf{g}^{W^+W^-})^2$, so the MHC amplitude is

$$\begin{aligned}
[\mathcal{M}(1^{+1}, 2^{-1}, 3^0, 4^0)]_0 = & \frac{(\mathbf{g}^{W^+W^-})^2}{2} \frac{\langle \eta_1 | P_{14} | 1 \rangle \langle 2 | P_{14} | \eta_2 \rangle}{s_{14} \tilde{m}_1 m_2} + \frac{(\mathbf{g}^{W^+W^-})^2}{2} \frac{\langle \eta_1 | P_{13} | 1 \rangle \langle 2 | P_{13} | \eta_2 \rangle}{s_{13} \tilde{m}_1 m_2} \\
& + \frac{(\mathbf{g}^{W^+W^-})^2}{2} \frac{\langle \eta_1 2 \rangle [\eta_2 1]}{\tilde{m}_1 m_2}.
\end{aligned} \tag{6.83}$$

Bolding it, we obtain

$$\mathbf{M}_1 = \frac{(\mathbf{g}^{W^+W^-})^2}{2\mathbf{m}_W^2} \frac{\langle \mathbf{1} | \mathbf{p}_3 | \mathbf{1} \rangle \langle \mathbf{2} | \mathbf{p}_4 | \mathbf{2} \rangle}{\mathbf{P}_{13}^2 - \mathbf{m}_W^2} + \frac{(\mathbf{g}^{W^+W^-})^2}{2\mathbf{m}_W^2} \frac{\langle \mathbf{1} | \mathbf{p}_4 | \mathbf{1} \rangle \langle \mathbf{2} | \mathbf{p}_3 | \mathbf{2} \rangle}{\mathbf{P}_{14}^2 - \mathbf{m}_W^2} + \frac{(\mathbf{g}^{W^+W^-})^2}{2\mathbf{m}_W^2} [\mathbf{12}] \langle \mathbf{21} \rangle. \tag{6.84}$$

In $(0, 0, 0, 0)$, we need to rewrite another coupling to massive coefficient as $12\lambda \rightarrow \mathbf{g}^{W^+W^-} \lambda_3$. The MHC amplitude include the following terms

$$[\mathcal{M}(1^0, 2^0, 3^0, 4^0)]_0 \supset \frac{\mathbf{g}^{W^+W^-} \lambda_3}{\mathbf{m}_W} \frac{[12]\langle 21 \rangle}{s_{12}}. \tag{6.85}$$

Bolding it, we get the following AHH structure

$$\mathbf{M}_2 = \frac{\mathbf{g}^{W^+W^-} \lambda_3}{\mathbf{m}_W} \frac{[\mathbf{12}] \langle \mathbf{21} \rangle}{\mathbf{P}_{12}^2 - \mathbf{m}_h^2} + \frac{(\mathbf{g}^{W^+W^-})^2}{2\mathbf{m}_W^2} \frac{2\mathbf{m}_W^2 [12]\langle 21 \rangle}{\mathbf{P}_{13}^2 - \mathbf{m}_W^2} + \frac{(\mathbf{g}^{W^+W^-})^2}{2\mathbf{m}_W^2} \frac{2\mathbf{m}_W^2 [12]\langle 21 \rangle}{\mathbf{P}_{14}^2 - \mathbf{m}_W^2}. \tag{6.86}$$

The other MHC terms in $(0, 0, 0, 0)$ will match to Eq. (6.84).

Sum over these two contributions, we obtain the total AHH amplitude,

$$\begin{aligned}
\mathbf{M}(W^+W^-hh) = & \mathbf{M}_1 + \mathbf{M}_2 \\
= & \frac{\mathbf{g}^{W^+W^-} \mathbf{g}^{W^+W^-}}{2\mathbf{m}_W^2} \frac{\langle 1|\mathbf{p}_3|1\rangle \langle 2|\mathbf{p}_4|2\rangle + 2\mathbf{m}_W^2 [12]\langle 21\rangle}{\mathbf{P}_{13}^2 - \mathbf{m}_W^2} \\
& + \frac{\mathbf{g}^{W^+W^-} \mathbf{g}^{W^+W^-}}{2\mathbf{m}_W^2} \frac{\langle 1|\mathbf{p}_4|1\rangle \langle 2|\mathbf{p}_3|2\rangle + 2\mathbf{m}_W^2 [12]\langle 21\rangle}{\mathbf{P}_{14}^2 - \mathbf{m}_W^2} \\
& + \frac{\mathbf{g}^{W^+W^-} \lambda_3}{\mathbf{m}_W} \frac{[12]\langle 21\rangle}{\mathbf{P}_{12}^2 - \mathbf{m}_h^2} + \frac{\mathbf{g}^{W^+W^-} \mathbf{g}^{W^+W^-}}{2\mathbf{m}_W^2} [12]\langle 21\rangle.
\end{aligned} \tag{6.87}$$

6.4 Sub-leading MHC matching

After obtained the leading matching, let us consider the sub-leading matching for MHC amplitudes. We continue to use the $WWhh$ amplitude as an example to illustrate the matching procedure.

In the leading matching, the 4-pt massless amplitude is matched to the leading MHC amplitude $[\mathcal{M}]_0$. For the $WWhh$ amplitude, this gives

$$\begin{aligned}
\mathcal{A}(1^+, 2^-, 3^0, 4^0) & \rightarrow [\mathcal{M}(1^+, 2^-, 3^0, 4^0)]_0, \\
\mathcal{A}(1^0, 2^0, 3^0, 4^0) & \rightarrow [\mathcal{M}(1^0, 2^0, 3^0, 4^0)]_0,
\end{aligned} \tag{6.88}$$

where the superscripts denote the helicity.

In the subleading matching, we match $(4+l)$ -pt massless amplitudes with l additional Higgs bosons to subleading MHC amplitude $[\mathcal{M}]_{l>0}$. Once the leading matching ($l=0$) is known, the sub-leading matching ($l>0$) can be obtained by attaching additional Higgs bosons to particle lines, following what we call *Higgsing rules*. Depending on whether the additional Higgs bosons are attached to external or internal particles, there are two types of Higgsing rules.

Below, we illustrate these two kinds of rules using two typical sub-leading matchings for $l=1$ and $l=2$:

$$\begin{aligned}
\mathcal{A}(1^+, 2^0, 3^0, 4^0; 5^0) & \rightarrow [\mathcal{M}(1^+, 2^0, 3^0, 4^0)]_1, \\
\mathcal{A}(1^+, 2^-, 3^0, 4^0; 5^0, 6^0) & \rightarrow [\mathcal{M}(1^+, 2^-, 3^0, 4^0)]_2.
\end{aligned} \tag{6.89}$$

where massless particles 5 and 6 are the additional Higgs bosons. Subleading matching for other helicity categories and higher orders can be obtained similarly using these two Higgsing rules.

External Higgsing rule We first consider the subleading matching for massless amplitude with helicity $(+0000)$, which contains one additional Higgs boson. This additional Higgs boson can be viewed as having split from one of the external particles of the 4-pt massless amplitude used in the leading matching. The 4-pt amplitude can have helicity $(+-00)$ and (0000) . To obtain the complete subleading MHC amplitude, both cases must be considered.

Let us begin with the $(+-00)$ 4-pt amplitude. Focusing on particle 2, we recall that in the leading matching this gauge boson with negative helicity corresponds to

$$\bullet \text{~~~~~} - \rightarrow \bullet \text{~~~~~} \times \text{~~~~~} - = \frac{1}{\tilde{m}_2} |2\rangle |\eta_2\rangle. \tag{6.90}$$

Going from $(+-00)$ to $(+0000)$, the helicity of particle 2 changes from -1 to 0 , while particle 5 (the additional Higgs boson) is created. This process can be interpreted as a *Higgs splitting*: a gauge boson with negative helicity splits into a scalar boson (zero helicity) and an extra Higgs boson, illustrated as

(6.91)

The internal particle need to be slightly off-shell, so its momentum P_{25} can be decomposed as

$$P_{25} = p_\chi + q = |\chi\rangle\langle\chi| + q, \quad (6.92)$$

where p_χ is the on-shell part and q is the off-shell part. Assuming $p_\chi \gg q$, the line with the Higgs insertion factorizes into the original line multiplied by a 3-pt amplitude,

$$\frac{|\eta_\chi]_\alpha|\chi\rangle_\alpha}{[\eta_\chi\xi]} \times \frac{[5\chi][\chi 2]}{[52]} \sim \frac{1}{2} \left(\frac{(|5])_\alpha(P|2])_\alpha}{[52]} - (2 \leftrightarrow 5) \right). \quad (6.93)$$

We now treat the two massless particles 2 and 5 as a single massive particle. Taking the on-shell limit $p_5 \rightarrow \eta_2$, the momentum of the extra Higgs boson becomes the subleading part of the massive momentum. Consequently, the splitting structure matches the massive MHC state,

$$\begin{aligned} \bullet \overbrace{\text{---}}^h 0 &= \frac{1}{2} \lim_{p_5 \rightarrow \eta_2} \left(\frac{(|5])_\alpha(P|2])_\alpha}{[52]} - (2 \leftrightarrow 5) \right) \\ &\sim \frac{1}{2} (|\eta_2]_\alpha|\eta_2\rangle_\alpha - |2]_\alpha|2\rangle_\alpha) \\ &\rightarrow \bullet \overbrace{\text{---}}^h 0 + \bullet \overbrace{\text{---}}^h 0. \end{aligned} \quad (6.94)$$

Here both the leading and subleading terms appear. Since we are focusing on the subleading matching, only the term $|\eta\rangle|\eta\rangle$ contributes to the subleading MHC amplitude. Thus we can extract a matching rule from leading to subleading order

$$\begin{aligned} \bullet \overbrace{\text{---}}^h 0 &\rightarrow \bullet \overbrace{\text{---}}^h 0 = |\eta_2]|2\rangle \\ \text{split } \downarrow & \\ \bullet \overbrace{\text{---}}^h 0 &\rightarrow \bullet \overbrace{\text{---}}^h 0 = |\eta_2]|\eta_2\rangle \end{aligned} \quad (6.95)$$

This is called the external Higgsing rule. Using it, we can match the massless amplitude with helicity $(+0000)$ to the subleading MHC amplitude. As an explicit example, let us consider the following

diagrammatic matching:

$$\begin{aligned}
 & \text{Top row:} \\
 & \text{Bottom row:} \\
 & \text{Right side:} \\
 & \text{Equation:} \quad (6.96)
 \end{aligned}$$

Other subleading MHC terms can be derived in a similar way, as illustrated in figure 8. Note, however, that this external Higgsing rule does not produce all subleading MHC amplitudes. Contributions from other helicity must also be taken into account.

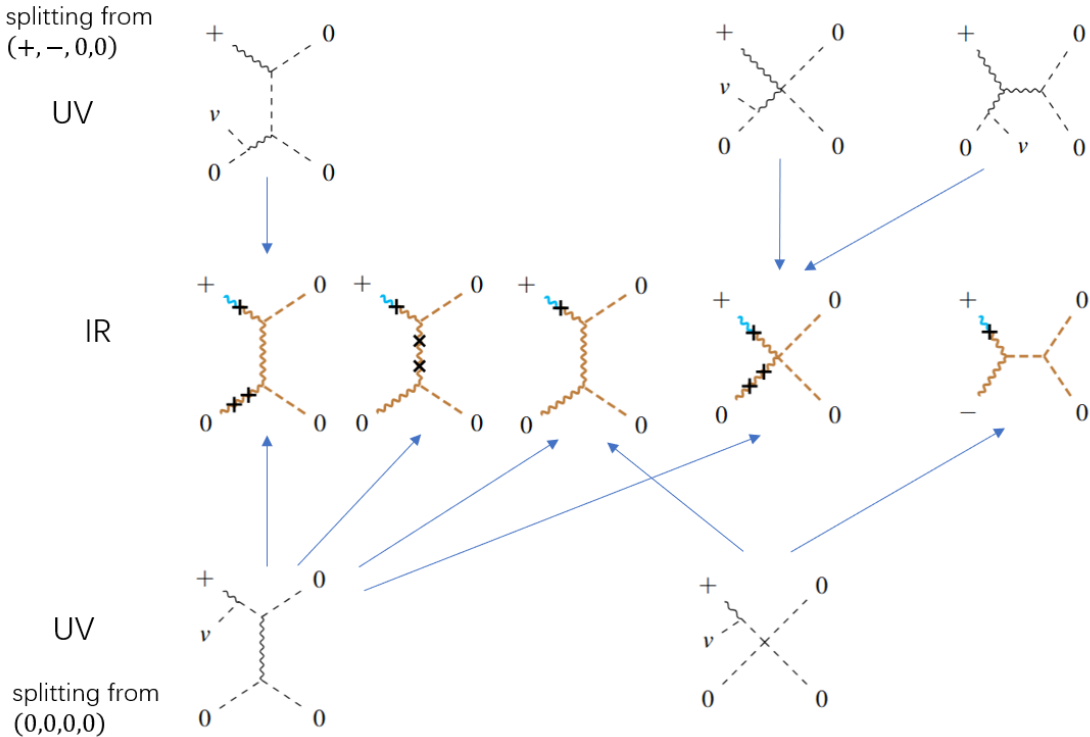


Figure 8: The diagrammatic matching for helicity category $(+1, 0, 0, 0)$ of W^+W^-hh amplitude.

Then we consider the helicity (0000). From (0000) to (+0000), the helicity of particle 1 is

changed from 0 to +1. This requires another kind of external Higgsing rules:

$$\begin{array}{ccc}
 \bullet \text{---} 0 & \rightarrow & \bullet \text{wavy} 0 = |p\rangle|p] \\
 \text{split} \downarrow & & \\
 \bullet \text{---} \text{wavy} + & \rightarrow & \bullet \text{wavy} \times \text{blue} + = |\eta\rangle|p]
 \end{array} \quad (6.97)$$

Using this Higgsing rule, we can obtain the other subleading MHC amplitudes that are cannot be given from $(+-00)$, such as

$$\begin{array}{ccc}
 \bullet \text{---} 0 & \rightarrow & \bullet \text{wavy} 0 = -12\lambda \frac{\langle 12 \rangle [21]}{s_{12}} \\
 \text{split} \downarrow & & \\
 \bullet \text{---} \text{wavy} + & \rightarrow & \bullet \text{wavy} \times \text{blue} + = -12\lambda \frac{m_1 \langle \eta_1 2 \rangle [21]}{s_{12}}
 \end{array} \quad (6.98)$$

Using the external Higgsing rules, we can find all MHC subleading terms. The final result is

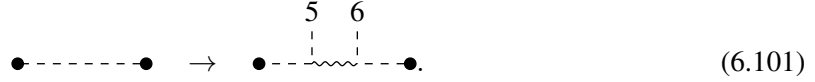
$$\begin{aligned}
 [\mathcal{M}]_1 = & \frac{g^2}{2} \left(\frac{\langle \eta_1 | P_{13} | 1 \rangle (\langle 2 | \eta_{24} | 2 \rangle - \langle \eta_2 | P_{24} | \eta_2 \rangle) + \langle \eta_1 | \eta_{13} | 1 \rangle \langle 2 | P_{24} | 2 \rangle + 2\mathbf{m}_W^2 \langle \eta_1 2 \rangle [21]}{m_1 \mathbf{m}_2 s_{13}} \right. \\
 & \left. - \frac{\langle \eta_1 | P_{13} | 1 \rangle \langle 2 | P_{24} | 2 \rangle 2p_1 \cdot \eta_3 + 2p_3 \cdot \eta_1 + \mathbf{m}_1^2 + \mathbf{m}_3^2 - \mathbf{m}_W^2}{s_{13} m_1 \mathbf{m}_2} \right) \\
 & + \frac{g^2}{2} \left(\frac{\langle \eta_1 | P_{14} | 1 \rangle (\langle 2 | \eta_{23} | 2 \rangle - \langle \eta_2 | P_{23} | \eta_2 \rangle) + \langle \eta_1 | \eta_{14} | 1 \rangle \langle 2 | P_{23} | 2 \rangle + 2\mathbf{m}_W^2 \langle \eta_1 2 \rangle [21]}{m_1 \mathbf{m}_2 s_{14}} \right. \\
 & \left. - \frac{\langle \eta_1 | P_{14} | 1 \rangle \langle 2 | P_{23} | 2 \rangle 2p_1 \cdot \eta_4 + 2p_4 \cdot \eta_1 + \mathbf{m}_1^2 + \mathbf{m}_4^2 - \mathbf{m}_W^2}{s_{14} m_1 \mathbf{m}_2} \right) \\
 & - 12\lambda \frac{m_1 \langle \eta_1 2 \rangle [21]}{s_{12}} - \frac{g^2}{2} \frac{\langle \eta_1 \eta_2 \rangle [\eta_2 1]}{m_1 \mathbf{m}_2}.
 \end{aligned} \quad (6.99)$$

Internal Higgsing rule Then we consider the matching for 6-pt massless amplitudes with helicity $(+-0000)$, which contains two additional Higgs boson. In this case, the additional Higgs boson can be split not only from external particles, but also from internal ones. This require us to consider the internal Higgsing rules.

We start from the 4-pt amplitude with helicity $(+-00)$. In the leading matching, the massless internal particle in the (14)-channel match to

$$\bullet \text{---} \bullet \rightarrow \bullet \text{wavy} \bullet = P_{14} P_{14}. \quad (6.100)$$

When going from $(+-00)$ to $(+-0000)$, two additional Higgs bosons are split from this internal massless, shown as



Here, particles 5 and 6 are the two extra Higgs bosons. This massless structure involves three propagators

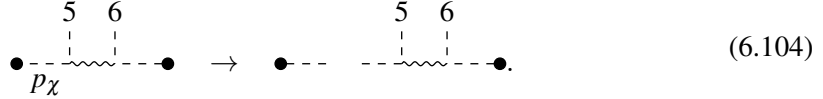
$$P_{14}^2, P_{145}^2, P_{1456}^2, \quad (6.102)$$

corresponding to the three internal particles in the massless diagrams. To match this to the MHC internal line, we combine the additional Higgs bosons with one of the internal particles into a massive particle. A convenient way to select this internal particle is to take its momentum to be nearly on-shell:

$$P_{ij\dots} \sim p_\chi \equiv |\chi]\langle \chi|, \quad (6.103)$$

where p_χ represents the on-shell internal momentum. The additional Higgs bosons and this on-shell internal particle are then packaged into a massive state. Since there are three internal particles, this yields three contributions:

- First we take the momentum $P_{14} \sim p_\chi$ to be nearly on-shell, which corresponds a scalar boson. The internal structure factorizes into two external pieces as



The first piece (without Higgs splitting) corresponds to the Goldstone structure $|\chi\rangle|\chi\rangle$, while the second gives

$$\text{---} \overset{5}{\underset{1}{\overset{|}{\underset{\sim}{\text{---}}}}} \overset{6}{\underset{1}{\overset{|}{\text{---}}}} \text{---} \bullet = \frac{(\langle \chi | [\chi] - \langle 5 | [5] \rangle)}{(p_\chi + p_5)^2}. \quad (6.105)$$

Therefore we obtain

$$\mathcal{I}_{(14)} = \bullet \underset{p_\chi}{\underset{|}{\underset{|}{\text{---}}}} \sim |\chi\rangle |\chi\rangle \times \frac{(\langle \chi | [\chi] - \langle 5 | [5])}{(p_\chi + p_5)^2}. \quad (6.106)$$

Here, particle 5 acts as the subleading spinor η_{14} of the internal momentum. Taking the appropriate on-shell limit gives

$$\lim_{\substack{p_5 \rightarrow \eta_{14} \\ p_6 \rightarrow 0}} \mathcal{I}_{(14)} \sim |\chi| |\chi\rangle \times \frac{(\langle \chi | \chi | - \langle \eta_{14} | [\eta_{14}] |)}{(p_\chi + p_5)^2}. \quad (6.107)$$

- Then we take the momentum $P_{145} \sim p_\chi$ to be nearly on-shell, which corresponds to an internal gauge boson. Since the gauge boson can have helicity ± 1 , the internal line factorizes into two terms

$$\mathcal{I}_{(145)} = \bullet \dashdot \overset{5}{\overset{|}{\overset{|}{\text{---}}}} \overset{6}{\overset{|}{\overset{|}{\text{---}}}} \bullet \sim \frac{|\chi| |5\rangle}{\langle \chi | 5 \rangle} \times \frac{|6\rangle \langle \chi|}{[6\chi]} + \frac{|5\rangle |\chi\rangle}{[5\chi]} \times \frac{|\chi\rangle \langle 6|}{\langle \chi | 6 \rangle}. \quad (6.108)$$

In this case, both particles 5 and 6 serve as the subleading spinor η_{14} , requiring a different on-shell limit

$$\lim_{\substack{p_5 \rightarrow -\eta_{14} \\ p_6 \rightarrow \eta_{14}}} \mathcal{I}_{(14)} \sim \frac{|\chi| |\eta_{14}\rangle \times |\eta_{14}| \langle \chi| + |\eta_{14}\rangle |\chi\rangle \times |\chi| \langle \eta_{14}|}{[\eta_{14}\chi] \langle \chi \eta_{14}\rangle}. \quad (6.109)$$

- The last contribution is to take the momentum $P_{1456} \sim p_\chi$ to be nearly on-shell, which also corresponds to a scalar boson. The internal line factorizes into

$$\mathcal{I}_{(1456)} = \bullet \dashdot \overset{5}{\overset{|}{\overset{|}{\text{---}}}} \overset{6}{\overset{|}{\overset{|}{\text{---}}}} \bullet \sim \frac{|\chi| |\chi\rangle - |6\rangle |6\rangle}{(-p_\chi + p_6)^2} \times \langle \chi | \chi |. \quad (6.110)$$

Particle 6 provides the subleading structure, leading to

$$\lim_{\substack{p_5 \rightarrow 0 \\ p_6 \rightarrow -\eta_{14}}} \mathcal{I}_{(1456)} \sim \frac{|\chi| |\chi\rangle - |6\rangle |6\rangle}{(-p_\chi + p_6)^2} \times \langle \chi | \chi |. \quad (6.111)$$

In the above, the three on-shell momenta p_χ can be identified with the same internal momentum

$$p_\chi \rightarrow P_{14}. \quad (6.112)$$

Combining the three contributions, we obtain

$$\begin{aligned} \bullet \dashdot \overset{5}{\overset{|}{\overset{|}{\text{---}}}} \overset{6}{\overset{|}{\overset{|}{\text{---}}}} \bullet &\rightarrow |P\rangle \langle P| |\eta\rangle \langle \eta| + |P\rangle |\eta\rangle [\eta| \langle P| + |\eta\rangle |P\rangle [P| \langle \eta| + |\eta\rangle \langle \eta| |P\rangle \langle P| \\ &= P\eta + \eta P - \mathbf{m}^2. \end{aligned} \quad (6.113)$$

This analysis can be summarized as the following internal Higgsing rules

$$\begin{array}{ccc} \bullet \dashdot \bullet & \rightarrow & \bullet \text{---} \bullet = PP \\ \text{split} \downarrow & & \\ h & & h \\ \bullet \dashdot \text{---} \bullet & \rightarrow & \bullet \text{---} \bullet = P\eta + \eta P - \mathbf{m}^2 \end{array} \quad (6.114)$$

A more detail discussion about the internal Higgsing rules for other states is given in Appendix A.

Using this internal Higgsing rule, we can derive the subleading matching for the $(+-00)$ amplitude. Recall that the leading matching in the (14) -channel gives

When two Higgs bosons are split from the internal line, we obtain the subleading MHC amplitude with the same helicity category,

Similarly, we can derive the subleading amplitude in the (13) -channel. The subleading amplitude in the (12) -channel can be obtained by applying the external Higgsing rule to the (0000) helicity amplitude.

7 Summary and Outlook

In this work, we have systematically developed the on-shell Minimal Helicity-Chirality (MHC) formalism for higher-point amplitudes to enable the efficient calculation of scattering amplitudes involving all massive particles, with a particular focus on massive gauge bosons in the spontaneous broken standard model. By establishing a constructive massless-massive correspondence, we bridge the gap between the highly streamlined methods of massless amplitude calculations and the phenomenological necessity of treating constructive amplitudes with massive external states.

The MHC framework achieves this by working with amplitudes of definite helicity that are directly analogous to massless amplitudes in the light-cone gauge, thereby inheriting their computational advantages. Through the extended little-group covariance, these MHC amplitudes are then combined to reconstruct the complete physical massive amplitude. This approach resolves key technical challenges intrinsic to massive calculations, such as the need for distinct treatments of longitudinal and transverse polarizations and provides motivation for necessary contact terms in the light-cone gauge, and systematic derivation of all contact 4-point SM amplitudes.

We have provided a complete prescription on the constructive massive amplitudes for the MHC formalism within the SM context and the following results are obtained

- The complete standard model MHC contact 3-point and 4-point amplitudes are derived as the building blocks of the constructive higher-point massive amplitudes. For the same spin amplitudes, different orders of MHC amplitudes should be related by the ladder operators.

- Analogy to the light-cone gauge massless amplitude construction, the light-cone gauge choice of the MHC amplitudes is specified. The AHH amplitudes should also contain such gauge dependence in the spontaneous broken theory, and thus 4-point contact AHH amplitudes is also needed.
- Using the contact 3-point and 4-point MHC amplitudes at the leading order as the building blocks, explicit constructive (bootstrap) and recursive (BCFW) methods are utilized to construct the higher-point massive amplitudes, analogous to massless amplitude construction in the light-cone gauge. Once the contact 4-point AHH amplitudes is identified, similar construction can be applied to the AHH amplitudes.
- A robust procedure for massless-massive amplitude matching is performed. First bootstrapping 3-point gauge-invariant massless amplitudes to obtain the higher point gauge-invariant ones, and then performing the amplitude deformation and pole separation to match to the massive amplitudes

All the construction and matching are at the leading MHC order, and the sub-leading matching is obtained with the generalized Higgsing rules. This procedure can be able to apply to the higher point massive amplitude construction than 4-point ones in the standard model.

In summary, the MHC formalism successfully extends the conceptual clarity and computational power of modern on-shell methods to the massive sector. It transforms the calculation of massive amplitudes, particularly those involving massive gauge boson, into a more transparent, efficient, and systematic endeavor. This work provides a unified and powerful toolkit for precision calculations in the electroweak sector and beyond, with direct applications to collider phenomenology and the study of effective field theories.

Acknowledgments

This work is supported by the National Science Foundation of China under Grants No. 12347105, No. 12375099 and No. 12447101, and the National Key Research and Development Program of China Grant No. 2020YFC2201501, No. 2021YFA0718304.

A Higgsing Rules for Internal Particles

A.1 MHC internal particles

In section 4, we showed that gluing two MHC external particle states gives an internal particle states. For completeness, we list all possible internal particle states with spin $s \leq 1$.

For a scalar boson, there is only one type of internal particle state:

$$\bullet \text{---} \bullet = 1. \quad (\text{A.1})$$

For a fermion, there are two chirality, denoted by red and cyan lines. Therefore, the internal fermion line can change chirality according to

$$\bullet \xrightarrow{\text{red}} \times \xrightarrow{\text{cyan}} \bullet = \mathbf{m}^2 \delta_{\alpha}^{\beta}, \quad (\text{A.2})$$

$$\bullet \xrightarrow{\text{cyan}} \times \xrightarrow{\text{red}} \bullet = \mathbf{m}^2 \delta_{\dot{\alpha}}^{\dot{\beta}}, \quad (\text{A.3})$$

where the upper and lower indices correspond to the left- and right-hand sides of the diagrams, respectively. When the chirality is not flipped, there are two contributions:

$$\bullet \xrightarrow{\text{blue}} \bullet = p_{\dot{\alpha}}^{\beta}, \quad \bullet \xrightarrow{\text{red}} \times \xrightarrow{\text{cyan}} \bullet = \mathbf{m}^2 \eta_{\dot{\alpha}}^{\beta}, \quad (\text{A.4})$$

$$\bullet \xrightarrow{\text{red}} \bullet = p_{\alpha}^{\dot{\beta}}, \quad \bullet \xrightarrow{\text{blue}} \times \xrightarrow{\text{red}} \bullet = \mathbf{m}^2 \eta_{\alpha}^{\dot{\beta}}. \quad (\text{A.5})$$

Including the appropriate coefficients, these two contributions are not independent and combine into a $p + \eta$ structure, which smoothly matches the $SU(2)$ covariant momentum \mathbf{p} .

For a vector boson, there are three chirality, denoted by red, brown and cyan lines. In this case, the chirality of the internal state can be flipped twice as

$$\bullet \xrightarrow{\text{red}} \times \xrightarrow{\text{brown}} \times \xrightarrow{\text{cyan}} \bullet = \mathbf{m}^4 \delta_{(\alpha_1}^{\beta_1} \delta_{\alpha_2)}^{\beta_2}, \quad (\text{A.6})$$

$$\bullet \xrightarrow{\text{cyan}} \times \xrightarrow{\text{brown}} \times \xrightarrow{\text{red}} \bullet = \mathbf{m}^4 \delta_{(\alpha_1}^{\beta_2} \delta_{\alpha_2)}^{\dot{\beta}_2}. \quad (\text{A.7})$$

When the chirality is flipped once, the internal particle state receives two contributions,

$$\bullet \xrightarrow{\text{brown}} \times \xrightarrow{\text{cyan}} \bullet = \mathbf{m}^2 p_{\dot{\alpha}_2}^{(\beta_2} \delta_{\alpha_1)}^{\beta_1)}, \quad \bullet \xrightarrow{\text{red}} \times \xrightarrow{\text{cyan}} \bullet = \mathbf{m}^4 \eta_{\dot{\alpha}_2}^{(\beta_2} \delta_{\alpha_1)}^{\beta_1)}, \quad (\text{A.8})$$

$$\bullet \xrightarrow{\text{red}} \times \xrightarrow{\text{brown}} \bullet = \mathbf{m}^2 p_{(\alpha_1}^{\beta_1} \delta_{\alpha_2)}^{\beta_2}, \quad \bullet \xrightarrow{\text{red}} \times \xrightarrow{\text{brown}} \bullet = \mathbf{m}^4 \eta_{(\alpha_1}^{\dot{\beta}_1} \delta_{\alpha_2)}^{\beta_2}, \quad (\text{A.9})$$

$$\bullet \xrightarrow{\text{cyan}} \times \xrightarrow{\text{brown}} \bullet = \mathbf{m}^2 p_{(\dot{\alpha}_1}^{\beta_1} \delta_{\dot{\alpha}_2)}^{\beta_2}, \quad \bullet \xrightarrow{\text{cyan}} \times \xrightarrow{\text{brown}} \bullet = \mathbf{m}^4 \eta_{(\dot{\alpha}_1}^{\beta_1} \delta_{\dot{\alpha}_2)}^{\dot{\beta}_2}, \quad (\text{A.10})$$

$$\bullet \xrightarrow{\text{brown}} \times \xrightarrow{\text{red}} \bullet = \mathbf{m}^2 p_{\alpha_1}^{(\dot{\beta}_1} \delta_{\alpha_2)}^{\dot{\beta}_2}, \quad \bullet \xrightarrow{\text{brown}} \times \xrightarrow{\text{red}} \bullet = \mathbf{m}^4 \eta_{\alpha_1}^{(\dot{\beta}_1} \delta_{\alpha_2)}^{\dot{\beta}_2}. \quad (\text{A.11})$$

If there is no chirality flip, three contributions appear,

$$\bullet \xrightarrow{\text{brown}} \bullet = p_{(\alpha_1}^{(\beta_1} p_{\alpha_2)}^{\beta_2)}, \quad \bullet \xrightarrow{\text{red}} \times \xrightarrow{\text{cyan}} \bullet = \mathbf{m}^2 p_{(\alpha_1}^{(\beta_1} \eta_{\alpha_2)}^{\beta_2)} + \mathbf{m}^2 \eta_{(\alpha_1}^{(\beta_1} p_{\alpha_2)}^{\beta_2)}, \quad \bullet \xrightarrow{\text{cyan}} \times \xrightarrow{\text{red}} \bullet = \mathbf{m}^4 \eta_{(\alpha_1}^{(\beta_1} \eta_{\alpha_2)}^{\beta_2)}, \quad (\text{A.12})$$

$$\bullet \xrightarrow{\text{brown}} \bullet = -p_{\dot{\alpha}_2}^{\beta_1} p_{\alpha_1}^{\dot{\beta}_2}, \quad \bullet \xrightarrow{\text{red}} \times \xrightarrow{\text{brown}} \bullet = 2\mathbf{m}^4 \delta_{\alpha_1}^{\beta_1} \delta_{\alpha_2}^{\dot{\beta}_2} - \mathbf{m}^2 p_{\dot{\alpha}_2}^{\beta_1} \eta_{\alpha_1}^{\dot{\beta}_2} - \mathbf{m}^2 \eta_{\dot{\alpha}_2}^{\beta_1} p_{\alpha_1}^{\dot{\beta}_2}, \quad \bullet \xrightarrow{\text{cyan}} \times \xrightarrow{\text{brown}} \bullet = -\mathbf{m}^4 \eta_{\dot{\alpha}_2}^{\beta_1} \eta_{\alpha_1}^{\dot{\beta}_2}, \quad (\text{A.13})$$

$$\bullet \xrightarrow{\text{red}} \bullet = p_{(\alpha_1}^{(\dot{\beta}_1} p_{\alpha_2)}^{\dot{\beta}_2)}, \quad \bullet \xrightarrow{\text{red}} \times \xrightarrow{\text{brown}} \bullet = \mathbf{m}^2 p_{(\alpha_1}^{(\dot{\beta}_1} \eta_{\alpha_2)}^{\dot{\beta}_2)} + \mathbf{m}^2 \eta_{(\alpha_1}^{(\dot{\beta}_1} p_{\alpha_2)}^{\dot{\beta}_2)}, \quad \bullet \xrightarrow{\text{cyan}} \times \xrightarrow{\text{red}} \bullet = \mathbf{m}^4 \eta_{(\alpha_1}^{(\dot{\beta}_1} \eta_{\alpha_2)}^{\dot{\beta}_2)}. \quad (\text{A.14})$$

A.2 Internal particle Higgsing

After enumerating all MHC internal particle states, we now present a systematic set of Higgsing rules for internal particles. This rules map the massless internal structure with additional Higgs bosons splitting from it, to the corresponding MHC internal particle states. Given the large number of MHC states, the rules are best illustrated diagrammatically.

Internal fermion We first consider the fermion case. Compared to the leading matching, the Higgs splitting introduces a chirality flip, represented by a cross in MHC diagrams. Therefore, the Higgsing rules will depend on the MHC diagram from the leading matching. Below we list three typical leading matching and their resulting Higgs splittings. Other cases can be derived similarly by changing the colors of the MHC diagrams.

Leading matching			
One Higgs splitting			-
Two Higgs splitting		-	-

(A.15)

Note that a single Higgs splitting changes the helicity of the external particles. Since an external particle can attach to either the left or the right side of the internal line, the corresponding MHC diagrams appear in two variants, as shown in the table above. In contrast, two Higgs splittings do not change the external helicity, so only one MHC diagram corresponds to that case.

Internal vector boson Then we consider internal vector bosons. These have more particle states than fermions, so we restrict ourselves to the leading matching without chirality flips. Other cases can be obtained by shifting the MHC diagrams upward within a column, analogous to the fermion case in Eq. (A.15). Below we show the leading matching with two chirality and the corresponding Higgsing rules,

Leading matching		
One Higgs splitting		
Two Higgs splitting		
Three Higgs splitting		
Four Higgs splitting		

As in the fermion case, splittings involving an odd number of Higgs bosons change the helicity of the external particles, so the corresponding MHC diagrams may have more than one variant.

B Contact 4-point Amplitudes from Conserved Current

In this section, we verify the contact amplitude using the conserved current structure. The 4-point amplitude can be written in the form of factorized and contact terms, and then it can be rewritten as

certain sub-amplitudes with the conserved currents

$$\mathcal{M} = \mathcal{M}_f + \mathcal{M}_{ct} \xrightarrow{\text{deform}} \mathcal{M}_f^{\text{conserved}} \quad (\text{B.1})$$

where \mathcal{M}_f denotes the factorized term containing poles, and \mathcal{M}_{ct} denotes the contact term. By gluing these conserved current MHC sub-amplitudes, we can determine the contact term at leading order.

B.1 Contact VVSS amplitudes

Let us first calculate the VVSS contact amplitude using the $WWhh$ amplitude. The $WWhh$ amplitude has the following structure

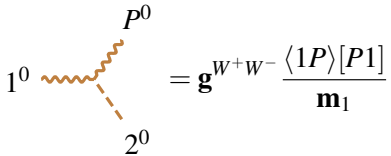
$$\mathcal{M} = \underbrace{\mathcal{M}_{(12)} + \mathcal{M}_{(13)} + \mathcal{M}_{(14)}}_{\mathcal{M}_f} + \mathcal{M}_{ct}. \quad (\text{B.2})$$

Using the gluing technique, the first three terms can be constructed. For each term, the corresponding internal particle and sub-amplitudes are listed below

channel	sub-amplitudes	internal particle
(12)-channel	$WWh \times hhh$	h
(13)-channel	$WWh \times WWh$	W
(14)-channel		

(B.3)

This shows that we can use two types of 3-point amplitudes, WWh and hhh , to construct the $WWhh$ amplitude. The only MHC amplitude related to a conserved current is the primary WWh amplitude,



$$= \mathbf{g}^{W^+W^-} \frac{\langle 1P \rangle [P1]}{\mathbf{m}_1}. \quad (\text{B.4})$$

This amplitude vanishes when momentum conservation $p_1 + p_2 + P = 0$ and the on-shell conditions for all particles are imposed. This primary amplitude can be decomposed into a product of an MHC current $[\mathbf{J}]_0$ and a vector $[\mathbf{A}]_0$,

$$\langle 1P \rangle [P1] = [\mathbf{J}]_0 \cdot [\mathbf{A}]_0, \quad (\text{B.5})$$

where the primary current and vector are defined as

$$[\mathbf{J}]_0 = |1\rangle |1\rangle, \quad [\mathbf{A}]_0 = |P\rangle |P\rangle, \quad (\text{B.6})$$

Note that $\partial \cdot [\mathbf{J}]_0 \neq 0$, so it does not directly correspond to a conserved current.

To find a truly conserved current, we can examine the massless 2-point structure in the UV theory. For two scalar particles, the Noether current is given by

$$J = \frac{1}{2} (|1\rangle |1\rangle - |2\rangle |2\rangle), \quad (\text{B.7})$$

which corresponds to $\phi^* D\phi - \phi D\phi^*$. This current satisfies the conservation condition

$$\partial \cdot J = \frac{1}{2}(\langle 1|1+2|1] - \langle 2|1+2|2]) = 0. \quad (\text{B.8})$$

We can match this Noether current J and a Goldstone mode $\partial\phi$ to the MHC current and vector

$$\begin{aligned} \partial\phi &= |P\rangle|P\rangle & \rightarrow & \quad [\mathbf{A}]_0 = |P\rangle|P\rangle, \\ J &= \frac{1}{2}(|1\rangle|1\rangle - |2\rangle|2\rangle) & \rightarrow & \quad [\mathbf{J}]_0 + \frac{1}{2}P = |1\rangle|1\rangle + \frac{1}{2}|P\rangle|P\rangle. \end{aligned} \quad (\text{B.9})$$

Therefore, the contraction $J \cdot \partial\phi$ corresponds to the MHC primary amplitude

$$J \cdot \partial\phi \rightarrow 1^0 \text{ (wavy line)} \text{ (dashed line)} = \mathbf{g}^{W^+W^-} \frac{\langle 1P\rangle[P1] + P^2}{\mathbf{m}_1}, \quad (\text{B.10})$$

which contains the off-shell quantity P^2 . When particle P is on-shell ($P^2 = 0$), this quantity vanishes and the amplitude returns to eq. (B.4). However, when P is glued as an internal particle, such a term must be retained.

We can now use this knowledge of the conserved current to determine the contact $WWhh$ amplitude. The $WWhh$ amplitude can be categorized into nine helicity categories, classified by the number of transverse vectors n_T :

$$\begin{aligned} n_T = 0: & \quad (0,0,0,0), \\ n_T = 1: & \quad (\pm,0,0,0), (0,\pm,0,0), \\ n_T = 2: & \quad (\pm,\mp,0,0), (\pm,\pm,0,0). \end{aligned} \quad (\text{B.11})$$

We will examine each case to see whether the primary WWh amplitude appears and whether the contact amplitude can be determined.

For $n_T = 0$, there is only one helicity category $(0,0,0,0)$. We first consider the (14)-channel, where the internal particle is a W boson. In this channel, we glue two WWh amplitudes of the form given in Eq. (B.10),

$$\begin{aligned} & 1^0 \text{ (wavy line)} \text{ (dashed line)} \quad 4^0 \\ & P^0 \quad \rightarrow \mathbf{g}^{W^+W^-} \mathbf{g}^{W^+W^-} \frac{(-\langle 1P_{14}\rangle[P_{14}1] + P_{14}^2) \times (-\langle 2P_{23}\rangle[P_{23}2] + P_{23}^2)}{s_{14}\mathbf{m}_1\mathbf{m}_2} \\ & P^0 \quad = \mathbf{g}^{W^+W^-} \mathbf{g}^{W^+W^-} \frac{\langle 1|P_{14}|1\rangle\langle 2|P_{23}|2\rangle}{s_{14}} - \mathbf{g}^{W^+W^-} \mathbf{g}^{W^+W^-} \frac{s_{14}}{\mathbf{m}_1\mathbf{m}_2}. \\ & 2^0 \quad \text{ (wavy line)} \text{ (dashed line)} \quad 3^0 \end{aligned} \quad (\text{B.12})$$

The second term contributes to the contact amplitude. Combining it with the contribution from the (13)-channel gives the full contact term

$$-\mathbf{g}^{W^+W^-} \mathbf{g}^{W^+W^-} \frac{s_{14}}{\mathbf{m}_1 \mathbf{m}_2} + (3 \leftrightarrow 4) \rightarrow \begin{array}{c} 1^0 \quad 4^0 \\ \diagup \quad \diagdown \\ \text{wavy line} \quad \text{dashed line} \\ \diagdown \quad \diagup \\ 2^0 \quad 3^0 \end{array} = \mathbf{g}^{W^+W^-} \mathbf{g}^{W^+W^-} \frac{\langle 12 \rangle [21]}{\mathbf{m}_1 \mathbf{m}_2}. \quad (\text{B.13})$$

which exhibits the correct Goldstone behavior $\tilde{\lambda} \lambda$ for both particles 1 and 2. Once this primary contact amplitude is known, descendant contact amplitudes can also be determined by the extended LG covariance. So far we have not used the (12)-channel. Although this channel also contains the primary WWh sub-amplitude in the factorized limit, the internal particle is a scalar boson. The corresponding diagram is

$$\begin{array}{c} 1^0 \quad 4^0 \\ \diagup \quad \diagdown \\ \text{wavy line} \quad \text{dashed line} \\ \diagdown \quad \diagup \\ 2^0 \quad 3^0 \end{array} \quad (\text{B.14})$$

This differs from the case in Eq. (B.10), where the internal particle is a vector boson. Therefore, the (12)-channel does not contribute to the contact term.

Similarly, we can determine the contact term for helicity categories with $n_T = 1$. As an example, we consider the $(+1, 0, 0, 0)$ as an example. In the (14)-channel, gluing the two sub-amplitudes gives,

$$\begin{array}{c} 1^+ \quad 4^0 \\ \text{blue cross} \quad \text{dashed line} \\ \text{wavy line} \quad \text{dashed line} \\ \text{wavy line} \quad \text{dashed line} \\ 2^0 \quad 3^0 \end{array} \rightarrow \mathbf{g}^{W^+W^-} \mathbf{g}^{W^+W^-} \frac{\langle \eta_1 P_{14} \rangle [P_{14} 1] \times (-\langle 2P_{23} \rangle [P_{23} 2] + P_{23}^2)}{m_1 \mathbf{m}_2 s_{14}} \\ = \mathbf{g}^{W^+W^-} \mathbf{g}^{W^+W^-} \frac{\langle \eta_1 |P_{14}| 1] \langle 2 |P_{23}| 2]}{m_1 \mathbf{m}_2 s_{14}} - \mathbf{g}^{W^+W^-} \mathbf{g}^{W^+W^-} \frac{\langle \eta_1 4 \rangle [41]}{m_1 \mathbf{m}_2}. \quad (\text{B.15})$$

Combining this with the contribution from the (13)-channel yields the contact term

$$-\mathbf{g}^{W^+W^-} \mathbf{g}^{W^+W^-} \frac{\langle \eta_1 4 \rangle [41]}{m_1 \mathbf{m}_2} + (3 \leftrightarrow 4) \rightarrow \begin{array}{c} 1^+ \quad 4^0 \\ \diagup \quad \diagdown \\ \text{wavy line} \quad \text{dashed line} \\ \diagdown \quad \diagup \\ 2^0 \quad 3^0 \end{array} = \mathbf{g}^{W^+W^-} \mathbf{g}^{W^+W^-} \frac{\langle \eta_1 2 \rangle [21]}{m_1 \mathbf{m}_2}. \quad (\text{B.16})$$

The corresponding descendant contact amplitude is

$$= g^{W^+W^-} g^{W^+W^-} \frac{\langle \eta_1 \eta_2 \rangle [\eta_2 1]}{m_1 m_2}. \quad (\text{B.17})$$

For helicity categories with $n_T = 2$, no primary WWh amplitude exists, so the conserved-current method cannot be used to fix the contact amplitude.

In summary, by rewriting the vanishing 3-point MHC amplitudes in terms of conserved currents from the UV theory, and employing these modified forms in the gluing procedure, we can determine certain contact amplitudes. This approach applies only to helicity categories where such vanishing MHC amplitudes are present.

B.2 Contact $VVVV$ amplitudes

Now we will determine $VVVV$ contact massive amplitude in the SM using the conserved current analysis in $WW \rightarrow ZZ$ amplitudes. The contact term has two origins: the massless contact term and the conserved current. The first origin only relate to the $\lambda \phi^4$ interaction, so we discuss this later. For now, we consider the second origin, the conserved current.

As previously discussion, the amplitude can be decomposed to a product of the current and the vector. This current may not equal to the massless Noether, so their difference can create a contact term. In the massless gauge theory with spin ≤ 1 , there are three kinds of Noether current J . Let us examine whether they equal to the MHC current \mathbf{J} in a specific order,

- The fermion Noether current $\bar{\psi} \gamma^\mu \psi$. It equals to primary FF current

$$J = |1\rangle |2\rangle \rightarrow [\mathbf{J}] = |1\rangle |2\rangle. \quad (\text{B.18})$$

Therefore, FFV amplitude will not generate the contact term.

- The scalar Noether current $\phi^* D\phi$. It equals is not equal to primary VS current

$$J = \frac{1}{2}(|1\rangle \langle 1| - |2\rangle \langle 2|) \rightarrow [\mathbf{J}] + \frac{1}{2}P = |1\rangle \langle 1| + \frac{1}{2}P. \quad (\text{B.19})$$

Therefore, VVS amplitude will generate the contact term.

- The Yang-Mills Noether current $F^{\mu\nu} A_\mu$. It equals to the 1st descendant VV current.

$$\begin{aligned} J(1^{-1}, 2^{-1}) &= \frac{\langle 12 \rangle}{[\xi_2 2]} [\xi_2]^\alpha \langle 1 |^\alpha + \frac{\langle 12 \rangle}{[\xi_1 1]} [\xi_1]^\alpha \langle 2 |^\alpha \\ &\rightarrow [\mathbf{J}(1^{-1}, 2^{-1})]_1 = -\frac{1}{m_2^2} m_2 \langle 12 \rangle [\eta_2]^\alpha \langle 1 |^\alpha - \frac{1}{m_1^2} m_1 \langle 12 \rangle [\eta_1]^\alpha \langle 2 |^\alpha. \end{aligned} \quad (\text{B.20})$$

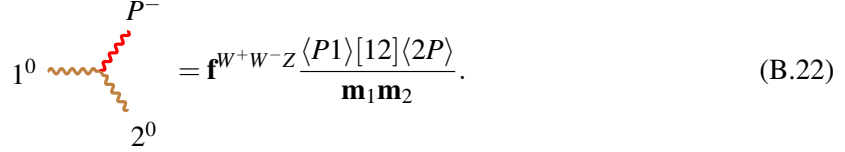
Therefore, the VVV amplitude will not generate contact term, if the internal particle is in $(\frac{1}{2}, \frac{1}{2})$ representation.

However, the above analysis do not consider the case that the internal vector boson can be a chiral particle, which has Lorentz representation $(1,0)$ or $(0,1)$. As an example, let us consider the W^+W^-ZZ amplitude. It has three channels. The corresponding internal particles and sub-amplitudes in the factorized limit are

channel	sub-amplitudes	internal particle	
(12)-channel	$WWh \times ZZh$	h	
(13)-channel	$WWZ \times WWZ$	W	
(14)-channel			

(B.21)

Since we are consider the case with internal vector boson, we can only pay attention to (13) and (14)-channel. The corresponding 3-pt amplitude is W^+W^-Z amplitude, with one particle will be labeled as P . This particle P will become internal vector, and it can be chiral or anti-chiral. We first consider the chiral case, the primary W^+W^-Z amplitude is



$$= \mathbf{f}^{W^+W^-Z} \frac{\langle P1 \rangle [12] \langle 2P \rangle}{\mathbf{m}_1 \mathbf{m}_2}. \quad (\text{B.22})$$

This primary amplitude can be decomposed into a product of an field strength tensor $[\mathbf{F}^\pm]_0$ and two vector $[\mathbf{A}]_0$.

$$\langle P1 \rangle [12] \langle 2P \rangle = [\mathbf{F}_{\alpha_2}^{\alpha_1}]_0 \times [\mathbf{A}_{\alpha_1 \dot{\alpha}}]_0 \times [\mathbf{A}^{\dot{\alpha} \alpha_2}]_0, \quad (\text{B.23})$$

where the field strength tensor and vectors are defined as

$$[\mathbf{F}_{\alpha_2}^{\alpha_1}]_0 = \langle P |^{\alpha_1} | P \rangle_{\alpha_2}, \quad [\mathbf{A}_{\alpha_1 \dot{\alpha}}]_0 = |1\rangle_{\alpha_1} [1|_{\dot{\alpha}}, \quad [\mathbf{A}^{\dot{\alpha} \alpha_2}]_0 = |2]^{\dot{\alpha}} \langle 2|^{\alpha_2}. \quad (\text{B.24})$$

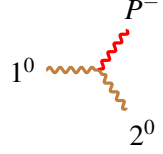
Now particles 1 and 2 are scalar boson, so they may relate to the scalar Noether current. For each particle, we associate a Noether current,

$$\begin{aligned} J_{\alpha_1 \dot{\alpha}} &= \frac{1}{2} (|1\rangle_{\alpha_1} [1|_{\dot{\alpha}} - |2\rangle_{\alpha_1} [2|_{\dot{\alpha}}), \\ J^{\dot{\alpha} \alpha_2} &= \frac{1}{2} (|1]^{\dot{\alpha}} \langle 1|^{\alpha_2} - |2]^{\dot{\alpha}} \langle 2|^{\alpha_2}). \end{aligned} \quad (\text{B.25})$$

Then we can match these two Noether current J and a field strength tensor \mathcal{F} to two MHC vectors and the MHC field strength tensor,

$$\begin{aligned} \mathcal{F}_{\alpha_2}^{\alpha_1} &= \langle P |^{\alpha_1} | P \rangle_{\alpha_2} & \rightarrow & \quad [\mathbf{F}_{\alpha_2}^{\alpha_1}]_0 = \langle P |^{\alpha_1} | P \rangle_{\alpha_2}, \\ J_{\alpha_1 \dot{\alpha}} &= \frac{1}{2} (|1\rangle_{\alpha_1} [1|_{\dot{\alpha}} - |2\rangle_{\alpha_1} [2|_{\dot{\alpha}}) & \rightarrow & \quad [\mathbf{A}_{\alpha_1 \dot{\alpha}}]_0 + \frac{1}{2} P_{\alpha_1 \dot{\alpha}} = |1\rangle_{\alpha_1} [1|_{\dot{\alpha}} + \frac{1}{2} P_{\alpha_1 \dot{\alpha}}, \\ -J^{\dot{\alpha} \alpha_2} &= \frac{1}{2} (|2]^{\dot{\alpha}} \langle 2|^{\alpha_2} - |1]^{\dot{\alpha}} \langle 1|^{\alpha_2}) & \rightarrow & \quad [\mathbf{A}^{\dot{\alpha} \alpha_2}]_0 + \frac{1}{2} P^{\dot{\alpha} \alpha_2} = |2]^{\dot{\alpha}} \langle 2|^{\alpha_2} + \frac{1}{2} P^{\dot{\alpha} \alpha_2}, \end{aligned} \quad (\text{B.26})$$

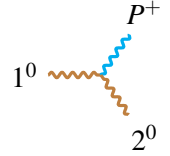
Therefore, the contraction $JJ\mathcal{F}$ corresponds to the MHC primary amplitude,



$$1^0 \text{ (orange wavy line)} \quad 2^0 \text{ (orange wavy line)} \quad P^- \text{ (red wavy line)} \\ = \frac{[\mathbf{F}_{\alpha_2}^{\alpha_1}]_0}{\mathbf{m}_1 \mathbf{m}_2} \times \left(|1\rangle_{\alpha_1} [12] \langle 2|^{\alpha_2} + \frac{|1\rangle_{\alpha_1} ([1|P])^{\alpha_2}}{2} + \frac{(P|2])_{\alpha_1} \langle 2|^{\alpha_2}}{2} + \frac{P^2 \delta_{\alpha_1}^{\alpha_2}}{4} \right). \quad (\text{B.27})$$

Contract with $[\mathbf{F}_{\alpha_2}^{\alpha_1}]_0$, the first term in the bracket return to the amplitude in eq. (B.22), while other three terms will contribute to the contact term.

Similarly, we can give the primary amplitude with particle P is anti-chiral,

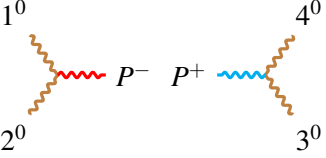


$$1^0 \text{ (orange wavy line)} \quad 2^0 \text{ (orange wavy line)} \quad P^+ \text{ (blue wavy line)} \\ = \frac{[\mathbf{F}_{\dot{\alpha}_1}^{\dot{\alpha}_2}]_0}{\mathbf{m}_1 \mathbf{m}_2} \times \left(|1\rangle^{\dot{\alpha}_1} \langle 12| [2|_{\dot{\alpha}_2} + \frac{|1\rangle^{\dot{\alpha}_1} (\langle 1|P)_{\dot{\alpha}_2}}{2} + \frac{(P|2])^{\dot{\alpha}_1} [2|_{\dot{\alpha}_2}}{2} + \frac{P_{12}^2 \delta_{\dot{\alpha}_1}^{\dot{\alpha}_2}}{4} \right). \quad (\text{B.28})$$

Now we can gluing the W^+W^-Z amplitude to determine the contact term. Here we choose the helicity category $(0, 0, 0, 0)$. Gluing the two field strength tensor can give an internal vector boson

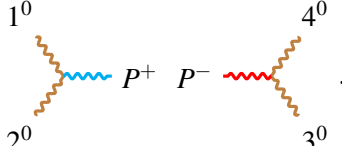
$$[\mathbf{F}_{\alpha_2}^{\alpha_1}]_0 \times [\mathbf{F}_{\dot{\beta}_2}^{\dot{\beta}_1}]_0 = \frac{1}{2} (P^{\alpha_1 \dot{\beta}_1} P_{\alpha_2 \dot{\beta}_2} + P_{\dot{\beta}_2}^{\alpha_1} P_{\alpha_2}^{\dot{\beta}_1}). \quad (\text{B.29})$$

Therefore, contracting two primary amplitudes, we get



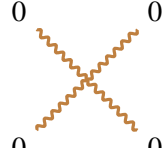
$$1^0 \quad 2^0 \quad P^- \quad P^+ \quad 3^0 \quad 4^0 \\ = \frac{\mathbf{f}^{W^+W^-Z}}{\mathbf{m}_1 \mathbf{m}_2} \left(|1\rangle_{\alpha_1} [12] \langle 2|^{\alpha_2} - \frac{|1\rangle_{\alpha_1} ([1|P_{12})^{\alpha_2}}{2} - \frac{(P_{12}|2])_{\alpha_1} \langle 2|^{\alpha_2}}{2} + \frac{P_{12}^2 \delta_{\alpha_1}^{\alpha_2}}{4} \right) \\ \times \frac{P_{12}^{\alpha_1 \dot{\beta}_1} P_{12, \alpha_2 \dot{\beta}_2} + P_{12}^{\alpha_1} P_{12 \alpha_2}^{\dot{\beta}_1}}{2s_{12}} \\ \times \frac{\mathbf{f}^{W^+W^-Z}}{\mathbf{m}_3 \mathbf{m}_4} \left(|3\rangle^{\dot{\beta}_1} \langle 34| [4|_{\dot{\beta}_2} + \frac{|3\rangle^{\dot{\beta}_1} (\langle 3|P_{12})_{\dot{\beta}_2}}{2} + \frac{(P_{12}|4])^{\dot{\beta}_1} [4|_{\dot{\beta}_2}}{2} + \frac{P_{12}^2 \delta_{\dot{\beta}_1}^{\dot{\beta}_2}}{4} \right) \\ = \frac{\mathbf{f}^{W^+W^-Z} \mathbf{f}^{W^+W^-Z}}{\mathbf{m}_1 \mathbf{m}_2 \mathbf{m}_3 \mathbf{m}_4} \frac{[12] (\langle 1|P_{12}|3] \langle 2|P_{12}|4] + \langle 1|P_{12}|4] \langle 2|P_{12}|3]) \langle 34\rangle}{2s_{12}} \\ + \frac{\mathbf{f}^{W^+W^-Z} \mathbf{f}^{W^+W^-Z}}{\mathbf{m}_1 \mathbf{m}_2 \mathbf{m}_3 \mathbf{m}_4} \frac{s_{12}(s_{14} - s_{13})}{2}. \quad (\text{B.30})$$

The second term contributes to the contact term. Similarly, the other helicity of internal line gives



$$\begin{aligned}
 &= \frac{\mathbf{f}^{W^+W^-Z} \mathbf{f}^{W^+W^-Z}}{\mathbf{m}_1 \mathbf{m}_2 \mathbf{m}_3 \mathbf{m}_4} \frac{\langle 12 \rangle ([1|P_{12}|3][2|P_{12}|4] + [1|P_{12}|4][2|P_{12}|3])[34]}{2s_{12}} \\
 &+ \frac{\mathbf{f}^{W^+W^-Z} \mathbf{f}^{W^+W^-Z}}{\mathbf{m}_1 \mathbf{m}_2 \mathbf{m}_3 \mathbf{m}_4} \frac{s_{12}(s_{14} - s_{13})}{2}
 \end{aligned} \tag{B.31}$$

Combining it with the contribution from (14)-channel gives the full contact term,



$$\begin{aligned}
 &= \frac{\mathbf{f}^{W^+W^-Z} \mathbf{f}^{W^+W^-Z}}{\mathbf{m}_1 \mathbf{m}_2 \mathbf{m}_3 \mathbf{m}_4} (\langle 12 \rangle [21] \langle 34 \rangle [34] + \langle 14 \rangle [41] \langle 23 \rangle [32] - 2 \langle 13 \rangle [31] \langle 24 \rangle [42]).
 \end{aligned} \tag{B.32}$$

The subleading order contribution in this helicity category can be obtained by applying ladder operators.

C $WW \rightarrow ZZ$ Amplitudes

In this section, we briefly calculate the $WW \rightarrow ZZ$ amplitudes in the MHC and AHH formalism.

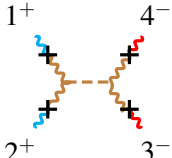
C.1 Bootstrapping MHC amplitudes

We can use gluing technique to obtain the $WW \rightarrow ZZ$ amplitudes. This amplitude has four contributions,

$$\mathcal{M}(WWZZ) = \mathcal{M}_{(12)} + \mathcal{M}_{(13)} + \mathcal{M}_{(14)} + \mathcal{M}_{\text{ct.}} \tag{C.1}$$

We choose helicity category $(+, +, -, -)$ to gluing the amplitude.

For (12)-channel, the internal particle is Higgs boson. We glue WWh and ZZh amplitude and get



$$= g^{W^+W^-} g^{ZZ} \frac{\tilde{m}_1 \tilde{m}_2 m_3 m_4 \langle \eta_1 \eta_2 \rangle [21] \langle 34 \rangle [\eta_4 \eta_3]}{s_{12} \mathbf{m}_1^2 \mathbf{m}_2^2 \mathbf{m}_3^2 \mathbf{m}_4^2} \tag{C.2}$$

For the (14)-channel, the internal particle is a W boson. In this case, we glue two WWZ amplitudes. Since the WWZ amplitude has six primary vertices, this results in a total of 36 terms. These terms fall into three categories, which we illustrate with the following examples. They can be grouped by the number of internal chirality flip:

- Three internal chirality flips:

$$= \frac{(\mathbf{f}^{W^+W^-Z})^2}{2\mathbf{m}_2^2\mathbf{m}_4^2\mathbf{m}^2 s_{14}} \tilde{m}_2 m_4 [1|\eta_4]\langle\eta_2 3\rangle\langle 4|P_{14}|1]\langle 3|P_{14}|2]. \quad (\text{C.3})$$

- Two internal chirality flips:

$$= \frac{(\mathbf{f}^{W^+W^-Z})^2}{2\mathbf{m}_1^2\mathbf{m}_2^2\mathbf{m}_4^2 s_{14}} \tilde{m}_1 \tilde{m}_2 m_4 \langle\eta_1 4\rangle\langle\eta_2 3\rangle([\eta_4|P_{14}|3\rangle[12] + [1|P_{14}|3\rangle[\eta_4 2]]). \quad (\text{C.4})$$

- One internal chirality flip:

$$= \frac{(\mathbf{f}^{W^+W^-Z})^2}{2\mathbf{m}_1^2\mathbf{m}_2^2\mathbf{m}_3^2\mathbf{m}_4^2 s_{14}} \tilde{m}_1 \tilde{m}_2 m_3 m_4 \mathbf{m}^2 \langle\eta_1 4\rangle[2\eta_3]([4\eta_2][\eta_1 3] + [43][\eta_1 \eta_2]). \quad (\text{C.5})$$

The internal line with more cross can be obtained by applying J^+J^- . Similarly, we can derive other terms in the (14)-channel. For the (13)-channel, we can apply a symmetry argument to obtain the amplitude directly. This is possible because particles 3 and 4 are both Z bosons and have identical helicities. The relation is given by

$$\mathcal{M}_{(13)}(1, 2, 3, 4) = \mathcal{M}_{(14)}(1, 2, 4, 3). \quad (\text{C.6})$$

The contact term is given by

$$= (\mathbf{f}^{W^+W^-Z})^2 \times (\langle\eta_1 \eta_2\rangle[21]\langle 34\rangle[\eta_3 \eta_4] + \langle\eta_1 4\rangle[\eta_4 1]\langle\eta_2 3\rangle[\eta_3 2] - 2\langle\eta_1 3\rangle[\eta_3 1]\langle\eta_2 4\rangle[\eta_4 2]). \quad (\text{C.7})$$

The final MHC result is just summing over the above four contributions.

C.2 Bootstrapping AHH amplitudes

We can also derive the $WW \rightarrow ZZ$ amplitude within the AHH formalism. The building blocks are the 3-pt and 4-pt contact AHH amplitudes. In this formalism, the 3-pt VVV amplitude can be expressed in two forms.

- When all three vector bosons are described by the $(\frac{1}{2}, \frac{1}{2})$ Lorentz representation, we have

$$\mathbf{M}(\mathbf{1}, \mathbf{2}, \mathbf{3}) = \frac{\langle \mathbf{12} \rangle [\mathbf{21}] \langle \mathbf{31} | \mathbf{3}] + \langle \mathbf{23} \rangle [\mathbf{32}] \langle \mathbf{12} | \mathbf{1}] + \langle \mathbf{31} \rangle [\mathbf{13}] \langle \mathbf{23} | \mathbf{2}]}{\mathbf{m}_1 \mathbf{m}_2 \mathbf{m}_3}. \quad (\text{C.8})$$

This form is similar to the Feynman amplitude, where each term corresponds to a contraction of three polarization vector ε and one massive momentum \mathbf{p} .

- Alternatively, two vector bosons can be assigned the $(\frac{1}{2}, \frac{1}{2})$ representation while the third is in the $(1, 0)$ or $(0, 1)$ representation:

$$\mathbf{M}(\mathbf{1}, \mathbf{2}, \mathbf{3}) = \left(\frac{[\mathbf{12}] \langle \mathbf{23} \rangle [\mathbf{31}] + \langle \mathbf{12} \rangle [\mathbf{23}] \langle \mathbf{31}]}{\mathbf{m}_2 \mathbf{m}_3} + \frac{[\mathbf{12}] [\mathbf{23}] \langle \mathbf{31}] + \langle \mathbf{12} \rangle \langle \mathbf{23} \rangle [\mathbf{31}]}{\mathbf{m}_1 \mathbf{m}_3} + \frac{[\mathbf{12}] \langle \mathbf{23} \rangle \langle \mathbf{31}] + \langle \mathbf{12} \rangle [\mathbf{23}] [\mathbf{31}]}{\mathbf{m}_1 \mathbf{m}_2} \right). \quad (\text{C.9})$$

This form can be obtained by bolding the MHC VVV amplitude.

Then, let us discuss the gluing technique for AHH amplitudes, using $WW \rightarrow ZZ$ as an example. In the (12)-channel, two VVV amplitudes can be glued together as

$$= \mathbf{M}(\mathbf{1}, \mathbf{4}, -\mathbf{P}_{14}) \otimes \mathbf{M}(\mathbf{P}_{14}, \mathbf{2}, \mathbf{3}), \quad (\text{C.10})$$

where \mathbf{P}_{14} denotes the momentum of the on-shell internal line, and \otimes indicates the contraction over the corresponding LG indices from the 3-pt amplitudes.

Writing the LG indices explicitly, the on-shell gluing gives

$$\begin{aligned} [\mathbf{P}]^{\dot{\alpha}} [\mathbf{P}]^{\alpha} \otimes [\mathbf{P}]_{\dot{\beta}} \langle \mathbf{P} \rangle_{\beta} &= [\mathbf{P}]^{\dot{\alpha}(I_1} [\mathbf{P}]^{\alpha I_2)} \times [\mathbf{P}]_{\dot{\beta} I_1} \langle \mathbf{P} \rangle_{\beta I_2} = \mathbf{m}^2 \delta_{\dot{\beta}}^{\dot{\alpha}} \delta_{\beta}^{\alpha} - \frac{1}{2} \mathbf{P}^{\dot{\alpha}\alpha} \mathbf{P}_{\beta\dot{\beta}}, \\ [\mathbf{P}]^{\dot{\alpha}_1} [\mathbf{P}]^{\dot{\alpha}_2} \otimes [\mathbf{P}]_{\dot{\beta}} \langle \mathbf{P} \rangle_{\beta} &= [\mathbf{P}]^{\dot{\alpha}_1(I_1} [\mathbf{P}]^{\dot{\alpha}_2 I_2)} \times [\mathbf{P}]_{\dot{\beta} I_1} \langle \mathbf{P} \rangle_{\beta I_2} = \mathbf{m} \delta_{\dot{\beta}}^{(\dot{\alpha}_1} \mathbf{P}^{\dot{\alpha}_2)\beta}, \\ [\mathbf{P}]^{\dot{\alpha}_1} [\mathbf{P}]^{\dot{\alpha}_2} \otimes [\mathbf{P}]_{\dot{\beta}_1} [\mathbf{P}]_{\dot{\beta}_2} &= [\mathbf{P}]^{\dot{\alpha}_1(I_1} [\mathbf{P}]^{\dot{\alpha}_2 I_2)} \times \mathbf{m} [\mathbf{P}]_{\dot{\beta}_1 I_1} [\mathbf{P}]_{\dot{\beta}_2 I_2} = \mathbf{m}^2 \delta_{\dot{\beta}_1}^{(\dot{\alpha}_1} \delta_{\dot{\beta}_2}^{\dot{\alpha}_2)}, \\ &\vdots \end{aligned} \quad (\text{C.11})$$

To compare with the gluing results from MHC amplitudes, we select specific terms of the 3-pt massive amplitude and glue them in three cases:

$$[\mathbf{14}] \langle \mathbf{4P} \rangle [\mathbf{P1}] \otimes \langle \mathbf{23} \rangle \langle \mathbf{3P} \rangle [\mathbf{P2}] = [\mathbf{14}] \langle \mathbf{23} \rangle (\mathbf{m}^2 \langle \mathbf{43} \rangle [\mathbf{21}] - \frac{1}{2} \langle \mathbf{4} | \mathbf{P}_{14} | \mathbf{1}] \langle \mathbf{3} | \mathbf{P}_{14} | \mathbf{2}]), \quad (\text{C.12})$$

$$\langle 14 \rangle [4P][P1] \otimes \langle 23 \rangle [3P][P2] = \frac{1}{2} \mathbf{m} \langle 14 \rangle \langle 23 \rangle ([4|P_{14}|3][12] + [1|P_{14}|3][42]), \quad (C.13)$$

$$\langle 14 \rangle [4P][P1] \otimes \langle 23 \rangle [3P][P2] = \frac{1}{2} \mathbf{m}^2 \langle 14 \rangle \langle 23 \rangle ([42][13] + [43][12]). \quad (C.14)$$

These results are consistent with Eqs. (C.3–C.5), if we bold the massless spinors.

References

- [1] S. J. Parke and T. R. Taylor, *An Amplitude for n Gluon Scattering*, *Phys. Rev. Lett.* **56** (1986) 2459.
- [2] Z. Xu, D.-H. Zhang, and L. Chang, *Helicity Amplitudes for Multiple Bremsstrahlung in Massless Nonabelian Gauge Theories*, *Nucl. Phys. B* **291** (1987) 392–428.
- [3] Z. Bern, L. J. Dixon, and D. A. Kosower, *Progress in one loop QCD computations*, *Ann. Rev. Nucl. Part. Sci.* **46** (1996) 109–148, [[hep-ph/9602280](#)].
- [4] L. J. Dixon, *Calculating scattering amplitudes efficiently*, in *Theoretical Advanced Study Institute in Elementary Particle Physics (TASI 95): QCD and Beyond*, pp. 539–584, 1, 1996. [hep-ph/9601359](#).
- [5] H. Elvang and Y.-t. Huang, *Scattering Amplitudes*, [arXiv:1308.1697](#).
- [6] C. Cheung, *TASI lectures on scattering amplitudes*, in *Theoretical Advanced Study Institute in Elementary Particle Physics: Anticipating the Next Discoveries in Particle Physics*, pp. 571–623, 2018. [arXiv:1708.03872](#).
- [7] G. Travaglini et al., *The SAGEX review on scattering amplitudes*, *J. Phys. A* **55** (2022), no. 44 443001, [[arXiv:2203.13011](#)].
- [8] S. Badger, J. Henn, J. C. Plefka, and S. Zoia, *Scattering Amplitudes in Quantum Field Theory*, *Lect. Notes Phys.* **1021** (2024) pp., [[arXiv:2306.05976](#)].
- [9] P. Benincasa and F. Cachazo, *Consistency Conditions on the S-Matrix of Massless Particles*, [arXiv:0705.4305](#).
- [10] E. Witten, *Perturbative gauge theory as a string theory in twistor space*, *Commun. Math. Phys.* **252** (2004) 189–258, [[hep-th/0312171](#)].
- [11] Z. Bern, L. J. Dixon, D. C. Dunbar, and D. A. Kosower, *One loop n point gauge theory amplitudes, unitarity and collinear limits*, *Nucl. Phys. B* **425** (1994) 217–260, [[hep-ph/9403226](#)].
- [12] Z. Bern, L. J. Dixon, D. C. Dunbar, and D. A. Kosower, *Fusing gauge theory tree amplitudes into loop amplitudes*, *Nucl. Phys. B* **435** (1995) 59–101, [[hep-ph/9409265](#)].
- [13] R. Britto, F. Cachazo, and B. Feng, *Generalized unitarity and one-loop amplitudes in N=4 super-Yang-Mills*, *Nucl. Phys. B* **725** (2005) 275–305, [[hep-th/0412103](#)].
- [14] R. Britto, F. Cachazo, and B. Feng, *New recursion relations for tree amplitudes of gluons*, *Nucl. Phys. B* **715** (2005) 499–522, [[hep-th/0412308](#)].
- [15] R. Britto, F. Cachazo, B. Feng, and E. Witten, *Direct proof of tree-level recursion relation in Yang-Mills theory*, *Phys. Rev. Lett.* **94** (2005) 181602, [[hep-th/0501052](#)].
- [16] N. Arkani-Hamed, T.-C. Huang, and Y.-t. Huang, *Scattering amplitudes for all masses and spins*, *JHEP* **11** (2021) 070, [[arXiv:1709.04891](#)].

[17] R. Franken and C. Schwinn, *On-shell constructibility of Born amplitudes in spontaneously broken gauge theories*, *JHEP* **02** (2020) 073, [[arXiv:1910.13407](https://arxiv.org/abs/1910.13407)].

[18] B. Bachu and A. Yelleshpur, *On-Shell Electroweak Sector and the Higgs Mechanism*, *JHEP* **08** (2020) 039, [[arXiv:1912.04334](https://arxiv.org/abs/1912.04334)].

[19] S. Ballav and A. Manna, *Recursion relations for scattering amplitudes with massive particles*, *JHEP* **03** (2021) 295, [[arXiv:2010.14139](https://arxiv.org/abs/2010.14139)].

[20] C. Wu and S.-H. Zhu, *Massive on-shell recursion relations for n -point amplitudes*, *JHEP* **06** (2022) 117, [[arXiv:2112.12312](https://arxiv.org/abs/2112.12312)].

[21] S. Ballav and A. Manna, *Recursion relations for scattering amplitudes with massive particles II: Massive vector bosons*, *Nucl. Phys. B* **983** (2022) 115935, [[arXiv:2109.06546](https://arxiv.org/abs/2109.06546)].

[22] D. Liu and Z. Yin, *Gauge invariance from on-shell massive amplitudes and tree-level unitarity*, *Phys. Rev. D* **106** (2022), no. 7 076003, [[arXiv:2204.13119](https://arxiv.org/abs/2204.13119)].

[23] B. Bachu, *Spontaneous Symmetry Breaking from an On-Shell Perspective*, [arXiv:2305.02502](https://arxiv.org/abs/2305.02502).

[24] Y. Ema, T. Gao, W. Ke, Z. Liu, K.-F. Lyu, and I. Mahbub, *Momentum shift and on-shell recursion relation for electroweak theory*, *Phys. Rev. D* **110** (2024), no. 10 105002, [[arXiv:2407.14587](https://arxiv.org/abs/2407.14587)].

[25] Y. Shadmi and Y. Weiss, *Effective Field Theory Amplitudes the On-Shell Way: Scalar and Vector Couplings to Gluons*, *JHEP* **02** (2019) 165, [[arXiv:1809.09644](https://arxiv.org/abs/1809.09644)].

[26] R. Aoude and C. S. Machado, *The Rise of SMEFT On-shell Amplitudes*, *JHEP* **12** (2019) 058, [[arXiv:1905.11433](https://arxiv.org/abs/1905.11433)].

[27] G. Durieux, T. Kitahara, Y. Shadmi, and Y. Weiss, *The electroweak effective field theory from on-shell amplitudes*, *JHEP* **01** (2020) 119, [[arXiv:1909.10551](https://arxiv.org/abs/1909.10551)].

[28] T. Ma, J. Shu, and M.-L. Xiao, *Standard model effective field theory from on-shell amplitudes**, *Chin. Phys. C* **47** (2023), no. 2 023105, [[arXiv:1902.06752](https://arxiv.org/abs/1902.06752)].

[29] G. Durieux and C. S. Machado, *Enumerating higher-dimensional operators with on-shell amplitudes*, *Phys. Rev. D* **101** (2020), no. 9 095021, [[arXiv:1912.08827](https://arxiv.org/abs/1912.08827)].

[30] H.-L. Li, Z. Ren, J. Shu, M.-L. Xiao, J.-H. Yu, and Y.-H. Zheng, *Complete Set of Dimension-8 Operators in the Standard Model Effective Field Theory*, [arXiv:2005.00008](https://arxiv.org/abs/2005.00008).

[31] H.-L. Li, Z. Ren, M.-L. Xiao, J.-H. Yu, and Y.-H. Zheng, *Complete set of dimension-nine operators in the standard model effective field theory*, *Phys. Rev. D* **104** (2021), no. 1 015025, [[arXiv:2007.07899](https://arxiv.org/abs/2007.07899)].

[32] H.-L. Li, Z. Ren, M.-L. Xiao, J.-H. Yu, and Y.-H. Zheng, *Low energy effective field theory operator basis at $d \leq 9$* , *JHEP* **06** (2021) 138, [[arXiv:2012.09188](https://arxiv.org/abs/2012.09188)].

[33] H.-L. Li, J. Shu, M.-L. Xiao, and J.-H. Yu, *Depicting the Landscape of Generic Effective Field Theories*, [arXiv:2012.11615](https://arxiv.org/abs/2012.11615).

[34] G. Durieux, T. Kitahara, C. S. Machado, Y. Shadmi, and Y. Weiss, *Constructing massive on-shell contact terms*, *JHEP* **12** (2020) 175, [[arXiv:2008.09652](https://arxiv.org/abs/2008.09652)].

[35] H.-L. Li, Z. Ren, M.-L. Xiao, J.-H. Yu, and Y.-H. Zheng, *Operator bases in effective field theories with sterile neutrinos: $d \leq 9$* , *JHEP* **11** (2021) 003, [[arXiv:2105.09329](https://arxiv.org/abs/2105.09329)].

[36] M. Accettulli Huber and S. De Angelis, *Standard Model EFTs via on-shell methods*, [JHEP **11** \(2021\) 221](#), [[arXiv:2108.03669](#)].

[37] Z.-Y. Dong, T. Ma, and J. Shu, *Constructing on-shell operator basis for all masses and spins*, [Phys. Rev. D **107** \(2023\), no. 11 L111901](#), [[arXiv:2103.15837](#)].

[38] H.-L. Li, Z. Ren, M.-L. Xiao, J.-H. Yu, and Y.-H. Zheng, *Operators for generic effective field theory at any dimension: on-shell amplitude basis construction*, [JHEP **04** \(2022\) 140](#), [[arXiv:2201.04639](#)].

[39] R. Balkin, G. Durieux, T. Kitahara, Y. Shadmi, and Y. Weiss, *On-shell Higgsing for EFTs*, [JHEP **03** \(2022\) 129](#), [[arXiv:2112.09688](#)].

[40] S. De Angelis, *Amplitude bases in generic EFTs*, [JHEP **08** \(2022\) 299](#), [[arXiv:2202.02681](#)].

[41] Z.-Y. Dong, T. Ma, J. Shu, and Y.-H. Zheng, *Constructing generic effective field theory for all masses and spins*, [Phys. Rev. D **106** \(2022\), no. 11 116010](#), [[arXiv:2202.08350](#)].

[42] Z. Ren and J.-H. Yu, *A complete set of the dimension-8 Green's basis operators in the Standard Model effective field theory*, [JHEP **02** \(2024\) 134](#), [[arXiv:2211.01420](#)].

[43] H. Liu, T. Ma, Y. Shadmi, and M. Waterbury, *An EFT hunter's guide to two-to-two scattering: HEFT and SMEFT on-shell amplitudes*, [JHEP **05** \(2023\) 241](#), [[arXiv:2301.11349](#)].

[44] J. M. Goldberg, H. Liu, and Y. Shadmi, *Dimension-8 SMEFT contact-terms for vector-pair production via on-shell Higgsing*, [JHEP **12** \(2024\) 057](#), [[arXiv:2407.07945](#)].

[45] A. Guevara, A. Ochirov, and J. Vines, *Scattering of Spinning Black Holes from Exponentiated Soft Factors*, [JHEP **09** \(2019\) 056](#), [[arXiv:1812.06895](#)].

[46] M.-Z. Chung, Y.-T. Huang, J.-W. Kim, and S. Lee, *The simplest massive S-matrix: from minimal coupling to Black Holes*, [JHEP **04** \(2019\) 156](#), [[arXiv:1812.08752](#)].

[47] A. Guevara, A. Ochirov, and J. Vines, *Black-hole scattering with general spin directions from minimal-coupling amplitudes*, [Phys. Rev. D **100** \(2019\), no. 10 104024](#), [[arXiv:1906.10071](#)].

[48] Z. Bern, C. Cheung, R. Roiban, C.-H. Shen, M. P. Solon, and M. Zeng, *Scattering Amplitudes and the Conservative Hamiltonian for Binary Systems at Third Post-Minkowskian Order*, [Phys. Rev. Lett. **122** \(2019\), no. 20 201603](#), [[arXiv:1901.04424](#)].

[49] B. Maybee, D. O'Connell, and J. Vines, *Observables and amplitudes for spinning particles and black holes*, [JHEP **12** \(2019\) 156](#), [[arXiv:1906.09260](#)].

[50] N. Arkani-Hamed, Y.-t. Huang, and D. O'Connell, *Kerr black holes as elementary particles*, [JHEP **01** \(2020\) 046](#), [[arXiv:1906.10100](#)].

[51] A. Ochirov, *Helicity amplitudes for QCD with massive quarks*, [JHEP **04** \(2018\) 089](#), [[arXiv:1802.06730](#)].

[52] A. Falkowski and C. S. Machado, *Soft Matters, or the Recursions with Massive Spinors*, [JHEP **05** \(2021\) 238](#), [[arXiv:2005.08981](#)].

[53] A. Lazopoulos, A. Ochirov, and C. Shi, *All-multiplicity amplitudes with four massive quarks and identical-helicity gluons*, [JHEP **03** \(2022\) 009](#), [[arXiv:2111.06847](#)].

[54] J. M. Campbell and R. K. Ellis, *Top tree amplitudes for higher order calculations*, [JHEP **10** \(2023\) 125](#), [[arXiv:2309.03323](#)].

- [55] Y. Ema, T. Gao, W. Ke, Z. Liu, K.-F. Lyu, and I. Mahbub, *Momentum shift and on-shell constructible massive amplitudes*, Phys. Rev. D **110** (2024), no. 10 105003, [[arXiv:2403.15538](https://arxiv.org/abs/2403.15538)].
- [56] Y.-H. Ni, C. Wu, and J.-H. Yu, *Massless-Massive Amplitude Correspondence I: Helicity-chirality Matching and On-shell Higgsing*, . arXiv:2401.xxxxx.
- [57] Y.-H. Ni, Y.-N. Wang, C. Wu, and J.-H. Yu, *Extended Poincare Symmetry Dictates Massive Scattering Amplitudes*, [arXiv:2412.03762](https://arxiv.org/abs/2412.03762).
- [58] Y.-H. Ni, Y.-N. Wang, C. Wu, and J.-H. Yu, *Massive Helicity-Chirality Spinor Formalism from Massless Amplitudes with On-shell Mass Insertion*, [arXiv:2501.09062](https://arxiv.org/abs/2501.09062).
- [59] K. Risager, *A Direct proof of the CSW rules*, JHEP **12** (2005) 003, [[hep-th/0508206](https://arxiv.org/abs/hep-th/0508206)].
- [60] T. Cohen, H. Elvang, and M. Kiermaier, *On-shell constructibility of tree amplitudes in general field theories*, JHEP **04** (2011) 053, [[arXiv:1010.0257](https://arxiv.org/abs/1010.0257)].
- [61] C. Cheung, K. Kampf, J. Novotny, C.-H. Shen, and J. Trnka, *On-Shell Recursion Relations for Effective Field Theories*, Phys. Rev. Lett. **116** (2016), no. 4 041601, [[arXiv:1509.03309](https://arxiv.org/abs/1509.03309)].